

AN ABSTRACT OF THE THESIS OF

Juan C. Valdes-Salazar for the degree of Master of Science in Mechanical Engineering presented on August 31, 1993.

Title: Six-Axis Force Sensors: A Comparative Study

Redacted for Privacy

Abstract approved: _____
Dr. Eugene Fichter

A comparative study of three six-axis force sensors selected after an extensive literature survey is presented. A sensor to measure ground contact force at each foot of a walking machine is recommended.

Principles of force sensing are reviewed and characteristics of sensing elements are discussed. Results of simulation of three six-axis force sensors are presented as behavior curves, sensitivity plots and compliance matrices. These simulations use finite element techniques.

Condition numbers of compliance matrices are presented as a measure of overall sensor performance. Estimates of manufacturing costs are included as a final selection criterion.

**Six-Axis Force Sensors:
A Comparative Study**

by

Juan C. Valdes-Salazar

A THESIS

submitted to

Oregon State University

in partial fulfillment of
the requirements for the
degree of

Master of Science

Completed August 31, 1993

Commencement June 1994

APPROVED:

Redacted for Privacy

Professor of Mechanical Engineering in charge of major

Redacted for Privacy

Head of department of Mechanical Engineering

Redacted for Privacy

Dean of Graduate School

Date thesis is presented August 31, 1993

TABLE OF CONTENTS

	<u>Page</u>
1.- Introduction	1
2.- Fundamental Concepts	6
2.1 Basic Relationships	6
3.- Design	10
3.1 Design Principles	10
3.1.1 Location	10
3.1.2 Size	13
3.1.3 Transducers	14
3.1.4 Construction	15
3.2 Force Sensor Requirements	16
3.2.1 Force Range	16
3.2.2 Accuracy	17
3.2.3 Sensitivity and Selectivity	17
3.3 Configuration of Elastic Elements	26
3.3.1 Column Type Elements	27
3.3.2 Cantilever Beams	28
3.3.3 Shear Elements	29
3.3.4 Spoked Wheels	30
4.- Description of Selected Sensors	32
4.1 Truss Sensor	32
4.1.1 Design Review	33
4.2 Stewart Platform Transducer	34
4.2.1 Design Review	35
4.3 Cross-Shape Structure	36
4.3.1 Design Review	37
5.- Comparative Analysis	41
5.1 The Finite Element Method	42
5.2 Truss Sensor Analysis	44
5.3 Stewart Platform Transducer Analysis	67
5.4 Cross-Shape Structure Analysis	79
5.5 Evaluation	90
5.6 Results	94

TABLE OF CONTENTS (CONTINUED)

	<u>Page</u>
6.- Conclusions	97
Bibliography	99
Appendices	101
Appendix A Mass Calculations	101
Appendix B Truss Sensor FEM Program and Output	106
Appendix C Stewart-Platform FEM Program and Output	117
Appendix D Cross-Shape Structure FEM Program and Output	126
Appendix E Sensitivity Analysis Program	139
Appendix F Singular Value Decomposition Program	146
Appendix G Time and Cost Estimation	153

LIST OF FIGURES

<u>Figure</u>	<u>Page</u>
1. Simple second-order model of force sensor integration.	11
2. Wrist force-sensing vs. finger force-sensing.	13
3. Rectangular bar fitted with strain gauges for measurements of a force F .	19
4. The Wheatstone bridge circuit.	20
5. Typical elastic elements.	27
6. Column type elements.	28
7. Bending elements.	28
8. Shear strain elements.	29
9. Spoked wheel elements.	30
10. Frame/truss design schematic.	32
11. Model for Stewart-Platform.	35
12. Cross-Shape Structure.	36
13. PPS on X, Y, and Z axis.	37
14. Model of PPS.	38
15. Truss sensor showing constraints and elements of interest.	45
16a. Cross-linking curves varying force f_x (Truss, elem.40).	48
16b. Cross-linking curves varying force f_y (Truss, elem.40).	49
16c. Cross-linking curves varying force f_z (Truss, elem.40).	50
16d. Cross-linking curves varying force f_x (Truss, elem.72).	51

LIST OF FIGURES (CONTINUED)

<u>Figure</u>	<u>Page</u>
16e. Cross-linking curves varying force f_y (Truss, elem.72).	52
16f. Cross-linking curves varying force f_z (Truss, elem.72).	53
16g. Cross-linking curves varying force f_x (Truss, elem.80).	54
16h. Cross-linking curves varying force f_y (Truss, elem.80).	55
16i. Cross-linking curves varying force f_z (Truss, elem.80).	56
17a. Sensitivity analysis (Truss, linear displacement).	58
17b. Sensitivity analysis (Truss, angular displacement).	58
18. Truss sensor fem model using solid elements.	60
19a. σ_x stress field under a force f_x (Truss, global coords.).	61
19b. σ_x stress field under a force f_x (Truss, local coords.).	62
19c. σ_x stress field under a force f_y (Truss, global coords.).	63
19d. σ_x stress field under a force f_y (Truss, local coords.).	64
19e. σ_x stress field under a force f_z (Truss, global coords.).	65
19f. σ_x stress field under a force f_z (Truss, local coords.).	66
20. Stewart-Platform: top, side, and isometric views.	69
21. Stewart-Platform fem model with elements of interest.	70
22a. Cross-linking curves varying force f_x (Stewart, elem.57).	72
22b. Cross-linking curves varying force f_y (Stewart, elem.57).	73
22c. Cross-linking curves varying force f_z (Stewart, elem.57).	74
22d. Cross-linking curves varying force f_x (Stewart, elem.67).	75

LIST OF FIGURES (CONTINUED)

<u>Figure</u>	<u>Page</u>
22e. Cross-linking curves varying force f_y (Stewart, elem.67).	76
22f. Cross-linking curves varying force f_z (Stewart, elem.67).	77
23a. Sensitivity analysis (Stewart, linear displacement).	78
23b. Sensitivity analysis (Stewart, angular displacement).	78
24. Cross-Structure section: top, front, and isometric views.	80
25. Cross-Structure section with constraints and applied forces.	82
26a. σ_x stress field under a force f_x (Cross).	83
26b. σ_x stress field under a force f_y (Cross).	84
26c. σ_x stress field under a force f_z (Cross).	85
26d. σ_x stress field under a moment m_x (Cross).	86
26e. σ_x stress field under a moment m_y (Cross).	87
26f. σ_x stress field under a moment m_z (Cross).	88
27a. Sensitivity analysis (Cross, linear displacement).	89
27b. Sensitivity analysis (Cross, angular displacement).	89
28. Truss sensor dimensions.	101
29. Model for Stewart Platform.	103
30. Cross sensor basic volume.	104

LIST OF TABLES

<u>Table</u>	<u>Page</u>
1. Time and cost estimates for the Truss sensor.	67
2. Time and cost estimates for the Stewart-Platform.	71
3. Time and cost estimates for the Cross-Structure.	90
4. Final results for the three sensors studied.	94
5. Time estimation for the Truss sensor.	153
6. Time estimation for the Stewart-Platform.	154
7. Time estimation for the Cross sensor.	155

Six-Axis Force Sensors: A Comparative Study

C H A P T E R 1

INTRODUCTION

The objective of this work is to select a force sensor for a walking machine. This machine will be an autonomous six-legged robot capable of adventuring in a variety of environments and, therefore, requiring a suitable, reliable means of feedback from a series of sensors properly designed. As the interaction between the robot and its surroundings is primarily physical, a force sensor is the most logical choice among the different kinds of sensors available.

Although several six-axis force sensing devices have been developed recently, industrial applications of these devices are rarely found [19]. In the endeavor to introduce real flexibility into the behavior of industrial machines, or any automated machine, the concept of force feedback is now generally recognized to be essential. In the recent past, several research and industrial laboratories have been supporting this statement by designing appropriate force sensors and force feedback strategies.

Nevertheless, today's reality reveals that industrial applications involving force feedback are rare. This is in sharp contrast with the growing penetration

of vision systems.

The main reasons behind this discrepancy are twofold. First, force sensors are difficult to incorporate into commercially available robot controllers. Although a vision system is more complex than a force sensor, its interaction with the robot controller is mainly geometrical [19]. Therefore, it only influences target coordinates. These data are easily understood by traditional controllers with suitable digital inputs. Force sensor data, however, influence the dynamics of the joint loops. Unfortunately, most available controllers do not allow such low level interaction with the robot. Moreover, the interpretation of force sensor data is much less straightforward than the processing of vision data.

A second reason can be found in the force sensor itself. Normally, it is a fragile instrument and thus prone to overloading. Mechanical overload protection is a must, but difficult to achieve properly.

Despite these difficulties, turning industrial robots into adaptive systems that adjust themselves to external changes is probably the best way to enhance robot capabilities without making robots too expensive or limiting their versatility. Many kinds of sensors could provide the robot with information about the process or the environment, but only a force sensor would have a suitable feedback in the case of physical interaction between a

tool or part held by the robot, or the robot itself, and its surroundings.

The first step in the analysis of force sensors was to research and analyze all the available literature on the subject. The main reason was to try to find something that could be analyzed, redesigned, and fitted into the walking machine.

Many force sensors are reported in the literature, and several six-axis force sensors are commercially available [1, 5, 7, 16, 18, 21]. However, there are still several unresolved problems. First, there have been very few analytical studies because of the complexity of the sensor elastic elements or large cross-coupling among strain gage outputs for each axial force element. As for the evaluation of designed sensors, only very recently have some theoretical approaches been proposed [20]. Second, many of the sensors need some data processing of the measured sensing device outputs due to the cross-coupling. It is desirable to develop a sensor with as little cross-coupling as possible.

The literature shows that most sensors consist of a series of elastic elements in shear or bending connected to a "rigid" frame. When the sensor is subjected to the action of a set of forces and moments, these forces and moments are transmitted from the frame to the elastic elements which deform in a certain way. These deformations are recorded and, from them, the set of

forces and moments can be determined.

There are two basic arrangements in the geometry of the sensors: rectangular frame and circular frame. The rectangular arrangement seems to be the most common type. This design seems to offer a better chance to reduce the coupling between the signals leading to less computational time in processing the strain measurements.

In reviewing the available literature, the following attributes were analyzed: cross-coupling, rigidity, compactness, and feasibility of monolithic construction in order to avoid non-linearities (hysteresis and friction) normally present in glued or bolted joints [20].

As a result of this research, three concepts were chosen and carefully redesigned and evaluated, to yield a recommendation for the most suitable force sensor.

This thesis consists of five chapters after this one. Chapter 2 deals with the fundamental relationships on which any force sensor is based. The compliance matrix concept is presented as well as its relevance in determination of unknown forces when strains at particular points of the sensor are known.

Chapter 3 describes rules that ease design of force sensors and introduces the Wheatstone bridge as a sensing circuit. This leads to a basic introduction to analysis of sensitivity and selectivity. In addition, different types of elastic elements most commonly employed with force sensors are described, and evaluated.

In chapter 4 the actual comparative study is presented with descriptions of selected sensors, reasons why they were selected and their main characteristics according to their inventors.

Chapter 5 describes, in detail, the analyses performed on each of the sensors. The finite element method as a tool for analysis of force sensors is also presented as well as a cost estimate for manufacturing each sensor. Results of finite element analyses are shown in a series of behavior curves, and tables. Evaluation of each sensor is presented at the end of the chapter.

Chapter 6 summarizes all results from the previous chapter and presents a series of recommendations for future study.

CHAPTER 2

FUNDAMENTAL CONCEPTS

Robot force control can be viewed as the manipulation of the exchange of forces between the robot and its environment. Force sensing is the means of measuring this interaction. As pointed out by Flatau [9], it is important to distinguish between three types of interaction forces. First, the principal forces are ones represented by a vector set of three mutually orthogonal forces and three orthogonal torques referred to a prechosen point on the robot. The second type of force is a contact force acting on the end effector of the robot. The third type is the inertia force caused by dynamic motion of the robot. The work for this thesis is solely focused on determination of the principal force set (PFS).

2.1 Basic Relationships

The PFS is usually determined by means of a six-axis force sensor placed between the wrist and the end effector of the robot. In our particular case, the sensor will be located between the foot, the ground-contact surface, and the lowest point of the terminal leg segment. These six basic forces are contained in the vector

$$\mathbf{f} = [f_x \ f_y \ f_z \ M_x \ M_y \ M_z]^T \quad (1)$$

The effects due to these external forces are measured at selected locations on the sensor body. For a particular set of forces, \mathbf{f} , the response strain vector

$$\mathbf{e} = [\epsilon_1 \ \epsilon_2 \ \epsilon_3 \dots \epsilon_m]^T \quad (2)$$

is obtained, where "m" is the total number of strain measurements. The matrix relationship between strains and forces is

$$\mathbf{e} = \mathbf{C} \mathbf{f} \quad (3)$$

where \mathbf{C} (the compliance matrix), represents the relation between the applied force and the resulting strain for each force component. This compliance matrix can be determined either analytically, using methods in structural analysis, numerically [10], or experimentally using calibration [18]. If the sensor body deformation is within the elastic region of the material, the compliance matrix is constant, and equation (3) is a linear relationship. To compensate for the difference in units between force and moment, the force vector \mathbf{f} is usually normalized with respect to the maximum forces and moments

$$\mathbf{f} = \left[\frac{f_x}{f_{xmax}}, \frac{f_y}{f_{ymax}}, \frac{f_z}{f_{zmax}}, \frac{M_x}{M_{xmax}}, \frac{M_y}{M_{ymax}}, \frac{M_z}{M_{zmax}} \right]^T \quad (4)$$

Then we obtain

$$\epsilon = \underline{C} f \quad (5)$$

where \underline{C} is the normalized compliance matrix given by

$$\underline{C} = C \text{diag}[f_{\max}, f_{\max}, f_{\max}, M_{\max}, M_{\max}, M_{\max}]^T \quad (6)$$

If the maximum PFS components are taken to be the maximum values for both forces and moments, the normalized maximum force set is

$$f = [1 \ 1 \ 1 \ 1 \ 1 \ 1]^T \quad (7)$$

With this normalization, the ij th element of \underline{C} becomes the strain component at gauge "i" due to load "j" and the sum of the elements of row "i" is the total strain measured by the i th strain gauge due to the simultaneous effect of the maximum PFS.

In order to determine the PFS from measured strain, Eq. (3) needs to be transformed into the following form:

$$f = B \epsilon \quad (8)$$

The determination of matrix B depends on whether matrix \underline{C} is square or rectangular. If \underline{C} is square and non-singular then

$$f = \underline{C}^{-1} \epsilon \quad (9)$$

This corresponds to the case where a total of six strain measurements are taken. When more than six strain measurements are present, \underline{C} will no longer be square. To find B , a pseudo-inverse of \underline{C} must be used. It has been shown that one appropriate pseudo-inverse is the Moore-Penrose inverse [1].

CHAPTER 3

DESIGN

In order for a design to be successful, the designer must follow a systematic procedure, a series of rules that result in an efficient and organized job. These rules can be called the **design principles** and are developed based both on empirical experience and theoretical analysis.

In this chapter, the design principles for the development of most of the force sensors generated so far are presented, the different type of elements employed in the design are described, and the advantages and disadvantages of each type of element is presented. Examples of their most common application are included as well.

3.1 Design principles

3.1.1 Location

With respect to force sensing in robots, force can be measured at different locations. The purpose of using force sensors is always to know the interaction forces at the interface between the end effector of the robot and the environment.

The different possible measuring locations [20] are:

1. in the joints of the actuators. This method is mainly used in master-slave manipulators.

2. in the gripper fingers.
3. in the contact area between the fingers and the grasped object (artificial skin sensors).
4. in the robot environment.
5. in the interface between the robot extremity and the end effector. This is the application domain of multi-component force-torque wrist sensors, and therefore, the one applied in this work.

Another design principle, to consider, is the placement of the sensor. It is desirable to mount the sensor as close to the point of measurement as possible.

To see the reason for this, let us refer to Fig.1. This figure illustrates a simple mass-spring model of force sensor performance where force is measured by a

strain gauge mounted on an elastic member. $F_a(t)$ denotes the applied force being measured and $F_m(t)$ denotes the measured force as indicated by the output from a strain gauge. An equivalent system is a mass connected to a spring and dashpot. The measured force is proportional to the product of k_{eq} , the effective spring stiffness, and $x(t)$, the

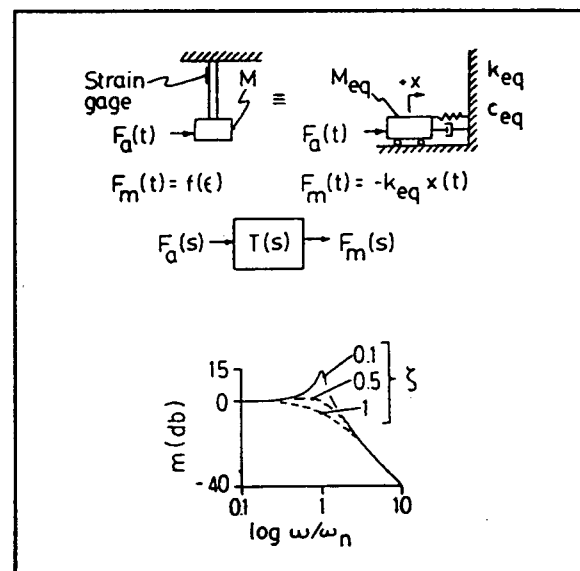


Figure 1 Simple second-order model of force sensor integration. (from [18])

displacement of the mass. The system is governed by a second-order differential

equation and has the transfer function:

$$T(s) = \frac{k_{eq}}{(M_{eq}s^2 + c_{eq}s + k_{eq})} \quad (10)$$

The frequency response plot for the transfer function is shown in the lower part of Fig.1, where m is the magnitude ratio in decibels, ω is the angular frequency of the input forcing function $F_a(t)$, ω_n is the natural frequency of the system, and ζ is the damping ratio [18].

Applied forces with frequency components greater than 20% of the system's natural frequency produce force output that is distorted in amplitude and phase [18]. The best measuring system has the highest natural frequency possible, so applied forces with high frequency components are measured accurately. System frequency response is increased by maximizing the natural frequency of the system.

Natural frequency can be expressed in terms of the equivalent spring constant and mass:

$$\omega_n = \sqrt{\frac{k_{eq}}{m_{eq}}} \quad (11)$$

When a force sensor is inserted at the wrist (in our case "ankle" would be

more appropriate) of a robot as shown in Fig.2, a larger equivalent mass, m_{eq} , is included in the force measuring system and the natural frequency of the system is decreased.

Based on this simple second-order model of sensor performance, force sensors should be inserted as closely as possible to the desired point of force measurement.

3.1.2 Size

Limiting the physical size of the sensor is important, especially for use on small robots, but difficult to achieve. In many cases, the weight of the sensor-end effector system represents more than 50% of the maximum payload [20]. Therefore, aluminum alloys are widely used as sensor materials. Stiffness requirements, rather than only sensitivity requirements, determine the diameter-to-height ratio of the sensor. There is always a compromise between stiffness and sensitivity. Because of the high sensitivity of strain gauges, sensors can be built stiff enough to not greatly reduce the natural frequencies. Therefore the goal is to build a sensor with the smallest mass possible, while still being within acceptable stiffness limits.

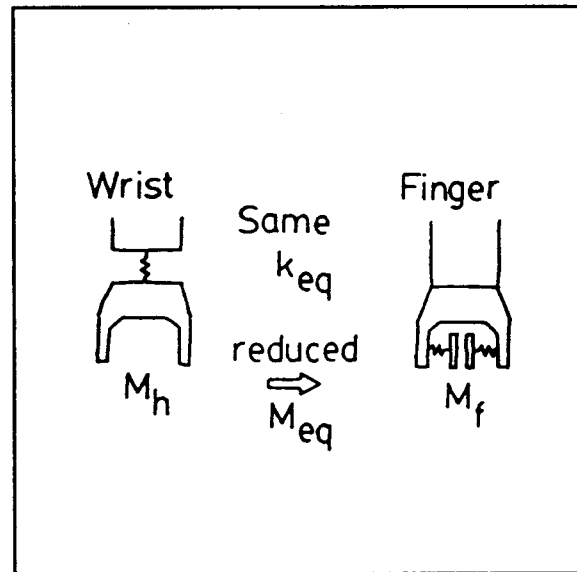


Figure 2. Wrist force-sensing vs. finger force sensing.(from [18])

3.1.3 Transducers

A force sensor consists of an elastic body which deforms under an applied force. Measurements of elastic deformations by appropriate transducers yield electrical signals from which the force vector components can be derived. Several measuring devices exist: displacement transducers (LVDT, inductive, capacitive, etc), piezo-electrical crystals, magneto-elastic devices, and strain gauges. Strain gauges are the smallest, easiest to use, and cheapest reliable transducers for use in robot force sensors [20]. The following favorable factors support this preference:

1. small size and low mass are instrumental in minimizing inertial effects and allowing operation over a broad frequency range, typically from static up to tens of kilohertz (where the upper limit depends upon gauge length).

2. absence of critical mechanical linkages, because strain gauges, being fully bonded to the elastic element, make a sturdy, shock-resistant, single piece.

3. outstanding linearity over a wide strain range, especially when strains of equal magnitude and opposite sign are measured, and ease of compensation of residual non-linearity at circuitry level, if required [6, 15].

4. low-sensitivity to temperature and ability to operate with proper compensation over a wide temperature range.

5. high stability, that is ability to retain calibration over a long time if adequately protected from abuse.

6. low sensitivity to a number of electrical or mechanical disturbances.

7. Relative change in resistance is readily exploited to compensate for

changes of supply voltage and frequency, and even intense magnetic fields may be tolerated with proper precautions [6, 15].

3.1.4 Construction

In building a sensor several options exist, but, in all cases, non-linearities must be minimized. These non-linearities can be caused by phenomena such as hysteresis or friction which normally occurs in bolted joints or glued interfaces. The best way to deal with this problem is to build the sensor from one single solid piece of material, that is, monolithic construction. Another major advantage of monolithic construction is found in the design process itself. As will be seen later, most design procedures deal with analysis of the sensor using finite element techniques. In modeling the sensor, one assumes that elastic elements undergo deformation without suffering separation from the body of the sensor. Another assumption is that deformation at the interface of the elastic elements with the body of the sensor is the same as deformation within the body and is within the elastic range. With these assumptions, we simplify the analysis from one non-linear, very complex problem to a linear and simpler problem. Monolithic construction also eliminates problems caused by joints. Bolted joints depend on friction forces to prevent motion between parts and separation of the jointed parts may be a serious problem. Glued joints may suffer different, but no less important problems; the glue may degrade easily when exposed to different environments, suffer from creep effects and undergo plastic deformation. Interaction between glued parts may be extremely complex both to analyze and

to model. Obviously, the best way to deal with these problems is to consider a sensor manufactured from one single solid block of homogeneous material.

In summary, the following statements can be established as a good set of **design principles** for force sensors:

1) the sensor must be placed as close as possible to the point of measurement.

2) the sensor must be built from one solid block of material.

3) the sensor must have low mass.

3.2 Force Sensor Requirements

In addition to the previous principles, the following requirements influence the final layout of a force sensor.

3.2.1 Force Range

The required range of the force components depends on the application at hand. Mechanical stops in all measuring directions have to be provided to prevent excessive strains in the sensitive sensor elements. The sensitivities of the measuring circuits in the different possible directions have to be matched in order to provide equal measuring accuracy and force resolution in all directions. One way to achieve this is by using the same type of strain gauge at all locations where measurements are taken.

3.2.2 Accuracy

The accuracy of a sensor system is affected by placement of strain gauges, cross-sensitivities, non-linearities, errors in data-processing circuitry, and calibration errors. With reasonable care, overall error figures of around 5% can be obtained [20] which is sufficient for virtually every application of force feedback.

3.2.3 Sensitivity and Selectivity

Simple formulas for strength of material can be used for dimensioning as a first approximation; effects of end constraint and proximity, however, must be taken into account with short, thick elements. When load-induced strain is evaluated for load-measurement purposes, strains at gauged sections may also be induced by spurious sources such as forces in directions different than the direction under study. A conflict may then arise between the requirements of sensitivity to nominal load and the ability to reject unwanted signals, that is, selectivity. Some sacrifice in sensitivity may be required to achieve a satisfactory selectivity. A simple linear model, where output signal y is given in terms of input components x_1 and x_2 and the relevant sensitivities a_1 and a_2 can be written as

$$y = a_1x_1 + a_2x_2 \quad (12)$$

The ratio R of the nominal signal component a_1x_1 to overall output y is given

by

$$R = \frac{1}{1 + (x_2/x_1)(a_2/a_1)} \quad (13)$$

If we want to measure x_1 via y , with as small an influence of x_2 as possible, we ought to keep the product $(x_2/x_1)(a_2/a_1)$ small. The term a_2/a_1 is a measure of the component-separating capability of the element and is determined by the element's shape and size, arrangement of strain gauges, errors in strain gauge location, errors in gauge factors, and errors in sensing circuitry.

In a given section of the elastic element, the applied load may be shown to produce an axial force N , a shearing force T , and bending and twisting moments M_b and M_t , respectively. The elastic element shape, strain gauge location and strain gauge orientation are chosen in order to selectively exploit one of the aforementioned components for generation of the signal to be measured.

For example, if the elastic element is a prismatic bar, then, except for proximity effects, strains due to axial force and shear and twisting moments are constant over the bar's length. However, strain due to bending is linearly dependent on position along the bar's length. Consequently, transducers based on bending moment are designed accordingly.

Further considerations may be derived from equations relating strain, and the sensing circuitry output, to force and moment components according to simple theory from strength of materials. A full sensing circuitry made up of four active gauges, with gauge factor S_g , is considered to always increase sensitivity. If gauges 3 and 4 are placed diametrically opposite to gauges 1 and 2 respectively

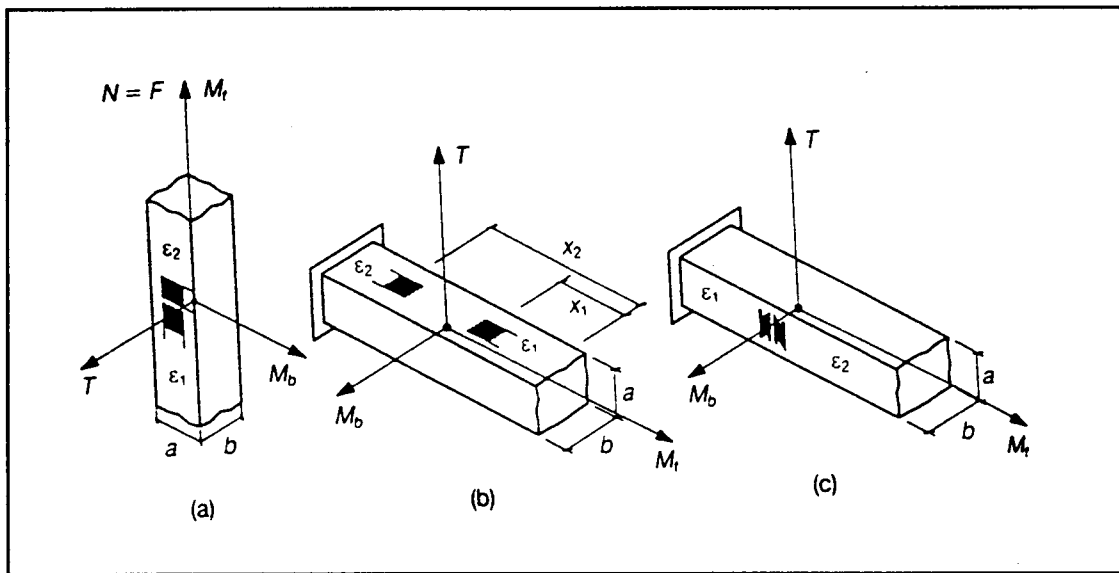


Figure 3. Rectangular bar fitted with strain gauges for measurements of a force F . (a) axial load N , (b) bending moment M_b , (c) side-force T . (from [2])

(Fig. 3) the following relationships are found :

$$\epsilon_3 = \epsilon_1 \quad \text{and} \quad \epsilon_4 = \epsilon_2 \quad (14)$$

where ϵ_i represents the strain measured by the 'ith' strain gauge.

Before analyzing the different load cases shown in Fig.3, it is convenient to describe the sensing circuitry system. The usual sensing circuitry involved with

strain measurements is the Wheatstone bridge [6].

The Wheatstone bridge is a circuit which can be employed to determine the change in resistance which a gauge undergoes when it is subjected to strain, and can be used to determine both static and dynamic strain-gauge readings. The bridge may be used as a direct-readout device where the output voltage ΔE is measured and related to strain. The bridge may also be used as a null-balance system where the output voltage ΔE is adjusted to a zero value by adjusting the resistive balance of the bridge. In either mode of operation the bridge can be effectively employed in a wide variety of strain-gauge applications.

To show the principle of operation of the Wheatstone bridge as a direct-readout device (where ΔE is measured to determine the strain), consider the circuit shown in Fig.4. The voltage drop across R_1 is denoted as V_{AB} and is given by the following expression:

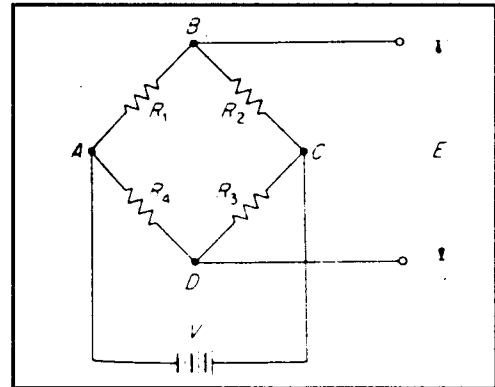


Figure 4. The Wheatstone bridge circuit.

$$V_{AB} = \frac{R_1}{R_1 + R_2} V \quad (15)$$

and, similarly, the voltage drop across R_4 is denoted as V_{AD} and is given by

$$V_{AD} = \frac{R_4}{R_3 + R_4} V \quad (16)$$

The output voltage from the bridge V is equivalent to V_{BD} , which is

$$E = V_{BD} = V_{AB} - V_{AD} \quad (17)$$

Substituting Eqns.(15) and (16) into Eq.(17) and simplifying give

$$E = \frac{R_1 R_3 - R_2 R_4}{(R_1 + R_2)(R_3 + R_4)} V \quad (18)$$

The voltage E will go to zero and the bridge will be considered in balance when

$$R_1 R_3 = R_2 R_4 \quad (19)$$

It is this feature of balancing which permits the Wheatstone bridge to be employed for static strain measurements. The bridge is initially balanced before strains are applied to the gauges in the bridge; thus the voltage E is initially zero, and the strain-induced voltage ΔE can be measured directly for both static and dynamic applications.

Consider an initially balanced bridge so that $E = 0$ and then change each value of resistance $R_1, R_2, R_3,$ and R_4 by an incremental amount $\Delta R_1, \Delta R_2, \Delta R_3,$ and ΔR_4 . The voltage output ΔE of the bridge can be obtained from Eq.(18), which becomes

$$\Delta E = V \frac{\begin{vmatrix} R_1 + \Delta R_1 & R_2 + \Delta R_2 \\ R_4 + \Delta R_4 & R_3 + \Delta R_3 \end{vmatrix}}{\begin{vmatrix} R_1 + \Delta R_1 + R_2 + \Delta R_2 & 0 \\ 0 & R_3 + \Delta R_3 + R_4 + \Delta R_4 \end{vmatrix}} = V \frac{A}{B} \quad (20)$$

where **A** is the determinant in the numerator and **B** is the determinant in the denominator. By expanding each of these determinants, neglecting second-order terms, and noting the balance condition (Eq.19), it is possible to show that

$$A = R_1 R_3 \left(\frac{\Delta R_1}{R_1} - \frac{\Delta R_2}{R_2} + \frac{\Delta R_3}{R_3} - \frac{\Delta R_4}{R_4} \right) \quad (21)$$

$$B = \frac{R_1 R_3 (R_1 + R_2)^2}{R_1 R_2} \quad (22)$$

Combining Eqs.(20) to (22) yields

$$\Delta E = V \frac{R_1 R_2}{(R_1 + R_2)^2} \left(\frac{\Delta R_1}{R_1} - \frac{\Delta R_2}{R_2} + \frac{\Delta R_3}{R_3} - \frac{\Delta R_4}{R_4} \right) \quad (23)$$

By letting $R_2/R_1 = r$ it is possible to rewrite Eq.(23) as

$$\Delta E = V \frac{r}{(1 + r)^2} \left(\frac{\Delta R_1}{R_1} - \frac{\Delta R_2}{R_2} + \frac{\Delta R_3}{R_3} - \frac{\Delta R_4}{R_4} \right) \quad (24)$$

Finally, if we make $r=1$, knowing that

$$\frac{\Delta R}{R} = S_g \epsilon \quad (25)$$

Eq.(24) can be rewritten as

$$\frac{\Delta E}{V} = \frac{S_g}{4} (\epsilon_1 - \epsilon_2 + \epsilon_3 - \epsilon_4) \quad (26)$$

provided that the gauge factors are the same for all gauges.

Equation (26) represents the basic equation which governs the behavior of the Wheatstone bridge in strain measurement and the one to be used here.

Taking a bar with rectangular cross-section axb (see Fig.3), for the case of axial load F we have $N = F$, $T = 0$, $M_b = M_t = 0$. Therefore, with ν being Poisson's ratio and considering the bridge output (Eq.26) we have the following

$$\epsilon_1 = \frac{F}{Eab}; \quad \epsilon_2 = -\nu \frac{F}{Eab}; \quad S_1 = \frac{\Delta E}{V} = S_g (1+\nu) \frac{F}{2Eab} \quad (27)$$

The notation ΔE must be taken as a single entity representing the change in the output voltage of the Wheatstone bridge and must not be confused with E , the modulus of elasticity.

If the applied force F is orthogonal to the bar's axis, then $N = 0$, $T = F$, and $M_b = Fx$; either the bending moment or shear-originated strain may be

exploited. To use bending moment

$$e_1 = \frac{6Fx_1}{Ea^2b}; \quad e_2 = \frac{6Fx_2}{Ea^2b}; \quad S_2 = \frac{\Delta E}{V} = \frac{6S_g F(x_1 - x_2)}{2Ea^2b} \quad (28)$$

To use shear

$$e_1 = \frac{\alpha F(1 + \nu)}{Eab}; \quad e_2 = \frac{-\alpha F(1 + \nu)}{Eab}; \quad S_2 = \frac{\Delta E}{V} = \frac{\alpha S_g F(1 + \nu)}{Eab} \quad (29)$$

where α represents the shear factor of the given cross-section (1.5 for rectangular sections) [2].

Let us consider as a reference the first loading condition examined, axial. Sensitivities of bending and shear cases with respect to the axial load case can be obtained as the ratio of bridge outputs as follows:

$$\frac{S_2}{S_1} = \frac{6(x_1 - x_2)}{a(1 + \nu)} \quad \frac{S_3}{S_1} = 2\alpha \quad (30)$$

where S_1 , S_2 , and S_3 , represent the bridge output signal for the axial, bending, and shear load respectively.

The sensitivity ratio for the case of shear is constant for the case at hand, as it is determined uniquely by the shear factor α . On the other hand, in the case of bending, both bar thickness and distance between gauged sections enter the picture, enabling sensitivity ratios in excess of 20 to be obtained easily [2].

Selectivity may be considered using elementary methods to treat the three loading conditions considered. For the sake of simplicity, spurious effects such as those caused by gauge misalignment are pooled together and treated as a difference (d_{sg}) among gauge factors. The unwanted components that originate from a deviation (d_f) of the point of application of force F , with the most critical direction being taken into account, are considered. Because of gauge misalignment Eq.(5) is no longer valid. Only the first loading case (axial) will be illustrated, as the same analysis applies for all three cases.

In the first case, a bending moment $M_b = Fd_f$ is present (see Fig.3) as well as the axial load $N = F$. Therefore

$$e_1 = \frac{F}{Eab} + \frac{6Fd_f}{Ea^2b}; \quad e_2 = -\nu e_1; \quad e_3 = \frac{F}{Eab} - \frac{6Fd_f}{Ea^2b}; \quad e_4 = -\nu e_3 \quad (31)$$

and, taking a worst-case scenario,

$$S_{g1} = S_{g2} = S_g - \frac{d_{sg}}{2}; \quad S_{g3} = S_{g4} = S_g + \frac{d_{sg}}{2} \quad (32)$$

we obtain

$$\frac{\Delta E}{V} = S_g(1 + \nu) \frac{F}{2Eab} + d_{sg}(1 + \nu) \frac{3Fd_f}{2Ea^2b} \quad (33)$$

If we analyze the remaining two cases in a similar way, it can be shown [2] that on a relative basis, variation in sensitivity in the three cases considered

are given by

$$\frac{\Delta S_1}{S_1} = \frac{d_{sg}}{S_g} \frac{6d_f}{a} \quad (34)$$

$$\frac{\Delta S_2}{S_2} = \frac{d_{sg}}{S_g} \frac{(x_1 + x_2)2d_f}{(x_1 - x_2)} \quad (35)$$

$$\frac{\Delta S_3}{S_3} = \frac{d_{sg}}{S_g} \frac{(3a + 1.8b)d_f}{3ab} \quad (36)$$

The element loaded in shear (eq.36) is seen to be less affected than the axially loaded element (Eq.34) by shifts in the line of action of external load. If the load is symmetrical ($x_2 = -x_1$), the element small, and some conditions on dimensional tolerances and proportioning are met, the element loaded in bending is seen to be unaffected.

3.3 Configuration of Elastic Elements

As previously stated, a force sensor consists of a number of elastic elements connected to the body or frame of the sensor. This frame is said to be "rigid" to the extent that when a general force is acting on the sensor, its deformation is negligible in comparison with deformations of the elastic elements.

From the deformations of the elastic elements, the PFS can be obtained. Other considerations that still need to be addressed concern the existence of special types of elastic elements for use in force sensors and the application each element is best suited for. This section is intended to answer these questions.

An elastic element may be classified according to several criteria, such as the shape or configuration, stress exploited by the transducing element, or the intended use of the sensor (weighing, general-purpose force measurement). Some typical shapes are shown in Fig.5.

3.3.1 Column-type elements

Column-type elastic elements are simple and inexpensive to manufacture; in most cases no other configuration may be available for very large loads. Some examples of this type of element are shown in Fig.6.

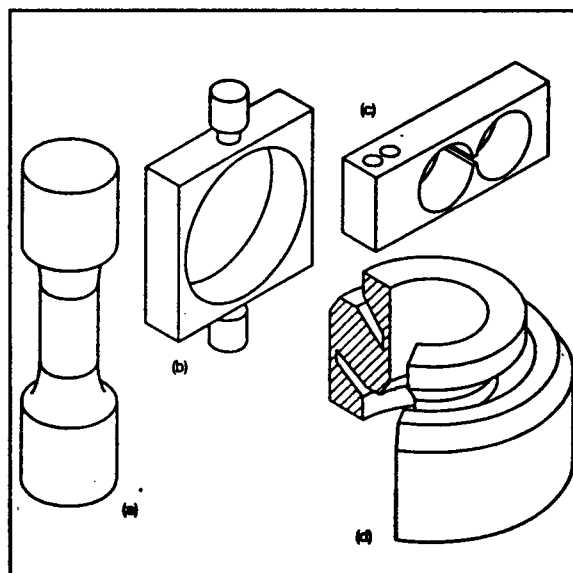


Figure 5. Typical elastic elements. (a) column, (b) "square" ring, (c) "binocular" beam, (d) toroid (from [2])

Some of these variations allow an increase in resistance to bending moments and an increase of sensitivity when placed in particular arrangements. Basically, column-type elements are designed to measure large tension or compression loads.

3.3.2 Cantilever beams

Sensitivity to force measured through bending strain may be varied over a broad range by altering the lever arm. Reasonable stiffness may be retained even at low force levels by selecting cross-sections with a high ratio of moment of inertia to modulus of resistance, that is, hollow or slotted elements. (Fig. 7).

In order to dispense with the requirement of tight control of the effective lever arm, elastic devices with parallel linkage are frequently used. A dual beam arrangement offers an inherently larger stiffness to spurious load components. Very simple devices were proved to be quite effective with parallel strip linkages [2]. Departures from parallelism of beams were found to affect sensitivity to moments far more than differences of the same order in effective beam length

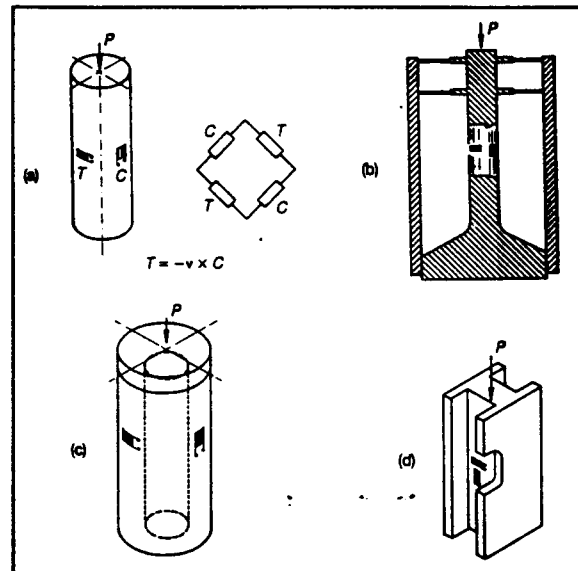


Figure 6. Column type elements. (a) simple solid, showing strain-gauge bridge, (b) load cell with diaphragms. (c) hollow beam, (d) H-section (from [2])

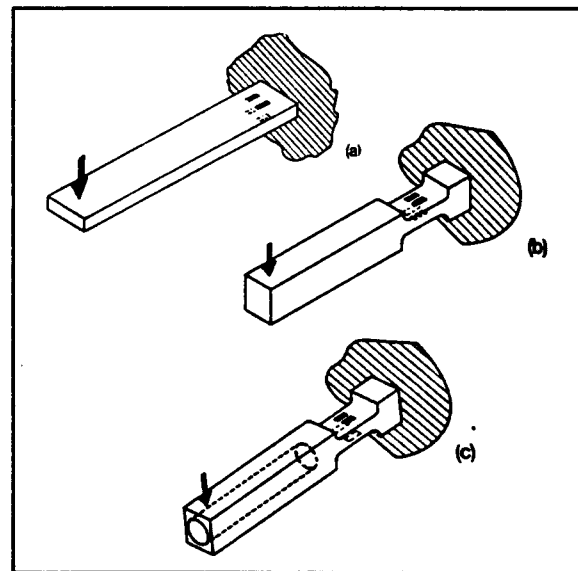


Figure 7. Bending elements. (a) simple cantilever, (b) Stiffness improvement by strain concentration, (c) hollow beams enhances natural frequency (from [2])

(Mana et al., 1989). Adoption of integral beams, where flexures are slotted or bored out from a solid piece, leads to enhanced stiffness with low hysteresis. Also, flexure thickness may be made smaller at the strain-gauge location as long as this thickness is increased in the adjacent zones to reduce the risk of elastic instability. This type of element is mostly used at medium to low load ranges, typically in weighing systems, where their excellent repeatability is an advantage over other units.

3.3.3 Shear elements

Exploitation of shear strain (Fig.8), offers a number of advantages, namely low sensitivity to even large shifts in line of action of load without the need for a linkage, fair sensitivity, and good linearity. In view of these advantages, it is hard to explain why shear-type load cells only appeared on the market some thirty years after the invention of the wire strain gauge [2].

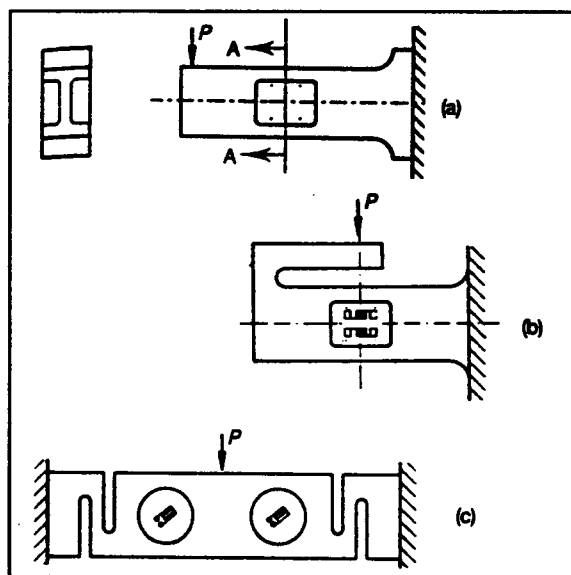


Figure 8. Shear strain elements. (a) shear stress increased by milling pockets in the web, (b) reduction of unwanted effects by making bending equal to zero, (c) symmetry protects against side-loads (from [2])

Since the moment arm can be controlled, short cantilever beams can be made to fairly large load capacities. Suitable pockets enhance sensitivity without

greatly affecting ultimate strength. Shear-type elements can take larger loads than other elements without requiring overload stops.

3.3.4 Spoked Wheels

Elements of the bending type or shear type already examined require an external load-application structure. This structure may be, in certain cases, quite complex and cumbersome due to the intrinsically asymmetric shape of the cantilever-type element in the direction of the highest sensitivity. This causes difficulty in correct load application, a condition that must be satisfied to avoid non-repeatability, hysteresis, and, in certain instances, non-linearity.

A rewarding load-application method exploits a symmetric structure obtained by linking a number of bending or shear-type beams in the pattern of wheel spokes or radial segments. Although it is possible to obtain 45, 60, 90, 120 and 180 degree symmetries, as a rule 90 degree symmetry is employed, while 120 and 60 degree symmetries are seldom

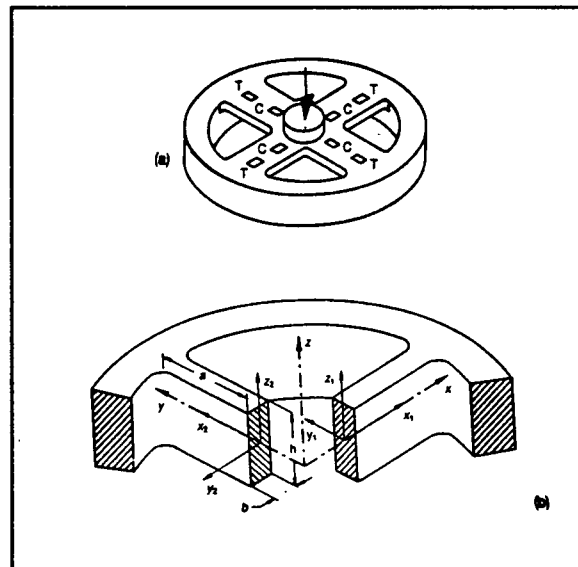


Figure 9. Spoked wheel elements. (a) typical four-spoked element, (b) reference systems used in their analysis (from [2])

adopted because of constructional difficulties. Fig.9 shows one typical example of this type of element. Unfortunately, it is not possible to simultaneously avoid

the effect of the external bending moment and the redundant axial constraint in the spokes. Very complex arrangements must be built to try to avoid this effect which, lead to non-repeatability and hysteresis problems. The characteristics of force flow through the measurement sections depend on the redundant constraints.

CHAPTER 4

DESCRIPTION OF SELECTED SENSORS

Among sensors found in the literature survey, most have some characteristics in common, namely, rectangular or circular arrangements of the elastic elements and extensive use of simple cantilever or shear type elements, which are the common elements employed in all the commercial sensors available today. However, a few sensors described in the literature exploited different elements in a unique way. These sensors are not commercially available but all of them are very promising choices. In this section each of these sensors is described and its main characteristics (according to each inventor) are reported.

4.1 Truss Sensor [1]

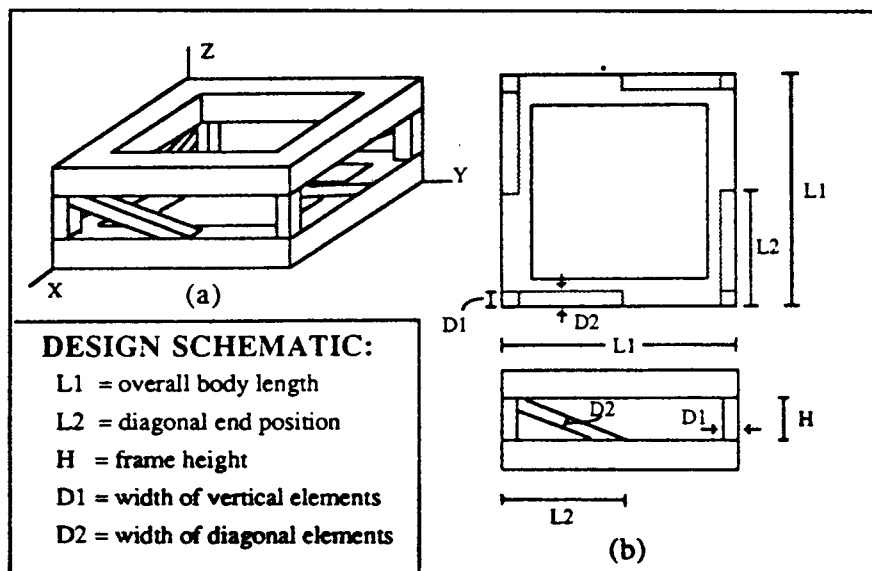


Figure 10. Frame/truss design schematic. (from [1])

The schematic design of the truss sensor is depicted in Fig.10. The uniqueness of this design lies in the elastic members that exhibit truss (axial deformation) behavior, as opposed to the commonly used beam (bending) behavior. Some of the improvements claimed are: increased force sensitivity with a consistently low condition number, increased rigidity, and improved design flexibility.

4.1.1 Design Review

The key to the truss force sensor is truss behavior. The aim is to eliminate the use of beam theory and coupling and rigidity problems normally encountered in sensors using these elements. In a truss the strain measured in a member is due solely to axial deformation, thus

$$\epsilon = P / EA \quad (37)$$

where ϵ is the strain measured, P is the axial local force acting on the member, cross sectional area A , and elastic modulus E . For a truss, only one measurement is needed to determine the force P from the strain ϵ , as opposed to the beam element, where two gauges are required to decouple the load. It is known from strength of materials [3] that in general a truss element under axial loading will have less nodal (end) displacement than a beam element under equivalent transverse loading. This means that a truss element under axial loading is stiffer than the equivalent beam under transverse loading.

Although there is still coupling between forces and moments in the truss sensor, the strain contribution due to bending is an order of magnitude smaller than that due to axial loading. The ideal location for strain measurement is in the middle of each elastic element.

The strain matrix of the sensor exhibits decoupled behavior in the sense that certain members are affected primarily by certain forces and not by others. The vertical members are affected mainly by f_z , M_x , and M_y , and not by f_x , f_y and M_z , which are picked up by the diagonal members (Fig.10). This leads to a small cross-coupling between strain outputs and therefore a nicely banded compliance matrix. This feature allows good condition numbers to be obtained, where the condition number is an index of structural performance of the sensor (see chapter 5 section 5.4).

With the truss sensor global deflections are held to a minimum, making this type of force sensor very rigid. This is due in part to truss behavior and in part to the orientation of the elastic members. The net result is a sensor equally resistant to motion in all directions. Also, the truss sensor may be made very compact from a single piece of material.

4.2 Stewart-Platform Transducer [11]

Although the Stewart-Platform is a well-studied subject [11], its application as a transducer was not studied until 1988 [11]. The idealized model that is used

for its study is shown in Fig.11. A platform of radius b is supported by six symmetrically-disposed elastic legs of equal length L , in turn mounted on a fixed base of radius a . The separation of the platform from the base is given by h . In the first instance, the legs are regarded as being connected to base and platform by means of spherical joints, thus imposing no bending or torsion on the leg themselves.

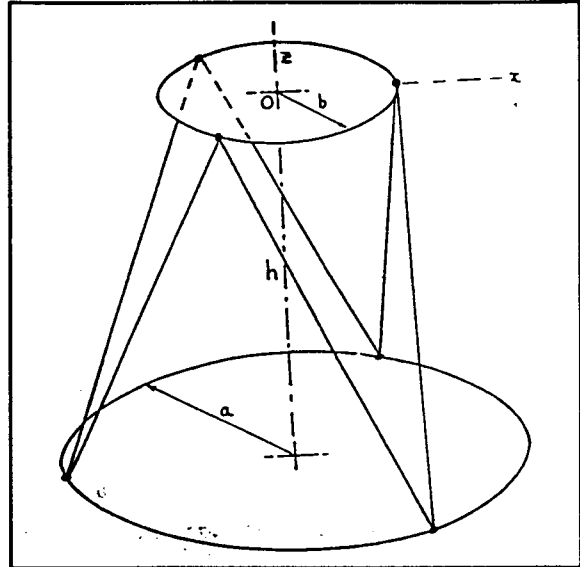


Figure 11. Model for Stewart-Platform. (from [11])

Consequently, remaining restraints offered to the platform by the set of legs are wholly dependent on the axial stiffness of these legs which are each of stiffness k . Axial deflections of the legs are assumed to be sufficiently small so that the geometrical shape of the device remains fixed, to a first order of approximation, and thus the externally-observed characteristics of the device are linear.

4.2.1 Design Review

In practical terms, it will not usually be feasible to construct a platform transducer of this kind with spherical joints at the ends of the legs. However, a stiff structure can be obtained with relatively slender legs. This will have the

advantage of high natural frequency of the device with its outboard load, but at the cost of relatively low transducer sensitivity. Typical leg diameters, in the case of circular sections, can be much smaller than their length, and then the bending stiffness of the legs imposes insignificant distortions in the form of the stiffness matrix. Similar arguments apply to the effect of axial torsional stiffness of the leg elements.

4.3 Cross-Shape Structure [21]

The cross-shape sensor is shown in fig.12. It has three pairs of elastic elements aligned on three axes which are orthogonal and cross at the center of the sensor. Each elastic element consists of a pair of thin parallel plates which form the parallel plate structure. From the outputs of strain gauges placed on the elastic elements, the six force

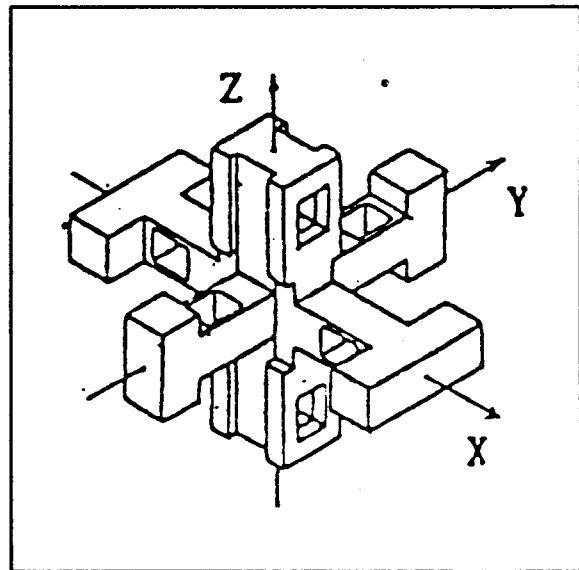


Figure 12. Cross-Shape Structure. (from [21])

components are obtained. Merits of the sensor include: (1) The whole characteristic of the sensor is obtainable just by analyzing the force-strain relation of a pair of elastic elements on an axis, making it simpler to design a sensor for a given specification. (2) The cross-coupling between the strain gauge outputs and the six force components can be made small. (3) It is easy to design a

sensor exhibiting better rigidity than other cantilever-based sensors.

4.3.1 Design Review

To understand how the sensor deforms under the applied load, let us look at Figs.13a and 13b.

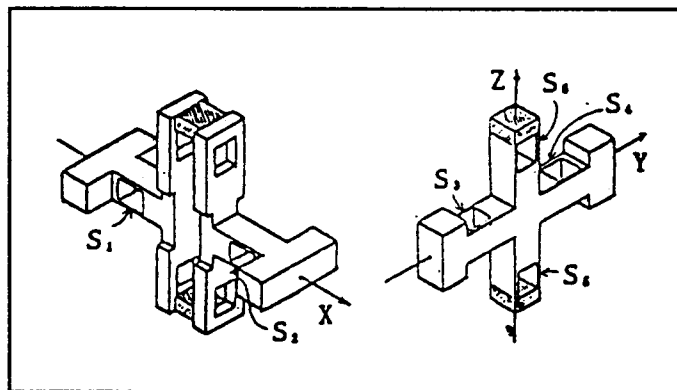


Figure 13. PPS on X, Y, and Z axis. (a) PPS on X axis (b) PPS on Y and Z axis. Strain gauges are labeled $S_1 - S_6$ (from [21])

These figures show an exploded view of the sensor for ease of understanding. The location where strain gauges are placed are labeled as $S_1 - S_6$. The hatched areas are the only common parts of these figures, which means that there is a slot running parallel to the Z axis from top to bottom of the sensor allowing free movement in three directions.

Fig.14 shows the model of a pair of parallel plate structures (PPS). As shown in the figure, each PPS is divided into three parts: the central block, end block, and plate.

It is assumed that the central and end block parts do not deform at all under the application of a force, and that the plate part can be modeled as two cantilevers. The notation d means

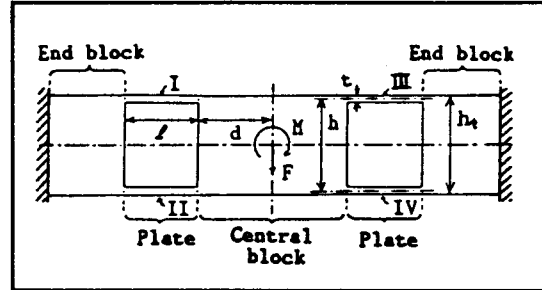


Figure 14. Model of PPS. (from [21])

the distance from the center of the beam to the PPS, L is the length of the plate, t is the thickness of the plate, b is the width of the plate, h is the distance between the center lines of two plates, and h_c is the thickness of the central block part. Note that $h_c = h + t$.

It can be shown [21] that strain on the outer surface of the plate for a force F and moment M applied on the center of the PPS model can be derived analytically. Three cases are considered: (1) force F only, (2) moment M only, and (3) force F and moment M combined.

(1) Case of force F only

When only a force F is applied on the center of PPS model [21], the strain on the upper surface of the plate II (and plate III) is given by

$$e(\xi) = \frac{3}{4Ebt^2} (2\xi - L)F \quad (38)$$

Similarly strain on the lower surface of the plate II (and plate IV) is given by

$$\epsilon(\xi) = - \frac{3}{4Ebt^2}(2\xi - L)F \quad (39)$$

(2) Case of Moment M only

When only a moment M is applied on the center of the PPS model, the symmetry of plates I-IV allows the following assumptions to be made [21]: the center block does not deflect, the deflections of plates I and IV are the same, and the deflections of plates II and III are the same. Strain on the upper surface of plate I (or the lower surface of plate IV) is given by

$$\epsilon_{M1}(\xi) = \frac{3[hL^2 - 2tL(L + 3d) + 6t(2d + L)\xi]M}{Ebt[6h^2L^2 + 8t^2(3d^2 + 3dL + L^2)]} \quad (40)$$

Similarly, strain on the lower surface of plate II (or the upper surface of plate III) is given by

$$\epsilon_{M2}(\xi) = - \epsilon_{M1}(\xi) \quad (41)$$

(3) Case of force F and moment M combined

With the assumption that the deflections are small, the strain for the case of combined F and M is given by the superposition of the cases of F only and M only [21]. For plates I and IV

$$\epsilon(\xi) = \frac{3}{4Ebt^2} \left[\left(\frac{2thL^2 - 4t^2L(L+3d) + 12t^2(2d+L)\xi}{3h^2L^2 + 4t^2(3d^2 + 3dL + L^2)} \right) M_{\pm}(2\xi - L)F \right] \quad (42)$$

where the sign \pm is "+" for plate I, and "-" for plate IV.

Similarly, for plates II and III

$$\epsilon(\xi) = -\frac{3}{4Ebt^2} \left[\left(\frac{2thL^2 + 4t^2L(L+3d) - 12t^2(2d+L)\xi}{3h^2L^2 + 4t^2(3d^2 + 3dL + L^2)} \right) M_{\pm}(2\xi - L)F \right] \quad (43)$$

where the sign \pm is "+" for plate II and "-" for plate III.

The pair of PPS on the X axis detect the F_x and M_y components. Similarly, with the other two pairs of PPS on Y and Z axis, the F_x , M_x , F_y , and M_x components are detected.

The best place for placing the strain gauges is the boundary between the central block or the end block and the plates.

CHAPTER 5

COMPARATIVE ANALYSIS

In this chapter, analysis and evaluation of the three sensors described in Chapter 4 is presented. The analysis was performed by the use of the finite element analysis software COSMOS/M. From the results, cross-coupling and sensitivity analyses were performed and the compliance matrix for each of the sensors was obtained. Using the compliance matrix, the evaluation was carried out by performing a singular value decomposition using an available subroutine [17]. The analysis is completed by a cost estimation for each of the sensors. The results of the analyses are presented and a comparison of each of the analyses is made, leading to a recommendation of the most suitable sensor for its future use with the walking machine.

The first part of this chapter introduces the finite element method (FEM) as a tool for the design of six-axis force sensors. Next, the truss sensor was analyzed. In order to perform the analyses, a preliminary geometry was designed and a FEM model was developed. The model was tested and with the obtained results, both cross-linking and sensitivity analyses were performed. The geometry was then modified and the analyses were repeated. This process continued until satisfactory results were obtained. Finally a cost estimation is provided. The above method was repeated for the Stewart-Platform and the Cross-Structure sensor.

All results are shown in a series of graphs, plots and tables for each sensor. Finally, compliance matrices were obtained and the condition numbers calculated.

5.1 The Finite Element Method (FEM) [10]

In problems of structural mechanics the design analyst seeks to determine the distribution, or field, of stresses throughout the structure to be designed. On occasion it is necessary to calculate the displacements at certain points of the structure to ensure that specified clearances are not violated. The calculated stress field should represent a system of internal and external forces which are in equilibrium and simultaneously the displacements should be continuous (the condition of compatibility). When the behavior being examined is of a two or three-dimensional nature, the solutions take the form of partial differential equations. Rarely do exact solutions exist for such equations and only slightly more often does it prove feasible to construct an adequate solution with an approximation consisting of a few terms. Many such terms are needed for an accurate solution.

The finite element method is an analytical procedure whose active development has been pursued for a relatively short period of time [10]. The basic concept of the method, when applied to problems of structural analysis, is that a continuum (the total structure) can be modeled analytically by its subdivisions into regions (the finite elements). In each of these regions, the

behavior is described by a separate set of assumed functions representing the stresses or displacements in that region. These sets of functions are often chosen in a form that ensures continuity of the described behavior throughout the complete continuum. If the behavior of the structure is characterized by a single differential equation, then the finite element method, in common with the series and finite differences schemes, represents an approach to the approximate solution of that equation. If the total structure is heterogeneous, being composed of many separate structural forms in each of which the behavior is described by a distinct differential equation, the finite element approach continues to be directly applicable [10].

In common with the alternative procedures for the accomplishment of numerical solutions for practical problems in structural mechanics, the finite element method requires the formation and solution of systems of algebraic equations. The special advantages of the method reside in its suitability for automation of the equation formation process and in the ability to represent highly irregular and complex structures and loading situations.

Therefore, the finite element method provides an excellent tool to analyze a given force sensor design and to introduce the necessary modifications for a better design. By creating a detailed and accurate finite element model the analyst can estimate the response of a given design, calculate the strains at the desired points, get the corresponding compliance matrix and then perform the

singular value decomposition which will yield the condition number (design index). This process may be repeated for several different designs, under the given loading conditions, until the desired singular values are obtained.

In summary, the finite element method ensures accuracy in the final response, and as such should be considered as a very effective tool in the design phase of a force sensor.

5.2 Truss Sensor Analysis

The force requirements from the preliminary walking machine design are:

Forces: 67.44 lb (300 N) along the sensor's x, y, and z axis.

Moments: 88.5 lb in (10 N m) along the sensor's x, y, and z axis.

Mass: 0.044 lb (0.02 kg) without mounting plates.

With these requirements, a preliminary geometry of the truss sensor was designed and the finite element model shown in Fig.15 was constructed as a first approximation. The model consists of thick-plate type finite elements forming the upper part of the support and 3D-beam type finite elements forming the 'elastic' vertical and diagonal elements. The numbers represent the elements where the strain gauges must be located, and the "tree-like" symbols at the lower part of each column represent the restraints. As it can be seen, the lower part of the support is modeled as the "ground". The reason for this "ground" is that the sensor is going to be placed between the lower part of the leg and the foot. In

TRUSS SENSOR
WIRE-FRAME MODEL

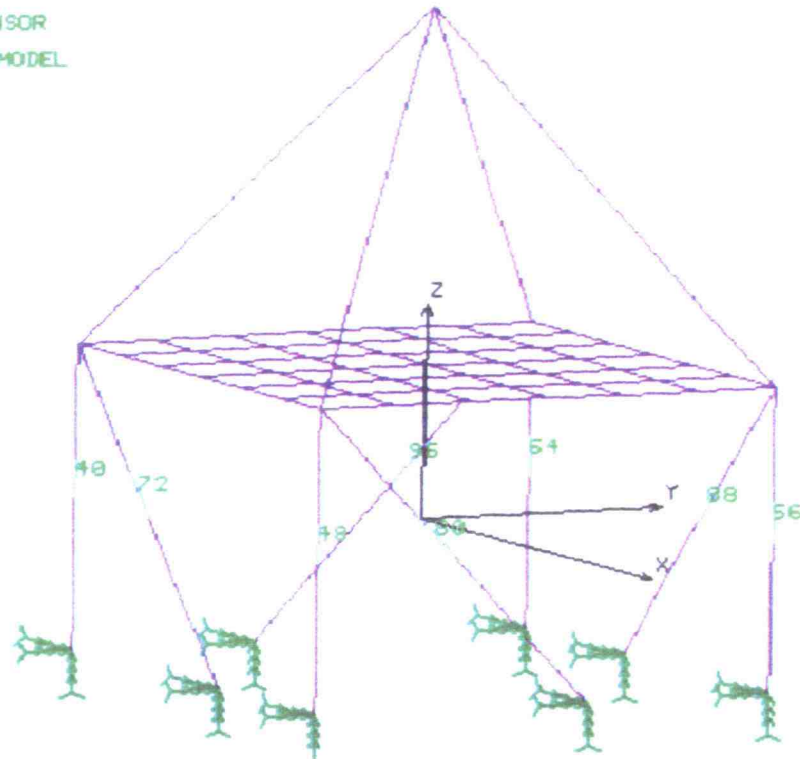


Figure 15. Truss sensor model showing constraints and elements of interest.

this model the foot is represented by the support (the pyramid-like structure at the top of the sensor) where the load is to be applied. Therefore, the sensor must be constrained in the lower part and there was no need to explicitly represent this body. In addition, the lower and upper supports are considered perfectly rigid and, therefore, don't deform at all. The first analysis was to check the stress distribution under the maximum load for possible yielding of the structure, and to study the strain magnitudes in order to find the best location for the placement of the strain gauges. To assure that the number of finite elements was appropriate, the elastic beams were each meshed using five 3D-beam elements. The analysis was performed and the results recorded. Then the number of finite elements was increased and the analysis performed again and the results were compared with those of the first analysis. This process was repeated until the results agreed within 0.5%. It was found that the minimum required number of finite elements was eight. The best placement of the strain gauges was at the middle of each beam, on each of the numbered elements in Fig.15.

The second analysis was the cross-coupling of the signals. Cross-coupling can be defined as the influence that other forces, different from the one we are interested in, have in the desired force's measurement. To determine this relationship, a set of loading conditions was designed. The force range was from 5.62 lb (25 N) to 22.48 lb (100 N) in increments of 5.62 lb (25 N), which gives a total of four points for each set of loads. The first step was to apply a single

force in the x direction and run the finite element analysis. The first loading condition consisted of forces in the x direction with values of 5.62, 11.24, 16.86, and 22.48 lb. The second loading condition consisted of forces in the x direction, but this time with a constant force in the y direction equal to 50% of the range, (11.24 lb). The final loading condition consisted of forces in the x direction but this time along with a constant force in the -z direction of magnitude 11.24 lb. This analysis was then repeated for the y and z directions, and results were obtained for each one of the eight elements of interest, giving a total of 72 set of load cases. Some results are shown in Figs.16.a-16.f, and the elements correspond to those in Fig.15.

Results are shown in a series of stress-force plots for representative elements of the sensor. Only the normal stress caused by a force parallel to the axis of the beam was considered because signals due to bending moments can be easily canceled in the Wheatstone bridge by proper arrangement of the strain gauges. From these results we notice that the vertical beams (elements 40, 48, 56, and 64) exhibit a high cross-coupling (Figs.16a-16c), while the diagonal beams (elements 72, 80, 88, and 96) do not. For example, from Figs.16d-16i, it is clearly shown that element 72 (and 88) is primarily affected by forces in the x direction, while element 80 (and 96) is primarily affected by forces in the y direction.

Stress - Force

truss sensor

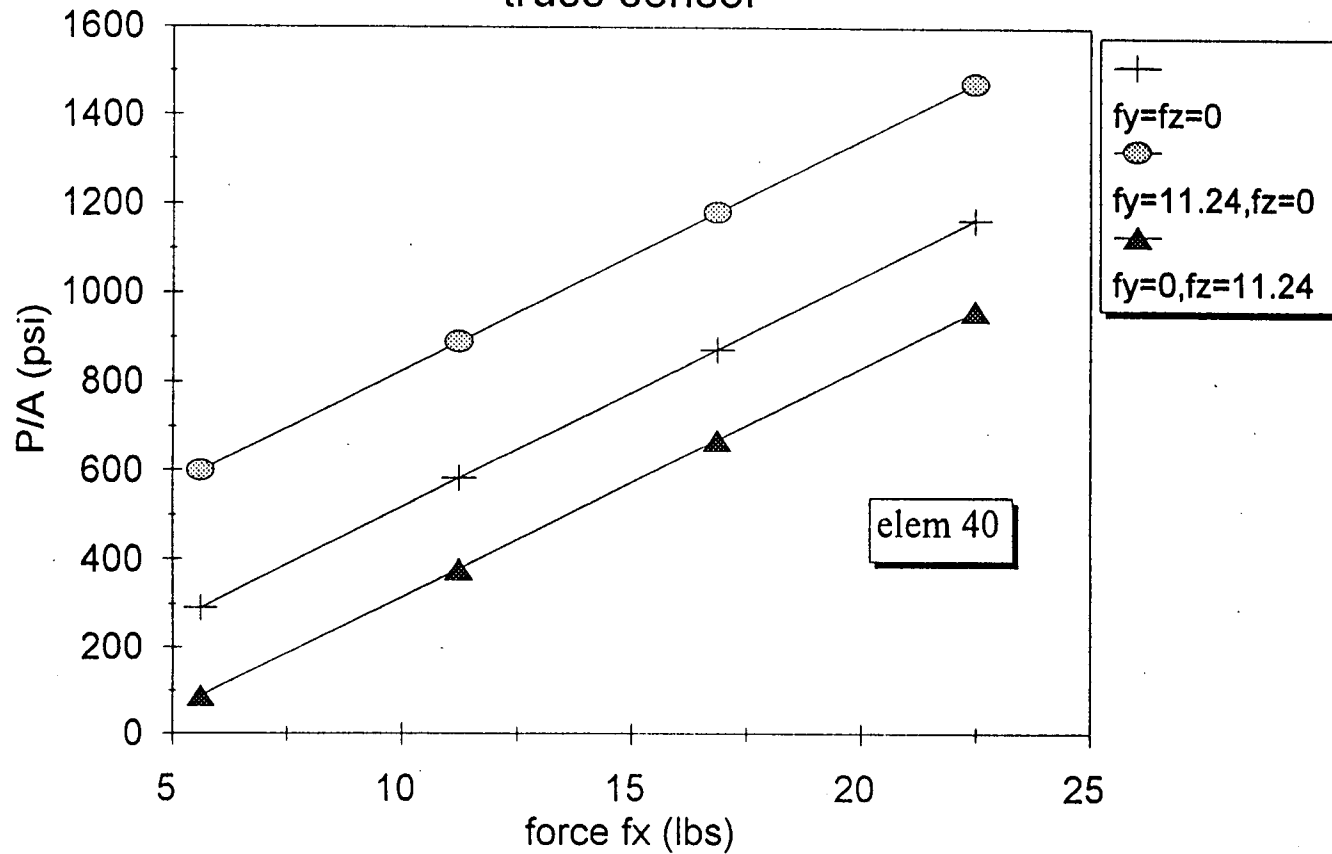


Figure 16a. Cross-linking curves varying force f_x (Truss, elem.40).

Stress - Force

truss sensor

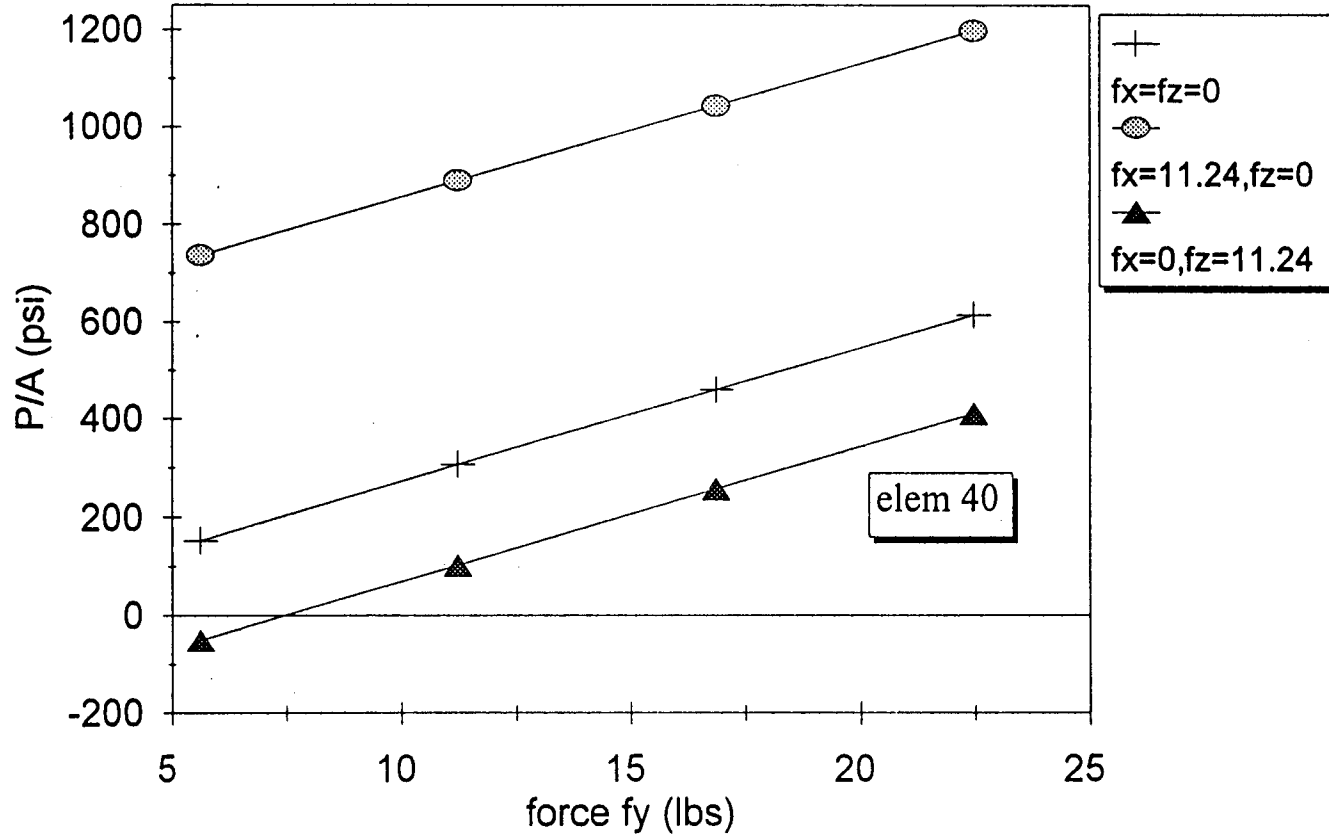


Figure 16b. Cross-linking curves varying force f_y (Truss, elem.40).

Stress - Force

truss sensor

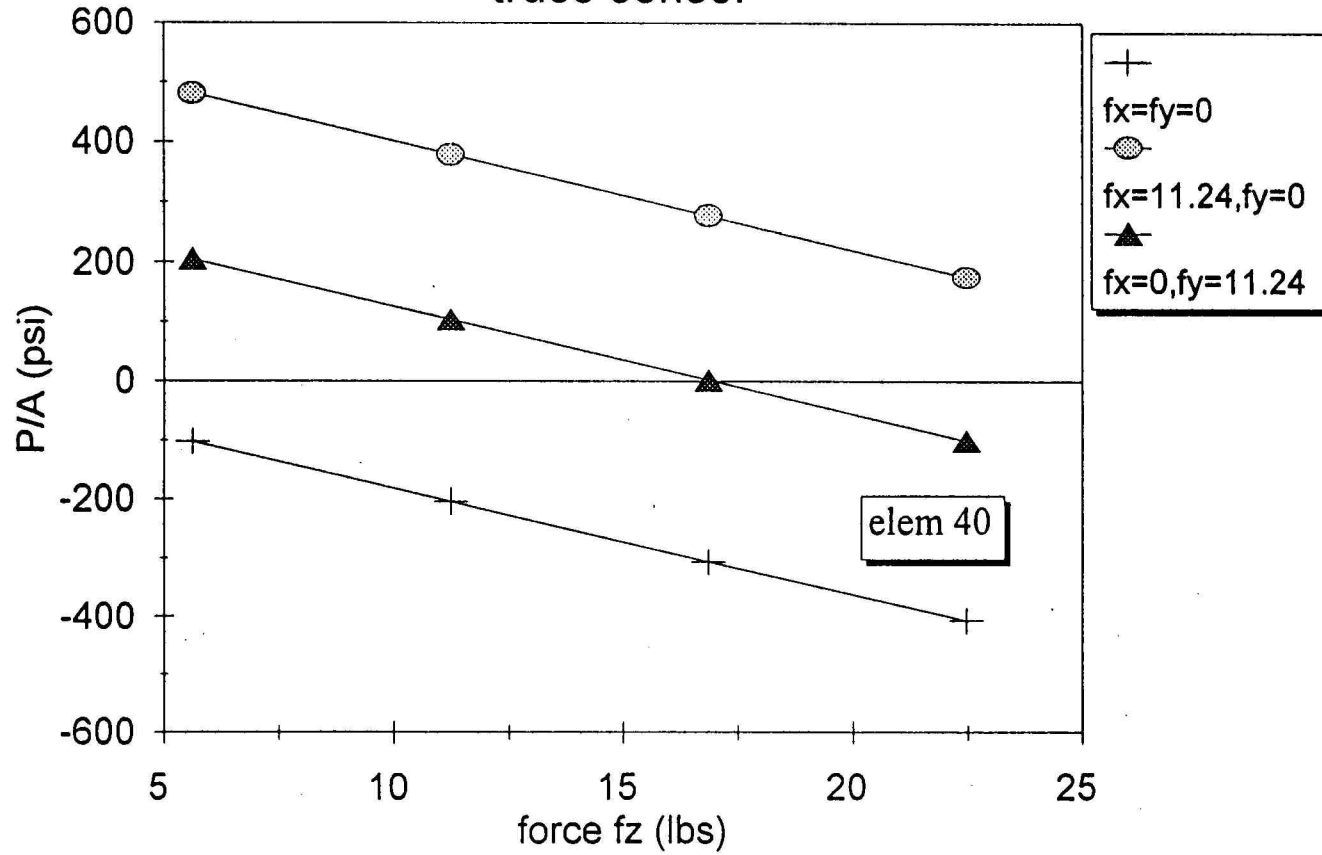


Figure 16c. Cross-linking curves varying force f_z (Truss, elem.40).

Stress - Force

truss sensor

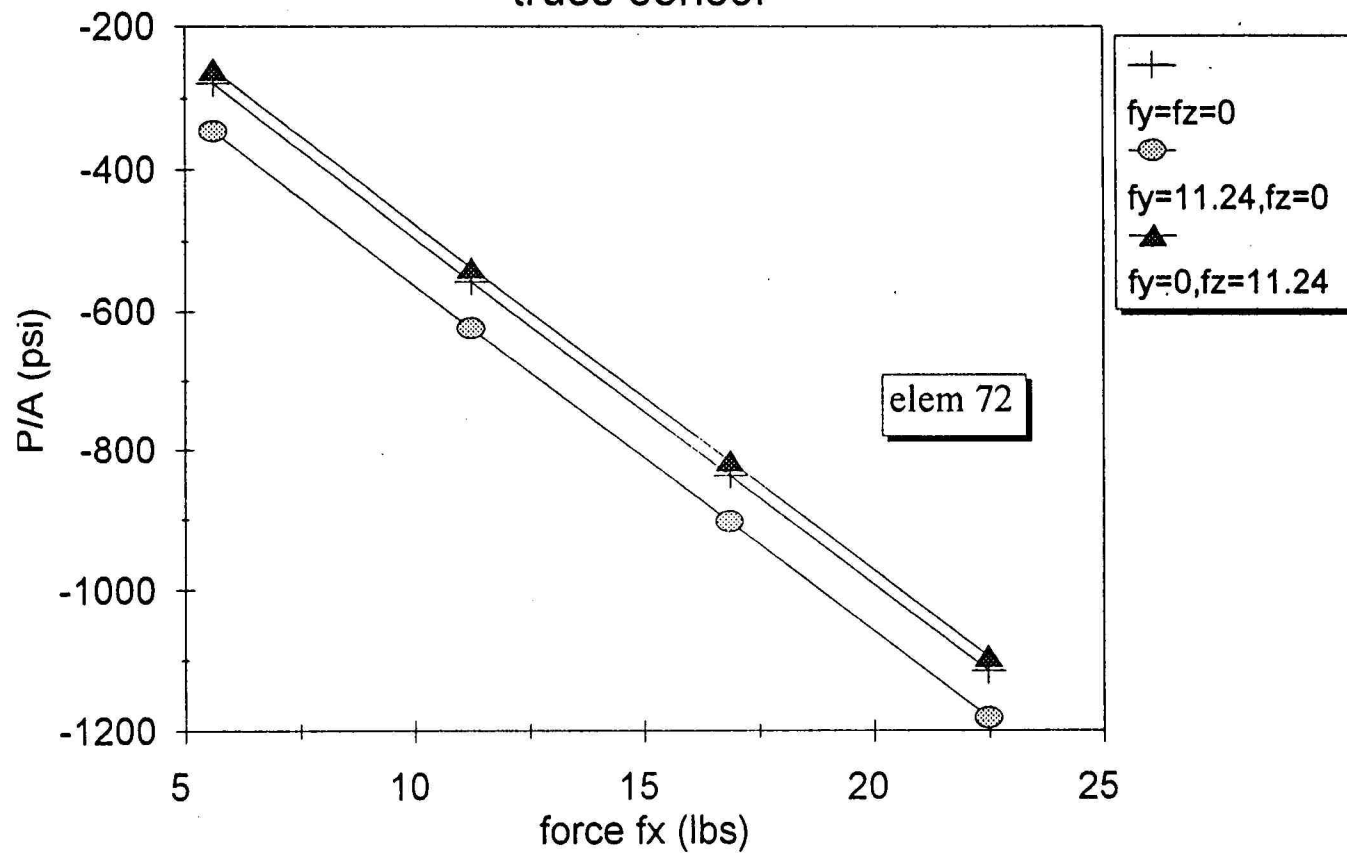


Figure 16d. Cross-linking curves varying force f_x (Truss, elem.72).

Stress - Force

truss sensor

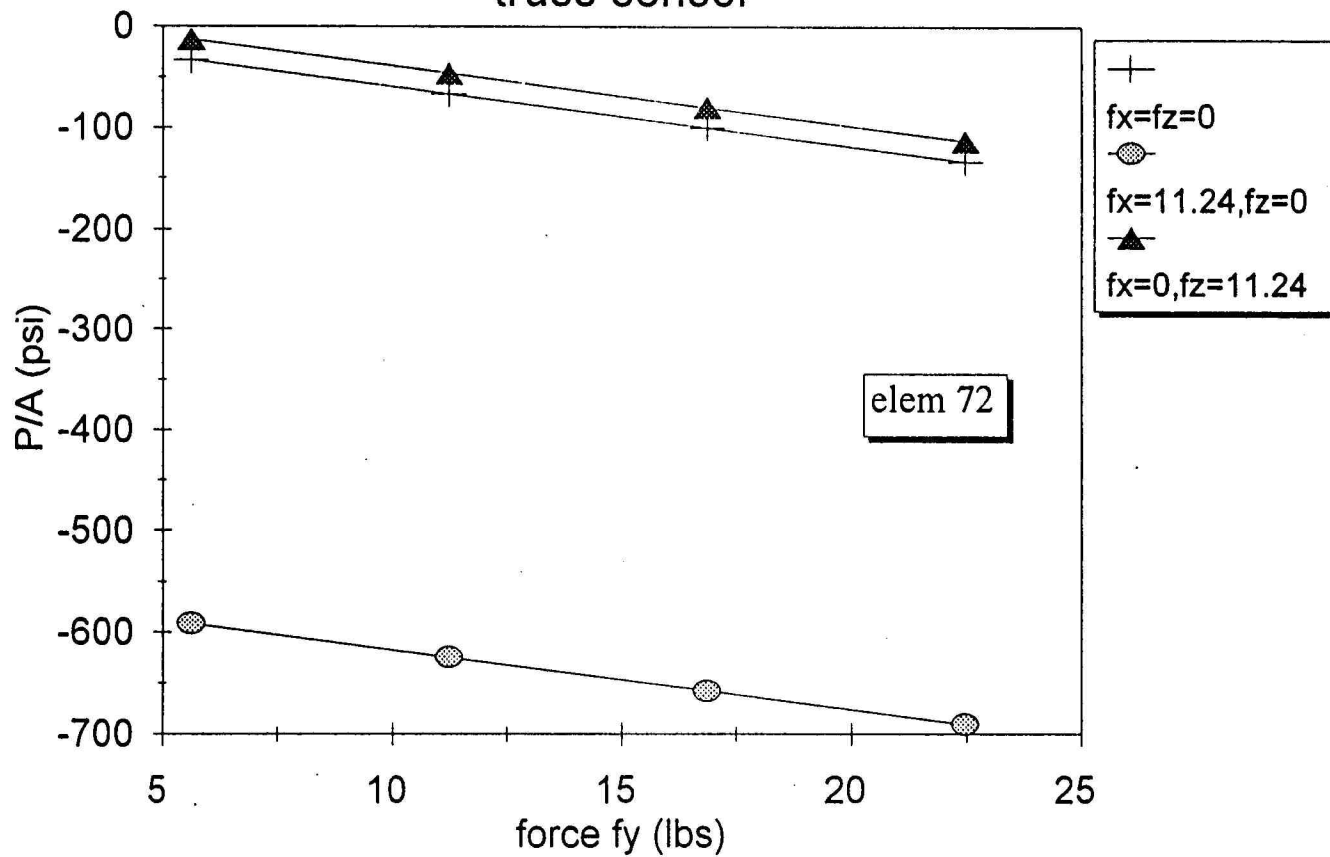


Figure 16e. Cross-linking curves varying force f_y (Truss, elem.72).

Stress - Force

truss sensor

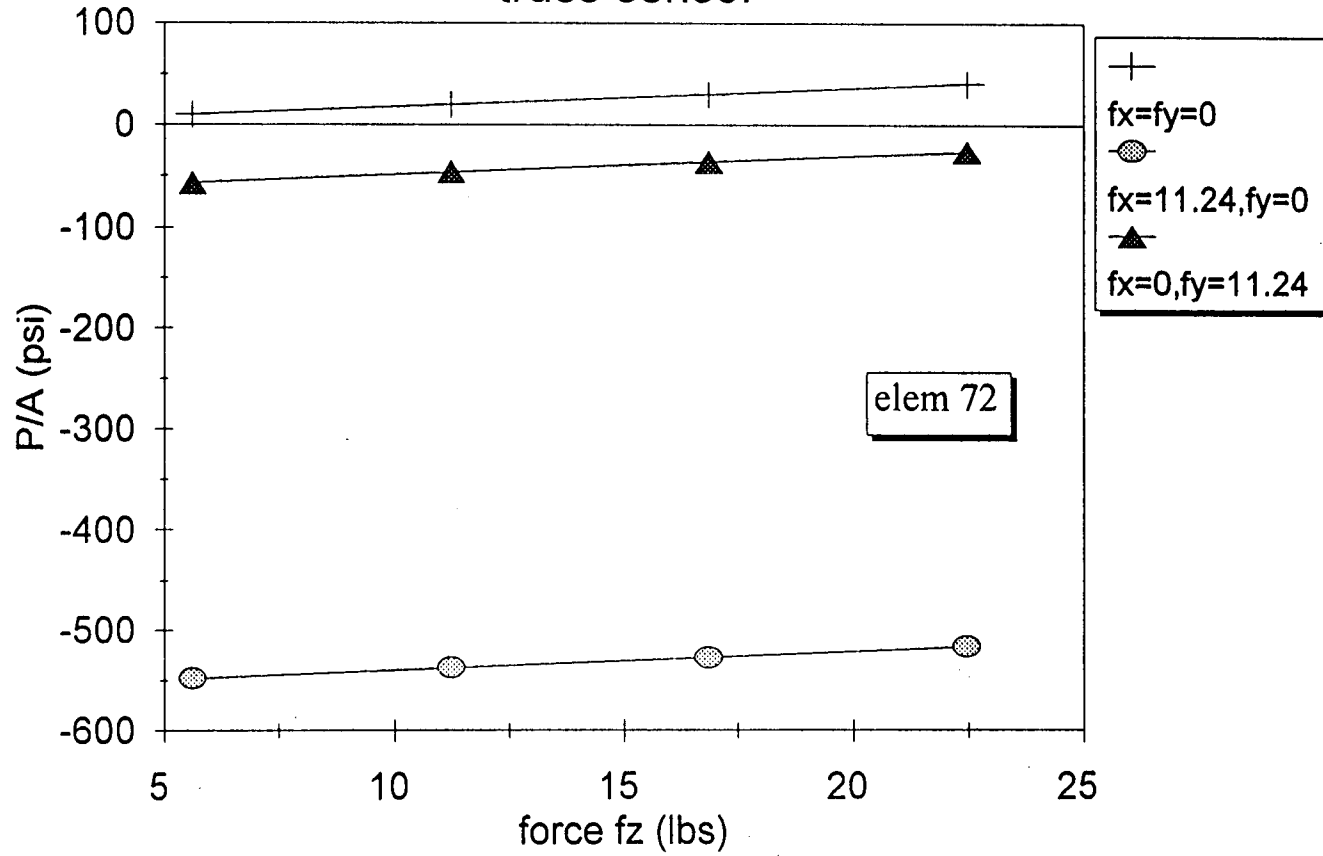


Figure 16f. Cross-linking curves varying force f_z (Truss, elem.72).

Stress - Force

truss sensor

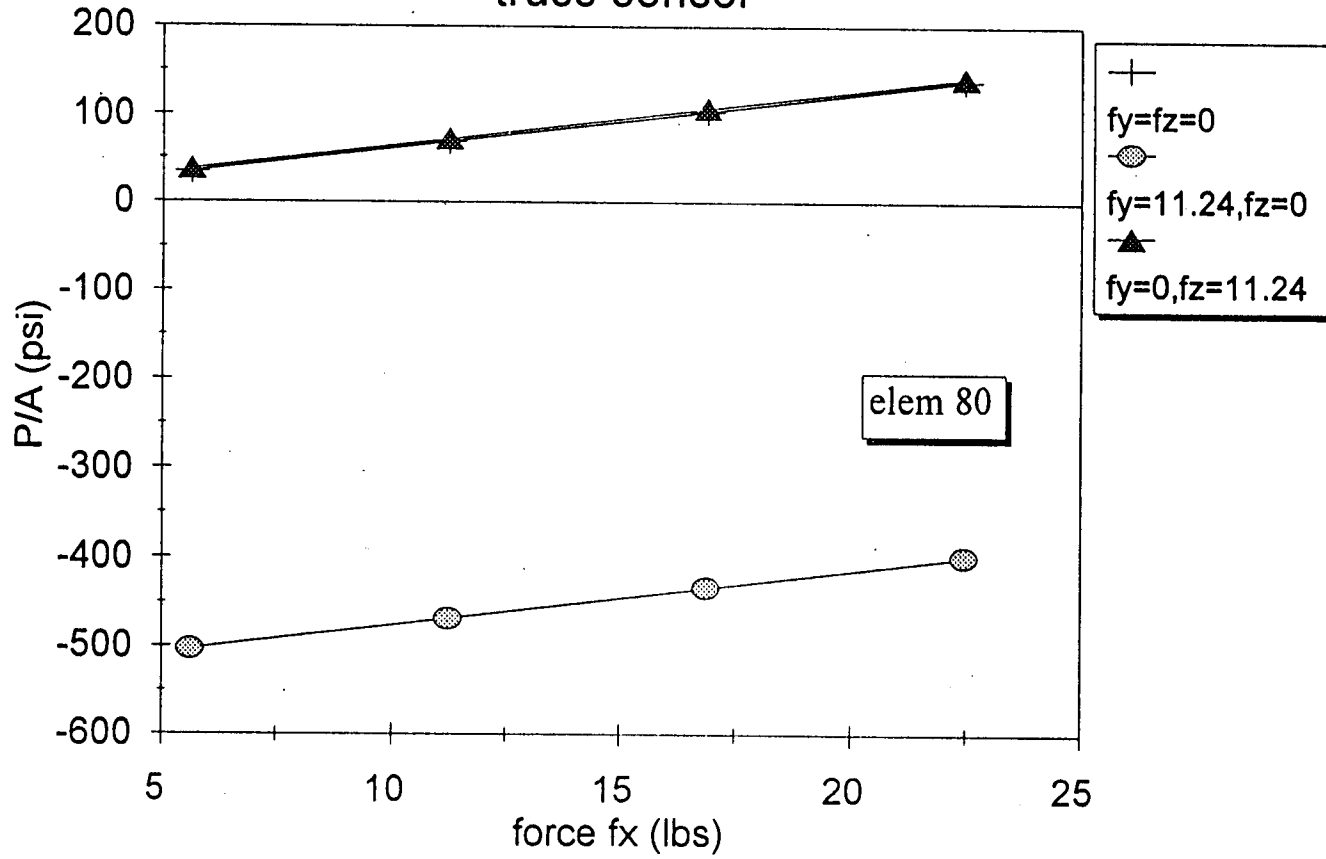


Figure 16g. Cross-linking curves varying force f_x (Truss, elem.80).

Stress - Force

truss sensor

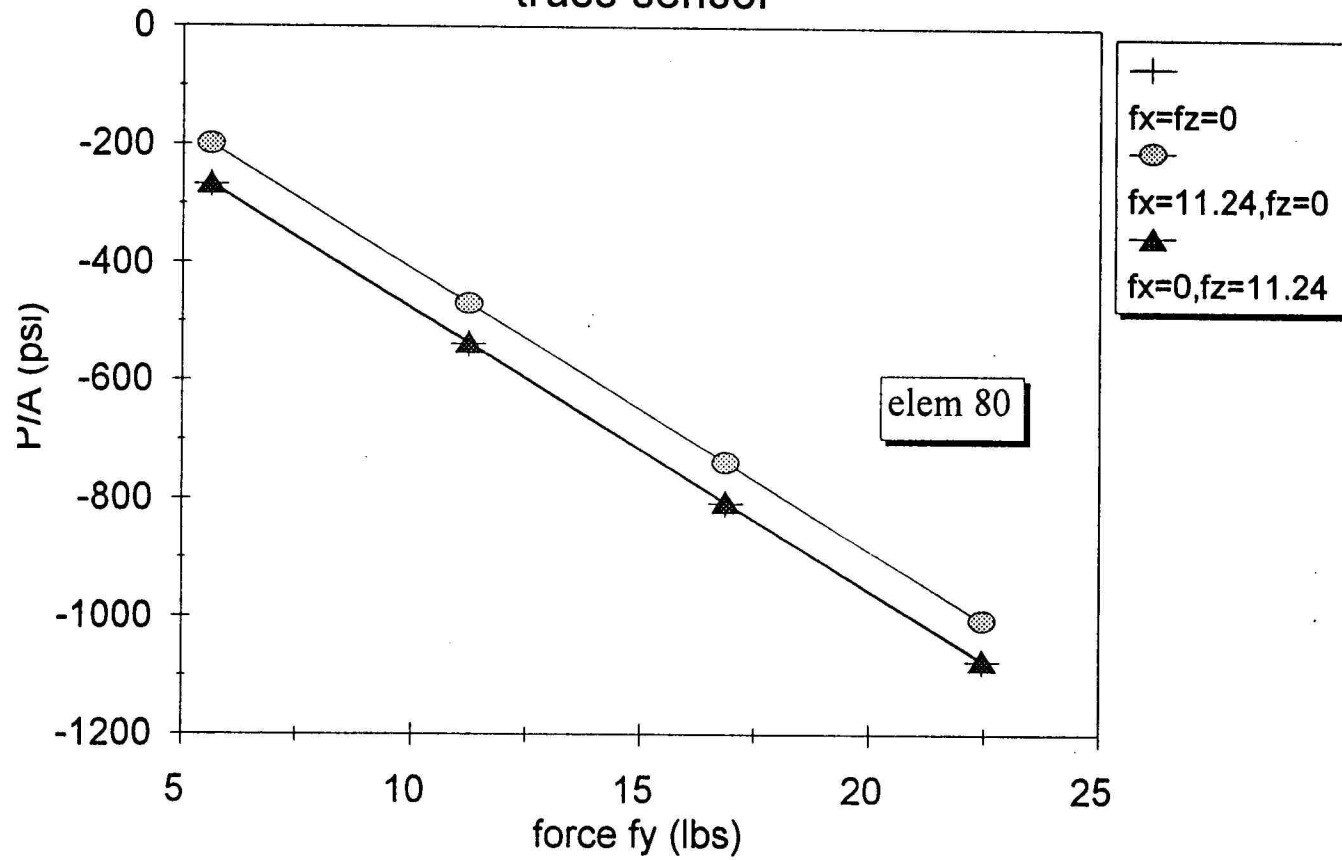


Figure 16h. Cross-linking curves varying force f_y (Truss, elem.80).

Stress - Force

truss sensor

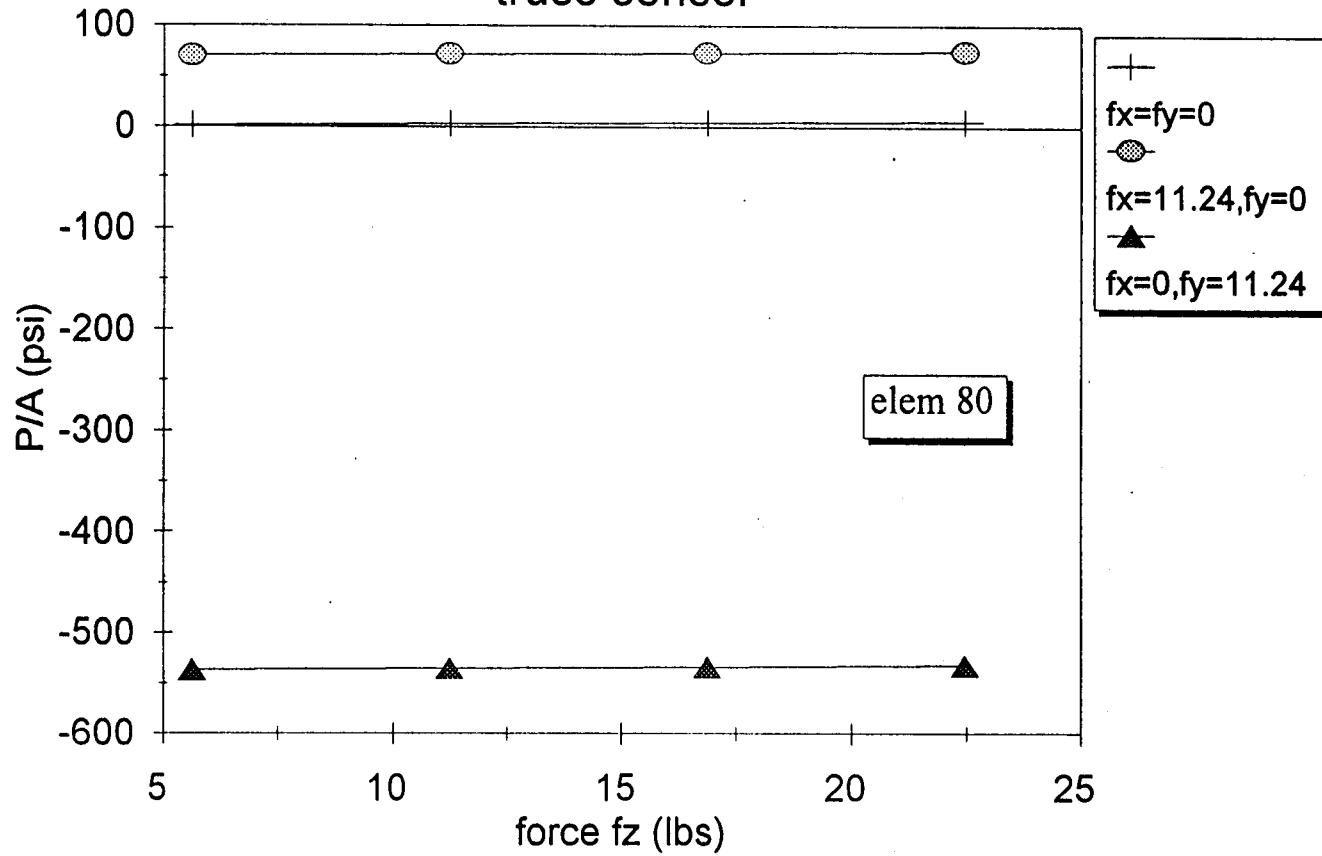


Figure 16i. Cross-linking curves varying force fz (Truss, elem.80).

After stress distribution and cross-coupling analyses were performed, the initial geometry was modified with the intention of reducing the mass of the sensor as much as possible and at the same time, improving both sensitivity and selectivity of the sensor without affecting its load capacity. This process was repeated until the behavior curves did not show a significant improvement. The resulting geometry is shown in appendix A.

The third step was the sensitivity analysis. This analysis reveals errors in the cancellation of the bending moment signal due to a linear or angular misplacement of strain gauges. To better understand this situation, refer to Fig.3. If we want to cancel the signal produced by a bending moment, two strain gauges (1 and 3) must be placed at the top and bottom faces of the rectangular beam at exactly the same distance from the fixed or the free end of the beam. Obviously this requirement is never going to be satisfied, so we must know how sensitive our beam is to a misalignment of the strain gauges, not only in the axial direction, but angularly as well.

The analysis was carried out by a computer program written in FORTRAN (appendix E) making the assumption that one of the gauges is placed exactly in the reference position and only one gauge is shifted from this reference position. The results are shown in Figs.(17a and 17b). These plots show the variation of the signal in percent versus absolute position. The linear analysis reference point in Fig.17a corresponds to a position at the midpoint of the diagonal elements.

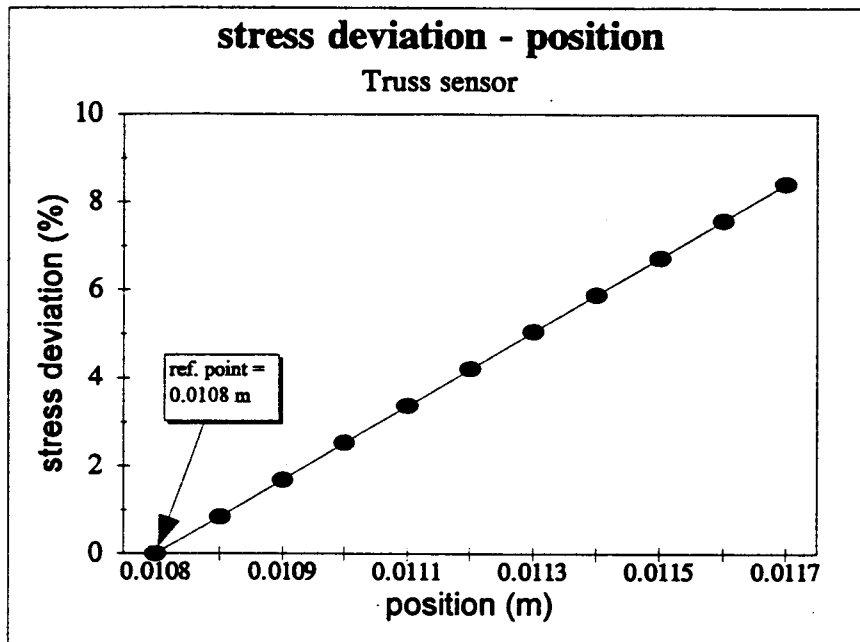


Figure 17a. Sensitivity analysis (Truss, linear displacement).

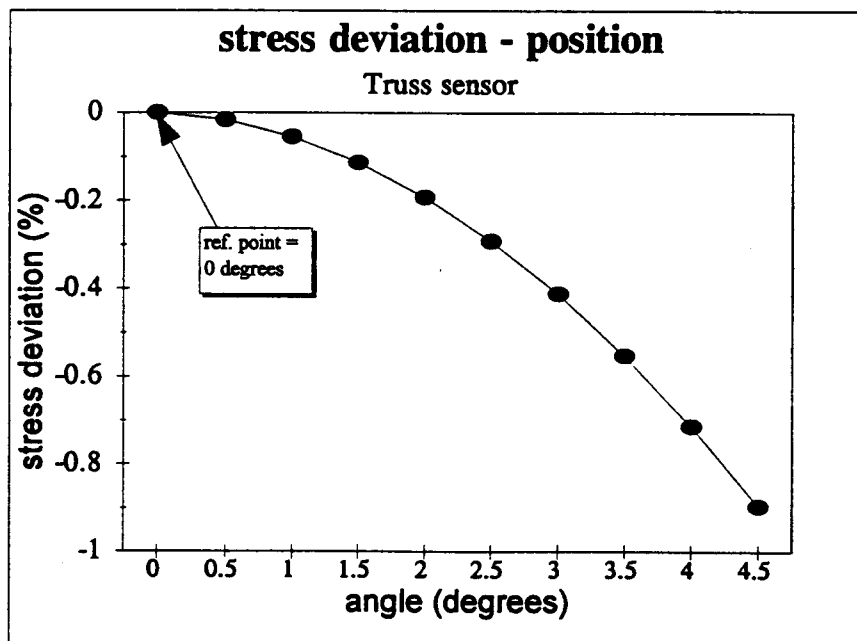


Figure 17b. Sensitivity analysis (Truss, angular displacement).

The angular analysis reference point in Fig.17b corresponds to the axis of the element. From these figures, it appears that a linear shift from the reference position has a greater influence than an angular misalignment.

At this point, the geometry of the sensor is well defined and now a more accurate model of the sensor was generated. This model is shown in Fig. 18. This model consists of 20-node solid finite elements for accuracy reasons. Using this model, the entire stress field can be easily analyzed; the results are shown in graphical display (Figs.19a-19f). By using solid elements in the model, it is possible not only to know the stresses in each coordinate direction, but the Von Mises stress (used for failure analysis) and the set of principal stresses as well. Is it possible to verify that we are dealing with plane or tridimensional stresses too. The disadvantage is that this model is not as easy to generate and the computational time is much greater than that of the first model. In addition, changes in geometry cannot be performed easily.

Figures 19a and 19b show the global coordinate stress field on the sensor when a force of 1 lb. is acting in the global x direction. However, the local or element coordinate systems of the diagonal beams do not coincide with the global coordinate system and, even more, each one of the diagonal elements is described in an individual coordinate system. The duality of the coordinate systems made it necessary to perform the finite element analysis both in global and in local coordinate systems. Consequently, the vertical beams were

Lin DEF Lc=3

TRUSS SENSOR

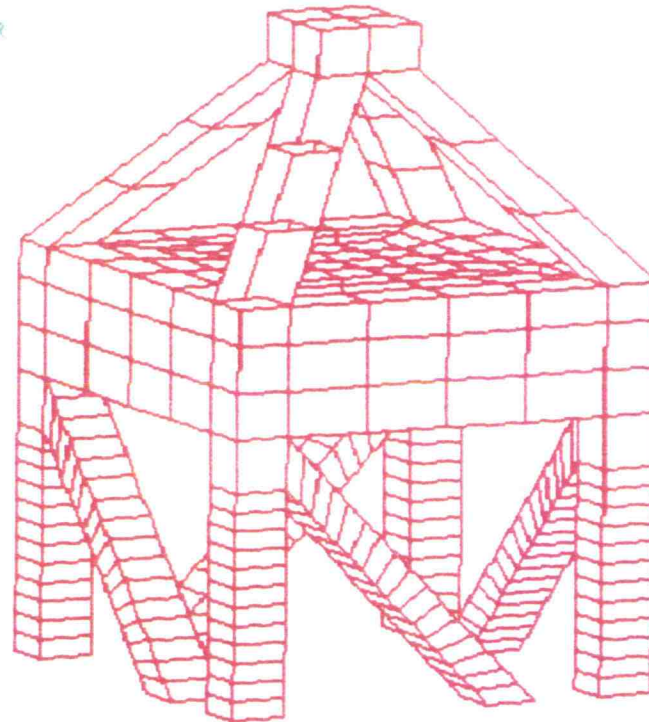


Figure 18. Truss sensor fem model using solid elements.

Lin STRESS Lc=1

TRUSS SENSOR
LOADED IN (+)X DIRECTION
FORCE = 1 LB

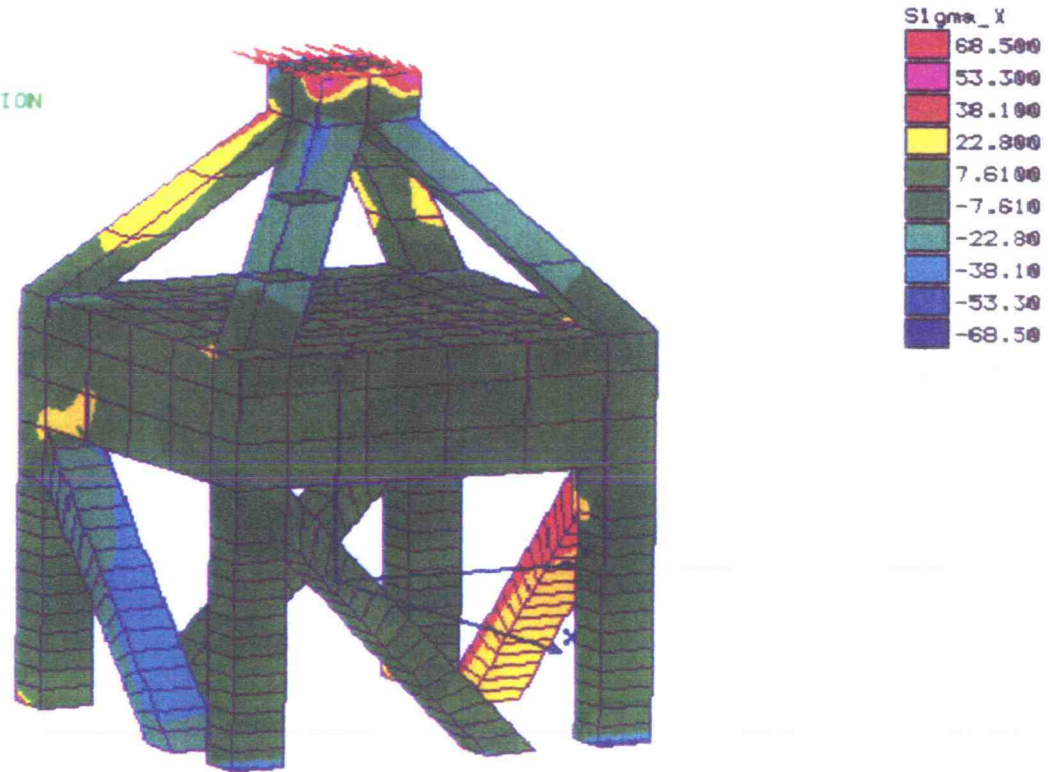


Figure 19a. σ_x stress field under a force f_x (Truss, global coords.).

L1n STRESS Lc=1

TRUSS SENSOR
LOADED IN (+)X DIRECTION

STRESSES IN LOCAL COORDINATES

FORCE = 1 LB

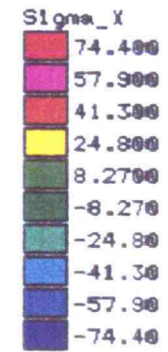
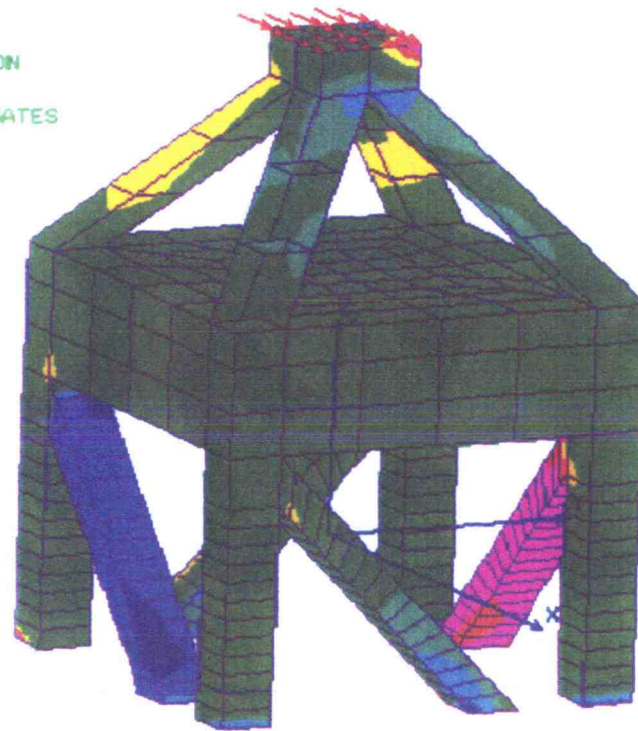


Figure 19b. σ_x stress field under a force f_x (Truss, local coords.).

L1n STRESS Lc=2

TRUSS SENSOR
LOADED IN (+)Y DIRECTION

FORCE = 1 LB

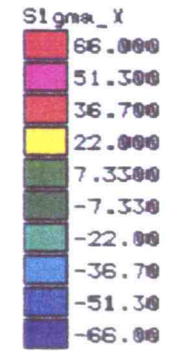
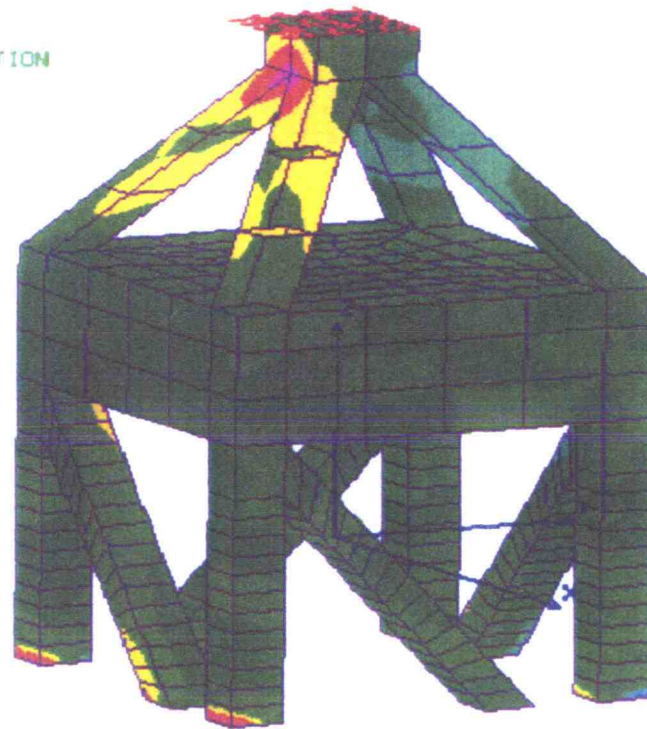


Figure 19c. σ_x stress field under a force f_y (Truss, global coords.).

Lin STRESS Lc=2

TRUSS SENSOR
LOADED IN (+)Y DIRECTION
STRESSES IN LOCAL COORDINATES
FORCE = 1 LB

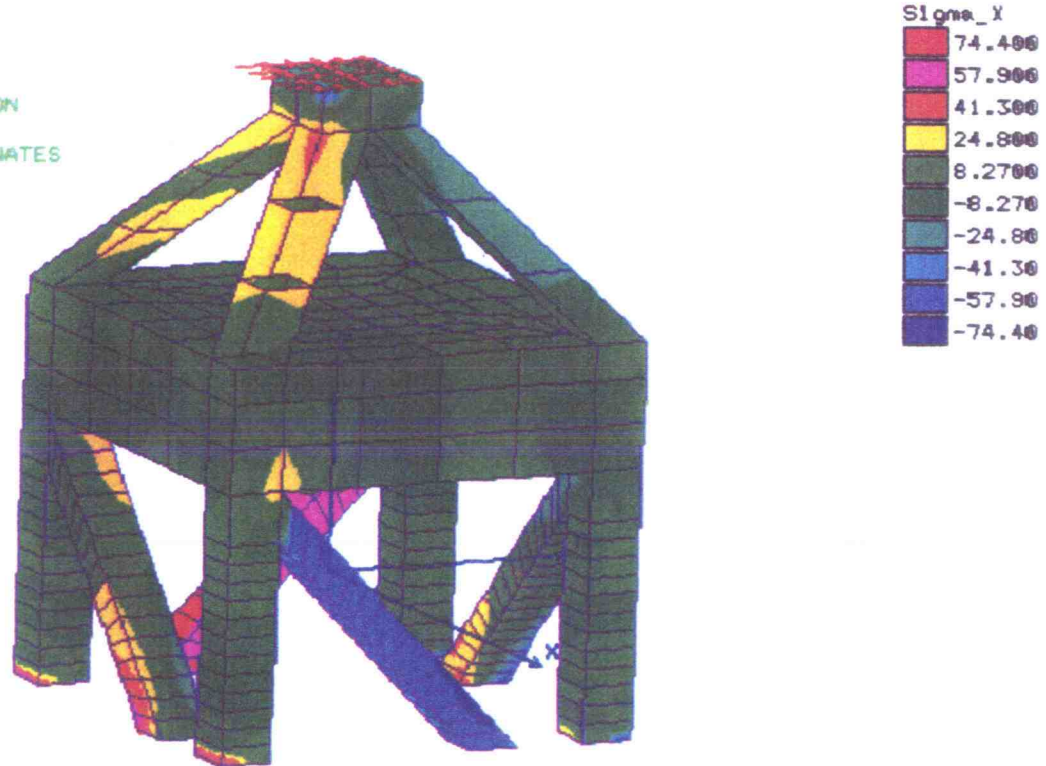


Figure 19d. σ_x stress field under a force f_y (Truss, local coords.).

L1n STRESS Lc=3

TRUSS SENSOR
LOADED IN (-) Z DIRECTION

FORCE = 1 LB

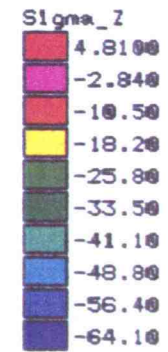
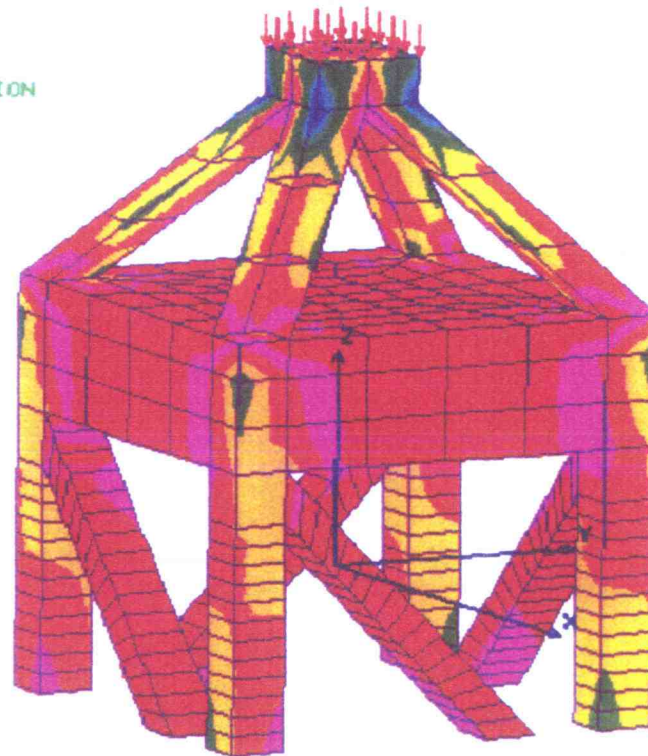


Figure 19e. σ_z stress field under a force f_z (Truss, global coords.).

L1n STRESS Lc=3

TRUSS SENSOR
LOADED IN (-) Z DIRECTION

STRESSES IN LOCAL COORDINATES

FORCE = 1 LB

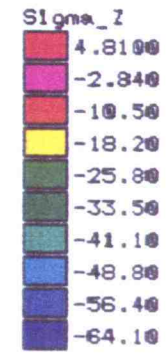
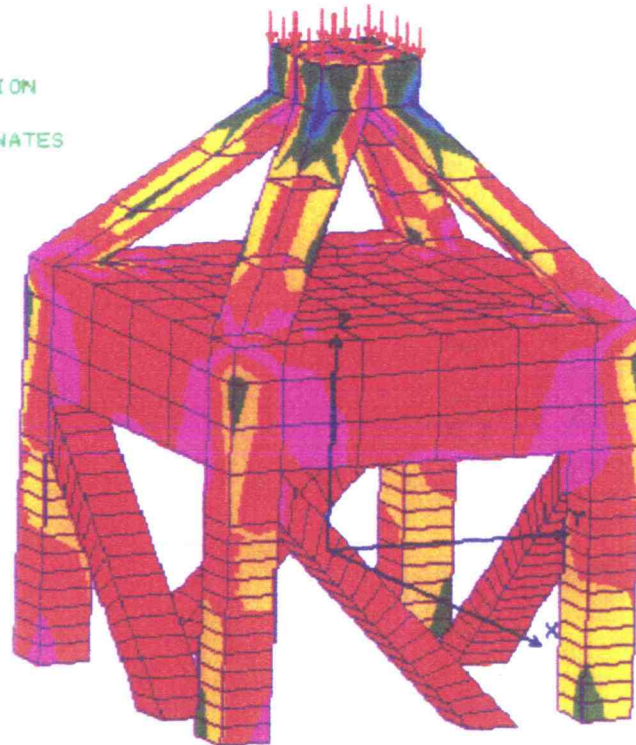


Figure 19f. σ_z stress field under a force f_z (Truss, local coords.).

analyzed using the global coordinate system while the diagonal beams were analyzed in the local coordinate system.

Finally, a cost estimation was obtained for the construction of a single sensor and the construction of a set of six sensors (one sensor for leg of the walking machine). This cost estimation was based on the fact that the sensor must be built from one single solid block of material. The most likely manufacturing process to be adopted is the electro discharge manufacturing (EDM) process because it can easily do the monolithic construction. Table 1 shows the estimated manufacturing time and cost (appendix G).

	TIME (HRS)	COST (DOLLARS)
ONE PART	28	728.00
SIX PARTS	114	2,964.00

Table 1. Time and cost estimates for the truss sensor.

5.3 Stewart Platform Transducer Analysis

The force requirements for the Stewart Platform are the same as the truss sensor and are as follows:

Forces: 67.44 lb (300 N) along the sensor's x , y , and z axis.

Moments: 88.5 lb in (10 N m) along the sensor's axis.

Mass: 0.044 lb (0.02 kg) without mounting plates.

Given these requirements, a finite model was generated. This model is shown in Figs.20 and 21. The model is composed of thick plates and 3D beam finite elements, and in this case, the lower platform is not modeled explicitly for reasons analogous to those explained for the truss sensor. In this model, the force is transmitted by means of the rigid triangular structure mounted at the top platform. Fig.20 shows the model from three different views in order to get a better understanding of the geometry. Fig.21 shows the model's constraints as well as the elements of interest which are located at the middle of each leg. The stress distribution analysis performed was exactly the same as the analysis performed for the truss sensor. The minimum required number of finite elements was found to be ten. The final dimensions are given in appendix A. Again, the best location to place the strain gauges was at the middle of each leg due to the uniformity of the stresses.

The second analysis was the cross-coupling of the signals. The analysis was performed using exactly the same sets of load conditions used for the truss sensor and the results are shown in Figs.22a-22f. As can be seen from these figures, the cross coupling is high, and there was no way found to reduce it, although this has no relevance when forming the compliance matrix.

For this sensor, a solid model was not necessary because the actual geometry is accurately represented by the model presented here, since the legs can be treated as beams (as well as the support) and the two platforms as

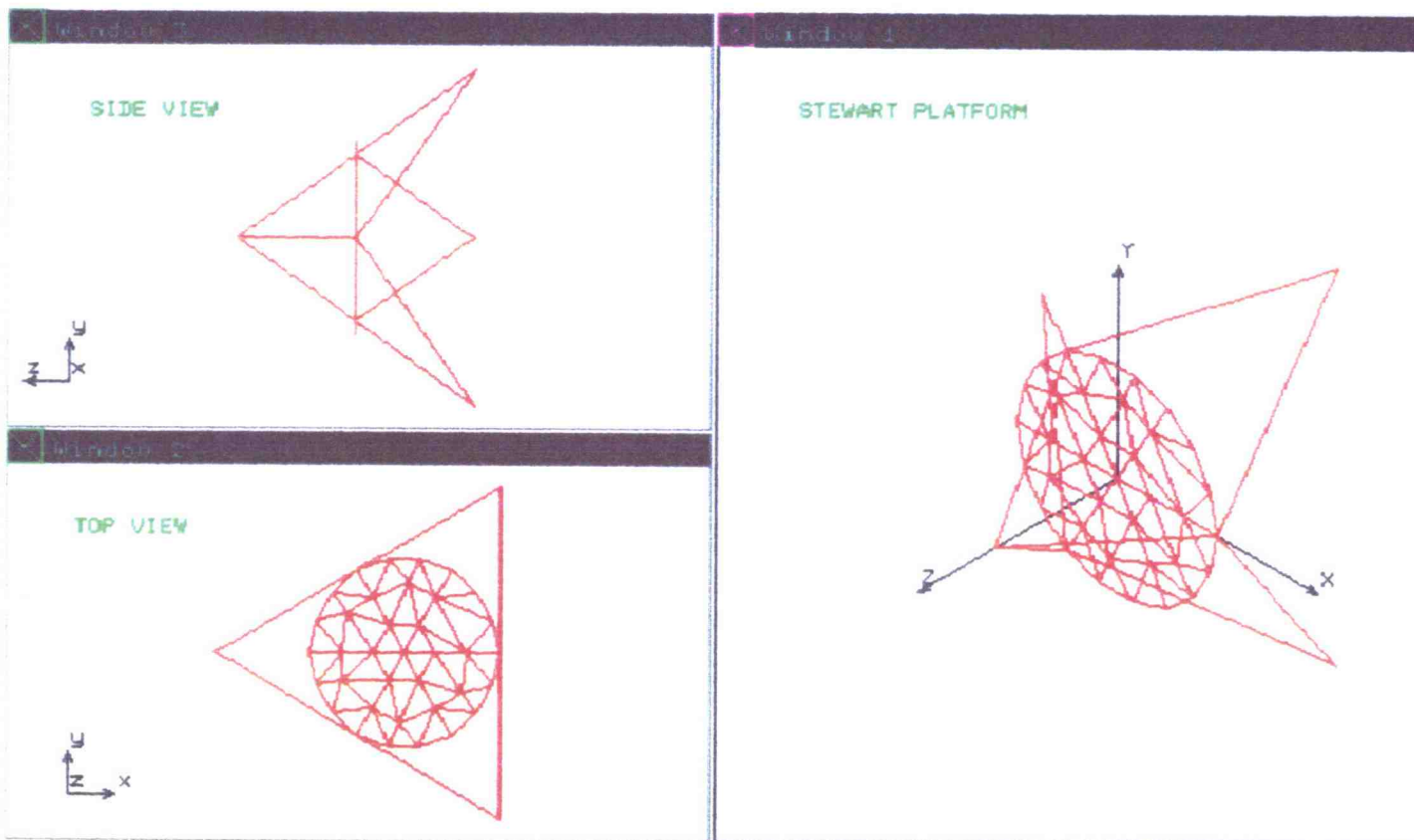


Figure 20. Stewart-Platform: top, side, and isometric views.

STEWART-PLATFORM
WIRE-FRAME MODEL

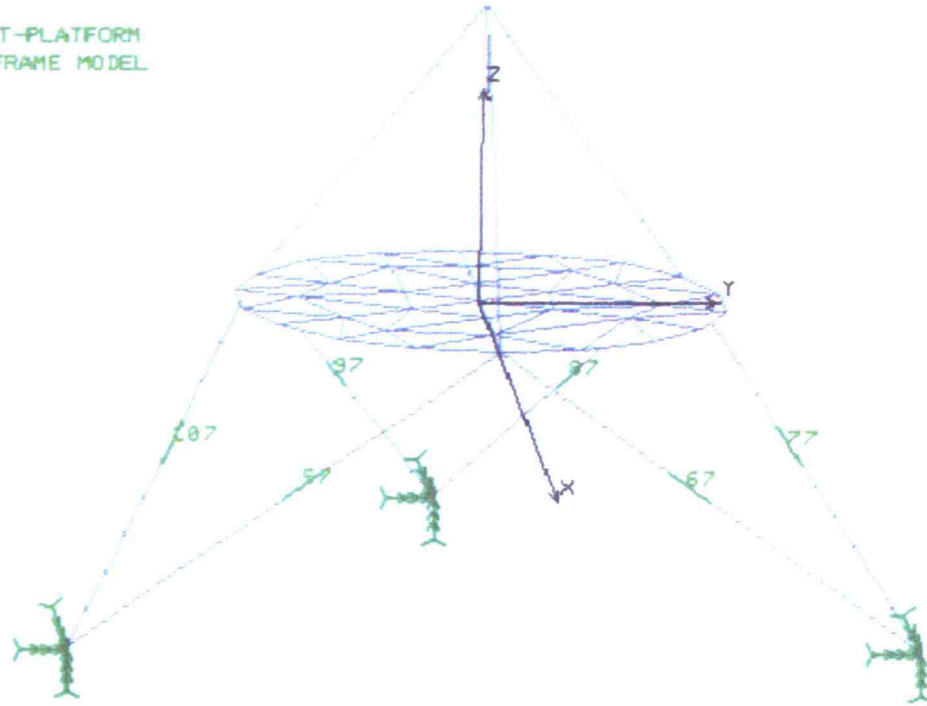


Figure 21. Stewart-Platform fem model showing elements of interest.

plates.

The third analysis was the sensitivity analysis, which again, was carried out by the same computer program written in FORTRAN (appendix E). The results are shown in Figs.23a and 23b. Like the truss sensor, the linear analysis reference point is the midpoint of each leg and the angular reference point corresponds to the axis of the leg. Also it can be seen that the strain measurement is much more sensitive to a linear displacement than to an angular deviation.

Finally, a cost estimation was obtained for the construction of one sensor and construction of six sensors. Monolithic construction of this sensor is extremely difficult to achieve, so this estimation was based considering the legs being glued to the plates. Table 2 shows the estimated manufacturing time and cost (see appendix G).

	TIME (HRS)	COST (DOLLARS)
ONE PART	28	728.00
SIX PARTS	114	2,964.00

Table 2. Time and cost estimates for the Stewart Platform.

Stress - Force

Stewart Platform

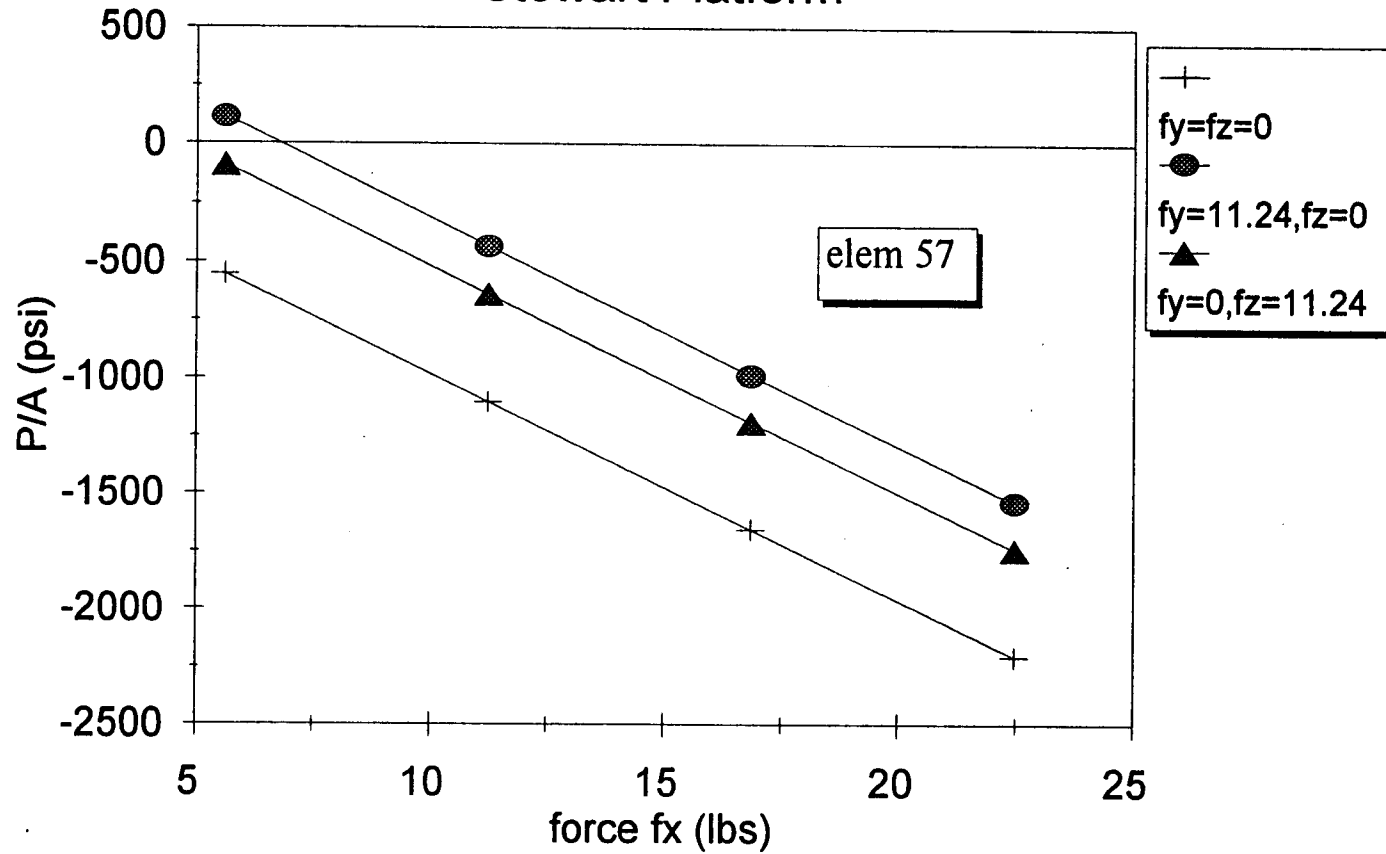


Figure 22a. Cross-linking curves varying force f_x (Stewart, elem.57).

Stress - Force

Stewart Platform

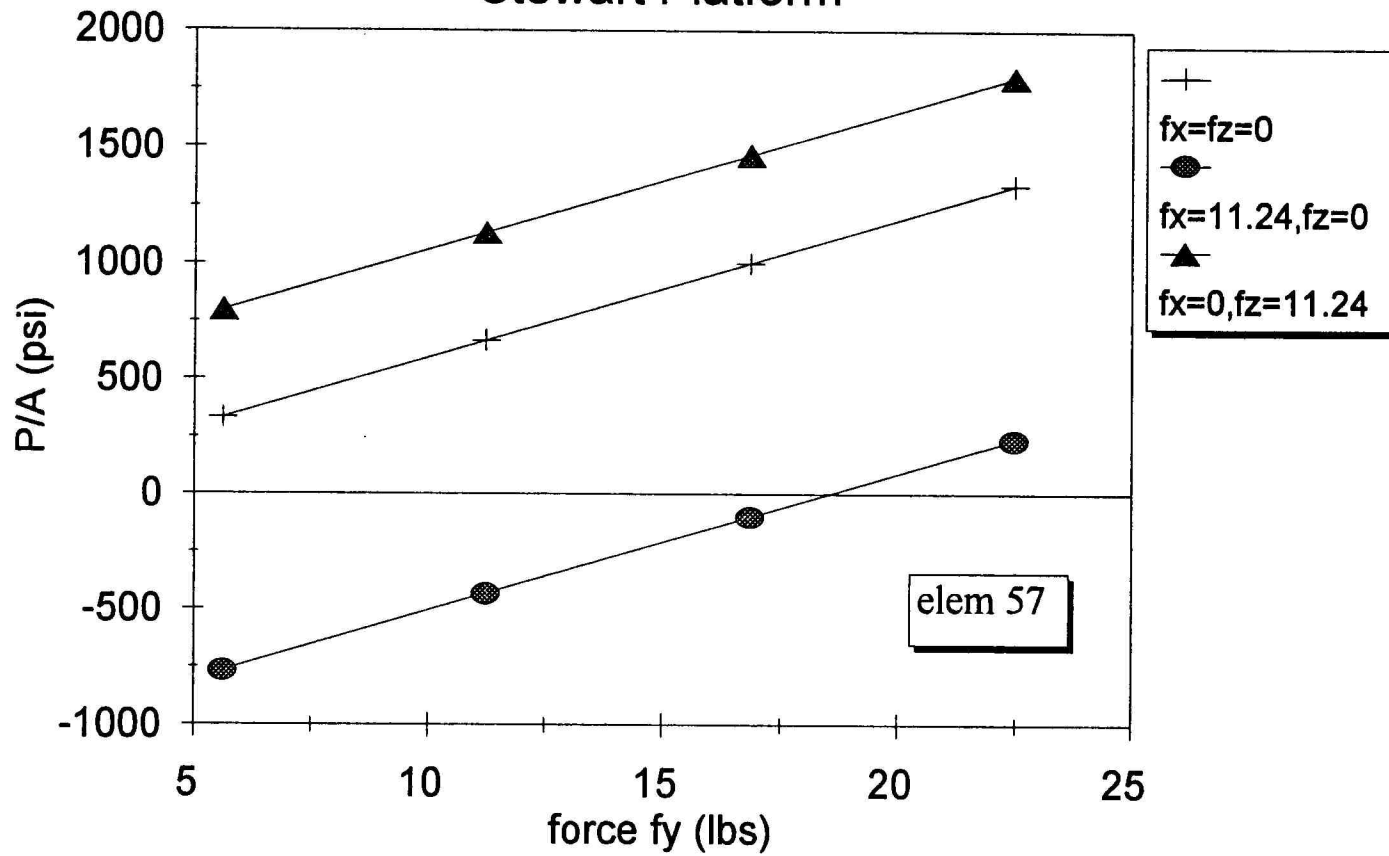


Figure 22b. Cross-linking curves varying force f_y (Stewart, elem.57).

Stress - Force

Stewart Platform

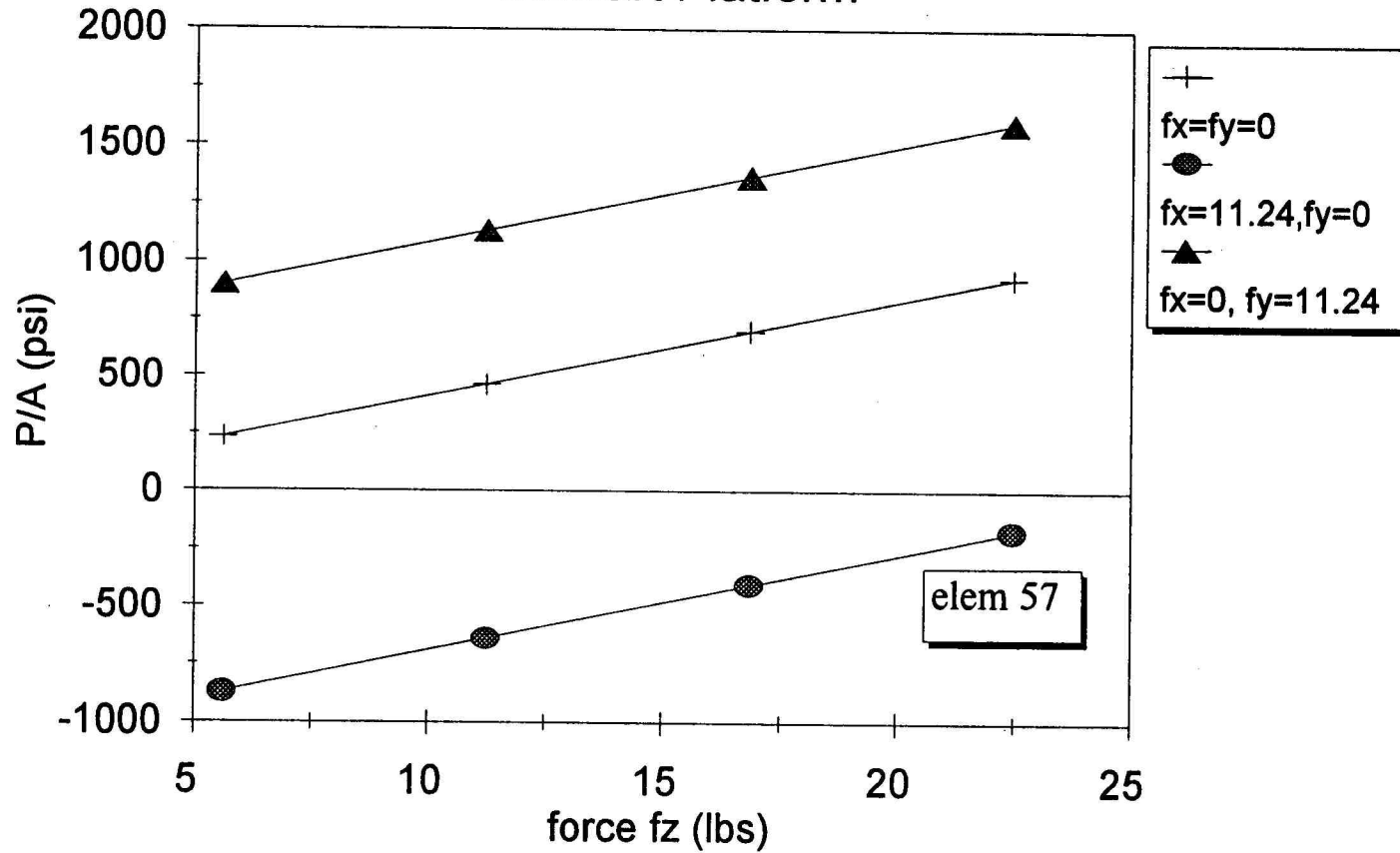


Figure 22c. Cross-linking curves varying force f_z (Stewart, elem.57).

Stress - Force

Stewart Platform

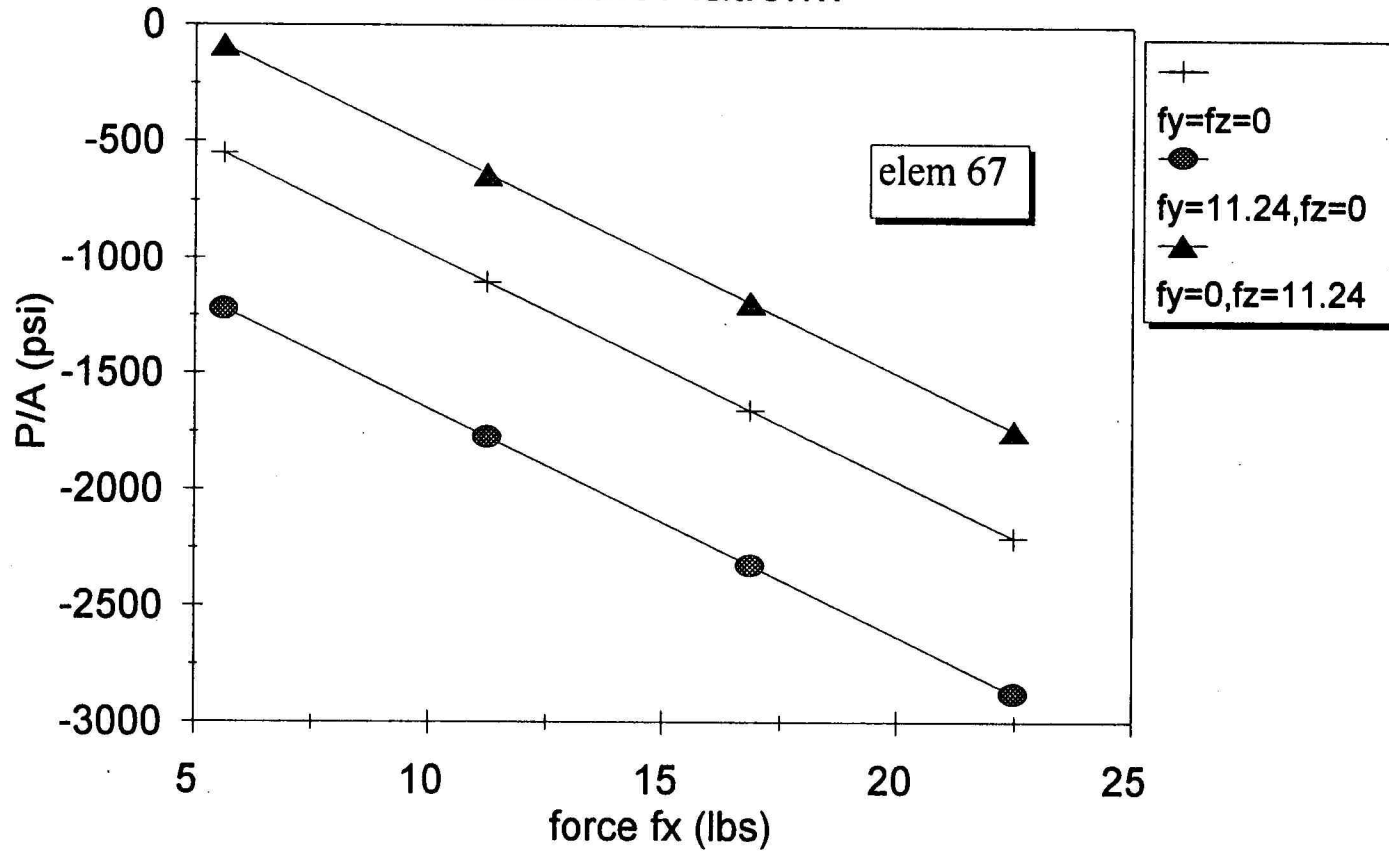


Figure 22d. Cross-linking curves varying force f_x (Stewart, elem.67).

Stress - Force

Stewart Platform

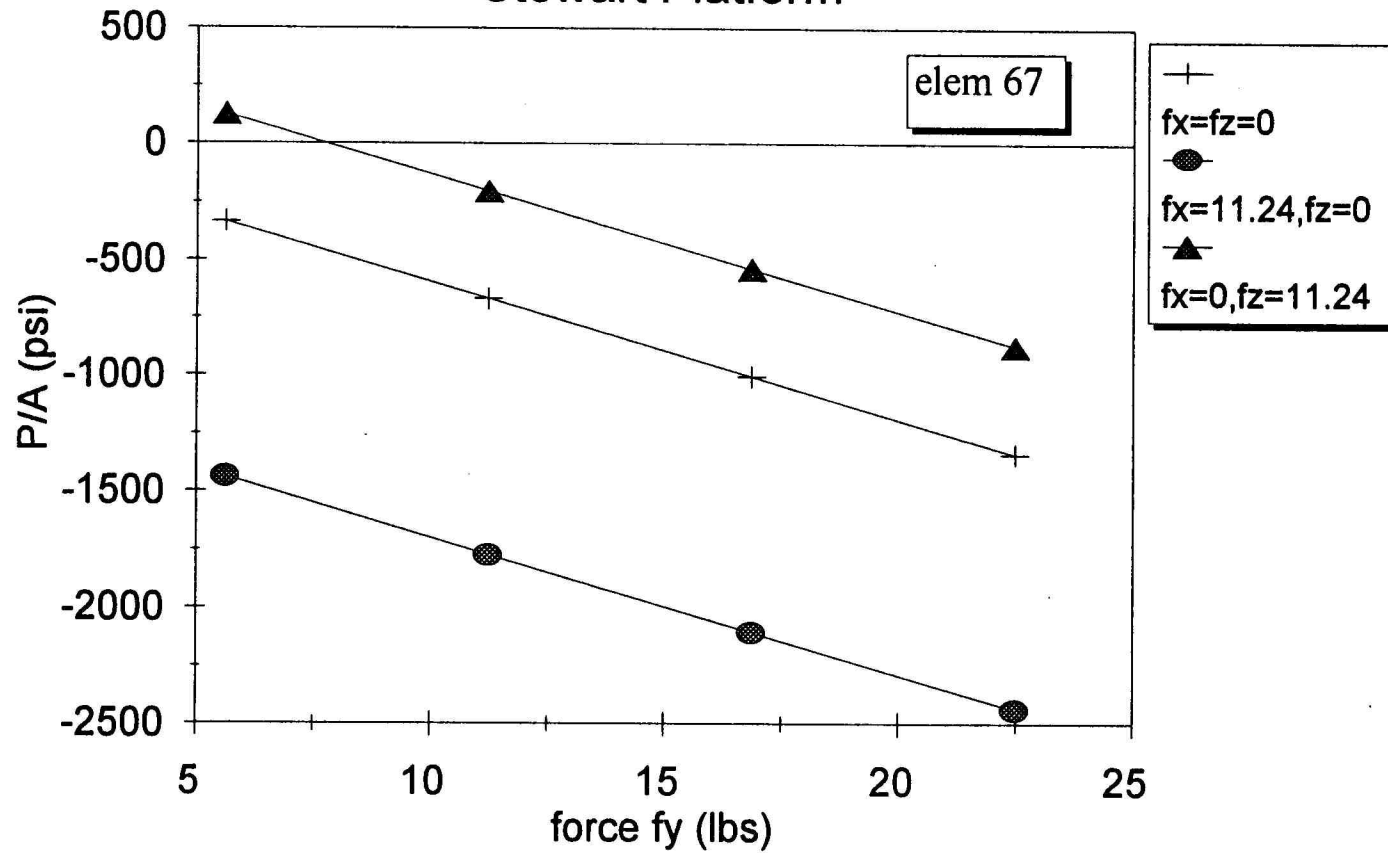


Figure 22e. Cross-linking curves varying force f_y (Stewart, elem.67).

Stress - Force

Stewart Platform

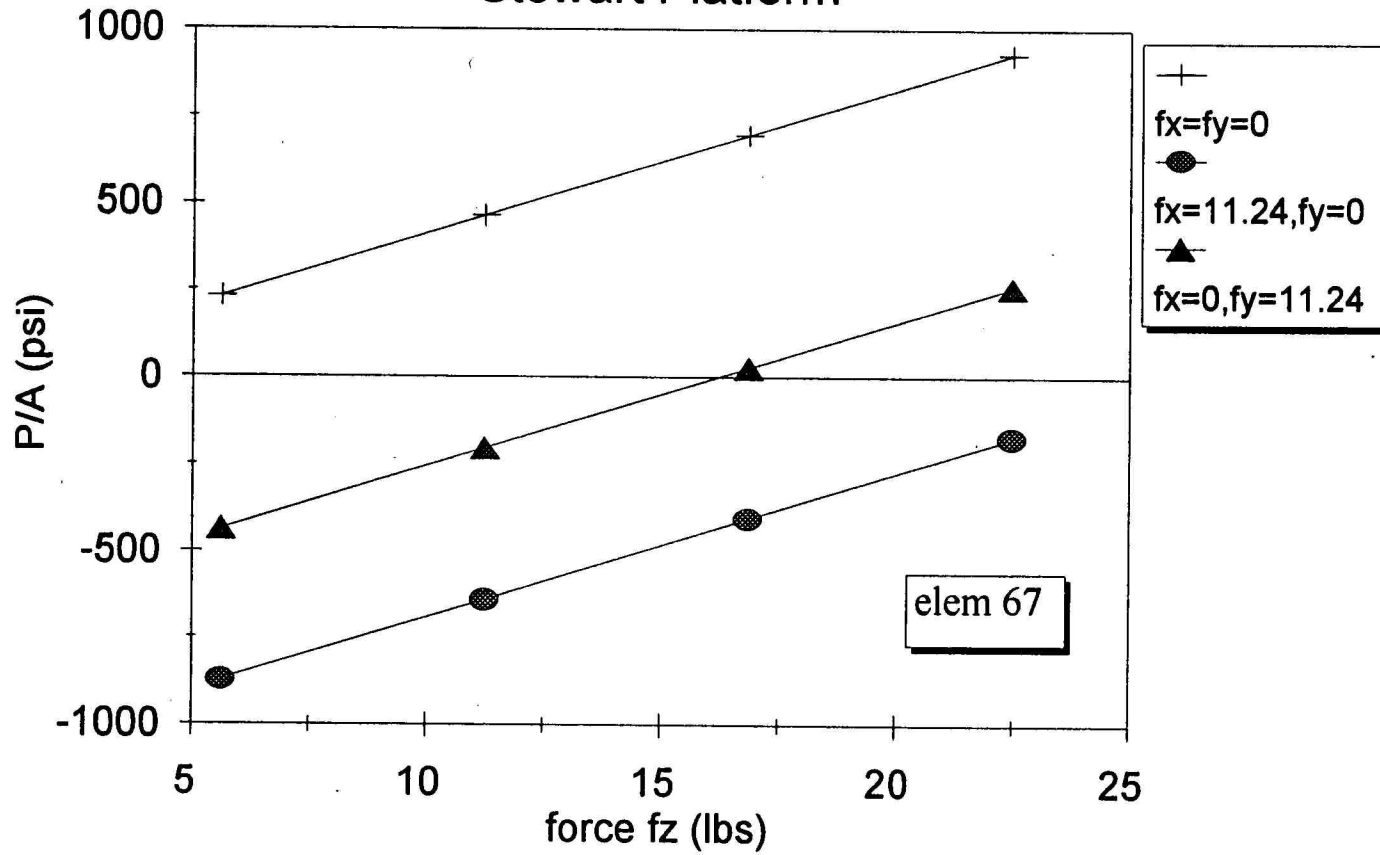


Figure 22f. Cross-linking curves varying force f_z (Stewart, elem.67).

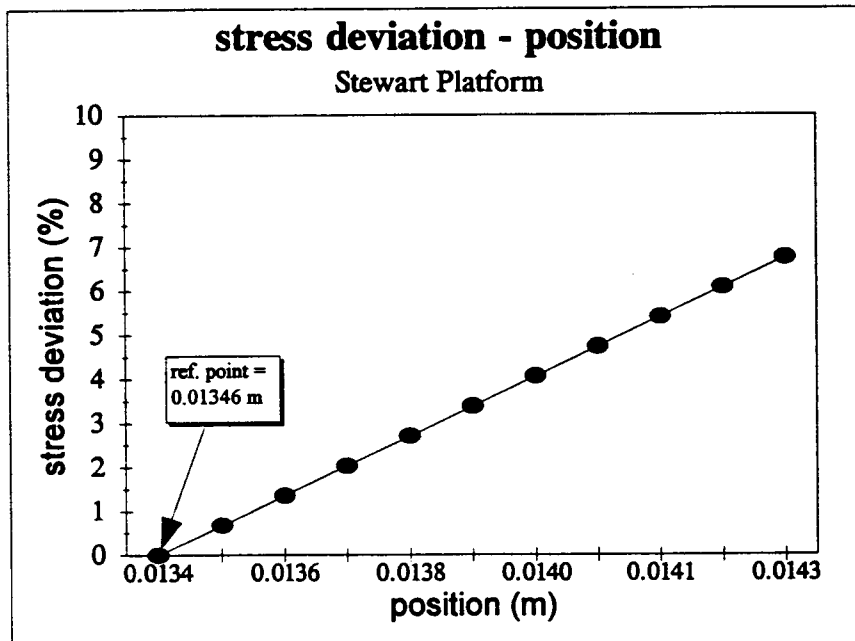


Figure 23a. Sensitivity analysis (Stewart, linear displacement).

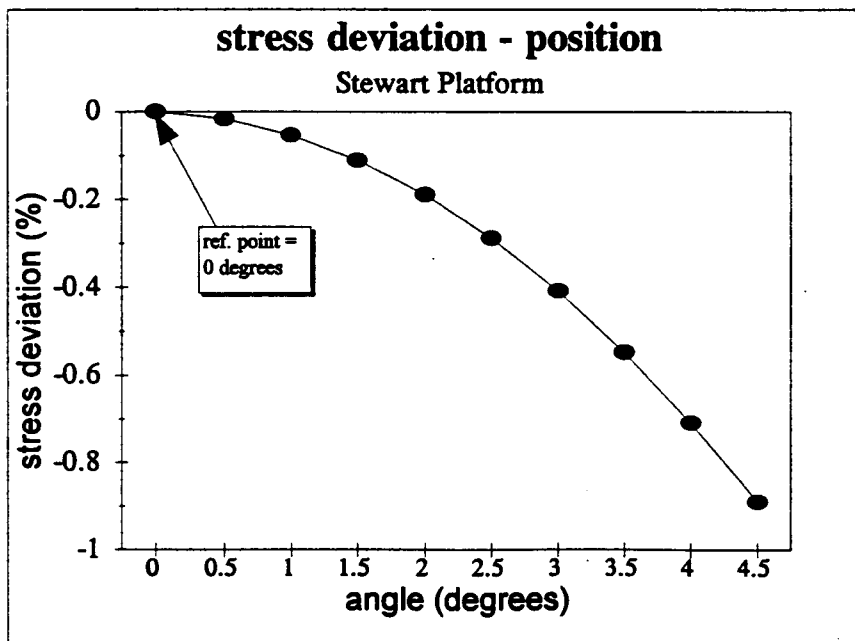


Figure 23b. Sensitivity analysis (Stewart, angular displacement).

5.4 Cross-Shape Structure Analysis

The force requirements for the cross sensor are the same as the truss sensor and the Stewart Platform and are as follows:

Forces: 67.44 lb (300 N) along the sensor's x , y , and z axis.

Moments: 88.5 lb in (10 N m) along the sensor's x , y , and z axis.

Mass: 0.044 lb (0.02 kg) without mounting plates.

With these requirements, the finite element model (Fig.24) was generated. This figure represents one third of the whole sensor (Fig.12) since symmetry of the structure allows analysis of this part to yield the analysis for the complete sensor (see section 4.3), provided that the two parts shown in Fig.13 be rigidly attached. The figure presents the model from three different views for a better understanding of the geometry.

In this case, due to the geometry of the element, the model was generated using solid elements directly. It was found that using 20 nodes did not make any significant improvement over use of 8 nodes and use of 20 nodes increases the computation time by a factor of four. Hence, 8 nodes were used throughout the analysis.

Similar to the other two sensors, the first analysis was to check the stress distribution under the maximum load for possible yielding of the structure and to study strain magnitudes in order to find the best placement of strain gauges.

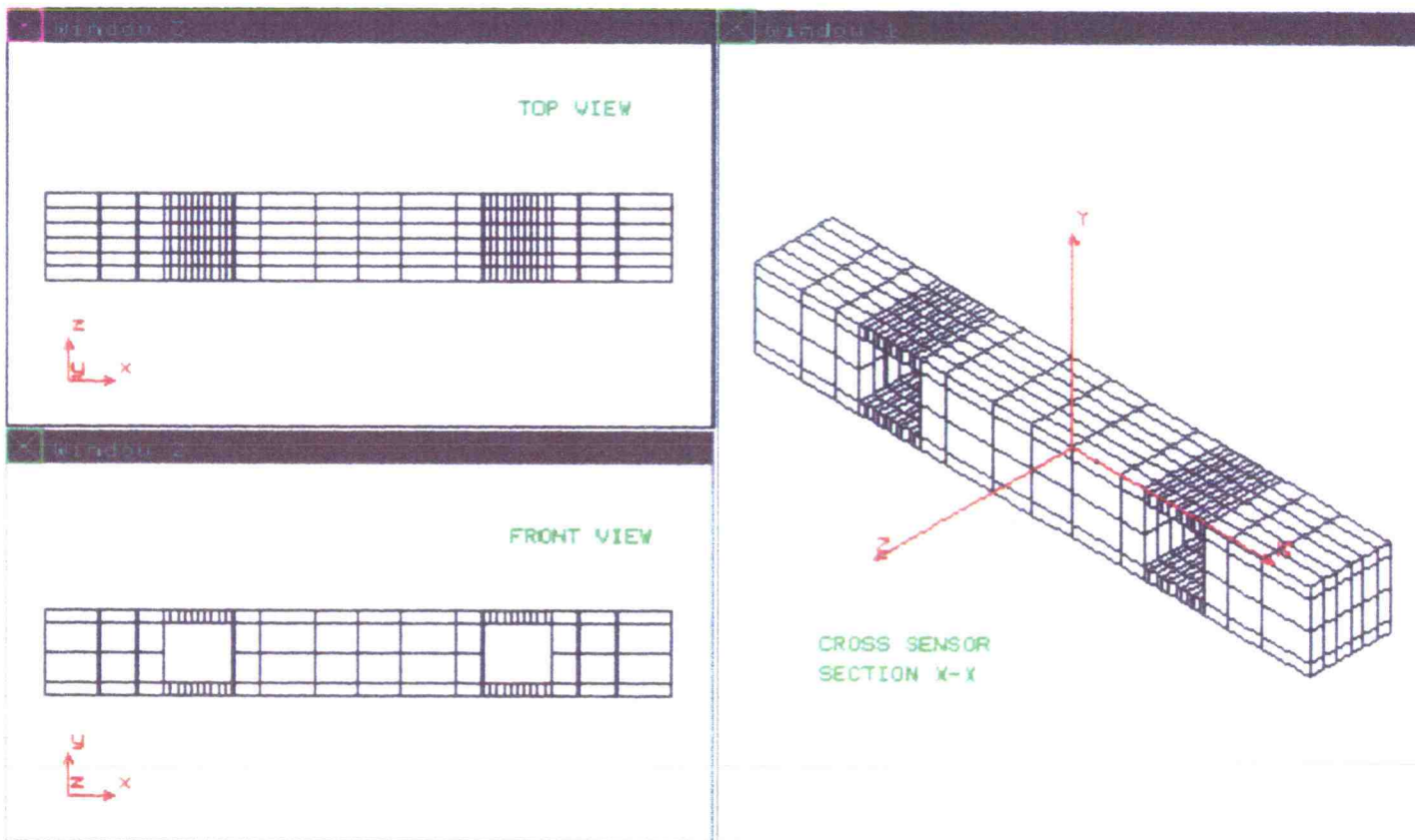


Figure 24. Cross-Structure section: top, front, and isometric views.

In this model, forces are applied at the center of the element in the form of distributed pressure over an area equal to the cross-sectional area of the bar and the ends are fully constrained as shown in Fig.25.

After the first analysis was completed, the geometry was dimensioned (see appendix A) and it was found that the best location for the strain gauges was 1 mm from the base of the parallel plates structure and either the center block or the end block. For convenience, the base of the parallel plates with the end block was selected. Next, cross-linking analysis was performed and the most important results are shown in Figs.26a-26f. The close-up of the area of interest was necessary in order to get a detailed image. Analyzing Figs.26a-26c, it is observed that this section of the sensor is almost insensitive to forces in the x and z directions, but very sensitive to the force in the y direction. In addition, the analysis of Figs.26d-26f, shows that this section is almost insensitive to moments in the x and y directions, but is very sensitive to the moments in the z direction.

Finally, sensitivity analysis was performed using the same FORTRAN program (appendix E) and results are shown in Figs.27a and 27b. Although the parallel plate structure is not very sensitive to angular misalignments, it was found to be very sensitive to linear misalignments (Fig.27a).

As the last step in the analysis, the manufacturing time and cost were estimated for one sensor and for a set of six sensors. Similar to the Stewart

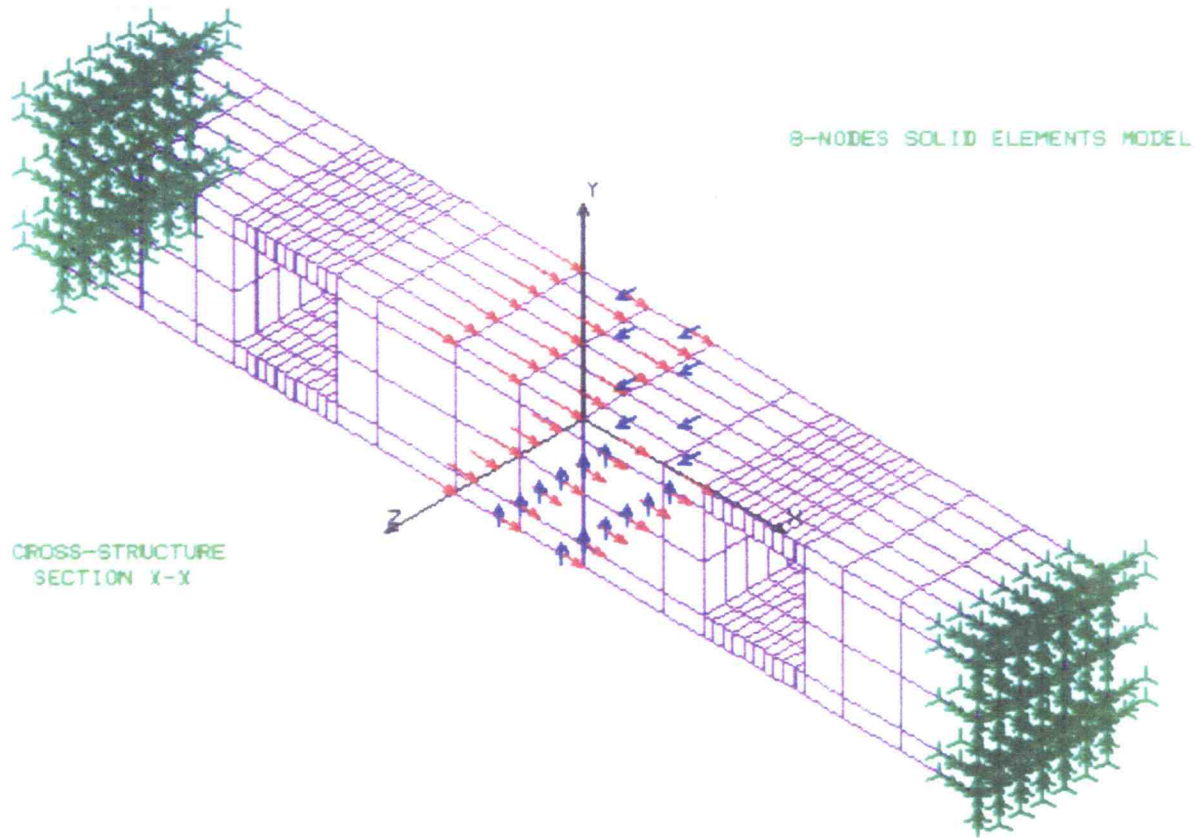


Figure 25. Cross-Structure section with constraints and applied forces.

LIn STRESS Lc=1

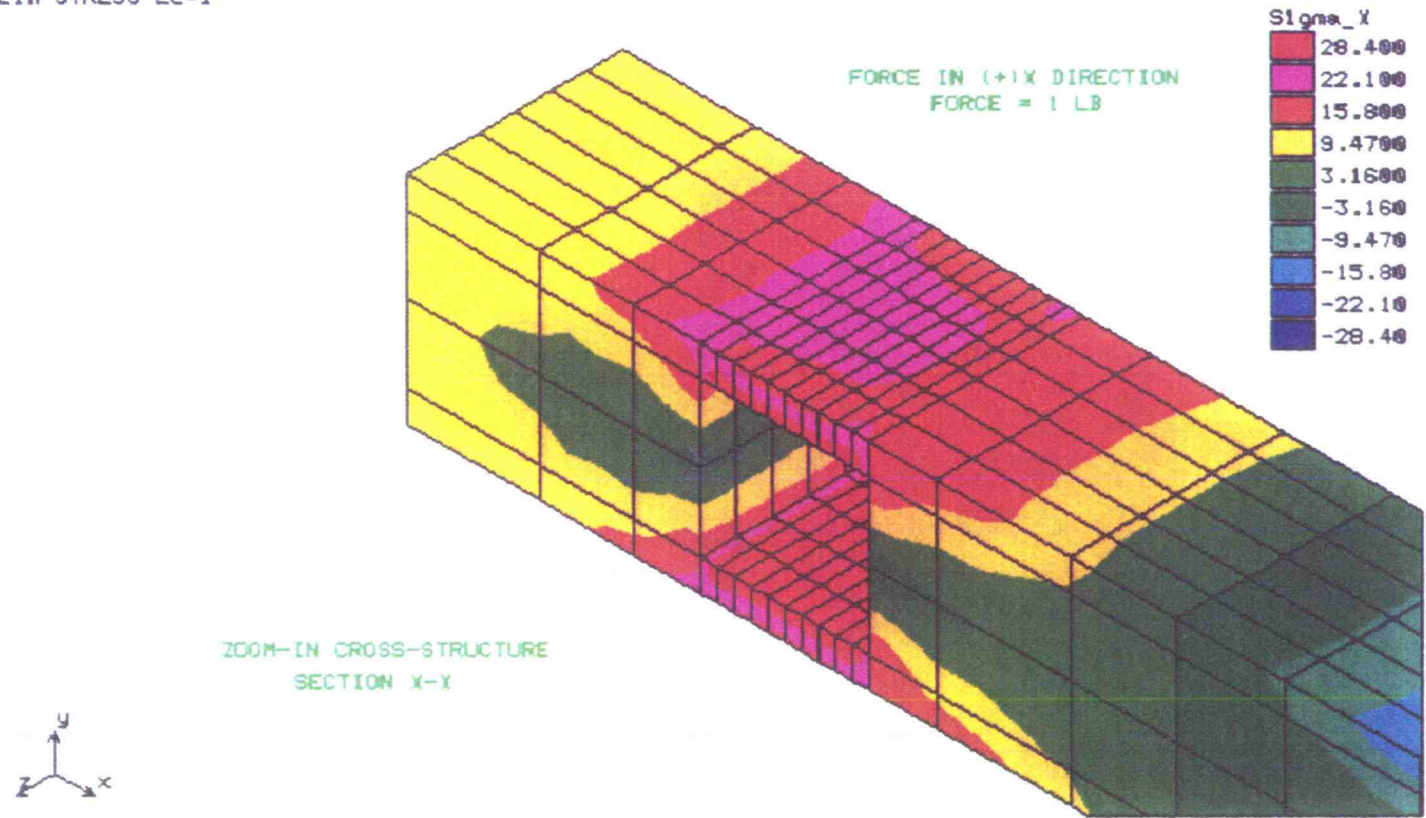


Figure 26a. σ_x stress field under a force f_x (Cross).

L1n STRESS Lc=2

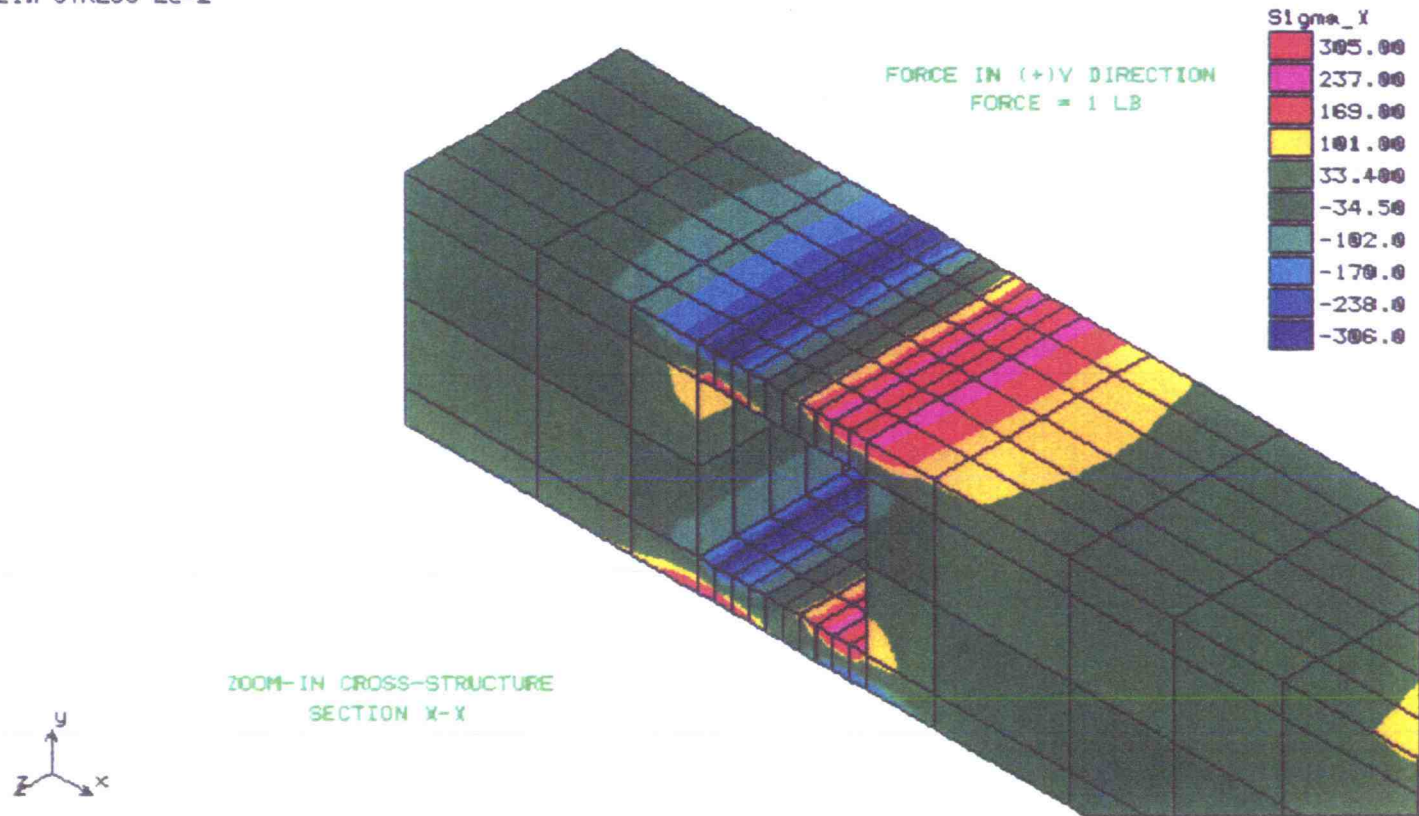


Figure 26b. σ_x stress field under a force f_y (Cross).

L1n STRESS Lc=3

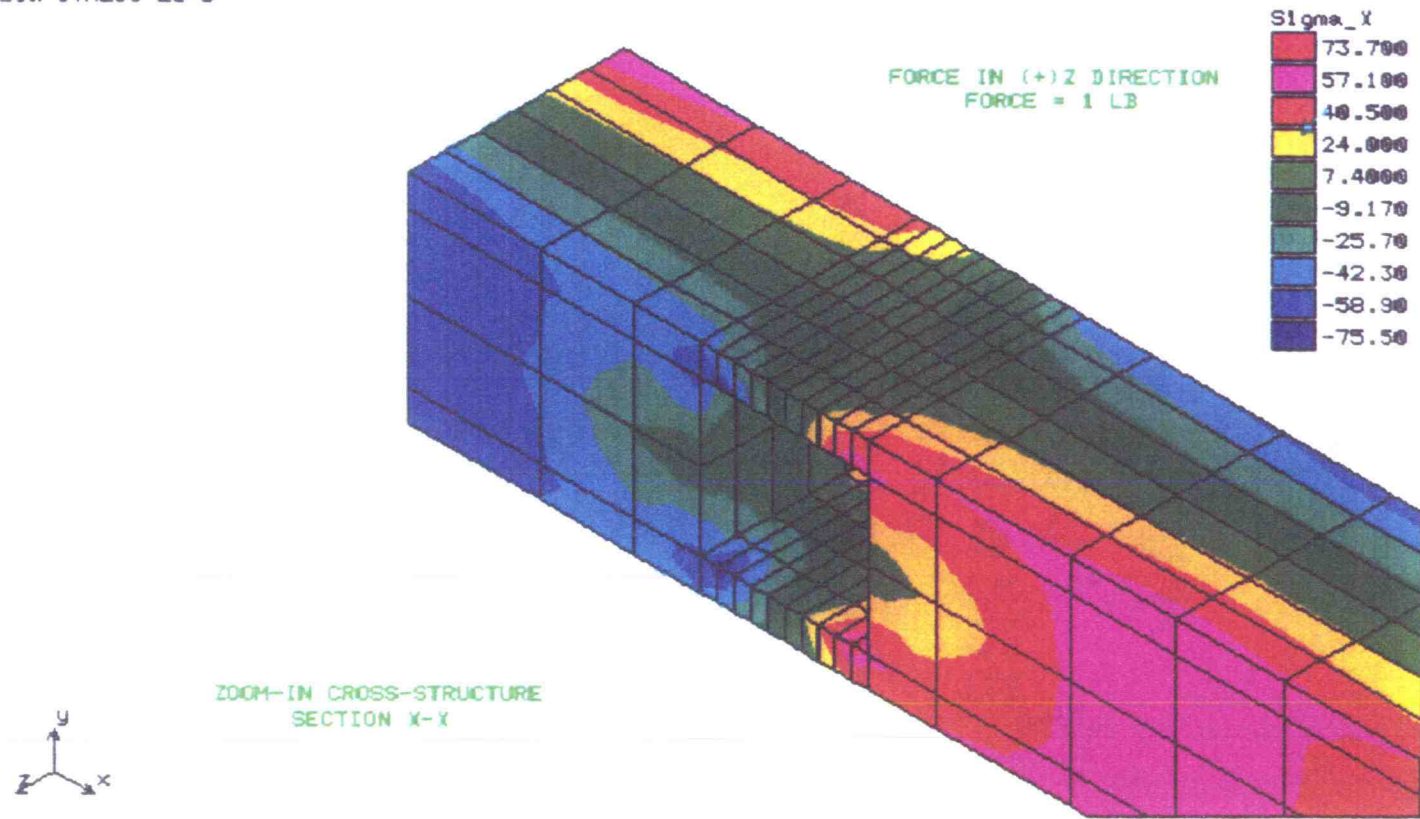


Figure 26c. σ_x stress field under a force f_z (Cross).

L1n STRESS Lc=1

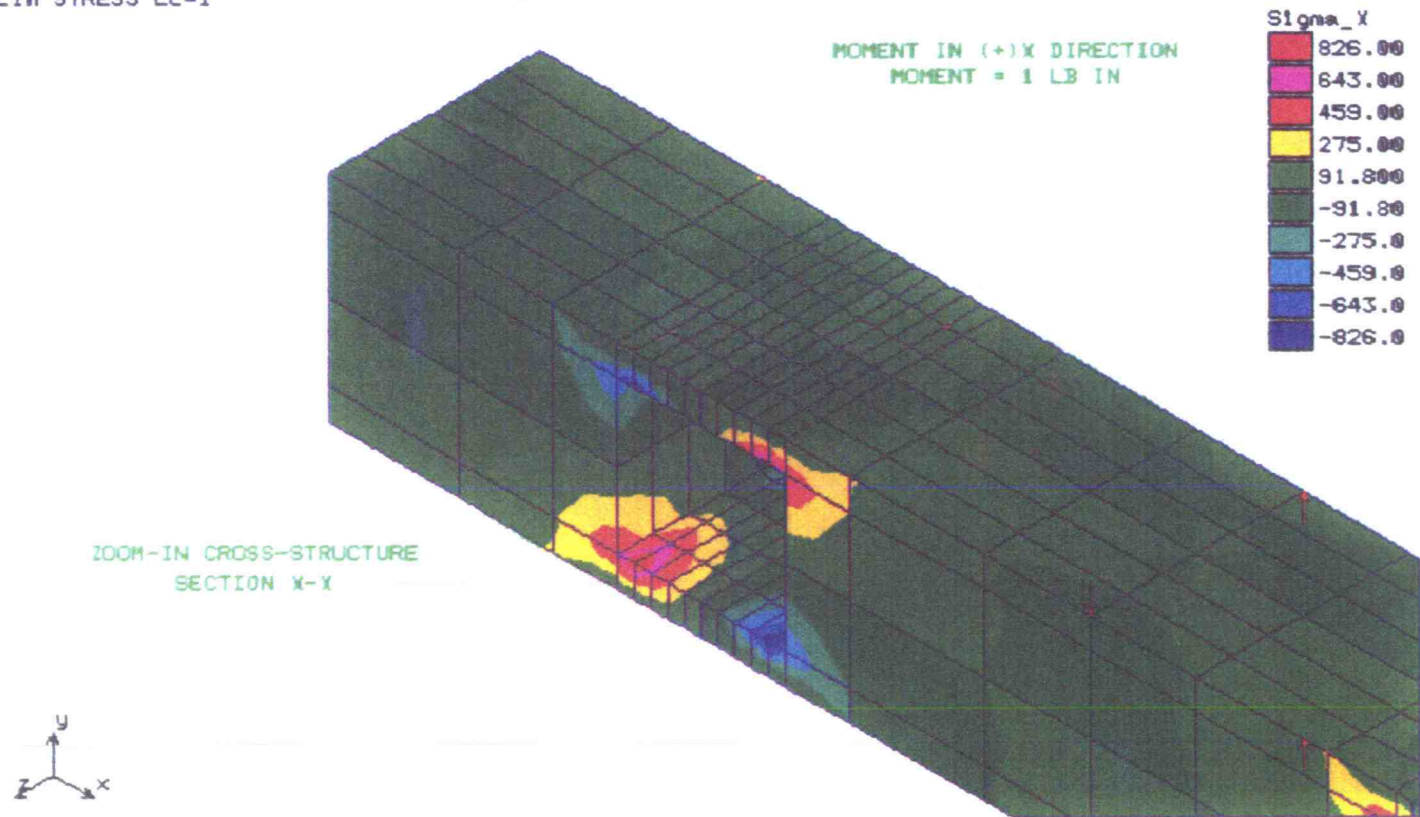
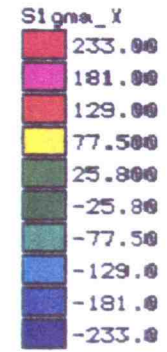


Figure 26d. σ_x stress field under a moment m_x (Cross).

L1n STRESS Lc=2

MOMENT IN (+)Y DIRECTION
MOMENT = 1 LB IN



ZOOM-IN CROSS-STRUCTURE
SECTION X-X

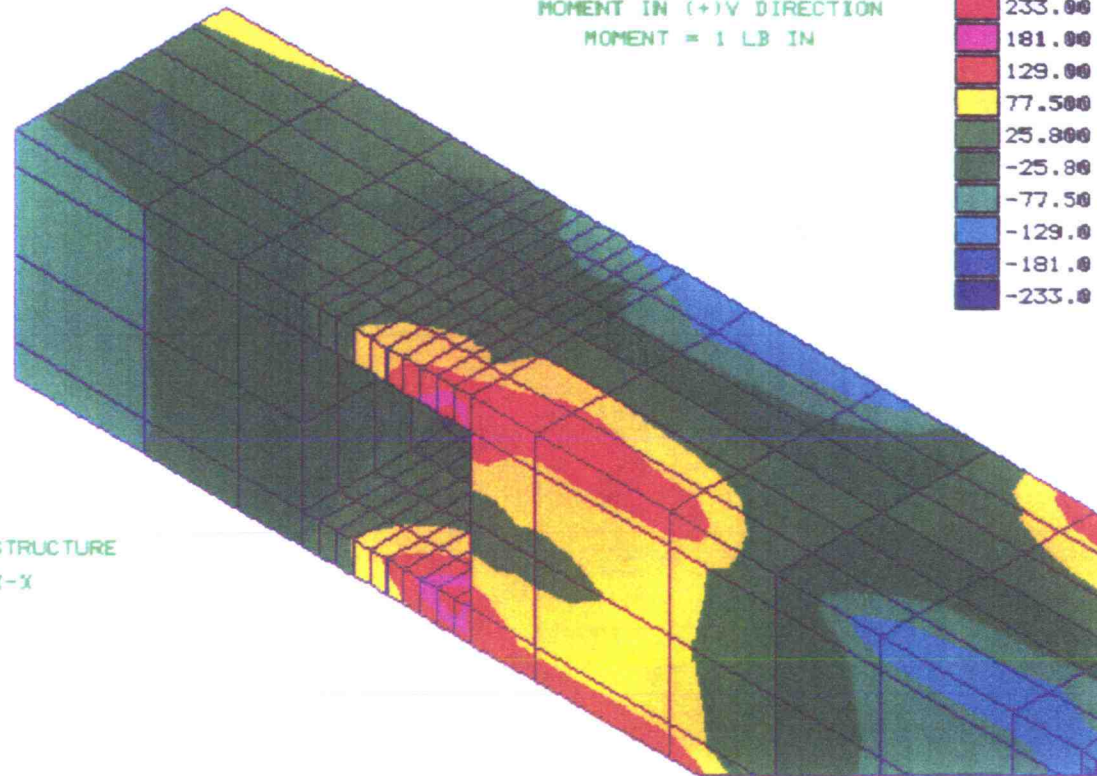
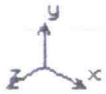
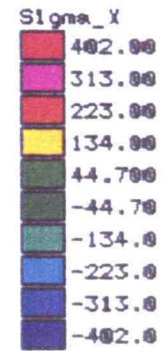


Figure 26e. σ_x stress field under a moment m_y (Cross).

L1n STRESS Lc=3

MOMENT IN (+)Z DIRECTION
MOMENT = 1 LB IN



ZOOM-IN CROSS-STRUCTURE
SECTION X-X

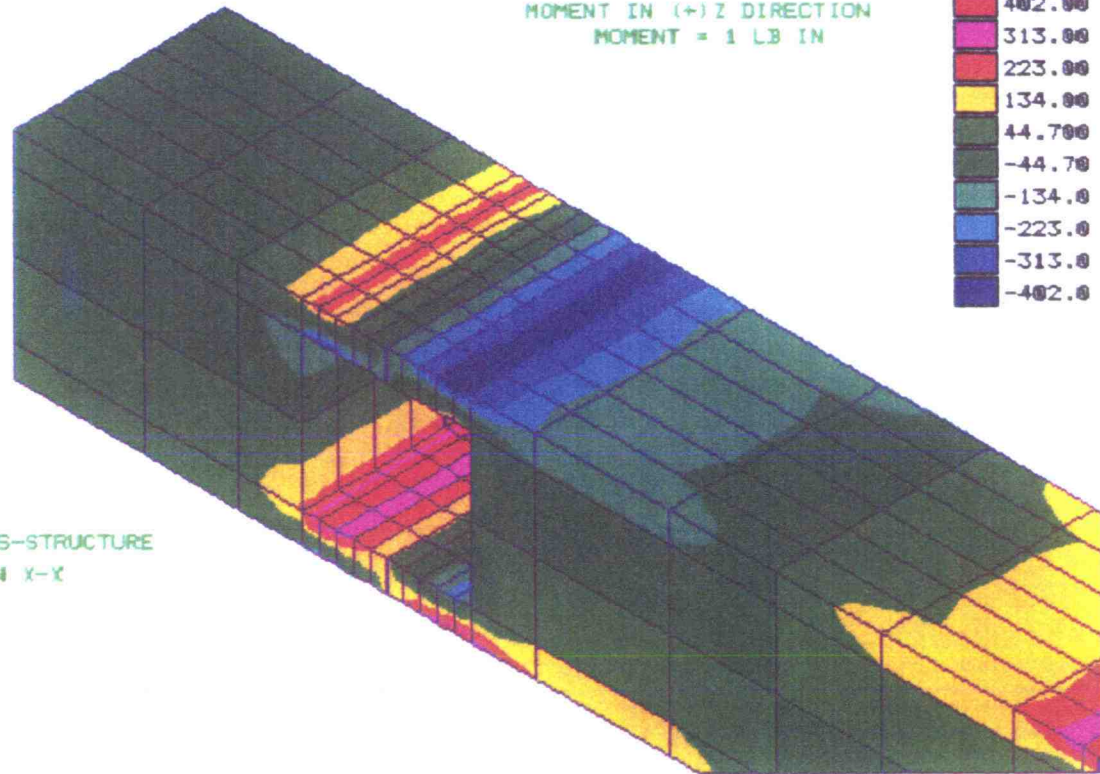
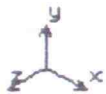


Figure 26f. σ_x stress field under a moment m_z (Cross).

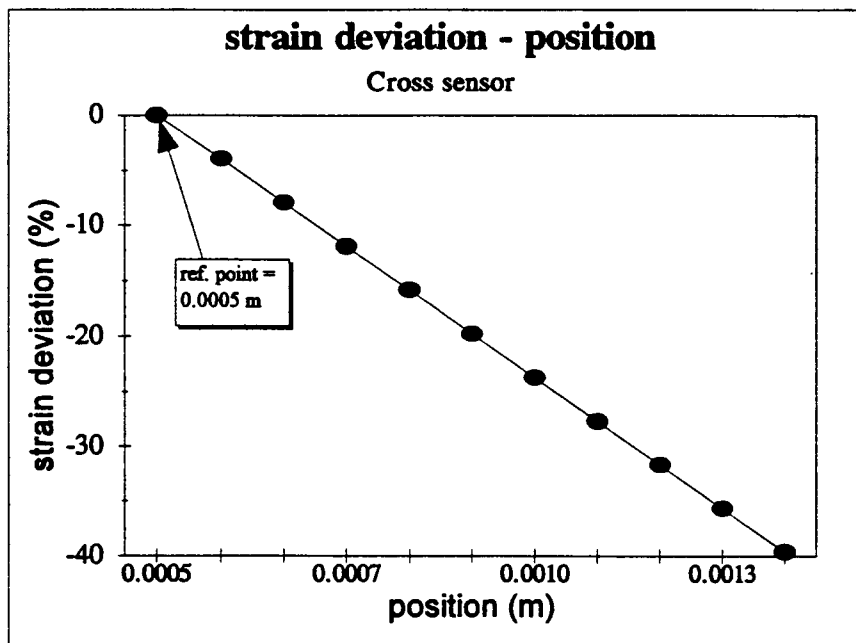


Figure 27a. Sensitivity analysis (Cross, linear displacement).

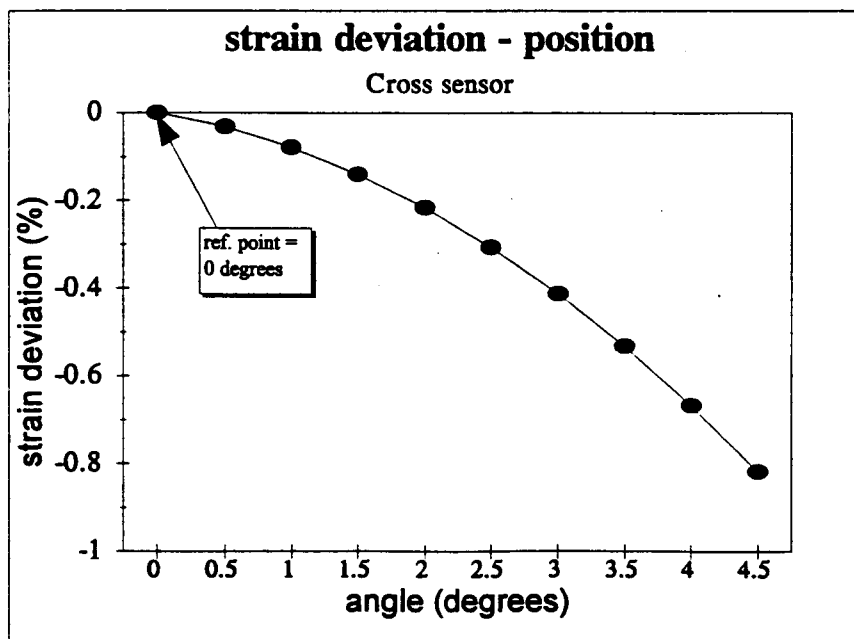


Figure 27b. Sensitivity analysis (Cross, angular displacement).

Platform, monolithic construction would not be practical because of the slots along the Z axis of the sensor. Consequently, these estimates consider two pieces as shown in Figs.13a and 13b. Table 3 shows these estimates.

	TIME (HRS)	COST (DOLLARS)
ONE PART	37	962.00
SIX PARTS	130	3,380.00

Table 3. Time and cost estimates for the Cross-Structure

5.5 Evaluation

As was stated in chapter 2, the compliance matrix C is a constant matrix which depends on the structural properties of the sensor body. It was established that this matrix is important in the measurement process because its Moore-Penrose inverse can be used to calculate the principal set of forces f from the measured strain vector ϵ . The measurement error in ϵ propagates to the error in f by means of the compliance matrix C . The compliance matrix C that gives the smallest error in f can be regarded as that corresponding to the best structural design. From this point of view an index for the evaluation of the structure of the sensor may be derived directly from C . To obtain this index, a singular value decomposition (SVD) of C is performed (appendix F). From the SVD three matrices are obtained. One of these matrices is a diagonal matrix whose elements are called "singular values". It can be shown that the ratio of the

maximum singular value (s_{\max}) to the minimum singular value (s_{\min}), limits the maximum possible error in f and can be used as an index to evaluate the structural performance of the sensor [12].

The better the structure the smaller the ratio of the singular values. This ratio is called the condition number of the C matrix and it is written as

$$\text{cond } C = \frac{s_{\max}}{s_{\min}} \quad (44)$$

The condition number is a measure of isotropy of the structural compliance with respect to the sensor strains [12]. The condition number is equal to one in the limitcase when the sensor has perfect isotropy of the structural compliance, therefore, this is also the best structure in the sense that it minimizes the error in f . The compliance matrices are obtained from the results of the finite element method (appendices B, C, and D) and the singular values were obtained by means of the program shown in appendix E. The resulting compliance matrices and corresponding singular values for each sensor are as follows:

Truss sensor

The normalized compliance matrix is

$$C = \begin{bmatrix} 5.03 & 2.65 & 1.76 & -3.1 & 5.5 & 3.61 \\ -2.82 & 5.13 & 1.65 & -3.84 & -4.79 & 1.21 \\ -4.88 & -2.84 & 1.81 & 3.69 & -1.73 & 3.47 \\ 2.6 & -4.93 & 1.59 & 3.32 & 1.85 & 1.57 \\ -4.81 & -0.57 & -0.17 & -0.078 & -1.997 & -4.82 \\ 0.598 & -4.64 & -0.026 & 1.18 & 0.85 & -4.44 \\ 4.38 & 0.35 & -0.24 & -1.15 & -0.51 & -4.86 \\ -0.019 & 4.87 & 0.17 & 0 & 0.071 & -5.59 \end{bmatrix}$$

and the singular values are

$$w = [12.6889 \ 12.32 \ 11.11 \ 4.18 \ 3.26 \ 2.91]$$

therefore, from eq.(44), the condition number is

$$\text{cond } C = 4.36$$

Stewart Platform

The normalized compliance matrix is

$$C = \begin{bmatrix} -9.527 & 5.77 & 4 & -0.15 & -15.5 & 5.69 \\ -9.527 & -5.77 & 4 & 0.15 & -15.5 & -5.69 \\ -0.24 & -11.1 & 4 & 13.5 & 7.64 & 5.69 \\ 9.76 & -5.36 & 4 & 13.4 & 7.9 & -5.69 \\ 9.76 & 5.36 & 4 & -13.4 & 7.9 & 5.69 \\ -0.24 & 11.1 & 4 & -13.5 & 7.64 & -5.69 \end{bmatrix}$$

and the singular values are

$$w = [32.03 \ 32.02 \ 13.94 \ 9.79 \ 8.26 \ 8.25]$$

therefore, the condition number from Eq.44 is

$$\text{cond } C = 3.88$$

Cross Structure

The normalized compliance matrix is

$$C = \begin{bmatrix} 1.67 & 0 & -29.7 & 0 & -19.16 & 0 \\ -1.67 & 0 & -29.7 & 0 & 19.16 & 0 \\ -29.7 & 1.67 & 0 & 0 & 0 & -19.16 \\ -29.7 & -1.67 & 0 & 0 & 0 & 19.16 \\ 0 & 29.7 & -1.67 & -19.16 & 0 & 0 \\ 0 & 29.7 & 1.67 & 19.16 & 0 & 0 \end{bmatrix}$$

and the singular values are

$$w = [42.3 \ 42.09 \ 41.98 \ 27.08 \ 27.03 \ 26.93]$$

therefore, from eq.(44), the condition number is

$$\text{cond } C = 1.57$$

With this evaluation, the comparative analysis is completed. Discussion of results and a recommendation for the suitable sensor to be employed with the walking machine are presented next, taking into consideration that the condition number for available commercial sensors range between 3.8 and 15.7.

5.6 Results

All results for the three sensors are summarized in the following table:

	TRUSS SENSOR	STEWART PLAT.	CROSS
COND.NUMBER	4.3	3.8	1.6
COST/UNIT (DOLLARS)	728	728	962
MASS (GRAMS)	18	37	21.5
STRAIN GAUGES (MIN.)	16	12	6
MONOLITHIC STRUCTURE	EASY TO ACHIEVE	EXTREMELY DIFFICULT	EXTREMELY DIFFICULT

Table 4. Final results for the three sensors studied.

Let us analyze the results for each of the sensors separately. Let us begin with the cross-sensor. From the table, the cross-sensor presents the lowest condition number (1.6), meaning an excellent structural behavior, an intermediate mass, and the lowest required number of strain gauges since the cancellation of the bending signals is not necessary (see section 5.4). However, the cross-sensor presents serious disadvantages too. First, although the condition number is extremely low, this number was the result of assuming monolithic construction which, from the manufacturing point of view, is not a recommended option

(appendix G). Second, although it requires the minimal number of strain gauges, the sensitivity of the cross sensor to strain gauge misplacements is the highest of the three sensors (see Figs.28a and 28b). Finally, but not less important, it is the most expensive sensor.

The Stewart Platform shows a very low condition number (3.8) but several disadvantages. First, its mass cannot be reduced too much because of the two solid end plates. Second, monolithic construction is almost impossible to achieve. Third, because of the small size and geometry of the legs, combined with the high number of strain gauges, instrumentation is very difficult, increasing the possibility of transducer misalignment. The sensor also has high cross-linking.

Finally, the truss sensor requires the greatest number of strain gauges but presents several advantages. First, it has a low condition number (4.3) compared to commercially available sensors. Second, a very compact and stiff sensor can be easily built giving it a low mass and high resistance to overload conditions, which are very important factors in the walking machine design. Third, monolithic construction is easy to achieved. Fourth, it is relatively inexpensive to build. One additional advantage is that this sensor is not as sensitive as the cross-sensor to strain gauge misalignment.

From these results, even though the cross-sensor exhibits the lowest

condition number, the truss sensor is considered to be the best choice because its good structural behavior, low cost, low mass and the possibility of monolithic construction.

CHAPTER 6

CONCLUSIONS

This chapter summarizes all observations and results obtained during this work. In addition, some recommendations for future study are given.

- 1.- The systematic six-axis force sensor design is a relatively new field of study and research.
- 2.- Analytical studies are almost non-existent due to the complexity of the geometries.
- 3.- To overcome these difficulties, numerical techniques are employed, and among these, the finite element method is shown to be a valuable tool in the design of six-axis force sensors.
- 4.- Although most force sensors present many similar characteristics, e.g. geometrical arrangements and type of elastic elements, this does not mean that innovative ideas and uncommon use of elastic elements cannot be successful, as proved by the three force sensors studied here.
- 5.- The truss sensor presented several of the advantages claimed by its inventors, mainly its sensitivity to lateral forces and its compactness, important factors in its use in the walking machine. In addition, low cost and easy instrumentation, together with the ease of monolithic construction, made this sensor the most suitable option for its use with the walking machine. One disadvantage is that the vertical elements greatly reduce its sensitivity to

vertical forces. A reduction in cross-sectional area at the points where the strain gauges are located is recommended.

6.- The Stewart Platform presented a low condition number but several disadvantages with respect to mass reduction and the difficulty of monolithic construction.

7.- Although the cross-structure exhibited the lowest condition number, several disadvantages seriously limit its use.

Recommendations for future study:

1.- Perform an optimization for the truss sensor having the cross sectional area of the vertical elements as the variable to be optimized.

2.- Build the selected sensor and perform the experimental calibration. This calibration is necessary for two main reasons. First, the finite element discretization is an approximation of a continuum and as a consequence, some errors are involved, which encompass uncertainties in material properties and physical characteristics of the sensor. Second, finite element analysis cannot simulate performance of strain gauges and accompanying electronic equipment.

BIBLIOGRAPHY

- 1) Bayo, E. and Stubbe, J.R.
Six-axis force sensor evaluation and a new type of optimal frame truss design for robotics applications. Journal of Robotic Systems 6(2), pp.191-208. 1989.
- 2) Bray, A., Barbato, G. and Levi, R.
Theory and Practice of Force Measurement. pp.142-182, 260-289. Academic Press 1990.
- 3) Budynas, R.G.
Advanced Strength and Applied Stress Analysis. pp.349-442. McGraw-Hill 1977.
- 4) Carignan et al.
Force Measuring Platform and Load Cell therefore Using Strain Gages to Measure Shear Forces. U.S. Patent #4,493,220. Jan 15, 1985.
- 5) Ch'Hayder et al.
Process for Producing Sensors for Measuring Spatial Forces and Sensors Obtained. U.S. Patent #3,000,700. Nov 12, 1991.
- 6) Dally and Riley.
Experimental Stress Analysis. 2nd Ed. pp.217-272. McGraw-Hill 1985.
- 7) Draisey.
Force and Moment Sensor. U.S. Patent #5,033,314. Jul 23, 1991.
- 8) Faulkner, M.G., Hay, H., Fuchshuber, P., Haberstock, D.
Development of a System for The Measurement of Forces and Moments Created by Orthodontic Appliances. Proceedings of the VI International Congress on Experimental Mechanics Vol.1. pp. 384-389. 1987.
- 9) Flatau, C.R.
Force Sensing in Robots and Manipulators. Proceedings of the 2nd International CISM-IFTOMM Symposium on the Theory and Practice of Robots and Manipulators. pp.294-306. Warsaw, 1976.
- 10) Gallagher, R.H.
Finite Element Analysis Fundamentals. pp. 53-84. Prentice Hall 1975.
- 11) Kerr, D.R.
Analysis, Properties, and Design of a Stewart-Platform Transducer. pp.139-145. Trends and Developments in Mechanisms, Machines and

- Robotics. A.S.M.E.DE-vol 15-3. 1988.
- 12) Kobayashi, A.S.
Handbook on Experimental Mechanics. pp.41-77. Prentice Hall Inc. 1987.
 - 13) Kovacevic et al.
Calibration Stand for Sensor. U.S. Patent #5,020,357. June 4, 1991.
 - 14) Kroll, E. and Weill, R.
Decoupling Load Components and Improving Robot Interfacing With an Easy-to-Use Six-Axis Force Sensor. The Theory of Machines and Mechanisms: Proceedings of the 7th World Congress. Sevilla, Spain. pp.1155-1158. September 1987.
 - 15) Murray, W.M., Miller, W.R.
The Bonded Electrical Resistance Strain Gage. pp.253-281, 360-382. Oxford University Press 1992.
 - 16) Nakamura, Y., Yoshikawa, T., Futamata, I.
Design and Signal Processing of Six-Axis Force Sensors. pp.75-81. Robotics Research: 4th International Symposium, M.I.T Press, Cambridge, MA. 1988.
 - 17) Press, Flannery, Teukolsky, and Vetterling.
Numerical Recipes. pp.52-64. Cambridge University Press. 1990.
 - 18) Reuber, M., Regan, K.
Design and Integration of a 3-D Force Sensor. pp.1090-1096. IEEE International Conference on Robotics & Automation vol.2. 1987.
 - 19) Uchiyama, M., Bayo, E., Palma-Villalon, E.
A Systematic Design Procedure to Minimize a Performance Index for Robot Force Sensors. Transactions of the ASME vol.113. pp.388-394. Sept 1991.
 - 20) Van Brussel, H., Belien, H., Thielemans, H.
Force Sensing for Advanced Robot Control. Robotics vol.2. pp.139-148. 1986.
 - 21) Yoshikawa, T., Miyazaki, T.
A Six-Axis Force Sensor with Three-Dimensional Cross-Shape Structure. IEEE International Conference on Robotics & Automation, vol.1. pp.249-255. 1989.

APPENDICES

APPENDIX A

MASS CALCULATIONS

In this section, the mass of each sensor is determined. All dimensions are expressed in inches. Material is Aluminum T6061 having a mass density of 0.098 lb/in³.

Truss Sensor

Dimensions of the sensor are shown in Fig.28. As can be seen, the total volume of the sensor is the volume of the top and bottom supports, the vertical elements and the diagonal elements. The volume of the supports is calculated as:

$$V_f = 2(V_1 - V_2) \text{ where:}$$

V_f = volume of both upper and lower support.

V_1 = volume of one support with no hole.

V_2 = volume of the hole of the support.

Therefore we have the following:

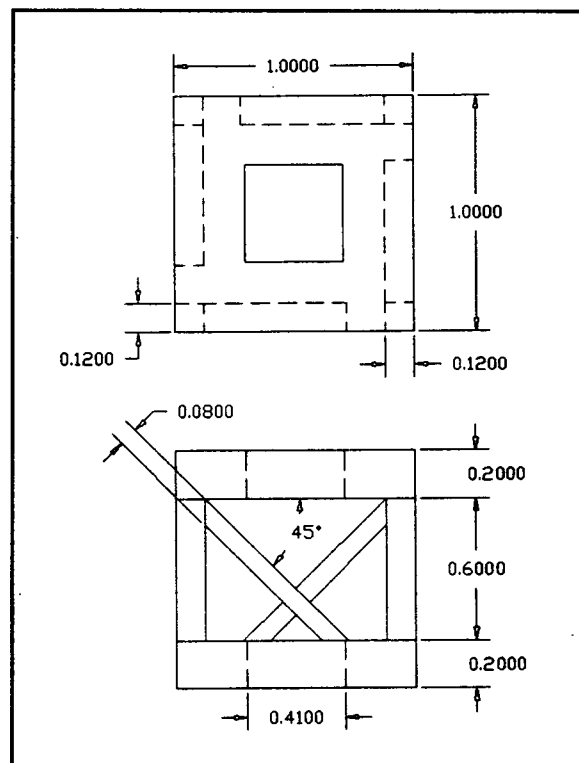


Figure 28. Truss sensor dimensions.

$$V_1 = 1.0 \times 1.0 \times 0.2 = 0.2 \text{ in}^3$$

$$V_2 = 0.41 \times 0.41 \times 0.2 = 0.03362 \text{ in}^3$$

$$2(V_1 - V_2) = 0.33276 \text{ in}^3$$

Volume of the vertical elements V_v is simply $4V_3$ with V_3 the volume of one single element:

$$V_v = 4(0.12 \times 0.12 \times 0.6) = 0.03456 \text{ in}^3.$$

Volume of the diagonal elements V_d is given by $4V_4$ where V_4 is the volume of one single diagonal element. It can be shown, that the volume of each diagonal element can be calculated as the product of the area of one trapezoid times the thickness of the element. Therefore:

$$V_d = 4[0.12 \times ((0.848722 + 0.688722)/2) \times 0.08] = 0.02951 \text{ in}^3.$$

So, the total volume V_t is given by

$$V_t = V_1 + V_v + V_d = 0.39683 \text{ in}^3.$$

Finally, the mass is calculated from the expression

$$\rho = m / V$$

where ρ is the mass density and V the volume. From this expression, the mass is found to be $m = (0.098)(0.39683)$

$$m = 0.03888 \text{ lb} = 17.64 \text{ g}$$

Stewart Platform

The Stewart Platform (Fig.29) consists of two circular plates and six legs having circular cross-sectional area. The dimensions are the following:

upper plate: diameter = 1.0",

thickness = 0.2"

lower plate: diameter = 2.0", thickness

= 0.2"

legs: diameter = 0.09375", length =

1.06"

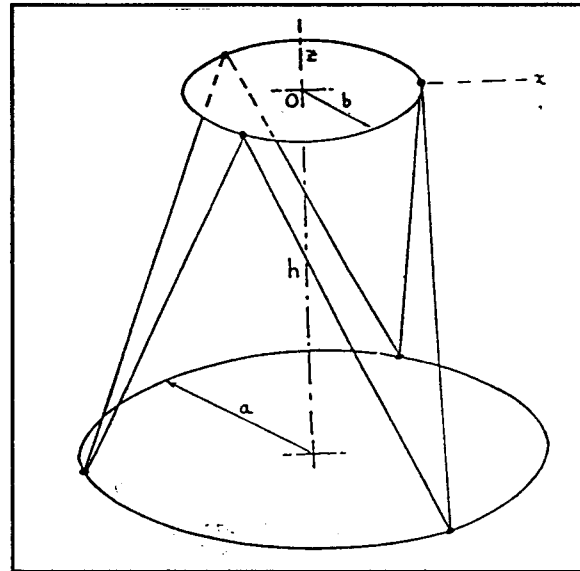


Figure 29. Model for Stewart Platform.
(From [11])

The volumes are calculated

using the formula

$$V = \frac{\pi D^2}{4} l$$

where V = volume

D = diameter

l = thickness or length

So, for the upper platform the volume V_u is:

$$V_u = \pi(1)^2 (0.2)/4 = 0.157079 \text{ in}^3$$

For the lower platform, the volume V_l is:

$$V_l = \pi(2)^2 (0.2)/4 = 0.628318 \text{ in}^3$$

Finally, for volume of the six legs V_{el} is:

$$V_{el} = 6\pi(0.09375)^2 (1.06)/4 = 0.0439 \text{ in}^3$$

The total volume V_t is given by:

$$V_t = V_u + V_l + V_{el} = 0.829298 \text{ in}^3.$$

The mass is

$$m = (0.098)(0.829298) = 0.081271 \text{ lb. So we can write:}$$

$$m = 0.081271 \text{ lb} = 36.864 \text{ g}$$

Cross Structure

Basically, the cross-structure volume can be approximated by one solid cube and six elements like the one shown in the Fig.30. The cube has 0.28" by side and its volume V_o is therefore:

$$V_o = (0.28)^3 = 0.021952".$$

The volume of one of the elements like the one in fig.30 can be divided in three sub-volumes. Two solid boxes and one hole. The volume of the solid boxes V_{b1} and V_{b2} are calculated as follows:

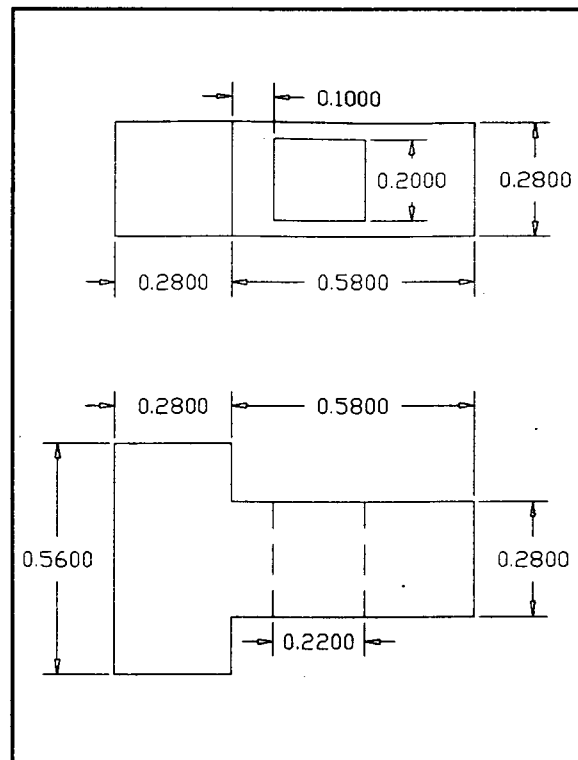


Figure 30. Cross sensor basic volume.

$$V_{b1} = (0.56 \times 0.28 \times 0.28) = 0.043904 \text{ in}^3$$

$$V_{b2} = (0.58 \times 0.28 \times 0.28) = 0.045472 \text{ in}^3$$

The volume of the hole V_h is:

$$V_h = (0.22 \times 0.20 \times 0.28) = 0.01232 \text{ in}^3$$

So the total volume of one element V_o is:

$$V_o = V_{b1} + V_{b2} - V_h = 0.077056 \text{ in}^3$$

and the volume of the six elements V_{6o} is

$$V_{6o} = 6(0.077056) = 0.462336 \text{ in}^3$$

The total volume V is given by

$$V = V_o + V_{6o} = 0.484288 \text{ in}^3$$

Finally, the mass is calculated as

$$m = (0.098)(0.484288) = 0.04746.$$

$$m = 0.04746 \text{ lb} = 21.53 \text{ g}$$

It is important to recognize that these values cannot be used for a direct comparison because, for manufacturing reasons, the sensors cannot be built within the same volume.

APPENDIX B

TRUSS SENSOR FEM PROGRAM AND OUTPUT

In the next pages, the finite element program written to model and analyze the truss sensor is shown together with its output. The finite element software used was COSMOS/M.

The program generates the model composed of plate and 3D beam finite elements. This program was created to perform the numerical calibration of the sensor, but the behavior curves were also obtained with this program by setting appropriate loading conditions. The compliance matrix of the sensor was obtained from data generated by this program. The output shows forces, moments, and stresses at each of the nodes which form the elements of interest (Fig.15). The values used to obtain the compliance matrix are shown in the stresses section, node 2, stress (P/A). For example, from the first page of the output, element 40 is formed by node 1 (52) and node 2 (53). The stress (P/A) at node 2 (53) is 51.87. The first part of the output deals with forces while the second part shows results for the applied external moments.

C*
 C* COSMOS/M Geostar V1.65
 C* Problem :truss sensor calib. Date : 02-MAY-93 Time : 15:44:33
 C*

PICK_MAT,1,ALUMINUM,FPS,
 C* MATL:ALUMINUM : ALUMINUM ALLOY

C* EX 10.3E+6 p.s.i.
 C* NUXY 0.36
 C* GXY 3.80E+6 p.s.i.
 C* ALPX 12.8E-6 /Fahrenheit
 C* DENS 2.51E-4 lb.s.s/in**4
 C* KX 2.194E-3 BTU/in.s.F
 C* C (Cp) 88.9493 BTUin/lbssF
 EGROUP,1,SHELL4T,1,0,0,0,0,0,
 RCONST,1,1,1,6,0.32,0,0,0,0,0,
 EGROUP,2,BEAM3D,0,0,0,0,0,0,
 RCONST,2,1,1,10,0.0144,17.28E-6,17.28E-6,0.12,0.12,0,0,3.45E-5,0.85,0.&
 85,
 RCONST,2,1,11,4,0,0,0,0.096,
 RCONST,2,2,1,10,0.010182,6.11E-6,1.22E-5,0.12,0.08485,0,0,1.8327E-5,0.&
 85,0.85,
 RCONST,2,2,11,4,0,0,0,9.06E-2,
 RCONST,2,3,1,10,0.072,8.64E-5,2.16E-3,0.6,0.12,0,0,2.246E-3,0.85,0.85,&
 RCONST,2,3,11,4,0,0,0,0.8736
 PT,1,-0.5,-0.5,0.3,
 PTGEN,1,1,1,1,0,1,0,0,
 SCALE,0,
 PTGEN,1,1,2,1,0,0,1,0,
 SCALE,0,
 CRLINE,1,1,3,
 CRLINE,2,3,4,
 CRLINE,3,4,2,
 CRLINE,4,2,1,
 SF4CR,1,1,2,3,4,0,
 PTGEN,1,1,4,1,0,0,0,-0.6,
 SCALE,0,
 CRLINE,5,1,5,
 CRLINE,6,3,7,
 CRLINE,7,4,8,
 CRLINE,8,2,6,
 PTGEN,1,6,6,1,0,0,0.6,0,
 PTGEN,1,8,8,1,0,-0.6,0,0,
 PTGEN,1,7,7,1,0,0,-0.6,0,
 PTGEN,1,5,5,1,0,0.6,0,0,
 CRLINE,9,1,12,
 CRLINE,10,2,9,
 CRLINE,11,4,10,
 CRLINE,12,3,11,
 PT,13,0,0,1,
 CRLINE,13,1,13,
 CRLINE,14,2,13,
 CRLINE,15,4,13,
 CRLINE,16,3,13,
 ACTSET,EG,1,

ACTSET,RC,1,
M_SF,1,1,1,4,6,6,1,1,
ACTSET,EG,2,
ACTSET,RC,1,
M_CR,5,5,1,3,8,1,2,
M_CR,8,8,1,3,8,1,4,
M_CR,7,7,1,3,8,1,3,
M_CR,6,6,1,3,8,1,1,
ACTSET,RC,2,
M_CR,9,9,1,3,8,1,3,
M_CR,10,10,1,3,8,1,1,
M_CR,11,11,1,3,8,1,2,
M_CR,12,12,1,3,8,1,4,
ACTSET,RC,3,
M_CR,13,13,1,3,5,1,3,
M_CR,14,14,1,3,5,1,1,
M_CR,15,15,1,3,5,1,2,
M_CR,16,16,1,3,5,1,1,
NMERGE,1,157,1,0.0001,0,1,0,
NCOMPRESS,1,155,1,
DND,81,ALL,0,81,1,
DND,113,ALL,0,113,1,
DND,105,ALL,0,105,1,
DND,73,ALL,0,73,1,
DND,97,ALL,0,97,1,
DND,65,ALL,0,65,1,
DND,57,ALL,0,57,1,
DND,89,ALL,0,89,1,
FND,118,FX,1,118,1,
PRINT_ELSET,8,40,40,48,48,56,56,64,64,72,72,80,80,88,88,96,96
ACTSET,LC,2
FND,118,FY,1,118,1,
PRINT_ELSET,8,40,40,48,48,56,56,64,64,72,72,80,80,88,88,96,96
ACTSET,LC,3
FND,118,FZ,1,118,1,
PRINT_ELSET,8,40,40,48,48,56,56,64,64,72,72,80,80,88,88,96,96
R_STATIC

DATE: 6/23/1993 TIME: 18:12:37

TITLE : Truss sensor calibration
CASE 1 CASE 2 CASE 3
SUBTITLE : FX = 1 FY = 1 FZ = 1

STRESS EVALUATION FOR STATIC ANALYSIS

STRESS OUTPUT FOR BEAM ELEMENT GROUP 2 CASE NO. 1

ELEMENT NUMBER	FORCES		MOMENTS		STRESSES			
	NODE1	NODE2	NODE1	NODE2	NODE1	NODE2		
40	[52 ,	53]	Fr=-.7469E+00	0.7469E+00	Tr=0.8108E-03	-.8108E-03	(P/A) =-.5187E+02	0.5187E+02
			Vs=0.3262E-01	-.3262E-01	Ms=0.3163E-02	-.9185E-03	(Ms/Ss)=0.1098E+02	-.3189E+01
			Vt=-.2992E-01	0.2992E-01	Mt=-.2578E-02	0.5025E-02	(Mt/St)=-.8953E+01	0.1745E+02
					(Tr*CTOR/Jp)=0.2256E+01	-.2256E+01	Smax =-.3193E+02	0.7251E+02
							Smin =-.7180E+02	0.3123E+02
48	[60 ,	61]	Fr=0.4180E+00	-.4180E+00	Tr=-.4204E-03	0.4204E-03	(P/A) =0.2903E+02	-.2903E+02
			Vs=-.2504E-01	0.2504E-01	Ms=-.5214E-02	-.2352E-02	(Ms/Ss)=-.1810E+02	-.8166E+01
			Vt=0.1009E+00	-.1009E+00	Mt=-.2319E-02	0.4410E-03	(Mt/St)=-.8051E+01	0.1531E+01
					(Tr*CTOR/Jp)=-.1170E+01	0.1170E+01	Smax =0.5518E+02	-.1933E+02
							Smin =0.2871E+01	-.3872E+02
56	[68 ,	69]	Fr=0.7240E+00	-.7240E+00	Tr=-.1755E-02	0.1755E-02	(P/A) =0.5028E+02	-.5028E+02
			Vs=-.3468E-01	0.3468E-01	Ms=-.4133E-02	0.7306E-03	(Ms/Ss)=-.1435E+02	0.2537E+01
			Vt=0.4537E-01	-.4537E-01	Mt=0.1581E-02	-.4182E-02	(Mt/St)=0.5489E+01	-.1452E+02
					(Tr*CTOR/Jp)=-.4884E+01	0.4884E+01	Smax =0.7012E+02	-.3322E+02
							Smin =0.3043E+02	-.6733E+02
64	[76 ,	77]	Fr=-.3866E+00	0.3866E+00	Tr=-.7713E-03	0.7713E-03	(P/A) =-.2685E+02	0.2685E+02
			Vs=0.1165E-01	-.1165E-01	Ms=0.4164E-02	0.2917E-02	(Ms/Ss)=0.1446E+02	0.1013E+0
			Vt=-.9441E-01	0.9441E-01	Mt=0.6184E-03	0.2553E-03	(Mt/St)=0.2147E+01	0.8865E+00
					(Tr*CTOR/Jp)=-.2146E+01	0.2146E+01	Smax =-.1024E+02	0.3786E+02
							Smin =-.4345E+02	0.1583E+02
72	[84 ,	85]	Fr=0.5052E+00	-.5052E+00	Tr=0.3951E-03	-.3951E-03	(P/A) =0.4962E+02	-.4962E+02
			Vs=0.5335E-02	-.5335E-02	Ms=0.1107E-02	-.1256E-02	(Ms/Ss)=0.7689E+01	-.8724E+01
			Vt=0.1406E-02	-.1406E-02	Mt=0.5015E-03	0.6435E-04	(Mt/St)=0.2466E+01	0.3165E+00
					(Tr*CTOR/Jp)=0.1953E+01	-.1953E+01	Smax =0.5978E+02	-.4058E+02
							Smin =0.3947E+02	-.5866E+02
80	[92 ,	93]	Fr=-.6277E-01	0.6277E-01	Tr=0.3484E-03	-.3484E-03	(P/A) =-.6164E+01	0.6164E+01
			Vs=-.2535E-01	0.2535E-01	Ms=0.5588E-03	-.1103E-03	(Ms/Ss)=0.3880E+01	-.7656E+00
			Vt=-.4228E-02	0.4228E-02	Mt=-.1657E-02	-.1032E-02	(Mt/St)=-.8152E+01	-.5074E+01
					(Tr*CTOR/Jp)=0.1722E+01	-.1722E+01	Smax =0.5867E+01	0.1200E+02
							Smin =-.1820E+02	0.3252E+00
ELEMENT NUMBER	FORCES		MOMENTS		STRESSES			
	NODE1	NODE2	NODE1	NODE2	NODE1	NODE2		
88	[100 ,	101]	Fr=-.4593E+00	0.4593E+00	Tr=-.6092E-03	0.6092E-03	(P/A) =-.4511E+02	0.4511E+02

Vs=-.6413E-02 0.6413E-02 Ms=-.8072E-03 0.1046E-02 (Ms/Ss)=-.5604E+01 0.7260E+01
 Vt=-.2248E-02 0.2248E-02 Mt=-.9686E-04 -.5834E-03 (Mt/St)=-.4764E+00 -.2869E+01
 (Tr*CTOR/Jp)=-.3011E+01 0.3011E+01 Smax =-.3903E+02 0.5524E+02
 Smin =-.5119E+02 0.3498E+02

96 [108 , 109]

Fr=0.1990E-02 -.1990E-02 Tr=-.7755E-03 0.7755E-03 (P/A)=0.1954E+00 -.1954E+00
 Vs=0.2744E-01 -.2744E-01 Ms=-.1728E-03 -.6383E-04 (Ms/Ss)=-.1200E+01 -.4432E+00
 Vt=0.2231E-02 -.2231E-02 Mt=0.2250E-02 0.6600E-03 (Mt/St)=0.1107E+02 0.3246E+01
 (Tr*CTOR/Jp)=-.3834E+01 0.3834E+01 Smax =0.1246E+02 0.3494E+01
 Smin =-.1207E+02 -.3885E+01

STRESS OUTPUT FOR BEAM ELEMENT GROUP 2 CASE NO. 2

ELEMENT NUMBER	FORCES		MOMENTS		STRESSES	
	NODE1	NODE2	NODE1	NODE2	NODE1	NODE2
40	[52 ,	53]	Fr=-.3940E+00 0.3940E+00	Tr=-.5752E-03 0.5752E-03	(P/A)=-.2736E+02 0.2736E+02	
			Vs=0.2400E-01 -.2400E-01	Ms=0.3516E-02 0.2454E-02	(Ms/Ss)=0.1221E+02 0.8523E+00	
			Vt=-.7960E-01 0.7960E-01	Mt=0.2248E-02 -.4480E-03	(Mt/St)=0.7807E+01 -.1556E+01	
				(Tr*CTOR/Jp)=-.1600E+01 0.1600E+01	Smax =-.7347E+01 0.3744E+02	
					Smin =-.4738E+02 0.1728E+02	
48	[60 ,	61]	Fr=-.7610E+00 0.7610E+00	Tr=0.9389E-03 -.9389E-03	(P/A)=-.5285E+02 0.5285E+02	
			Vs=0.3130E-01 -.3130E-01	Ms=0.4522E-02 -.8634E-03	(Ms/Ss)=0.1570E+02 -.2998E+01	
			Vt=-.4879E-01 0.4879E-01	Mt=-.2677E-02 0.5025E-02	(Mt/St)=-.9296E+01 0.1745E+02	
				(Tr*CTOR/Jp)=0.2613E+01 -.2613E+01	Smax =-.2785E+02 0.7329E+02	
					Smin =-.7785E+02 0.3240E+02	
56	[68 ,	69]	Fr=0.4219E+00 -.4219E+00	Tr=0.1342E-03 -.1342E-03	(P/A)=0.2930E+02 -.2930E+02	
			Vs=-.2650E-01 0.2650E-01	Ms=-.4274E-02 -.2436E-02	(Ms/Ss)=-.1484E+02 -.8457E+01	
			Vt=0.8946E-01 -.8946E-01	Mt=-.2869E-02 0.8814E-03	(Mt/St)=-.9962E+01 0.3060E+01	
				(Tr*CTOR/Jp)=0.3733E+00 -.3733E+00	Smax =0.5410E+02 -.1778E+02	
					Smin =0.4497E+01 -.4082E+02	
64	[76 ,	77]	Fr=0.7311E+00 -.7311E+00	Tr=-.5518E-03 0.5518E-03	(P/A)=0.5077E+02 -.5077E+02	
			Vs=-.4388E-01 0.4388E-01	Ms=-.4353E-02 0.2815E-03	(Ms/Ss)=-.1511E+02 0.9774E+00	
			Vt=0.5428E-01 -.5428E-01	Mt=0.4601E-03 -.3751E-02	(Mt/St)=0.1597E+01 -.1303E+02	
				(Tr*CTOR/Jp)=-.1535E+01 0.1535E+01	Smax =0.6748E+02 -.3677E+02	
					Smin =0.3406E+02 -.6478E+02	
72	[84 ,	85]	Fr=0.6033E-01 -.6033E-01	Tr=-.6330E-03 0.6330E-03	(P/A)=0.5925E+01 -.5925E+01	
			Vs=0.2290E-01 -.2290E-01	Ms=-.5419E-03 0.1120E-03	(Ms/Ss)=-.3762E+01 0.7778E+00	
			Vt=0.4053E-02 -.4053E-02	Mt=0.1838E-02 0.5908E-03	(Mt/St)=0.9038E+01 0.2906E+01	
				(Tr*CTOR/Jp)=-.3129E+01 0.3129E+01	Smax =0.1872E+02 -.2241E+01	
					Smin =-.6875E+01 -.9608E+01	
80	[92 ,	93]	Fr=0.4870E+00 -.4870E+00	Tr=0.4183E-03 -.4183E-03	(P/A)=0.4783E+02 -.4783E+02	
			Vs=0.9918E-02 -.9918E-02	Ms=0.1116E-02 -.1256E-02	(Ms/Ss)=0.7746E+01 -.8724E+01	
			Vt=0.1327E-02 -.1327E-02	Mt=0.9067E-03 0.1452E-03	(Mt/St)=0.4459E+01 0.7141E+00	
				(Tr*CTOR/Jp)=0.2068E+01 -.2068E+01	Smax =0.6004E+02 -.3840E+02	
					Smin =0.3563E+02 -.5727E+02	

ELEMENT NUMBER	FORCES		MOMENTS		STRESSES	
	NODE1	NODE2	NODE1	NODE2	NODE1	NODE2
88	[100	, 101]				
	Fr=-.3705E-01	0.3705E-01	Tr=0.5122E-03	-.5122E-03	(P/A)=-.3638E+01	0.3638E+01
	Vs=-.2410E-01	0.2410E-01	Ms=0.7253E-03	-.2204E-03	(Ms/Ss)=0.5036E+01	-.1530E+02
	Vt=-.4761E-02	0.4761E-02	Mt=-.1761E-02	-.7955E-03	(Mt/St)=-.8659E+01	-.3912E+01
			(Tr*CTOR/Jp)=0.2532E+01	-.2532E+01	Smax =0.1006E+02	0.9081E+01
			Smin =-.1733E+02	-.1804E+01		
96	[108	, 109]				
	Fr=-.5104E+00	0.5104E+00	Tr=-.2016E-03	0.2016E-03	(P/A)=-.5013E+02	0.5013E+02
	Vs=-.1260E-01	0.1260E-01	Ms=-.5635E-03	0.9379E-03	(Ms/Ss)=-.3912E+01	0.6513E+01
	Vt=-.3530E-02	0.3530E-02	Mt=-.1172E-02	-.1651E-03	(Mt/St)=-.5763E+01	-.8119E+00
			(Tr*CTOR/Jp)=-.9968E+00	0.9968E+00	Smax =-.4045E+02	0.5745E+02
			Smin =-.5981E+02	0.4281E+02		

STRESS OUTPUT FOR BEAM ELEMENT GROUP 2 CASE NO. 3

ELEMENT NUMBER	FORCES		MOMENTS		STRESSES	
	NODE1	NODE2	NODE1	NODE2	NODE1	NODE2
40	[52	, 53]				
	Fr=-.2611E+00	0.2611E+00	Tr=0.2534E-03	-.2534E-03	(P/A)=-.1813E+02	0.1813E+02
	Vs=0.1996E-01	-.1996E-01	Ms=0.1257E-02	-.4258E-03	(Ms/Ss)=0.4364E+01	-.1478E+01
	Vt=-.1108E-01	0.1108E-01	Mt=0.2495E-02	-.9978E-03	(Mt/St)=0.8663E+01	-.3465E+01
			(Tr*CTOR/Jp)=0.7050E+00	-.7050E+00	Smax =-.5103E+01	0.2307E+02
			Smin =-.3116E+02	0.1319E+02		
48	[60	, 61]				
	Fr=-.2446E+00	0.2446E+00	Tr=0.2264E-03	-.2264E-03	(P/A)=-.1699E+02	0.1699E+02
	Vs=0.1607E-01	-.1607E-01	Ms=0.2220E-02	-.5136E-03	(Ms/Ss)=0.7710E+01	-.1783E+01
	Vt=-.2276E-01	0.2276E-01	Mt=0.2007E-02	-.8024E-03	(Mt/St)=0.6970E+01	-.2786E+01
			(Tr*CTOR/Jp)=0.6300E+00	-.6300E+00	Smax =-.2309E+01	0.2156E+02
			Smin =-.3167E+02	0.1242E+02		
56	[68	, 69]				
	Fr=-.2687E+00	0.2687E+00	Tr=0.5041E-03	-.5041E-03	(P/A)=-.1866E+02	0.1866E+02
	Vs=0.1651E-01	-.1651E-01	Ms=0.2326E-02	-.4209E-03	(Ms/Ss)=0.8076E+01	-.1461E+01
	Vt=-.2540E-01	0.2540E-01	Mt=0.1746E-02	-.5079E-03	(Mt/St)=0.6063E+01	-.1764E+01
			(Tr*CTOR/Jp)=0.1403E+01	-.1403E+01	Smax =-.4520E+01	0.2188E+02
			Smin =-.3280E+02	0.1543E+02		
64	[76	, 77]				
	Fr=-.2360E+00	0.2360E+00	Tr=0.6252E-03	-.6252E-03	(P/A)=-.1639E+02	0.1639E+02
	Vs=0.1395E-01	-.1395E-01	Ms=0.2132E-02	-.3244E-03	(Ms/Ss)=0.7403E+01	-.1126E+01
	Vt=-.2410E-01	0.2410E-01	Mt=0.1886E-02	-.8399E-03	(Mt/St)=0.6550E+01	-.2916E+01
			(Tr*CTOR/Jp)=0.1740E+01	-.1740E+01	Smax =-.2433E+01	0.2043E+02
			Smin =-.3034E+02	0.1234E+02		
72	[84	, 85]				
	Fr=0.1845E-01	-.1845E-01	Tr=0.1506E-03	-.1506E-03	(P/A)=0.1812E+01	-.1812E+01
	Vs=0.2125E-02	-.2125E-02	Ms=-.6395E-03	0.2495E-03	(Ms/Ss)=-.4441E+01	0.1732E+01
	Vt=0.3678E-02	-.3678E-02	Mt=0.2543E-03	-.2888E-04	(Mt/St)=0.1250E+01	-.1420E+00
			(Tr*CTOR/Jp)=0.7445E+00	-.7445E+00	Smax =0.7504E+01	0.6182E-01
			Smin =-.3879E+01	-.3687E+01		
80	[92	, 93]				

$Fr=0.2699E-02$ $-0.2699E-02$ $Tr=0.1606E-03$ $-0.1606E-03$ $(P/A)=0.2651E+00$ $-0.2651E+00$
 $Vs=0.5300E-02$ $-0.5300E-02$ $Ms=-0.5270E-03$ $0.2006E-03$ $(Ms/Ss)=-0.3659E+01$ $0.1393E+01$
 $Vt=0.3077E-02$ $-0.3077E-02$ $Mt=0.6350E-03$ $-0.7280E-04$ $(Mt/St)=0.3123E+01$ $-0.3580E+00$
 $(Tr^*CTOR/Jp)=0.7940E+00$ $-0.7940E+00$ $Smax=0.7047E+01$ $0.1486E+01$
 $Smin=-0.6517E+01$ $-0.2016E+01$

ELEMENT NUMBER	FORCES		MOMENTS		STRESSES	
	NODE1	NODE2	NODE1	NODE2	NODE1	NODE2
88	[100	, 101]				
	$Fr=0.2467E-01$	$-0.2467E-01$	$Tr=0.2162E-03$	$-0.2162E-03$	$(P/A)=0.2423E+01$	$-0.2423E+01$
	$Vs=0.5115E-02$	$-0.5115E-02$	$Ms=-0.4400E-03$	$0.1270E-03$	$(Ms/Ss)=-0.3055E+01$	$0.8817E+00$
	$Vt=0.2951E-02$	$-0.2951E-02$	$Mt=0.4495E-03$	$0.9302E-04$	$(Mt/St)=0.2211E+01$	$0.4575E+00$
	$(Tr^*CTOR/Jp)=0.1069E+01$		$-0.1069E+01$		$Smax=0.7688E+01$	
					$-0.1084E+01$	
					$Smin=-0.2843E+01$	
					$-0.3762E+01$	
96	[108	, 109]				
	$Fr=-0.1859E-01$	$0.1859E-01$	$Tr=0.2295E-03$	$-0.2295E-03$	$(P/A)=-0.1826E+01$	$0.1826E+01$
	$Vs=0.4385E-02$	$-0.4385E-02$	$Ms=-0.5150E-03$	$0.2100E-03$	$(Ms/Ss)=-0.3576E+01$	$0.1458E+01$
	$Vt=0.2876E-02$	$-0.2876E-02$	$Mt=0.2800E-03$	$0.1851E-03$	$(Mt/St)=0.1377E+01$	$0.9102E+00$
	$(Tr^*CTOR/Jp)=0.1135E+01$		$-0.1135E+01$		$Smax=0.3127E+01$	
					$0.4194E+01$	
					$Smin=-0.6779E+01$	
					$-0.5425E+00$	

DATE: 6/23/1993 TIME: 18:24:21

TITLE : Truss sensor calibration

CASE 1 CASE 2 CASE 3

SUBTITLE : MX = 1 MY = 1 MZ = 1

STRESS EVALUATION FOR STATIC ANALYSIS

STRESS OUTPUT FOR BEAM ELEMENT GROUP 2 CASE NO. 1

ELEMENT NUMBER	FORCES		MOMENTS		STRESSES	
	NODE1	NODE2	NODE1	NODE2	NODE1	NODE2
40	[52 ,	53]				
	Fr=0.4599E+00	- .4599E+00	Tr=-.7211E-03	0.7211E-03	(P/A) =0.3194E+02	- .3194E+02
	Vs=-.5228E-01	0.5228E-01	Ms=0.5098E-02	- .3737E-02	(Ms/Ss)=0.1770E+02	- .1298E+02
	Vt=-.1814E-01	0.1814E-01	Mt=-.8070E-02	0.4148E-02	(Mt/St)=-.2802E+02	0.1440E+02
			(Tr*CTOR/Jp)=-.2006E+01	0.2006E+01	Smax =0.7766E+02	- .4557E+01
					Smin =-.1378E+02	- .5932E+02
48	[60 ,	61]				
	Fr=0.5702E+00	- .5702E+00	Tr=-.6493E-04	0.6493E-04	(P/A) =0.3959E+02	- .3959E+02
	Vs=-.2334E-01	0.2334E-01	Ms=-.6731E-02	0.1221E-02	(Ms/Ss)=-.2337E+02	0.4239E+01
	Vt=0.7347E-01	- .7347E-01	Mt=-.7032E-03	- .1047E-02	(Mt/St)=-.2442E+01	- .3636E+01
			(Tr*CTOR/Jp)=-.1807E+00	0.1807E+00	Smax =0.6541E+02	- .3172E+02
					Smin =0.1378E+02	- .4747E+02
56	[68 ,	69]				
	Fr=-.5474E+00	0.5474E+00	Tr=-.1737E-02	0.1737E-02	(P/A) =-.3802E+02	0.3802E+02
	Vs=0.4932E-01	- .4932E-01	Ms=-.7582E-02	0.3231E-02	(Ms/Ss)=-.2633E+02	0.1122E+02
	Vt=0.5802E-01	- .5802E-01	Mt=0.5708E-02	- .2009E-02	(Mt/St)=0.1982E+02	- .6976E+01
			(Tr*CTOR/Jp)=-.4832E+01	0.4832E+01	Smax =0.8132E+01	0.5621E+02
					Smin =-.8416E+02	0.1982E+02
64	[76 ,	77]				
	Fr=-.4922E+00	0.4922E+00	Tr=-.1055E-02	0.1055E-02	(P/A) =-.3418E+02	0.3418E+02
	Vs=-.1754E-01	0.1754E-01	Ms=0.7922E-02	- .2109E-02	(Ms/Ss)=0.2751E+02	- .7322E+02
	Vt=-.7751E-01	0.7751E-01	Mt=-.5261E-02	0.3946E-02	(Mt/St)=-.1827E+02	0.1370E+02
			(Tr*CTOR/Jp)=-.2936E+01	0.2936E+01	Smax =0.1159E+02	0.5520E+02
					Smin =-.7995E+02	0.1316E+02
72	[84 ,	85]				
	Fr=0.8191E-02	- .8191E-02	Tr=0.5396E-03	- .5396E-03	(P/A) =0.8045E+00	- .8045E+00
	Vs=0.7097E-02	- .7097E-02	Ms=0.2117E-02	- .1037E-02	(Ms/Ss)=0.1470E+02	- .7202E+01
	Vt=-.1018E-01	0.1018E-01	Mt=0.2418E-02	- .1665E-02	(Mt/St)=0.1189E+02	- .8187E+01
			(Tr*CTOR/Jp)=0.2668E+01	- .2668E+01	Smax =0.2739E+02	0.1458E+02
					Smin =-.2578E+02	- .1619E+02
80	[92 ,	93]				
	Fr=-.1235E+00	0.1235E+00	Tr=-.2561E-03	0.2561E-03	(P/A) =-.1213E+02	0.1213E+02
	Vs=-.1923E-01	0.1923E-01	Ms=0.8938E-04	0.2618E-03	(Ms/Ss)=0.6206E+00	0.1818E+00
	Vt=-.3311E-02	0.3311E-02	Mt=-.2440E-02	0.3999E-03	(Mt/St)=-.1200E+02	0.1967E+01
			(Tr*CTOR/Jp)=-.1266E+01	0.1266E+01	Smax =0.4861E+00	0.1592E+02
					Smin =-.2475E+02	0.8350E+01
ELEMENT NUMBER	FORCES		MOMENTS		STRESSES	
	NODE1	NODE2	NODE1	NODE2	NODE1	NODE2
88	[100 ,	101]				
	Fr=0.1204E+00	- .1204E+00	Tr=-.1093E-02	0.1093E-02	(P/A) =0.1183E+02	- .1183E+02

Vs=-.9819E-02 0.9819E-02 Ms=-.1389E-02 0.5023E-03 (Ms/Ss)=-.9646E+01 0.3488E+01
 Vt=0.8361E-02 -.8361E-02 Mt=-.1350E-02 0.3083E-03 (Mt/St)=-.6638E+01 0.1516E+01
 (Tr*CTOR/Jp)=-.5405E+01 0.5405E+01 Smax =0.2811E+02 -.6823E+01
 Smin =-.4456E+01 -.1683E+02

96 [108 , 109]

Fr=-.4638E-04 0.4638E-04 Tr=0.1324E-03 -.1324E-03 (P/A)=-.4555E-02 0.4555E-02
 Vs=0.2387E-01 -.2387E-01 Ms=0.1346E-02 -.9865E-03 (Ms/Ss)=0.9345E+01 -.6850E+01
 Vt=-.3388E-02 0.3388E-02 Mt=0.3782E-02 -.1250E-02 (Mt/St)=0.1860E+02 -.6148E+01
 (Tr*CTOR/Jp)=0.6543E+00 -.6543E+00 Smax =0.2794E+02 0.1300E+02
 Smin =-.2795E+02 -.1299E+02

STRESS OUTPUT FOR BEAM ELEMENT GROUP 2 CASE NO. 2

ELEMENT NUMBER	FORCES		MOMENTS		STRESSES	
	NODE1	NODE2	NODE1	NODE2	NODE1	NODE2
40	[52 , 53]					
	Fr=-.8164E+00	0.8164E+00	Tr=-.6123E-02	0.6123E-02	(P/A)=-.5670E+02	0.5670E+02
	Vs=0.2128E-01	-.2128E-01	Ms=0.8755E-02	-.4769E-02	(Ms/Ss)=0.3040E+02	-.1656E+02
	Vt=-.5314E-01	0.5314E-01	Mt=-.1640E-02	0.3236E-02	(Mt/St)=-.5695E+01	0.1124E+02
			(Tr*CTOR/Jp)=-.1704E+02	0.1704E+02	Smax =-.2060E+02	0.8449E+02
					Smin =-.9279E+02	0.2890E+02
48	[60 , 61]					
	Fr=0.7109E+00	-.7109E+00	Tr=-.1186E-02	0.1186E-02	(P/A)=0.4937E+02	-.4937E+02
	Vs=-.1014E+00	0.1014E+00	Ms=0.1473E-01	-.6179E-02	(Ms/Ss)=0.5115E+02	-.2146E+00
	Vt=-.1140E+00	0.1140E+00	Mt=-.1519E-01	0.7582E-02	(Mt/St)=-.5273E+02	0.2633E+02
			(Tr*CTOR/Jp)=-.3299E+01	0.3299E+01	Smax =0.1532E+03	-.1581E+01
					Smin =-.5452E+02	-.9715E+02
56	[68 , 69]					
	Fr=0.2561E+00	-.2561E+00	Tr=0.1672E-02	-.1672E-02	(P/A)=0.1778E+02	-.1778E+02
	Vs=-.4621E-02	0.4621E-02	Ms=-.1093E-01	0.3027E-02	(Ms/Ss)=-.3794E+02	0.1051E+02
	Vt=0.1053E+00	-.1053E+00	Mt=-.4488E-03	0.1022E-03	(Mt/St)=-.1558E+01	0.3549E+00
			(Tr*CTOR/Jp)=0.4652E+01	-.4652E+01	Smax =0.5728E+02	-.6916E+01
					Smin =-.2171E+02	-.2865E+02
64	[76 , 77]					
	Fr=-.2746E+00	0.2746E+00	Tr=0.1881E-02	-.1881E-02	(P/A)=-.1907E+02	0.1907E+02
	Vs=0.4649E-01	-.4649E-01	Ms=0.1881E-02	-.9726E-03	(Ms/Ss)=0.6530E+01	-.3377E+01
	Vt=-.1211E-01	0.1211E-01	Mt=0.7716E-02	-.4228E-02	(Mt/St)=0.2679E+02	-.1468E+02
			(Tr*CTOR/Jp)=0.5233E+01	-.5233E+01	Smax =0.1425E+02	0.3713E+02
					Smin =-.5239E+02	0.1009E+01
72	[84 , 85]					
	Fr=0.2095E+00	-.2095E+00	Tr=-.6933E-03	0.6933E-03	(P/A)=0.2057E+02	-.2057E+02
	Vs=0.3357E-01	-.3357E-01	Ms=0.5885E-03	-.8092E-03	(Ms/Ss)=0.4086E+01	-.5618E+01
	Vt=0.2081E-02	-.2081E-02	Mt=0.8179E-02	-.4618E-02	(Mt/St)=0.4022E+02	-.2271E+02
			(Tr*CTOR/Jp)=-.3427E+01	0.3427E+01	Smax =0.6488E+02	0.7758E+01
					Smin =-.2374E+02	-.4890E+02
80	[92 , 93]					
	Fr=-.8903E-01	0.8903E-01	Tr=0.8940E-03	-.8940E-03	(P/A)=-.8744E+01	0.8744E+01
	Vs=0.3395E-01	-.3395E-01	Ms=0.3882E-02	-.1896E-02	(Ms/Ss)=0.2695E+02	-.1316E+02
	Vt=-.1873E-01	0.1873E-01	Mt=0.6350E-02	-.2750E-02	(Mt/St)=0.3123E+02	-.1352E+02
			(Tr*CTOR/Jp)=0.4420E+01	-.4420E+01	Smax =0.4944E+02	0.3543E+02
					Smin =-.6693E+02	-.1794E+02

ELEMENT NUMBER	FORCES		MOMENTS		STRESSES	
	NODE1	NODE2	NODE1	NODE2	NODE1	NODE2
88	[100 , 101]					
	Fr=	-.5351E-01	-.5351E-01	Tr=	-.1482E-03	0.1482E-03
	(P/A)	=0.5255E+01	-.5255E+01			
	Vs=	-.3319E-01	0.3319E-01	Ms=	0.1753E-03	-.2556E-04
	(Ms/Ss)	=0.1217E+01	-.1775E+00			
	Vt=	-.1411E-02	0.1411E-02	Mt=	-.5391E-02	0.1870E-02
	(Mt/St)	=-.2651E+02	0.9196E+01			
	(Tr*CTOR/Jp)	=-.7326E+00	0.7326E+00	Smax	=0.3298E+02	0.4119E+01
				Smin	=-.2247E+02	-.1463E+02
96	[108 , 109]					
	Fr=	-.7444E-02	0.7444E-02	Tr=	0.6898E-03	-.6898E-03
	(P/A)	=-.7311E+00	0.7311E+00			
	Vs=	-.2788E-02	0.2788E-02	Ms=	-.2018E-02	0.1057E-02
	(Ms/Ss)	=-.1401E+02	0.7341E+01			
	Vt=	0.9054E-02	-.9054E-02	Mt=	-.8537E-03	0.5580E-03
	(Mt/St)	=-.4198E+01	0.2744E+01			
	(Tr*CTOR/Jp)	=0.3410E+01	-.3410E+01	Smax	=0.1748E+02	0.1082E+02
				Smin	=-.1894E+02	-.9354E+01

STRESS OUTPUT FOR BEAM ELEMENT GROUP 2 CASE NO. 3

ELEMENT NUMBER	FORCES		MOMENTS		STRESSES	
	NODE1	NODE2	NODE1	NODE2	NODE1	NODE2
40	[52 , 53]					
	Fr=	-.5360E+00	0.5360E+00	Tr=	-.7941E-02	0.7941E-02
	(P/A)	=-.3722E+02	0.3722E+02			
	Vs=	0.9666E-02	-.9666E-02	Ms=	-.1160E-02	-.3300E-02
	(Ms/Ss)	=-.4027E+01	-.1146E+02			
	Vt=	0.5946E-01	-.5946E-01	Mt=	-.6043E-02	0.6768E-02
	(Mt/St)	=-.2098E+02	0.2350E+02			
	(Tr*CTOR/Jp)	=-.2210E+02	0.2210E+02	Smax	=-.1221E+02	0.7218E+02
				Smin	=-.6223E+02	0.2264E+01
48	[60 , 61]					
	Fr=	-.1802E+00	0.1802E+00	Tr=	-.5813E-02	0.5813E-02
	(P/A)	=-.1251E+02	0.1251E+02			
	Vs=	-.1066E-01	0.1066E-01	Ms=	-.4009E-02	-.2294E-02
	(Ms/Ss)	=-.1392E+02	-.7964E+01			
	Vt=	0.8403E-01	-.8403E-01	Mt=	-.7989E-02	0.7190E-02
	(Mt/St)	=-.2774E+02	0.2496E+02			
	(Tr*CTOR/Jp)	=-.1618E+02	0.1618E+02	Smax	=0.2915E+02	0.4544E+02
				Smin	=-.5417E+02	-.2042E+02
56	[68 , 69]					
	Fr=	-.5140E+00	0.5140E+00	Tr=	-.5849E-02	0.5849E-02
	(P/A)	=-.3569E+02	0.3569E+02			
	Vs=	0.3580E-01	-.3580E-01	Ms=	-.1365E-01	0.7012E-03
	(Ms/Ss)	=-.4740E+02	0.2435E+01			
	Vt=	0.1727E+00	-.1727E+00	Mt=	-.1100E-02	0.3785E-02
	(Mt/St)	=-.3821E+01	0.1314E+02			
	(Tr*CTOR/Jp)	=-.1628E+02	0.1628E+02	Smax	=0.1553E+02	0.5127E+02
				Smin	=-.8692E+02	0.2012E+02
64	[76 , 77]					
	Fr=	-.2336E+00	0.2336E+00	Tr=	-.5637E-02	0.5637E-02
	(P/A)	=-.1622E+02	0.1622E+02			
	Vs=	0.4713E-01	-.4713E-01	Ms=	-.2476E-03	-.4071E-02
	(Ms/Ss)	=-.8598E+00	-.1414E+02			
	Vt=	0.5759E-01	-.5759E-01	Mt=	0.1288E-02	0.2247E-02
	(Mt/St)	=0.4471E+01	0.7803E+01			
	(Tr*CTOR/Jp)	=-.1568E+02	0.1568E+02	Smax	=-.1089E+02	0.3816E+02
				Smin	=-.2156E+02	-.5715E+01
72	[84 , 85]					
	Fr=	0.5050E+00	-.5050E+00	Tr=	-.1464E-02	0.1464E-02
	(P/A)	=0.4960E+02	-.4960E+02			
	Vs=	0.9568E-02	-.9568E-02	Ms=	0.2013E-02	-.1692E-02
	(Ms/Ss)	=0.1398E+02	-.1175E+02			
	Vt=	-.3028E-02	0.3028E-02	Mt=	0.5985E-02	-.4971E-02
	(Mt/St)	=0.2944E+02	-.2445E+02			
	(Tr*CTOR/Jp)	=-.7236E+01	0.7236E+01	Smax	=0.9302E+02	-.1341E+02
				Smin	=0.6185E+01	-.8580E+02
80	[92 , 93]					

Fr=0.4656E+00 -.4656E+00 Tr=-.1095E-02 0.1095E-02 (P/A)=0.4572E+02 -.4572E+02
Vs=-.3713E-02 0.3713E-02 Ms=0.2495E-02 -.1798E-02 (Ms/Ss)=0.1732E+02 -.1248E+02
Vt=-.6571E-02 0.6571E-02 Mt=0.3202E-02 -.3596E-02 (Mt/St)=0.1575E+02 -.1768E+02
(Tr*CTOR/Jp)=-.5415E+01 0.5415E+01 Smax =0.7879E+02 -.1556E+02
Smin =0.1266E+02 -.7589E+02

ELEMENT NUMBER	FORCES		MOMENTS		STRESSES	
	NODE1	NODE2	NODE1	NODE2	NODE1	NODE2
88	[100	, 101]				
	Fr=0.5096E+00	-.5096E+00	Tr=-.1691E-02	0.1691E-02	(P/A)=0.5005E+02	-.5005E+02
	Vs=-.2706E-01	0.2706E-01	Ms=0.7367E-03	-.9464E-03	(Ms/Ss)=0.5116E+01	-.6571E+01
	Vt=0.1976E-02	-.1976E-02	Mt=-.3140E-03	-.2556E-02	(Mt/St)=-.1544E+01	-.1257E+02
			(Tr*CTOR/Jp)=-.8358E+01	0.8358E+01	Smax =0.5671E+02	-.3091E+02
					Smin =0.4339E+02	-.6919E+02
96	[108	, 109]				
	Fr=0.5857E+00	-.5857E+00	Tr=-.7007E-03	0.7007E-03	(P/A)=0.5753E+02	-.5753E+02
	Vs=0.2721E-02	-.2721E-02	Ms=0.1983E-03	-.5619E-03	(Ms/Ss)=0.1377E+01	-.3901E+01
	Vt=0.3428E-02	-.3428E-02	Mt=0.4427E-02	-.4139E-02	(Mt/St)=0.2177E+02	-.2035E+02
			(Tr*CTOR/Jp)=-.3464E+01	0.3464E+01	Smax =0.8068E+02	-.3327E+02
					Smin =0.3438E+02	-.8178E+02

APPENDIX C

STEWART-PLATFORM TRANSDUCER FEM PROGRAM AND OUTPUT

In the next pages, the Finite Element program written to model and analyze the Stewart-Platform transducer is shown together with its output.

The program generates a model composed of plate and 3D beam elements (Fig.21). By using this program, the behavior curves of the Stewart-Platform were obtained. The compliance matrix for evaluation of the sensor is also obtained from the data generated from the program.

The output shows the result of the numerical calibration used to obtain the compliance matrix. Like the Truss sensor, the stress of interest is (P/A) at node 2 of each element. For example, from the first page of the output, element 57 is formed by node 1 (40) and node 2 (41). The stress (P/A) at node 2 (41) is -98.13. The first part shows the force calibration, while the second part shows the moment calibration.

C*
 C* COSMOS/M Geostar V1.65
 C* Problem : PLATFORM Date : 15-JUN-93 Time : 15:01:44
 C*
 EGROUP,1,SHELL4T,1,0,0,0,0,0,
 RCONST,1,1,1,6,0.3,0,0,0,0,
 PICK_MAT,1,A_STEEL,FPS,
 C* MATL:A_STEEL : ALLOY STEEL

 C* EX 30.0E+6 p.s.i.
 C* NUXY 0.28
 C* GXY 11.50E+6 p.s.i.
 C* ALPX 7.4E-6 /Fahrenheit
 C* DENS 7.246E-4 lb.s./in**4
 C* KX 6.688E-4 BTU/in.s.F
 C* C (Cp) 42.5426 BTUin/lbssF
 EGROUP,2,BEAM3D,0,0,0,0,0,0,
 RCONST,2,1,1,10,6.9E-3,3.79E-6,3.79E-6,9.375E-2,9.375E-2,0,0,7.58E-6,0&
 ,0,
 RCONST,2,1,11,4,0,0,0,0.046875,
 RCONST,2,2,1,10,2.761E-2,6.067E-5,6.067E-5,0.1875,0.1875,0,0,1.213E-4,&
 0,0,
 RCONST,2,2,11,4,0,0,0,0.09375,
 PICK_MAT,2,ALUMINUM,FPS,
 C* MATL:ALUMINUM : ALUMINUM ALLOY

 C* EX 10.3E+6 p.s.i.
 C* NUXY 0.36
 C* GXY 3.80E+6 p.s.i.
 C* ALPX 12.8E-6 /Fahrenheit
 C* DENS 2.51E-4 lb.s./in**4
 C* KX 2.194E-3 BTU/in.s.F
 C* C (Cp) 88.9493 BTUin/lbssF
 PLANE,Z,0,1,
 PT,1,0.5,0,0,
 PT,2,-0.5,0,0,
 SCALE,0,
 CRPCIRDIA,1,1,2,360,6,
 SCALE,0,
 CRLINE,7,3,4,
 CRLINE,8,3,5,
 CRLINE,9,3,2,
 CRLINE,10,3,6,
 CRLINE,11,3,7,
 CRLINE,12,3,1,
 PT,8,0.5,0.8660254,-0.6124,
 PT,9,-1,0,-0.6124,
 PT,10,0.5,-0.8660254,-0.6124,
 SCALE,0,
 CRLINE,13,1,10,
 CRLINE,14,1,8,
 CRLINE,15,5,8,
 CRLINE,16,5,9,
 CRLINE,17,6,9,
 CRLINE,18,6,10,
 SF3CR,1,1,7,12,0,

SF3CR,2,7,2,8,0,
SF3CR,3,8,3,9,0,
SF3CR,4,9,4,10,0,
SF3CR,5,10,5,11,0,
SF3CR,6,11,6,12,0,
SCALE,0,
PT,11,0,0,0.6124,
CRLINE,25,11,6,
CRLINE,26,11,1,
CRLINE,27,11,5,
SCALE,0,
ACTSET,EG,1,
ACTSET,RC,1,
ACTSET,MP,1,
MA_SF,1,6,1,0,0.2,
SCALE,0,
ACTSET,EG,2,
ACTSET,RC,1,
ACTSET,MP,2,
M_CR,13,18,1,3,10,1,3,
ACTSET,EG,2,
ACTSET,RC,2,
ACTSET,MP,1,
M_CR,25,27,1,3,3,1,3,
SCALE,0,
NMERGE,1,146,1,0.0001,0,1,0,
NCOMPRESS,1,144,1,
DND,56,ALL,0,56,1,
SCALE,0,
DND,46,ALL,0,46,1,
SCALE,0,
DND,75,ALL,0,75,1,
SCALE,0,
FND,94,FX,1,94,1,
SCALE,0,
PRINT_ELSET,6,57,57,67,67,77,77,87,87,97,97,107,107,
ACTSET,LC,2,
FND,94,FY,1,94,1,
PRINT_ELSET,6,57,57,67,67,77,77,87,87,97,97,107,107,
ACTSET,LC,3,
FND,94,FZ,1,94,1,
PRINT_ELSET,6,57,57,67,67,77,77,87,87,97,97,107,107,
SCALE,0,
PRINT_OPS,0,0,0,1,0,1,0,0,0,0,
R_STATIC

DATE: 6/19/1993 TIME: 13:30:42

TITLE : CALIBRATION FOR STEWART PLATFORM (FIRST PART)

SUBTITLE : FX=1 (CASE 1), FY=1 (CASE 2), FZ=1 (CASE 3)

STRESS EVALUATION FOR STATIC ANALYSIS

STRESS OUTPUT FOR BEAM ELEMENT GROUP 2 CASE NO. 1

ELEMENT NUMBER	FORCES		MOMENTS		STRESSES	
	NODE1	NODE2	NODE1	NODE2	NODE1	NODE2
57	[40	, 41]	(circular)			
	Fr=0.6771E+00	-0.6771E+00	Tr=-0.7367E-03	0.7367E-03	(P/A)=0.9813E+02	-0.9813E+02
	Vs=-0.3070E-02	0.3070E-02	Ms=-0.5987E-03	0.2309E-05	(Ms/Ss)=-0.7405E+01	0.2855E-01
	Vt=0.5623E-02	-0.5623E-02	Mt=0.3810E-03	-0.7066E-03	(Mt/St)=0.4712E+01	-0.8740E+01
			(Tr*CTOR/Jp)=-0.4556E+01	0.4556E+01	Smax =0.1069E+03	0.3446E-02
			(Hoop Stres)=0.3446E-02	0.3446E-02	Smin =0.8935E+02	-0.1069E+03
67	[50	, 51]	(circular)			
	Fr=0.6771E+00	-0.6771E+00	Tr=0.7371E-03	-0.7371E-03	(P/A)=0.9813E+02	-0.9813E+02
	Vs=-0.3075E-02	0.3075E-02	Ms=0.5914E-03	0.2283E-05	(Ms/Ss)=0.7314E+01	0.2824E-01
	Vt=-0.5597E-02	0.5597E-02	Mt=0.3797E-03	-0.7058E-03	(Mt/St)=0.4696E+01	-0.8730E+01
			(Tr*CTOR/Jp)=0.4558E+01	-0.4558E+01	Smax =0.1068E+03	0.3446E-02
			(Hoop Stres)=0.3446E-02	0.3446E-02	Smin =0.8944E+02	-0.1069E+03
77	[60	, 61]	(circular)			
	Fr=0.1696E-01	-0.1696E-01	Tr=0.1947E-03	-0.1947E-03	(P/A)=0.2457E+01	-0.2457E+01
	Vs=-0.3039E-03	0.3039E-03	Ms=-0.2042E-02	0.1560E-02	(Ms/Ss)=-0.2526E+02	0.1929E+02
	Vt=0.4547E-02	-0.4547E-02	Mt=-0.7141E-03	0.6819E-03	(Mt/St)=-0.8832E+01	0.8433E+01
			(Tr*CTOR/Jp)=0.1204E+01	-0.1204E+01	Smax =0.2922E+02	0.1860E+02
			(Hoop Stres)=0.3446E-02	0.3446E-02	Smin =-0.2430E+02	-0.2351E+02
87	[69	, 70]	(circular)			
	Fr=-0.6940E+00	0.6940E+00	Tr=-0.5393E-03	0.5393E-03	(P/A)=-0.1006E+03	0.1006E+03
	Vs=0.3431E-02	-0.3431E-02	Ms=-0.2637E-02	0.1560E-02	(Ms/Ss)=-0.3262E+02	0.1929E+02
	Vt=0.1016E-01	-0.1016E-01	Mt=0.3424E-03	0.2154E-04	(Mt/St)=0.4235E+01	0.2664E+00
			(Tr*CTOR/Jp)=-0.3335E+01	0.3335E+01	Smax =0.3446E-02	0.1199E+03
			(Hoop Stres)=0.3446E-02	0.3446E-02	Smin =-0.1335E+03	0.8129E+02
97	[79	, 80]	(circular)			
	Fr=-0.6941E+00	0.6941E+00	Tr=0.5395E-03	-0.5395E-03	(P/A)=-0.1006E+03	0.1006E+03
	Vs=0.3406E-02	-0.3406E-02	Ms=0.2641E-02	-0.1562E-02	(Ms/Ss)=0.3267E+02	-0.1932E+02
	Vt=-0.1017E-01	0.1017E-01	Mt=0.3388E-03	0.2241E-04	(Mt/St)=0.4191E+01	0.2772E+00
			(Tr*CTOR/Jp)=0.3336E+01	-0.3336E+01	Smax =0.3446E-02	0.1199E+03
			(Hoop Stres)=0.3446E-02	0.3446E-02	Smin =-0.1335E+03	0.8126E+02

ELEMENT NUMBER	FORCES		MOMENTS		STRESSES	
	NODE1	NODE2	NODE1	NODE2	NODE1	NODE2
107	[88	, 89]	(circular)			
	Fr=0.1692E-01	-0.1692E-01	Tr=-0.1954E-03	0.1954E-03	(P/A)=0.2452E+01	-0.2452E+01
	Vs=-0.3250E-03	0.3250E-03	Ms=0.2046E-02	-0.1562E-02	(Ms/Ss)=0.2531E+02	-0.1932E+02
	Vt=-0.4560E-02	0.4560E-02	Mt=-0.7164E-03	0.6819E-03	(Mt/St)=-0.8860E+01	0.8434E+01
			(Tr*CTOR/Jp)=-0.1208E+01	0.1208E+01	Smax =0.2926E+02	0.1863E+02
			(Hoop Stres)=0.3446E-02	0.3446E-02	Smin =-0.2436E+02	-0.2354E+02

STRESS OUTPUT FOR BEAM ELEMENT GROUP 2 CASE NO. 2

ELEMENT NUMBER	FORCES		MOMENTS		STRESSES	
	NODE1	NODE2	NODE1	NODE2	NODE1	NODE2
57	[40	, 41]	(circular)			
	Fr=-.4105E+00	0.4105E+00	Tr=0.2004E-03	-.2004E-03	(P/A)=-.5949E+02	0.5949E+02
	Vs=0.2202E-02	-.2202E-02	Ms=0.2696E-02	-.1798E-02	(Ms/Ss)=0.3334E+02	-.2223E+02
	Vt=-.8468E-02	0.8468E-02	Mt=0.6198E-03	-.3863E-03	(Mt/St)=0.7666E+01	-.4777E+01
			(Tr*CTOR/Jp)=0.1239E+01	-.1239E+01	Smax =0.3446E-02	0.8223E+02
			(Hoop Stres)=0.3446E-02	0.3446E-02	Smin =-.9370E+02	0.3675E+02
67	[50	, 51]	(circular)			
	Fr=0.4105E+00	-.4105E+00	Tr=0.2019E-03	-.2019E-03	(P/A)=0.5949E+02	-.5949E+02
	Vs=-.2159E-02	0.2159E-02	Ms=0.2696E-02	-.1798E-02	(Ms/Ss)=0.3334E+02	-.2223E+02
	Vt=-.8468E-02	0.8468E-02	Mt=-.6138E-03	0.3847E-03	(Mt/St)=-.7591E+01	0.4759E+01
			(Tr*CTOR/Jp)=0.1249E+01	-.1249E+01	Smax =0.9368E+02	0.3446E-02
			(Hoop Stres)=0.3446E-02	0.3446E-02	Smin =0.2529E+02	-.8223E+02
77	[60	, 61]	(circular)			
	Fr=0.7917E+00	-.7917E+00	Tr=-.7380E-03	0.7380E-03	(P/A)=0.1147E+03	-.1147E+03
	Vs=-.3728E-02	0.3728E-02	Ms=-.1863E-02	0.8986E-03	(Ms/Ss)=-.2304E+02	0.1111E+02
	Vt=0.9091E-02	-.9091E-02	Mt=0.2640E-04	-.4218E-03	(Mt/St)=0.3265E+00	-.5217E+01
			(Tr*CTOR/Jp)=-.4564E+01	0.4564E+01	Smax =0.1378E+03	0.3446E-02
			(Hoop Stres)=0.3446E-02	0.3446E-02	Smin =0.9170E+02	-.1270E+03
87	[69	, 70]	(circular)			
	Fr=0.3812E+00	-.3812E+00	Tr=0.5394E-03	-.5394E-03	(P/A)=0.5524E+02	-.5524E+02
	Vs=-.1575E-02	0.1575E-02	Ms=-.8322E-03	0.8986E-03	(Ms/Ss)=-.1029E+02	0.1111E+02
	Vt=-.6261E-03	0.6261E-03	Mt=0.6353E-03	-.8024E-03	(Mt/St)=0.7858E+01	-.9924E+01
			(Tr*CTOR/Jp)=0.3336E+01	-.3336E+01	Smax =0.6819E+02	0.3446E-02
			(Hoop Stres)=0.3446E-02	0.3446E-02	Smin =0.4229E+02	-.7014E+02
97	[79	, 80]	(circular)			
	Fr=-.3812E+00	0.3812E+00	Tr=0.5354E-03	-.5354E-03	(P/A)=-.5525E+02	0.5525E+02
	Vs=0.1554E-02	-.1554E-02	Ms=-.8329E-03	0.8990E-03	(Ms/Ss)=-.1030E+02	0.1112E+02
	Vt=-.6234E-03	0.6234E-03	Mt=-.6411E-03	0.8059E-03	(Mt/St)=-.7929E+01	0.9968E+01
			(Tr*CTOR/Jp)=0.3311E+01	-.3311E+01	Smax =0.3446E-02	0.7018E+02
			(Hoop Stres)=0.3446E-02	0.3446E-02	Smin =-.6825E+02	0.4031E+02

ELEMENT NUMBER	FORCES		MOMENTS		STRESSES	
	NODE1	NODE2	NODE1	NODE2	NODE1	NODE2
107	[88	, 89]	(circular)			
	Fr=-.7917E+00	0.7917E+00	Tr=-.7391E-03	0.7391E-03	(P/A)=-.1147E+03	0.1147E+03
	Vs=0.3763E-02	-.3763E-02	Ms=-.1864E-02	0.8990E-03	(Ms/Ss)=-.2305E+02	0.1112E+02
	Vt=0.9094E-02	-.9094E-02	Mt=-.1638E-04	0.4155E-03	(Mt/St)=-.2026E+00	0.5139E+01
			(Tr*CTOR/Jp)=-.4571E+01	0.4571E+01	Smax =0.3446E-02	0.1270E+03
			(Hoop Stres)=0.3446E-02	0.3446E-02	Smin =-.1378E+03	0.1025E+03

STRESS OUTPUT FOR BEAM ELEMENT GROUP 2 CASE NO. 3

ELEMENT NUMBER	FORCES		MOMENTS		STRESSES	
	NODE1	NODE2	NODE1	NODE2	NODE1	NODE2
57	[40	, 41]	(circular)			
	Fr=-.2853E+00	0.2853E+00	Tr=-.9449E-04	0.9449E-04	(P/A)=-.4135E+02	0.4135E+02
	Vs=0.1139E-02	-.1139E-02	Ms=0.2497E-03	0.6551E-06	(Ms/Ss)=0.3088E+01	0.8102E-02
	Vt=-.2360E-02	0.2360E-02	Mt=0.2148E-03	-.9399E-04	(Mt/St)=0.2656E+01	-.1162E+01

(Tr*CTOR/Jp)=-.5843E+00 0.5843E+00 Smax =0.3446E-02 0.4251E+02
 (Hoop Stres)=0.3446E-02 0.3446E-02 Smin =-.4542E+02 0.4019E+02
 67 [50 , 51] (circular)
 Fr=-.2853E+00 0.2853E+00 Tr=0.9688E-04 -.9688E-04 (P/A) =-.4135E+02 0.4135E+02
 Vs=0.1113E-02 -.1113E-02 Ms=-.2518E-03 0.6659E-06 (Ms/Ss)=-.3114E+01 0.8236E-02
 Vt=0.2368E-02 -.2368E-02 Mt=0.2074E-03 -.8941E-04 (Mt/St)=0.2565E+01 -.1106E+01
 (Tr*CTOR/Jp)=0.5991E+00 -.5991E+00 Smax =0.3446E-02 0.4246E+02
 (Hoop Stres)=0.3446E-02 0.3446E-02 Smin =-.4539E+02 0.4025E+02
 77 [60 , 61] (circular)
 Fr=-.2853E+00 0.2853E+00 Tr=-.9688E-04 0.9688E-04 (P/A) =-.4135E+02 0.4135E+02
 Vs=0.1118E-02 -.1118E-02 Ms=0.2510E-03 -.1947E-06 (Ms/Ss)=0.3105E+01 -.2408E-02
 Vt=-.2365E-02 0.2365E-02 Mt=0.2083E-03 -.8967E-04 (Mt/St)=0.2576E+01 -.1109E+01
 (Tr*CTOR/Jp)=-.5991E+00 0.5991E+00 Smax =0.3446E-02 0.4246E+02
 (Hoop Stres)=0.3446E-02 0.3446E-02 Smin =-.4539E+02 0.4024E+02
 87 [69 , 70] (circular)
 Fr=-.2853E+00 0.2853E+00 Tr=0.9468E-04 -.9468E-04 (P/A) =-.4135E+02 0.4135E+02
 Vs=0.1142E-02 -.1142E-02 Ms=-.2504E-03 -.1945E-06 (Ms/Ss)=-.3097E+01 -.2406E-02
 Vt=0.2363E-02 -.2363E-02 Mt=0.2150E-03 -.9390E-04 (Mt/St)=0.2659E+01 -.1161E+01
 (Tr*CTOR/Jp)=0.5855E+00 -.5855E+00 Smax =0.3446E-02 0.4251E+02
 (Hoop Stres)=0.3446E-02 0.3446E-02 Smin =-.4543E+02 0.4019E+02
 97 [79 , 80] (circular)
 Fr=-.2853E+00 0.2853E+00 Tr=-.9576E-04 0.9576E-04 (P/A) =-.4135E+02 0.4135E+02
 Vs=0.1136E-02 -.1136E-02 Ms=0.2515E-03 -.4654E-06 (Ms/Ss)=0.3111E+01 -.5756E-02
 Vt=-.2367E-02 0.2367E-02 Mt=0.2119E-03 -.9150E-04 (Mt/St)=0.2621E+01 -.1132E+01
 (Tr*CTOR/Jp)=-.5922E+00 0.5922E+00 Smax =0.3446E-02 0.4248E+02
 (Hoop Stres)=0.3446E-02 0.3446E-02 Smin =-.4542E+02 0.4022E+02

 ELEMENT FORCES MOMENTS STRESSES
 NUMBER NODE1 NODE2 NODE1 NODE2 NODE1 NODE2
 107 [88 , 89] (circular)
 Fr=-.2853E+00 0.2853E+00 Tr=0.9557E-04 -.9557E-04 (P/A) =-.4135E+02 0.4135E+02
 Vs=0.1138E-02 -.1138E-02 Ms=-.2500E-03 -.4657E-06 (Ms/Ss)=-.3092E+01 -.5759E-02
 Vt=0.2361E-02 -.2361E-02 Mt=0.2125E-03 -.9185E-04 (Mt/St)=0.2629E+01 -.1136E+01
 (Tr*CTOR/Jp)=0.5910E+00 -.5910E+00 Smax =0.3446E-02 0.4249E+02
 (Hoop Stres)=0.3446E-02 0.3446E-02 Smin =-.4541E+02 0.4022E+02

DATE: 6/19/1993 TIME: 13:40:56

TITLE : CALIBRATION OF STEWART PLATFORM (SECOND PART)

SUBTITLE : MX=1 (CASE 1), MY=1 (CASE 2), MY=1 (CASE 3)

STRESS EVALUATION FOR STATIC ANALYSIS

STRESS OUTPUT FOR BEAM ELEMENT GROUP 2 CASE NO. 1

ELEMENT NUMBER	FORCES		MOMENTS		STRESSES	
	NODE1	NODE2	NODE1	NODE2	NODE1	NODE2
57	[40 ,	41]	(circular)			
	Fr=0.1062E-01	- .1062E-01	Tr=0.4198E-03	- .4198E-03	(P/A) =0.1539E+01	- .1539E+01
	Vs=0.4543E-02	- .4543E-02	Ms=-.3825E-02	0.2394E-02	(Ms/Ss)=-.4731E+02	0.2961E+02
	Vt=0.1350E-01	- .1350E-01	Mt=0.1286E-02	- .8045E-03	(Mt/St)=0.1591E+02	- .9950E+01
			(Tr*CTOR/Jp)=0.2596E+01	- .2596E+01	Smax =0.5146E+02	0.2969E+02
			(Hoop Stres)=0.3446E-02	0.3446E-02	Smin =-.4838E+02	- .3277E+02
67	[50 ,	51]	(circular)			
	Fr=-.1065E-01	0.1065E-01	Tr=0.4197E-03	- .4197E-03	(P/A) =-.1544E+01	0.1544E+01
	Vs=-.4559E-02	0.4559E-02	Ms=-.3825E-02	0.2394E-02	(Ms/Ss)=-.4731E+02	0.2961E+02
	Vt=0.1350E-01	- .1350E-01	Mt=-.1288E-02	0.8045E-03	(Mt/St)=-.1593E+02	0.9950E+01
			(Tr*CTOR/Jp)=0.2596E+01	- .2596E+01	Smax =0.4838E+02	0.3278E+02
			(Hoop Stres)=0.3446E-02	0.3446E-02	Smin =-.5147E+02	- .2969E+02
77	[60 ,	61]	(circular)			
	Fr=-.9621E+00	0.9621E+00	Tr=0.3119E-03	- .3119E-03	(P/A) =-.1394E+03	0.1394E+03
	Vs=-.3036E-02	0.3036E-02	Ms=0.2751E-02	- .1195E-02	(Ms/Ss)=0.3402E+02	- .1478E+02
	Vt=-.1467E-01	0.1467E-01	Mt=-.1224E-02	0.9016E-03	(Mt/St)=-.1513E+02	0.1115E+02
			(Tr*CTOR/Jp)=0.1929E+01	- .1929E+01	Smax =0.3446E-02	0.1580E+03
			(Hoop Stres)=0.3446E-02	0.3446E-02	Smin =-.1767E+03	0.1209E+03
87	[69 ,	70]	(circular)			
	Fr=-.9515E+00	0.9515E+00	Tr=-.7312E-03	0.7312E-03	(P/A) =-.1379E+03	0.1379E+03
	Vs=0.1509E-02	- .1509E-02	Ms=0.1069E-02	- .1195E-02	(Ms/Ss)=0.1322E+02	- .1478E+02
	Vt=0.1189E-02	- .1189E-02	Mt=0.6193E-04	0.9808E-04	(Mt/St)=0.7660E+00	0.1213E+01
			(Tr*CTOR/Jp)=-.4522E+01	0.4522E+01	Smax =0.3446E-02	0.1527E+03
			(Hoop Stres)=0.3446E-02	0.3446E-02	Smin =-.1511E+03	0.1231E+03
97	[79 ,	80]	(circular)			
	Fr=0.9515E+00	- .9515E+00	Tr=-.7323E-03	0.7323E-03	(P/A) =0.1379E+03	- .1379E+03
	Vs=-.1498E-02	0.1498E-02	Ms=0.1075E-02	- .1199E-02	(Ms/Ss)=0.1329E+02	- .1482E+02
	Vt=0.1170E-02	- .1170E-02	Mt=-.6115E-04	- .9773E-04	(Mt/St)=-.7563E+00	- .1209E+01
			(Tr*CTOR/Jp)=-.4529E+01	0.4529E+01	Smax =0.1512E+03	0.3446E-02
			(Hoop Stres)=0.3446E-02	0.3446E-02	Smin =0.1246E+03	- .1528E+03

ELEMENT NUMBER	FORCES		MOMENTS		STRESSES	
	NODE1	NODE2	NODE1	NODE2	NODE1	NODE2
107	[88 ,	89]	(circular)			
	Fr=0.9621E+00	- .9621E+00	Tr=0.3121E-03	- .3121E-03	(P/A) =0.1394E+03	- .1394E+03
	Vs=0.3058E-02	- .3058E-02	Ms=0.2756E-02	- .1199E-02	(Ms/Ss)=0.3409E+02	- .1482E+02
	Vt=-.1469E-01	0.1469E-01	Mt=0.1228E-02	- .9032E-03	(Mt/St)=0.1518E+02	- .1117E+02
			(Tr*CTOR/Jp)=0.1930E+01	- .1930E+01	Smax =0.1768E+03	0.3446E-02
			(Hoop Stres)=0.3446E-02	0.3446E-02	Smin =0.1021E+03	- .1580E+03

STRESS OUTPUT FOR BEAM ELEMENT GROUP 2 CASE NO. 2

ELEMENT NUMBER	FORCES		MOMENTS		STRESSES	
	NODE1	NODE2	NODE1	NODE2	NODE1	NODE2
57	[40 ,	41]	(circular)			
	Fr=0.1105E+01	-.1105E+01	Tr=-.6003E-03	0.6003E-03	(P/A)=0.1601E+03	-.1601E+03
	Vs=0.8854E-03	-.8854E-03	Ms=-.9745E-03	0.2336E-05	(Ms/Ss)=-.1205E+02	0.2890E-01
	Vt=0.9166E-02	-.9166E-02	Mt=0.6735E-03	-.5796E-03	(Mt/St)=0.8330E+01	-.7169E+01
			(Tr*CTOR/Jp)=-.3712E+01	0.3712E+01	Smax =0.1748E+03	0.3446E-02
			(Hoop Stres)=0.3446E-02	0.3446E-02	Smin =0.1455E+03	-.1673E+03
67	[50 ,	51]	(circular)			
	Fr=0.1105E+01	-.1105E+01	Tr=0.6033E-03	-.6033E-03	(P/A)=0.1601E+03	-.1601E+03
	Vs=0.8525E-03	-.8525E-03	Ms=0.9671E-03	0.2295E-05	(Ms/Ss)=0.1196E+02	0.2838E-01
	Vt=-.9140E-02	0.9140E-02	Mt=0.6642E-03	-.5738E-03	(Mt/St)=0.8215E+01	-.7097E+01
			(Tr*CTOR/Jp)=0.3731E+01	-.3731E+01	Smax =0.1746E+03	0.3446E-02
			(Hoop Stres)=0.3446E-02	0.3446E-02	Smin =0.1456E+03	-.1672E+03
77	[60 ,	61]	(circular)			
	Fr=-.5431E+00	0.5431E+00	Tr=0.6675E-03	-.6675E-03	(P/A)=-.7871E+02	0.7871E+02
	Vs=0.3555E-02	-.3555E-02	Ms=-.2838E-02	0.2080E-02	(Ms/Ss)=-.3511E+02	0.2572E+02
	Vt=0.7151E-02	-.7151E-02	Mt=0.7929E-03	-.4158E-03	(Mt/St)=0.9806E+01	-.5143E+01
			(Tr*CTOR/Jp)=0.4128E+01	-.4128E+01	Smax =0.3446E-02	0.1049E+03
			(Hoop Stres)=0.3446E-02	0.3446E-02	Smin =-.1152E+03	0.5248E+02
87	[69 ,	70]	(circular)			
	Fr=-.5616E+00	0.5616E+00	Tr=0.6683E-04	-.6683E-04	(P/A)=-.8139E+02	0.8139E+02
	Vs=-.4407E-02	0.4407E-02	Ms=-.3809E-02	0.2080E-02	(Ms/Ss)=-.4711E+02	0.2572E+02
	Vt=0.1630E-01	-.1630E-01	Mt=-.1459E-02	0.9915E-03	(Mt/St)=-.1804E+02	0.1226E+02
			(Tr*CTOR/Jp)=0.4133E+00	-.4133E+00	Smax =0.3446E-02	0.1099E+03
			(Hoop Stres)=0.3446E-02	0.3446E-02	Smin =-.1318E+03	0.5289E+02
97	[79 ,	80]	(circular)			
	Fr=-.5616E+00	0.5616E+00	Tr=-.6789E-04	0.6789E-04	(P/A)=-.8139E+02	0.8139E+02
	Vs=-.4431E-02	0.4431E-02	Ms=0.3813E-02	-.2082E-02	(Ms/Ss)=0.4716E+02	-.2575E+02
	Vt=-.1632E-01	0.1632E-01	Mt=-.1465E-02	0.9948E-03	(Mt/St)=-.1812E+02	0.1230E+02
			(Tr*CTOR/Jp)=-.4198E+00	0.4198E+00	Smax =0.3446E-02	0.1099E+03
			(Hoop Stres)=0.3446E-02	0.3446E-02	Smin =-.1319E+03	0.5285E+02

ELEMENT NUMBER	FORCES		MOMENTS		STRESSES	
	NODE1	NODE2	NODE1	NODE2	NODE1	NODE2
107	[88 ,	89]	(circular)			
	Fr=-.5432E+00	0.5432E+00	Tr=-.6695E-03	0.6695E-03	(P/A)=-.7872E+02	0.7872E+02
	Vs=0.3563E-02	-.3563E-02	Ms=0.2842E-02	-.2082E-02	(Ms/Ss)=0.3515E+02	-.2575E+02
	Vt=-.7164E-02	0.7164E-02	Mt=0.7962E-03	-.4183E-03	(Mt/St)=0.9848E+01	-.5174E+01
			(Tr*CTOR/Jp)=-.4140E+01	0.4140E+01	Smax =0.3446E-02	0.1050E+03
			(Hoop Stres)=0.3446E-02	0.3446E-02	Smin =-.1152E+03	0.5245E+02

STRESS OUTPUT FOR BEAM ELEMENT GROUP 2 CASE NO. 3

ELEMENT NUMBER	FORCES		MOMENTS		STRESSES	
	NODE1	NODE2	NODE1	NODE2	NODE1	NODE2
57	[40 ,	41]	(circular)			

Fr=-.4046E+00 0.4046E+00 Tr=-.8065E-03 0.8065E-03 (P/A) =-.5864E+02 0.5864E+02
Vs=-.8744E-02 0.8744E-02 Ms=0.4243E-02 -.2763E-02 (Ms/Ss)=0.5248E+02 -.3417E+02
Vt=-.1395E-01 0.1395E-01 Mt=-.2473E-02 0.1546E-02 (Mt/St)=-.3059E+02 0.1912E+02
(Tr*CTOR/Jp)=-.4988E+01 0.4988E+01 Smax =0.2101E+01 0.9780E+02
(Hoop Stres)=0.3446E-02 0.3446E-02 Smin =-.1194E+03 0.1948E+02

67 [50 , 51] (circular)

Fr=0.4046E+00 -.4046E+00 Tr=-.8065E-03 0.8065E-03 (P/A) =0.5864E+02 -.5864E+02
Vs=0.8744E-02 -.8744E-02 Ms=0.4243E-02 -.2763E-02 (Ms/Ss)=0.5248E+02 -.3417E+02
Vt=-.1395E-01 0.1395E-01 Mt=0.2473E-02 -.1546E-02 (Mt/St)=0.3059E+02 -.1912E+02
(Tr*CTOR/Jp)=-.4988E+01 0.4988E+01 Smax =0.1194E+03 0.3446E-02
(Hoop Stres)=0.3446E-02 0.3446E-02 Smin =-.2101E+01 -.9780E+02

77 [60 , 61] (circular)

Fr=-.4046E+00 0.4046E+00 Tr=-.8065E-03 0.8065E-03 (P/A) =-.5864E+02 0.5864E+02
Vs=-.8744E-02 0.8744E-02 Ms=0.4243E-02 -.2763E-02 (Ms/Ss)=0.5248E+02 -.3417E+02
Vt=-.1395E-01 0.1395E-01 Mt=-.2473E-02 0.1546E-02 (Mt/St)=-.3059E+02 0.1912E+02
(Tr*CTOR/Jp)=-.4988E+01 0.4988E+01 Smax =0.2101E+01 0.9780E+02
(Hoop Stres)=0.3446E-02 0.3446E-02 Smin =-.1194E+03 0.1948E+02

87 [69 , 70] (circular)

Fr=0.4046E+00 -.4046E+00 Tr=-.8065E-03 0.8065E-03 (P/A) =0.5864E+02 -.5864E+02
Vs=0.8744E-02 -.8744E-02 Ms=0.4243E-02 -.2763E-02 (Ms/Ss)=0.5248E+02 -.3417E+02
Vt=-.1395E-01 0.1395E-01 Mt=0.2473E-02 -.1546E-02 (Mt/St)=0.3059E+02 -.1912E+02
(Tr*CTOR/Jp)=-.4988E+01 0.4988E+01 Smax =0.1194E+03 0.3446E-02
(Hoop Stres)=0.3446E-02 0.3446E-02 Smin =-.2101E+01 -.9780E+02

97 [79 , 80] (circular)

Fr=-.4046E+00 0.4046E+00 Tr=-.8065E-03 0.8065E-03 (P/A) =-.5864E+02 0.5864E+02
Vs=-.8744E-02 0.8744E-02 Ms=0.4243E-02 -.2763E-02 (Ms/Ss)=0.5248E+02 -.3417E+02
Vt=-.1395E-01 0.1395E-01 Mt=-.2473E-02 0.1546E-02 (Mt/St)=-.3059E+02 0.1912E+02
(Tr*CTOR/Jp)=-.4988E+01 0.4988E+01 Smax =0.2101E+01 0.9780E+02
(Hoop Stres)=0.3446E-02 0.3446E-02 Smin =-.1194E+03 0.1948E+02

ELEMENT NUMBER	FORCES		MOMENTS		STRESSES	
	NODE1	NODE2	NODE1	NODE2	NODE1	NODE2

107 [88 , 89] (circular)

Fr=0.4046E+00 -.4046E+00 Tr=-.8065E-03 0.8065E-03 (P/A) =0.5864E+02 -.5864E+02
Vs=0.8744E-02 -.8744E-02 Ms=0.4243E-02 -.2763E-02 (Ms/Ss)=0.5248E+02 -.3417E+02
Vt=-.1395E-01 0.1395E-01 Mt=0.2473E-02 -.1546E-02 (Mt/St)=0.3059E+02 -.1912E+02
(Tr*CTOR/Jp)=-.4988E+01 0.4988E+01 Smax =0.1194E+03 0.3446E-02
(Hoop Stres)=0.3446E-02 0.3446E-02 Smin =-.2101E+01 -.9780E+02

A P P E N D I X D

CROSS-SHAPE STRUCTURE FEM PROGRAM AND OUTPUT

In the next pages, the finite element program for analysis of the cross-structure sensor is shown together with the corresponding output. The program generates a model consisting of 8-nodes solid element and representing one third of the whole structure (Fig.25). The output shows the result of the numerical calibration performed in order to obtain the compliance matrix which was used to determine the condition number of the sensor. This output is composed of ten columns of stresses; the first three are the normal stresses in x, y, and z directions. The next three columns are shear stresses in xy, yz, and xz planes respectively. The next column is the Von Mises stress, and finally the last three columns are the principal stresses in x, y, and z directions. The elements of interest are 93, 94, 103, and 104 at their common node (285). This location is 0.5 mm from the base of the PPS and the end block on the center line. Both forces and moments calibration are shown.

C*
 C* COSMOS/M Geostar V1.65
 C* Problem : CROSS CALIBRATION Date : 25-JUN-93 Time : 18:43:30
 C*
 PT,1,-1,0.14,0.14,
 PTGEN,1,1,1,1,0,0.38,0,0,
 PTGEN,1,1,2,1,0,0,-0.04,0,
 CRPLINE,1,1,2,4,3,1,
 SF2CR,1,1,3,0,
 VLEXTR,1,1,1,Z,-0.28,
 PTGEN,1,2,4,2,0,0.22,0,0,
 CRLINE,14,2,9,
 CRLINE,15,4,10,
 SF2CR,7,14,15,0,
 VLEXTR,7,7,1,Z,-0.28,
 PTGEN,1,9,10,1,0,0.26,0,0,
 CRLINE,22,9,13,
 CRLINE,23,10,14,
 SF2CR,12,22,23,0,
 VLEXTR,12,12,1,Z,-0.28,
 PTGEN,1,13,14,1,0,0.28,0,0,
 CRLINE,30,13,17,
 CRLINE,31,14,18,
 SF2CR,17,30,31,0,
 VLEXTR,17,17,1,Z,-0.28,
 PTGEN,1,17,18,1,0,0.26,0,0,
 CRLINE,38,17,21,
 CRLINE,39,18,22,
 SF2CR,22,38,39,0,
 VLEXTR,22,22,1,Z,-0.28,
 PTGEN,1,21,22,1,0,0.22,0,0,
 CRLINE,46,21,25,
 CRLINE,47,22,26,
 SF2CR,27,46,47,0,
 VLEXTR,27,27,1,Z,-0.28,
 PTGEN,1,25,26,1,0,0.38,0,0,
 SCALE,0,
 CRLINE,54,25,29,
 CRLINE,55,26,30,
 SF2CR,32,54,55,0,
 VLEXTR,32,32,1,Z,-0.28,
 VLGEN,1,1,7,1,0,0,-0.24,0,
 VL8PT,15,8,33,37,39,35,3,6,8,4,
 VL8PT,16,8,41,43,47,45,10,12,16,14,
 VL8PT,17,8,45,47,51,49,14,16,20,18,
 VL8PT,18,8,49,51,55,53,18,20,24,22,
 VL8PT,19,8,57,59,63,61,26,28,32,30,
 EGROUP,1,SOLID,0,1,0,0,0,0,0,
 PICK_MAT,1,ALUMINUM,FPS,
 C* MATL:ALUMINUM : ALUMINUM ALLOY

 C* EX 10.3E+6 p.s.i.
 C* NUXY 0.36
 C* GXY 3.80E+6 p.s.i.
 C* ALPX 12.8E-6 /Fahrenheit
 C* DENS 2.51E-4 lb.s.s/in**4

C* KX 2.194E-3 BTU/in.s.F
C* C (Cp) 88.9493 BTUin/lbssF
M_VL,1,8,7,8,3,1,6,0.5,1,1,
M_VL,7,14,7,8,3,1,6,2,1,1,
M_VL,2,6,4,8,10,1,6,1,1,1,
M_VL,9,13,4,8,10,1,6,1,1,1,
M_VL,3,10,7,8,2,1,6,2,1,1,
M_VL,5,12,7,8,2,1,6,0.5,1,1,
M_VL,4,11,7,8,2,1,6,1,1,1,
M_VL,15,15,1,8,6,3,2,1,0.5,1,
M_VL,19,19,1,8,6,3,2,1,2,1,
M_VL,16,16,1,8,6,2,2,1,2,1,
M_VL,17,17,1,8,6,2,2,1,1,1,
M_VL,18,18,1,8,6,2,2,1,0.5,1,
SCALE,0,
NMERGE,1,1449,1,0.0001,0,1,0,
NCOMPRESS,1,1428,1,
DSF,4,ALL,0,4,1,
DSF,75,ALL,0,75,1,
DSF,40,ALL,0,40,1,
DSF,36,ALL,0,36,1,
DSF,99,ALL,0,99,1,
DSF,72,ALL,0,72,1,
FSF,19,FX,0.0238,56,37,
PRINT_ELSET,4,9,9,12,12,93,97,103,107,
ACTSET,LC,2,
PSF,56,12.755,56,1,12.755,12.755,
PRINT_ELSET,4,9,9,12,12,93,97,103,107,
ACTSET,LC,3,
PSF,18,12.755,18,1,12.755,12.755,
PSF,89,12.755,89,1,12.755,12.755,
PSF,54,12.755,54,1,12.755,12.755,
PRINT_ELSET,4,9,9,12,12,93,97,103,107,
PRINT_OPS,0,0,0,1,0,1,0,0,0,0,

DATE: 7/9/1993 TIME: 12:32: 5

TITLE: CROSS STRUCT. CALIB.
CASE 1 CASE 2 CASE 3
SUBTITLE: FX=1 FY=1 FZ=1

STRESS EVALUATION FOR STATIC ANALYSIS

STRESS OUTPUT FOR 3/D ELEMENT GROUP 1 CASE NO. 1

ELEMENT NUMBER	OUTPUT NODE	VON MISES SIGMA-X1	SIGMA-X2	SIGMA-X3	TAU-X12	TAU-X23	TAU-X13	STRESS	PRINCIPAL STRESSES
9	CENTER	1.4484E+01	-2.4174E-01	1.3864E+00	1.8091E+00	-1.9043E-01	-6.7029E-02	1.4334E+01	1.4703E+01 1.4071E+00 -4.8154E-01
19		1.9925E+01	2.8185E+00	4.5159E+00	1.7917E+00	-1.0041E-01	-8.9668E-02	1.6618E+01	2.0111E+01 4.5218E+00 2.6266E+00
20		1.9925E+01	-3.2015E+00	1.0997E+00	1.7917E+00	-2.8045E-01	-8.9668E-02	2.1535E+01	2.0063E+01 1.1179E+00 -3.3579E+00
24		9.0959E+00	-3.2015E+00	-1.4946E+00	1.7917E+00	-2.8045E-01	-4.4390E-02	1.1959E+01	9.3516E+00 -1.4544E+00 -3.4975E+00
23		9.0959E+00	2.8185E+00	1.4247E+00	1.7917E+00	-1.0041E-01	-4.4390E-02	7.7307E+00	9.5713E+00 2.3558E+00 1.4120E+00
27		1.9889E+01	2.7295E+00	4.5159E+00	1.8265E+00	-1.0041E-01	-8.9668E-02	1.6645E+01	2.0082E+01 4.5215E+00 2.5313E+00
28		1.9889E+01	-3.3135E+00	1.0997E+00	1.8265E+00	-2.8045E-01	-8.9668E-02	2.1581E+01	2.0033E+01 1.1174E+00 -3.4744E+00
32		9.0257E+00	-3.3135E+00	-1.4946E+00	1.8265E+00	-2.8045E-01	-4.4390E-02	1.1974E+01	9.2904E+00 -1.4566E+00 -3.6162E+00
31		9.0257E+00	2.7295E+00	1.4247E+00	1.8265E+00	-1.0041E-01	-4.4390E-02	7.7204E+00	9.5172E+00 2.2522E+00 1.4105E+00
12	CENTER	1.4484E+01	-2.4174E-01	1.3864E+00	1.8091E+00	1.9043E-01	6.7029E-02	1.4334E+01	1.4703E+01 1.4071E+00 -4.8154E-01
27		1.9889E+01	2.7295E+00	4.5159E+00	1.8265E+00	1.0041E-01	8.9668E-02	1.6645E+01	2.0082E+01 4.5215E+00 2.5313E+00
28		1.9889E+01	-3.3135E+00	1.0997E+00	1.8265E+00	2.8045E-01	8.9668E-02	2.1581E+01	2.0033E+01 1.1174E+00 -3.4744E+00
32		9.0257E+00	-3.3135E+00	-1.4946E+00	1.8265E+00	2.8045E-01	4.4390E-02	1.1974E+01	9.2904E+00 -1.4566E+00 -3.6162E+00
31		9.0257E+00	2.7295E+00	1.4247E+00	1.8265E+00	1.0041E-01	4.4390E-02	7.7204E+00	9.5172E+00 2.2522E+00 1.4105E+00
35		1.9925E+01	2.8185E+00	4.5159E+00	1.7917E+00	1.0041E-01	8.9668E-02	1.6618E+01	2.0111E+01 4.5218E+00 2.6266E+00
36		1.9925E+01	-3.2015E+00	1.0997E+00	1.7917E+00	2.8045E-01	8.9668E-02	2.1535E+01	2.0063E+01 1.1179E+00 -3.3579E+00
40		9.0959E+00	-3.2015E+00	-1.4946E+00	1.7917E+00	2.8045E-01	4.4390E-02	1.1959E+01	9.3516E+00 -1.4544E+00 -3.4975E+00
39		9.0959E+00	2.8185E+00	1.4247E+00	1.7917E+00	1.0041E-01	4.4390E-02	7.7307E+00	9.5713E+00 2.3558E+00 1.4120E+00
93	CENTER	2.2107E+01	3.3770E-01	3.2596E+00	-9.4076E-02	-1.6746E-01	-4.2304E-01	2.0481E+01	2.2117E+01 3.2595E+00 3.2791E-01
20		1.6984E+01	1.0630E+00	1.6223E+00	-9.5893E-02	-2.8045E-01	-2.4034E-01	1.5662E+01	1.6988E+01 1.7343E+00 9.4856E-01
265		1.6984E+01	-3.6573E-01	4.6012E-01	-9.5893E-02	-5.4478E-02	-2.4034E-01	1.6958E+01	1.6988E+01 4.6004E-01 -3.6967E-01
275		2.7153E+01	-3.6573E-01	4.3973E+00	-9.5893E-02	-5.4478E-02	-6.0575E-01	2.5496E+01	2.7169E+01 4.3817E+00 -3.6664E-01
24		2.7153E+01	1.0630E+00	6.5589E+00	-9.5893E-02	-2.8045E-01	-6.0575E-01	2.3851E+01	2.7171E+01 6.5551E+00 1.0485E+00
28		1.7158E+01	9.9803E-01	1.6223E+00	-9.2260E-02	-2.8045E-01	-2.4034E-01	1.5871E+01	1.7162E+01 1.7255E+00 8.9055E-01
285		1.7158E+01	-3.4446E-01	4.6012E-01	-9.2260E-02	-5.4478E-02	-2.4034E-01	1.7121E+01	1.7162E+01 4.6017E-01 -3.4848E-01
295		2.7134E+01	-3.4446E-01	4.3973E+00	-9.2260E-02	-5.4478E-02	-6.0575E-01	2.5464E+01	2.7151E+01 4.3817E+00 -3.4535E-01
32		2.7134E+01	9.9803E-01	6.5589E+00	-9.2260E-02	-2.8045E-01	-6.0575E-01	2.3876E+01	2.7152E+01 6.5549E+00 9.8378E-01
94	CENTER	2.2483E+01	-7.5418E-02	2.1867E+00	5.7094E-03	-4.3421E-02	-3.5337E-01	2.1526E+01	2.2490E+01 2.1814E+00 -7.6258E-02
265		1.7333E+01	-1.4294E-01	6.0105E-01	5.3051E-02	-5.4478E-02	-3.8353E-01	1.7129E+01	1.7342E+01 5.9645E-01 -1.4729E-01
266		1.7333E+01	5.8604E-02	-3.7128E-01	5.3051E-02	-3.2363E-02	-3.8353E-01	1.7506E+01	1.7341E+01 6.0994E-02 -3.8214E-01
276		2.7818E+01	5.8604E-02	3.8372E+00	5.3051E-02	-3.2363E-02	-3.2322E-01	2.5884E+01	2.7622E+01 3.8331E+00 5.8214E-02
275		2.7818E+01	-1.4294E-01	4.6797E+00	5.3051E-02	-5.4478E-02	-3.2322E-01	2.5698E+01	2.7622E+01 4.6758E+00 -1.4367E-01
285		1.7168E+01	-1.4389E-01	6.0105E-01	-4.1633E-02	-5.4478E-02	-3.8353E-01	1.6965E+01	1.7177E+01 5.9604E-01 -1.4787E-01
286		1.7168E+01	7.3442E-02	-3.7128E-01	-4.1633E-02	-3.2363E-02	-3.8353E-01	1.7406E+01	1.7177E+01 -7.0349E-02 -3.8286E-01
296		2.7815E+01	-7.3442E-02	3.8372E+00	-4.1633E-02	-3.2363E-02	-3.2322E-01	2.6159E+01	2.7819E+01 3.8331E+00 -7.3765E-02
295		2.7815E+01	-1.4389E-01	4.6797E+00	-4.1633E-02	-5.4478E-02	-3.2322E-01	2.5893E+01	2.7819E+01 4.6758E+00 -1.4456E-01
95	CENTER	2.2804E+01	5.8398E-02	1.4865E+00	2.5332E-02	-1.1515E-02	-2.7988E-01	2.2072E+01	2.2808E+01 1.4829E+00 5.8272E-02
266		1.7612E+01	2.6332E-01	-1.9861E-01	4.9233E-02	-3.2363E-02	-2.3975E-01	1.7589E+01	1.7615E+01 2.6562E-01 -2.0417E-01
267		1.7612E+01	2.5679E-02	-9.7881E-01	4.9233E-02	9.3335E-03	-2.3975E-01	1.8114E+01	1.7615E+01 2.5616E-02 -9.8198E-01
277		2.8115E+01	2.5679E-02	3.0978E+00	4.9233E-02	9.3335E-03	-3.2000E-01	2.6692E+01	2.8119E+01 3.0937E+00 2.5568E-02
276		2.8115E+01	2.6332E-01	4.0256E+00	4.9233E-02	-3.2363E-02	-3.2000E-01	2.6180E+01	2.8119E+01 4.0216E+00 2.6294E-01
286		1.7488E+01	8.2890E-02	-1.9861E-01	1.4320E-03	-3.2363E-02	-2.3975E-01	1.7552E+01	1.7491E+01 8.6526E-02 -2.0549E-01
287		1.7488E+01	-1.3830E-01	-9.7881E-01	1.4320E-03	9.3335E-03	-2.3975E-01	1.8066E+01	1.7491E+01 -1.3819E-01 -9.8203E-01
297		2.8003E+01	-1.3830E-01	3.0978E+00	1.4320E-03	9.3335E-03	-3.2000E-01	2.6677E+01	2.8007E+01 3.0937E+00 -1.3832E-01
296		2.8003E+01	8.2890E-02	4.0256E+00	1.4320E-03	-3.2363E-02	-3.2000E-01	2.6178E+01	2.8007E+01 4.0216E+00 8.2624E-02
96	CENTER	2.2988E+01	1.9618E-02	9.3035E-01	1.5018E-02	1.5014E-02	-1.5191E-01	2.2528E+01	2.2989E+01 9.2955E-01 1.9384E-02
267		1.7744E+01	1.0698E-01	-8.6991E-01	2.0073E-02	9.3335E-03	-1.2353E-01	1.8146E+01	1.7744E+01 1.0704E-01 -8.7082E-01
268		1.7744E+01	5.7548E-02	-1.2904E+00	2.0073E-02	2.0695E-02	-1.2353E-01	1.8398E+01	1.7744E+01 5.7838E-02 -1.2915E+00
278		2.8229E+01	5.7548E-02	2.6865E+00	2.0073E-02	2.0695E-02	-1.8028E-01	2.6955E+01	2.8230E+01 2.6854E+00 -5.7372E-02
277		2.8229E+01	1.0698E-01	3.1952E+00	2.0073E-02	9.3335E-03	-1.8028E-01	2.6714E+01	2.8230E+01 3.1939E+00 1.0694E-01
287		1.7755E+01	-1.3336E-02	-8.6991E-01	9.9622E-03	9.3335E-03	-1.2353E-01	1.8213E+01	1.7755E+01 -1.3242E-02 -8.7083E-01
288		1.7755E+01	-7.2717E-02	-1.2904E+00	9.9622E-03	2.0695E-02	-1.2353E-01	1.8468E+01	1.7755E+01 -7.2373E-02 -1.2915E+00
298		2.8224E+01	-7.2717E-02	2.6865E+00	9.9622E-03	2.0695E-02	-1.8028E-01	2.7025E+01	2.8225E+01 2.6854E+00 -7.2875E-02
297		2.8224E+01	-1.3336E-02	3.1952E+00	9.9622E-03	9.3335E-03	-1.8028E-01	2.6779E+01	2.8225E+01 3.1939E+00 -1.3367E-02
97	CENTER	2.3071E+01	2.2284E-02	6.6471E-01	-4.7169E-03	2.2495E-02	-5.0011E-02	2.2735E+01	2.3071E+01 6.6539E-01 2.1496E-02
268		1.7752E+01	9.2035E-02	-1.2486E+00	-3.9865E-03	2.0695E-02	-3.6616E-02	1.8367E+01	1.7752E+01 9.2354E-02 -1.2490E+00
269		1.7752E+01	5.6474E-02	-1.3888E+00	-3.9865E-03	2.2495E-02	-3.6616E-02	1.8461E+01	1.7752E+01 5.6882E-02 -1.3892E+00
279		2.8318E+01	5.6474E-02	2.5574E+00	-3.9865E-03	2.2495E-02	-6.3405E-02	2.7098E+01	2.8318E+01 2.5575E+00 5.6237E-02
278		2.8318E+01	9.2035E-02	2.7388E+00	-3.9865E-03	2.0695E-02	-6.3405E-02	2.7000E+01	2.8318E+01 2.7388E+00 9.1872E-02
288		1.7884E+01	-1.3168E-02	-1.2486E+00	-5.4474E-03	2.0695E-02	-3.6616E-02	1.8546E+01	1.7884E+01 -1.2823E-02 -1.2490E+00
289		1.7884E+01	-4.6204E-02	-1.3888E+00	-5.4474E-03	2.2495E-02	-3.6616E-02	1.8638E+01	1.7884E+01 -4.5766E-02 -1.3893E+00
299		2.8331E+01	-4.6204E-02	2.5574E+00	-5.4474E-03	2.2495E-02	-6.3405E-02	2.7170E+01	2.8331E+01 2.5575E+00 -4.6325E-02
298		2.8331E+01	-1.3168E-02	2.7388E+00	-5.4474E-03	2.0695E-02	-6.3405E-02	2.7074E+01	2.8331E+01 2.7388E+00 -1.3325E-02
103	CENTER	2.2107E+01	3.3770E-01	3.2596E+00	-9.4076E-02	1.6746E-01	4.2304E-01	2.0481E+01	2.2117E+01 3.2595E+00 3.2791E-01

Table with 10 columns: ID, X1, X2, X3, X4, X5, X6, X7, X8, X9. Rows 28-40 showing numerical data.

Table with 10 columns: ID, X1, X2, X3, X4, X5, X6, X7, X8, X9. Rows 104-116 showing numerical data.

Table with 10 columns: ID, X1, X2, X3, X4, X5, X6, X7, X8, X9. Rows 105-117 showing numerical data.

Table with 10 columns: ID, X1, X2, X3, X4, X5, X6, X7, X8, X9. Rows 106-118 showing numerical data.

Table with 10 columns: ID, X1, X2, X3, X4, X5, X6, X7, X8, X9. Rows 107-119 showing numerical data.

STRESS OUTPUT FOR 3/D ELEMENT GROUP 1 CASE NO. 2

Table with 10 columns: ELEMENT NUMBER, OUTPUT NODE, SIGMA-X1, SIGMA-X2, SIGMA-X3, TAU-X12, TAU-X23, TAU-X13, STRESS, PRINCIPAL STRESSES. Rows 9, 12, 13 showing stress output for various elements.

94
CENTER -6.1199E-01 -6.1693E+00 -1.0589E+00 2.3735E+01 6.1319E-01 2.1790E-01 4.1472E+01 2.0509E+01 -1.0478E+00 -2.7301E+01
265 -2.5959E+02 -1.7418E+01 -9.8641E+01 2.4122E+01 6.8819E-01 2.3483E-01 2.1753E+02 -1.5032E+01 -9.8646E+01 -2.6197E+02
266 -2.5959E+02 4.9804E+00 -9.2639E+01 2.4122E+01 5.3819E-01 2.3483E-01 2.3547E+02 7.1649E+00 -9.2642E+01 -2.6177E+02
276 2.5922E+02 4.9804E+00 9.7704E+01 2.4122E+01 5.3819E-01 6.7064E-01 2.2673E+02 2.6149E+02 9.7706E+01 2.7081E+00
275 2.5922E+02 -1.7418E+01 8.9340E+01 2.4122E+01 6.8819E-01 6.7064E-01 2.4523E+02 2.6131E+02 8.9343E+01 -1.9511E+01
285 -2.6304E+02 -1.6607E+01 -9.8641E+01 2.3347E+01 6.8819E-01 2.3483E-01 2.2109E+02 -1.4409E+01 -9.8646E+01 -2.6523E+02
286 -2.6304E+02 4.3675E+00 -9.2639E+01 2.3347E+01 5.3819E-01 2.3483E-01 2.3794E+02 6.3938E+00 -9.2642E+01 -2.6507E+02
296 2.6097E+02 4.3675E+00 9.7704E+01 2.3347E+01 5.3819E-01 6.7064E-01 2.2856E+02 2.6308E+02 9.7706E+01 2.2567E+00
295 2.6097E+02 -1.6607E+01 8.9340E+01 2.3347E+01 6.8819E-01 6.7064E-01 2.4597E+02 2.6292E+02 8.9343E+01 -1.8563E+01

95
CENTER -9.2750E-01 1.7330E+00 1.1154E+00 2.3045E+01 5.9504E-01 3.9467E-01 4.0008E+01 2.3488E+01 1.1345E+00 -2.2701E+01
266 -1.8490E+02 4.7740E+00 -6.5286E+01 2.3011E+01 5.3819E-01 9.6159E-01 1.7085E+02 7.5282E+00 -6.5280E+01 -1.8766E+02
267 -1.8490E+02 -8.9970E-01 -6.6868E+01 2.3011E+01 6.5190E-01 9.6159E-01 1.6632E+02 1.9385E+00 -6.6863E+01 -1.8775E+02
277 1.8374E+02 -8.9970E-01 6.6620E+01 2.3011E+01 6.5190E-01 -1.7224E-01 1.6666E+02 1.8657E+02 6.6625E+01 -3.7299E+00
276 1.8374E+02 4.7740E+00 6.9996E+01 2.3011E+01 5.3819E-01 -1.7224E-01 1.6186E+02 1.8665E+02 6.9999E+01 1.8588E+00
286 -1.8541E+02 4.2189E+00 -6.5286E+01 2.3080E+01 5.3819E-01 9.6159E-01 1.7091E+02 6.9899E+00 -6.5280E+01 -1.8819E+02
287 -1.8541E+02 -1.1611E+00 -6.6868E+01 2.3080E+01 6.5190E-01 9.6159E-01 1.6661E+02 1.6900E+00 -6.6863E+01 -1.8826E+02
297 1.8286E+02 -1.1611E+00 6.6620E+01 2.3080E+01 6.5190E-01 -1.7224E-01 1.6609E+02 1.8571E+02 6.6625E+01 -4.0171E+00
296 1.8286E+02 4.2189E+00 6.9996E+01 2.3080E+01 5.3819E-01 -1.7224E-01 1.6152E+02 1.8580E+02 6.9999E+01 1.2815E+00

96
CENTER -1.5056E+00 -4.2554E-01 -1.0519E-01 2.2426E+01 5.0511E-01 6.5297E-01 3.8891E+01 2.1468E+01 -7.6765E-02 -2.3427E+01
267 -1.1097E+02 -1.3158E+00 -4.0277E+01 2.2187E+01 6.5190E-01 9.6078E-01 1.0368E+02 3.0082E+00 -4.0267E+01 -1.1530E+02
268 -1.1097E+02 5.7287E-01 -3.9273E+01 2.2187E+01 5.3833E-01 9.6078E-01 1.0519E+02 4.8248E+00 -3.9260E+01 -1.1523E+02
278 1.0814E+02 5.7287E-01 3.9751E+01 2.2187E+01 3.5833E-01 9.6078E-01 1.0183E+02 1.1254E+02 3.9754E+01 -3.8276E+00
277 1.0814E+02 -1.3158E+00 3.9378E+01 2.2187E+01 6.5190E-01 9.6078E-01 1.0325E+02 1.1247E+02 3.9389E+01 -5.6530E+00
287 -1.1097E+02 -1.3954E+00 -4.0277E+01 2.2666E+01 6.5190E-01 9.6078E-01 1.0394E+02 3.1128E+00 -4.0267E+01 -1.1549E+02
288 -1.1097E+02 4.3613E-01 -3.9273E+01 2.2666E+01 5.3833E-01 9.6078E-01 1.0540E+02 4.8717E+00 -3.9260E+01 -1.1542E+02
298 1.0777E+02 4.3613E-01 3.9751E+01 2.2666E+01 3.5833E-01 9.6078E-01 1.0192E+02 1.1236E+02 3.9754E+01 -4.1580E+00
297 1.0777E+02 -1.3954E+00 3.9378E+01 2.2666E+01 6.5190E-01 3.4516E-01 1.0330E+02 1.1229E+02 3.9389E+01 -5.9254E+00

97
CENTER -2.1926E+00 1.5567E-01 -2.5872E-02 2.2090E+01 1.7793E-01 7.4267E-01 3.8351E+01 2.1110E+01 -1.3867E-02 -2.3159E+01
268 -3.8272E+01 1.5604E-01 -1.3205E+01 2.1824E+01 3.5833E-01 9.4173E-01 5.0731E+01 1.0018E+01 -1.3176E+01 -4.8164E+01
269 -3.8272E+01 1.9123E-01 -1.2834E+01 2.1824E+01 2.4624E-03 9.4173E-01 5.0790E+01 1.0055E+01 -1.2820E+01 -4.8150E+01
278 3.3899E+01 1.9123E-01 1.3026E+01 2.1824E+01 -2.4624E-03 5.4361E-01 4.7939E+01 4.4627E+01 1.3021E+01 -1.0532E+01
279 3.3899E+01 1.5504E-01 1.2910E+01 2.1824E+01 3.5833E-01 5.4361E-01 4.7970E+01 4.4616E+01 1.2920E+01 -1.0572E+01
288 -3.8065E+01 8.1078E-02 -1.3205E+01 2.2356E+01 3.5833E-01 9.4173E-01 5.1257E+01 1.0395E+01 -1.3176E+01 -4.8408E+01
289 -3.8065E+01 1.9532E-01 -1.2834E+01 2.2356E+01 -2.4624E-03 9.4173E-01 5.1353E+01 1.0496E+01 -1.2821E+01 -4.8379E+01
299 3.3668E+01 1.9532E-01 1.3026E+01 2.2356E+01 -2.4624E-03 5.4361E-01 4.8537E+01 4.4866E+01 1.3021E+01 -1.0998E+01
298 3.3668E+01 8.1078E-02 1.2910E+01 2.2356E+01 3.5833E-01 5.4361E-01 4.8605E+01 4.4839E+01 1.2920E+01 -1.1100E+01

103
CENTER -4.5964E-01 2.3200E+01 1.0540E+01 2.4300E+01 -6.2140E-01 2.5847E-01 4.6833E+01 3.8412E+01 1.0525E+01 -1.5656E+01
28 -3.4193E+02 6.2016E+01 -9.6222E+01 2.4031E+01 -5.5460E-01 8.1196E-01 3.5500E+02 6.3443E+01 -9.6222E+01 -3.4335E+02
285 -3.4193E+02 -1.6707E+01 -1.2728E+02 2.4031E+01 -6.8819E-01 8.1196E-01 2.8943E+02 -1.4936E+01 -1.2728E+02 -3.4370E+02
295 3.3913E+02 -1.6707E+01 1.1815E+02 2.4031E+01 -6.8819E-01 -2.9501E-01 3.1393E+02 3.4074E+02 1.1816E+02 -1.8326E+01
32 3.3913E+02 6.2016E+01 1.4751E+02 2.4031E+01 -5.5460E-01 -2.9501E-01 2.4928E+02 3.4119E+02 1.4752E+02 5.9944E+01
36 -3.3999E+02 6.4639E+01 -9.6222E+01 2.4568E+01 -5.5460E-01 8.1196E-01 3.5542E+02 6.8127E+01 -9.6222E+01 -3.4148E+02
305 -3.3999E+02 -1.7147E+01 -1.2728E+02 2.4568E+01 -6.8819E-01 8.1196E-01 2.8743E+02 -1.5283E+01 -1.2728E+02 -3.4185E+02
315 3.4095E+02 -1.7147E+01 1.1815E+02 2.4568E+01 -6.8819E-01 -2.9501E-01 3.1607E+02 3.4263E+02 1.1816E+02 -1.8828E+01
40 3.4095E+02 6.4639E+01 1.4751E+02 2.4568E+01 -5.5460E-01 -2.9501E-01 2.4926E+02 3.4312E+02 1.4752E+02 6.2467E+01

104
CENTER -6.1199E-01 -6.1693E+00 -1.0589E+00 2.3735E+01 -6.1319E-01 -2.1790E-01 4.1472E+01 2.0509E+01 -1.0478E+00 -2.7301E+01
285 -2.6304E+02 -1.6607E+01 -9.8641E+01 2.3347E+01 -6.8819E-01 2.3483E-01 2.2109E+02 -1.4409E+01 -9.8646E+01 -2.6523E+02
286 -2.6304E+02 4.3675E+00 -9.2639E+01 2.3347E+01 -5.3819E-01 2.3483E-01 2.3794E+02 6.3938E+00 -9.2642E+01 -2.6507E+02
296 2.6097E+02 4.3675E+00 9.7704E+01 2.3347E+01 -5.3819E-01 -6.7064E-01 2.2856E+02 2.6308E+02 9.7706E+01 2.2567E+00
295 2.6097E+02 -1.6607E+01 8.9340E+01 2.3347E+01 -6.8819E-01 -6.7064E-01 2.4597E+02 2.6292E+02 8.9343E+01 -1.8563E+01
305 -2.5959E+02 -1.7418E+01 -9.8641E+01 2.4122E+01 -6.8819E-01 2.3483E-01 2.1753E+02 -1.5032E+01 -9.8646E+01 -2.6197E+02
306 -2.5959E+02 4.9804E+00 -9.2639E+01 2.4122E+01 -5.3819E-01 2.3483E-01 2.3547E+02 7.1649E+00 -9.2642E+01 -2.6177E+02
316 2.5922E+02 4.9804E+00 9.7704E+01 2.4122E+01 -5.3819E-01 -6.7064E-01 2.2673E+02 2.6149E+02 9.7706E+01 2.7081E+00
315 2.5922E+02 -1.7418E+01 8.9340E+01 2.4122E+01 -6.8819E-01 -6.7064E-01 2.4523E+02 2.6131E+02 8.9343E+01 -1.9511E+01

105
CENTER -9.2750E-01 1.7330E+00 1.1154E+00 2.3045E+01 -5.9505E-01 -3.9467E-01 4.0008E+01 2.3488E+01 1.1345E+00 -2.2701E+01
286 -1.8541E+02 4.2189E+00 -6.5286E+01 2.3080E+01 -5.3819E-01 -9.6159E-01 1.7091E+02 6.9899E+00 -6.5280E+01 -1.8819E+02
287 -1.8541E+02 -1.1611E+00 -6.6868E+01 2.3080E+01 -6.5190E-01 -9.6159E-01 1.6661E+02 1.6900E+00 -6.6863E+01 -1.8826E+02
297 1.8286E+02 -1.1611E+00 6.6620E+01 2.3080E+01 -6.5190E-01 1.7224E-01 1.6609E+02 1.8571E+02 6.6625E+01 -4.0171E+00
296 1.8286E+02 4.2189E+00 6.9996E+01 2.3080E+01 -5.3819E-01 1.7224E-01 1.6152E+02 1.8580E+02 6.9999E+01 1.2815E+00
306 -1.8490E+02 4.7740E+00 -6.5286E+01 2.3011E+01 -5.3819E-01 -9.6159E-01 1.7085E+02 7.5282E+00 -6.5280E+01 -1.8766E+02
307 -1.8490E+02 -8.9970E-01 -6.6868E+01 2.3011E+01 -6.5190E-01 -9.6159E-01 1.6632E+02 1.9385E+00 -6.6863E+01 -1.8775E+02
317 1.8374E+02 -8.9970E-01 6.6620E+01 2.3011E+01 -6.5190E-01 1.7224E-01 1.6666E+02 1.8657E+02 6.6625E+01 -3.7299E+00
316 1.8374E+02 4.7740E+00 6.9996E+01 2.3011E+01 -5.3819E-01 1.7224E-01 1.6186E+02 1.8665E+02 6.9999E+01 1.8588E+00

106
CENTER -1.5056E+00 -4.2554E-01 -1.0519E-01 2.2426E+01 -5.0511E-01 -6.5297E-01 3.8891E+01 2.1468E+01 -7.6765E-02 -2.3427E+01
287 -1.1097E+02 -1.3954E+00 -4.0277E+01 2.2666E+01 -6.5190E-01 9.6078E-01 1.0394E+02 3.1128E+00 -4.0267E+01 -1.1549E+02
288 -1.1097E+02 4.3613E-01 -3.9273E+01 2.2666E+01 -5.3833E-01 9.6078E-01 1.0540E+02 4.8717E+00 -3.9260E+01 -1.1542E+02
298 1.0777E+02 4.3613E-01 3.9751E+01 2.2666E+01 -3.5833E-01 9.6078E-01 1.0192E+02 1.1236E+02 3.9754E+01 -4.1580E+00
297 1.0777E+02 -1.3954E+00 3.9378E+01 2.2666E+01 -6.5190E-01 3.4516E-01 1.0330E+02 1.1229E+02 3.9389E+01 -5.9254E+00
307 -1.1097E+02 -1.3158E+00 -4.0277E+01 2.2187E+01 -6.5190E-01 9.6078E-01 1.0368E+02 3.0082E+00 -4.0267E+01 -1.1530E+02
308 -1.1097E+02 5.7287E-01 -3.9273E+01 2.2187E+01 -5.3833E-01 9.6078E-01 1.0519E+02 4.8248E+00 -3.9260E+01 -1.1523E+02
318 1.0814E+02 5.7287E-01 3.9751E+01 2.2187E+01 -3.5833E-01 9.6078E-01 1.0183E+02 1.1254E+02 3.9754E+01 -3.8276E+00
317 1.0814E+02 -1.3158E+00 3.9378E+01 2.2187E+01 -6.5190E-01 3.4516E-01 1.0325E+02 1.1247E+02 3.9389E+01 -5.6530E+00

107
CENTER -2.1926E+00 1.5567E-01 -2.5872E-02 2.2090E+01 -1.7793E-01 -7.4267E-01 3.8351E+01 2.1110E+01 -1.3867E-02 -2.3159E+01
288 -3.8065E+01 8.1078E-02 -1.3205E+01 2.2356E+01 -3.5833E-01 9.4173E-01 5.1257E+01 1.0395E+01 -1.3176E+01 -4.8408E+01
289 -3.8065E+01 1.9532E-01 -1.2834E+01 2.2356E+01 2.4624E-03 9.4173E-01 5.1353E+01 1.0496E+01 -1.2821E+01 -4.8379E+01
299 3.3668E+01 1.9532E-01 1.3026E+01 2.2356E+01 -2.4624E-03 5.4361E-01 4.8537E+01 4.4866E+01 1.3021E+01 -1.0998E+01
298 3.3668E+01 8.1078E-02 1.2910E+01 2.2356E+01 -3.5833E-01 5.4361E-01 4.8605E+01 4.4839E+01 1.2920E+01 -1.1100E+01

Table with 10 columns: Element ID, SIGMA-X1, SIGMA-X2, SIGMA-X3, TAU-X12, TAU-X23, TAU-X13, STRESS, PRINCIPAL STRESSES. Rows 308-318 showing stress values for various elements.

STRESS OUTPUT FOR 3/D ELEMENT GROUP 1 CASE NO. 3

Table with 10 columns: ELEMENT NUMBER, OUTPUT NODE, SIGMA-X1, SIGMA-X2, SIGMA-X3, TAU-X12, TAU-X23, TAU-X13, STRESS, PRINCIPAL STRESSES.

9

Table with 10 columns: ELEMENT NUMBER, OUTPUT NODE, SIGMA-X1, SIGMA-X2, SIGMA-X3, TAU-X12, TAU-X23, TAU-X13, STRESS, PRINCIPAL STRESSES. Rows 19-31 for element 9.

12

Table with 10 columns: ELEMENT NUMBER, OUTPUT NODE, SIGMA-X1, SIGMA-X2, SIGMA-X3, TAU-X12, TAU-X23, TAU-X13, STRESS, PRINCIPAL STRESSES. Rows 27-39 for element 12.

93

Table with 10 columns: ELEMENT NUMBER, OUTPUT NODE, SIGMA-X1, SIGMA-X2, SIGMA-X3, TAU-X12, TAU-X23, TAU-X13, STRESS, PRINCIPAL STRESSES. Rows 20-32 for element 93.

94

Table with 10 columns: ELEMENT NUMBER, OUTPUT NODE, SIGMA-X1, SIGMA-X2, SIGMA-X3, TAU-X12, TAU-X23, TAU-X13, STRESS, PRINCIPAL STRESSES. Rows 265-295 for element 94.

95

Table with 10 columns: ELEMENT NUMBER, OUTPUT NODE, SIGMA-X1, SIGMA-X2, SIGMA-X3, TAU-X12, TAU-X23, TAU-X13, STRESS, PRINCIPAL STRESSES. Rows 266-296 for element 95.

96

Table with 10 columns: ELEMENT NUMBER, OUTPUT NODE, SIGMA-X1, SIGMA-X2, SIGMA-X3, TAU-X12, TAU-X23, TAU-X13, STRESS, PRINCIPAL STRESSES. Rows 267-297 for element 96.

97

Table with 10 columns: ELEMENT NUMBER, OUTPUT NODE, SIGMA-X1, SIGMA-X2, SIGMA-X3, TAU-X12, TAU-X23, TAU-X13, STRESS, PRINCIPAL STRESSES. Rows 268-298 for element 97.

103

Table with 10 columns: ELEMENT NUMBER, OUTPUT NODE, SIGMA-X1, SIGMA-X2, SIGMA-X3, TAU-X12, TAU-X23, TAU-X13, STRESS, PRINCIPAL STRESSES. Rows 28-285 for element 103.

295 2.1777E-01 6.4601E-01 2.9500E+00 9.8880E-06 1.6214E+00 3.6288E+01 6.2967E+01 3.7934E+01 6.4516E-01 -3.4766E+01
 32 2.1777E-01 2.4684E-01 1.4701E+00 9.8880E-06 7.5846E+00 3.6288E+01 6.4223E+01 3.7922E+01 2.4562E-01 -3.6233E+01
 36 4.3855E+00 -7.9076E-01 -1.0665E+00 2.4747E-01 7.5846E+00 2.1767E+01 4.0280E+01 2.4547E+01 -8.2526E-02 -2.1936E+01
 305 4.3855E+00 -2.8622E-01 -4.8131E-01 2.4747E-01 1.6214E+00 2.1767E+01 3.8108E+01 2.3888E+01 -2.2396E-01 -2.0046E+01
 315 1.7327E+01 -2.8622E-01 2.9500E+00 2.4747E-01 1.6214E+00 3.6288E+01 6.4979E+01 4.7146E+01 -2.2638E-01 -2.6930E+01
 40 1.7327E+01 -7.9076E-01 1.4701E+00 2.4747E-01 7.5846E+00 3.6288E+01 6.6450E+01 4.6983E+01 8.1956E-02 -2.9059E+01
104
 CENTER 4.4510E+00 8.7278E-03 9.6869E-01 3.0185E-01 1.2675E+00 2.9942E+01 5.2068E+01 3.2715E+01 4.2431E-02 -2.7329E+01
 285 -4.8941E-01 5.0625E-01 -6.4163E-01 -1.5541E-03 1.6214E+00 2.9369E+01 5.0958E+01 2.8850E+01 5.0305E-01 -2.9978E+01
 286 -4.8941E-01 6.6304E-01 -8.0941E-01 -1.5541E-03 9.1361E-01 2.9369E+01 5.0911E+01 2.8735E+01 6.6183E-01 -3.0033E+01
 296 4.0505E-01 6.6304E-01 3.2253E+00 -1.5541E-03 9.1361E-01 3.0515E+01 5.2946E+01 3.2376E+01 6.6272E-01 -2.8746E+01
 295 4.0505E-01 5.0625E-01 2.1005E+00 -1.5541E-03 1.6214E+00 3.0515E+01 5.2953E+01 3.1823E+01 5.0580E-01 -2.9317E+01
 305 4.4585E+00 -1.1563E+00 -6.4163E-01 6.0525E-01 1.6214E+00 2.9369E+01 5.1240E+01 3.1401E+01 -1.0722E+00 -2.7689E+01
 306 4.4585E+00 2.1877E-02 -8.0941E-01 6.0525E-01 9.1361E-01 2.9369E+01 5.1140E+01 3.1313E+01 6.3231E-02 -2.7705E+01
 316 1.3430E+01 2.1877E-02 3.2253E+00 6.0525E-01 9.1361E-01 3.0515E+01 5.4260E+01 3.9266E+01 7.3673E-01 -2.2663E+01
 315 1.3430E+01 -1.1563E+00 2.1005E+00 6.0525E-01 1.6214E+00 3.0515E+01 5.4574E+01 3.8810E+01 -1.0444E+00 -2.3391E+01
105
 CENTER 3.4305E+00 7.6565E-02 7.5726E-01 3.2857E-01 7.4149E-01 3.0825E+01 5.3497E+01 3.2950E+01 9.4420E-02 -2.8780E+01
 286 -5.6324E-01 4.0713E-01 -1.1539E+00 -3.1179E-03 9.1361E-01 3.1808E+01 5.5132E+01 3.0964E+01 4.0615E-01 -3.2680E+01
 287 -5.6324E-01 4.9025E-01 -3.0538E-01 -3.1179E-03 5.6938E-01 3.1808E+01 5.5109E+01 3.1379E+01 4.8980E-01 -3.2247E+01
 297 2.0526E-01 4.9025E-01 2.0666E+00 -3.1179E-03 5.6938E-01 2.9842E+01 5.1727E+01 3.0998E+01 4.9002E-01 -2.8726E+01
 296 2.0526E-01 4.0713E-01 2.4217E+00 -3.1179E-03 9.1361E-01 2.9842E+01 5.1756E+01 3.1190E+01 4.0675E-01 -2.8563E+01
 306 3.7663E+00 -8.7031E-01 -1.1539E+00 6.6026E-01 9.1361E-01 3.1808E+01 5.5334E+01 3.3209E+01 -8.2879E-01 -3.0638E+01
 307 3.7663E+00 2.7920E-01 -3.0538E-01 6.6026E-01 5.6938E-01 3.1808E+01 5.5245E+01 3.3603E+01 3.0363E-01 -3.0167E+01
 317 1.0314E+01 2.7920E-01 2.0666E+00 6.6026E-01 5.6938E-01 2.9842E+01 5.2535E+01 3.6318E+01 3.0949E-01 -2.3966E+01
 316 1.0314E+01 -8.7031E-01 2.4217E+00 6.6026E-01 9.1361E-01 2.9842E+01 5.2674E+01 3.6470E+01 -8.1566E-01 -2.3789E+01
106
 CENTER 2.1158E+00 3.0896E-02 3.9802E-01 2.8578E-01 4.2904E-01 3.1375E+01 5.4385E+01 3.2644E+01 3.9136E-02 -3.0139E+01
 287 -5.4060E-01 1.4396E-01 -7.3944E-01 -3.5160E-03 5.6938E-01 3.3172E+01 5.7462E+01 3.2537E+01 1.4364E-01 -3.3817E+01
 288 -5.4060E-01 3.2036E-01 -1.8251E-02 -3.5160E-03 2.8871E-01 3.3172E+01 5.7462E+01 3.2895E+01 3.2023E-01 -3.3454E+01
 298 -2.6216E-01 3.2036E-01 1.3281E+00 -3.5160E-03 2.8871E-01 2.9579E+01 5.1253E+01 3.0124E+01 3.2024E-01 -2.9058E+01
 297 -2.6216E-01 1.4396E-01 1.0217E+00 -3.5160E-03 5.6938E-01 2.9579E+01 5.1254E+01 2.9971E+01 1.4368E-01 -2.9211E+01
 307 2.8113E+00 -8.5354E-01 -7.3944E-01 5.7508E-01 5.6938E-01 3.3172E+01 5.7586E+01 3.4255E+01 -8.3269E-01 -3.2204E+01
 308 2.8113E+00 5.1280E-01 -1.8251E-02 5.7508E-01 2.8871E-01 3.3172E+01 5.7525E+01 3.4600E+01 5.2281E-01 -3.1817E+01
 318 6.4546E+00 5.1280E-01 1.3281E+00 5.7508E-01 2.8871E-01 2.9579E+01 5.1547E+01 3.3583E+01 5.2496E-01 -2.5812E+01
 317 6.4546E+00 -8.5354E-01 1.0217E+00 5.7508E-01 5.6938E-01 2.9579E+01 5.1671E+01 3.3441E+01 -8.2761E-01 -2.5991E+01
107
 CENTER 6.8020E-01 1.5646E-02 1.4210E-01 2.5443E-01 1.6320E-01 3.1624E+01 5.4781E+01 3.2037E+01 1.8298E-02 -3.1217E+01
 288 -5.3449E-01 -2.9311E-02 -5.7919E-01 -3.0976E-03 2.8871E-01 3.3825E+01 5.8592E+01 3.3270E+01 -2.9401E-02 -3.4383E+01
 289 -5.3449E-01 1.7473E-01 3.1790E-01 -3.0976E-03 3.7691E-02 3.3825E+01 5.8593E+01 3.3720E+01 1.7472E-01 -3.3936E+01
 299 -5.9586E-01 1.7473E-01 5.5564E-01 -3.0976E-03 3.7691E-02 2.9424E+01 5.0973E+01 2.9409E+01 1.7472E-01 -2.9449E+01
 298 -5.9586E-01 -2.9311E-02 2.7404E-01 -3.0976E-03 2.8871E-01 2.9424E+01 5.0971E+01 2.9267E+01 -2.9426E-02 -2.9589E+01
 308 1.3039E+00 -7.5255E-01 -5.7919E-01 5.1197E-01 2.8871E-01 3.3825E+01 5.8629E+01 3.4202E+01 -7.4362E-01 -3.3486E+01
 309 1.3039E+00 6.6972E-01 3.1790E-01 5.1197E-01 3.7691E-02 3.3825E+01 5.8600E+01 3.4643E+01 6.7078E-01 -3.3023E+01
 319 2.5473E+00 6.6972E-01 5.5564E-01 5.1197E-01 3.7691E-02 2.9424E+01 5.1008E+01 3.0996E+01 6.7100E-01 -2.7894E+01
 318 2.5473E+00 -7.5255E-01 2.7404E-01 5.1197E-01 2.8871E-01 2.9424E+01 5.1057E+01 3.0857E+01 -7.4184E-01 -2.8046E+01

DATE: 7/13/1993 TIME: 14:40:45

TITLE: CROSS STRUCT. CALIB. RESULTS
CASE 1 CASE 2 CASE 3
SUBTITLE: MX = 1 MY = 1 MZ = 1

STRESS EVALUATION FOR STATIC ANALYSIS

STRESS OUTPUT FOR 3/D ELEMENT GROUP 1 CASE NO. 1

Table with columns: ELEMENT NUMBER, OUTPUT NODE, SIGMA-X1, SIGMA-X2, SIGMA-X3, TAU-X12, TAU-X23, TAU-X13, STRESS, PRINCIPAL STRESSES. Contains data for elements 9, 12, 33, 34, 95, 96, and 97.


```

28 -1.4001E+01 2.1847E+00 -3.8603E+01 1.3381E-07 7.8977E+01 2.2324E+02 4.1169E+02 2.1183E+02 3.6623E-01 -2.6262E+02
285 -1.4001E+01 2.2237E+00 -4.3587E+01 1.3381E-07 3.1875E+01 2.2324E+02 3.9266E+02 1.9739E+02 1.8949E+00 -2.5464E+02
295 1.8409E+01 2.2237E+00 5.1532E+01 1.3381E-07 3.1875E+01 1.9341E+02 3.4229E+02 2.3151E+02 2.6604E+00 -1.6200E+02
32 1.8409E+01 2.1847E+00 4.6332E+01 1.3381E-07 7.8977E+01 1.9341E+02 3.6391E+02 2.4073E+02 4.5346E+00 -1.7834E+02
36 -1.2342E+02 4.2661E+01 -3.8603E+01 1.8885E+01 7.8977E+01 2.2324E+02 4.3587E+02 1.6686E+02 3.3804E+01 -3.2003E+02
305 -1.2342E+02 -1.2941E+01 -4.3587E+01 1.8885E+01 3.1875E+01 2.2324E+02 4.0422E+02 1.4426E+02 -9.8685E+00 -3.1434E+02
315 2.7332E+02 -1.2941E+01 5.1532E+01 1.8885E+01 3.1875E+01 1.9341E+02 4.2894E+02 3.8537E+02 7.2974E+00 -8.0758E+01
40 2.7332E+02 4.2661E+01 4.6332E+01 1.8885E+01 7.8977E+01 1.9341E+02 4.2939E+02 3.8566E+02 8.2307E+01 -1.0566E+02
104
CENTER 3.0979E+01 -2.7261E+00 4.2461E+00 9.4321E+00 2.6414E+01 2.1147E+02 3.7077E+02 2.3005E+02 1.2787E-01 -1.9768E+02
285 -1.1631E+01 7.5156E-01 -3.6225E+01 2.6643E-07 3.1875E+01 3.1197E+02 5.4414E+02 2.8998E+02 6.2304E-01 -3.3770E+02
286 -1.1631E+01 4.0253E+00 -3.3166E+01 2.6643E-07 2.0953E+01 3.1197E+02 5.4253E+02 2.9050E+02 3.9546E+00 -3.3522E+02
296 1.6408E+01 4.0253E+00 5.0752E+01 2.6643E-07 2.0953E+01 1.1097E+02 2.0005E+02 1.4764E+02 4.4709E+00 -8.0929E+01
295 1.6408E+01 7.5156E-01 3.5624E+01 2.6643E-07 3.1875E+01 1.1097E+02 2.0225E+02 1.4138E+02 1.9899E+00 -9.0590E+01
305 -7.6347E+01 -2.0016E+01 -3.6225E+01 1.8864E+01 3.1875E+01 3.1197E+02 5.4646E+02 2.5672E+02 -1.6816E+01 -3.7249E+02
306 -7.6347E+01 4.3348E+00 -3.3166E+01 1.8864E+01 2.0953E+01 3.1197E+02 5.4704E+02 2.5798E+02 6.4209E+00 -3.6958E+02
316 1.9549E+02 4.3348E+00 5.0752E+01 1.8864E+01 2.0953E+01 1.1097E+02 2.2962E+02 2.5578E+02 2.5620E+00 -8.0823E+01
315 1.9549E+02 -2.0016E+01 3.5624E+01 1.8864E+01 3.1875E+01 1.1097E+02 2.8037E+02 2.5234E+02 1.6353E+01 -5.7564E+01
105
CENTER 2.4127E+01 1.2736E+00 5.3547E+00 8.6000E+00 1.6960E+01 2.1665E+02 3.7727E+02 2.3172E+02 2.7570E+00 -2.0372E+02
286 -7.6273E+00 2.8623E+00 -2.8686E+01 2.6842E-07 2.0953E+01 3.5450E+02 6.1571E+02 3.3714E+02 2.8256E+00 -3.7342E+02
287 -7.6273E+01 3.1617E+00 -1.9712E+01 2.6842E-07 1.2967E+01 3.5450E+02 6.1474E+02 3.4113E+02 3.1473E+00 -3.6845E+02
297 1.3651E+01 3.1617E+00 3.1253E+01 2.6842E-07 1.2967E+01 7.8790E+01 1.4047E+02 1.0267E+02 3.4512E+00 -5.8060E+01
296 1.3651E+01 2.8623E+00 3.8563E+01 2.6842E-07 2.0953E+01 7.8790E+01 1.4473E+02 1.0831E+02 3.6146E+00 -5.6847E+01
306 -4.7751E+01 -2.2107E+00 -2.8686E+01 1.7200E+01 2.0953E+01 3.5450E+02 6.1708E+02 3.1844E+02 -3.9012E-01 -3.9470E+02
307 -4.7751E+01 1.2813E+00 -1.9712E+01 1.7200E+01 1.2967E+01 3.5450E+02 6.1662E+02 3.2107E+02 2.4304E+00 -3.8968E+02
317 1.3824E+02 1.2813E+00 3.1253E+01 1.7200E+01 1.2967E+01 7.8790E+01 1.8859E+02 1.8045E+02 1.5450E+01 -2.5127E+01
316 1.3824E+02 -2.2107E+00 3.8563E+01 1.7200E+01 2.0953E+01 7.8790E+01 1.9102E+02 1.8176E+02 2.3083E+01 -3.0258E+01
106
CENTER 1.4763E+01 -1.0726E-02 2.5663E+00 7.4746E+00 9.5834E+00 2.2012E+02 3.8209E+02 2.2888E+02 6.8940E-01 -2.1223E+02
287 -4.2440E+00 7.0078E-01 -1.6757E+01 1.9631E-07 1.2967E+01 3.8047E+02 6.5956E+02 3.7024E+02 6.9504E-01 -3.9124E+02
288 -4.2440E+00 2.1862E+00 -9.7074E+00 1.9631E-07 6.1999E+00 3.8047E+02 6.5916E+02 3.7365E+02 2.1845E+00 -3.8750E+02
298 7.1310E+00 2.1862E+00 1.8966E+01 1.9631E-07 6.1999E+00 5.9774E+01 1.0515E+02 7.3412E+01 2.2401E+00 -4.7368E+01
297 7.1310E+00 7.0078E-01 1.7764E+01 1.9631E-07 1.2967E+01 5.9774E+01 1.0699E+02 7.3721E+01 9.9795E-01 -4.9124E+01
307 -2.4187E+01 -6.7928E+00 -1.6757E+01 1.4949E+01 1.2967E+01 3.8047E+02 6.6005E+02 3.6002E+02 -5.8107E+00 -4.0194E+02
308 -2.4187E+01 3.8628E+00 -9.7074E+00 1.4949E+01 6.1999E+00 3.8047E+02 6.6003E+02 3.6369E+02 4.3221E+00 -3.9804E+02
318 8.0351E+01 3.8628E+00 1.8966E+01 1.4949E+01 6.1999E+00 5.9774E+01 1.2817E+02 1.1766E+02 9.3777E+00 -2.3856E+01
317 8.0351E+01 -6.7928E+00 1.7764E+01 1.4949E+01 1.2967E+01 5.9774E+01 1.3398E+02 1.1683E+02 6.8895E+00 -3.2400E+01
107
CENTER 4.7846E+00 1.7349E-01 9.9861E-01 6.8494E+00 3.1185E+00 2.2181E+02 3.8444E+02 2.2475E+02 3.6756E-01 -2.1916E+02
288 -1.3507E+00 -1.5179E-01 -8.3403E+00 1.5338E-07 6.1999E+00 3.9291E+02 6.8067E+02 3.8813E+02 -1.5208E-01 -3.9782E+02
289 -1.3507E+00 1.2752E+00 -2.8691E-01 1.5338E-07 3.7094E-02 3.9291E+02 6.8054E+02 3.9209E+02 1.2752E+00 -3.9373E+02
299 2.4741E+00 1.2752E+00 6.2480E+00 1.5338E-07 3.7094E-02 5.0719E+01 8.7963E+01 5.5115E+01 1.2752E+00 -4.6393E+01
298 2.4741E+00 -1.5179E-01 6.7377E+00 1.5338E-07 6.1999E+00 5.0719E+01 8.8685E+01 5.5540E+01 -1.1288E-01 -4.6731E+01
308 -8.2598E+00 -5.0246E+00 -8.3403E+00 1.3699E+01 6.1999E+00 3.9291E+02 6.8104E+02 3.8468E+02 -4.5977E+00 -4.0171E+02
309 -8.2598E+00 4.5951E+00 -2.8691E-01 1.3699E+01 3.7094E-02 3.9291E+02 6.8104E+02 3.8890E+02 4.5918E+00 -3.9744E+02
319 2.6275E+01 4.5951E+00 6.2480E+00 1.3699E+01 3.7094E-02 5.0719E+01 9.3366E+01 6.9692E+01 4.7278E+00 -3.7301E+01
318 2.6275E+01 -5.0246E+00 6.3737E+00 1.3699E+01 6.1999E+00 5.0719E+01 9.5647E+01 6.8623E+01 -4.5384E-01 -4.0545E+01
STRESS OUTPUT FOR 3/D ELEMENT GROUP 1 CASE NO. 2
ELEMENT OUTPUT VON MISES
NUMBER NODE SIGMA-X1 SIGMA-X2 SIGMA-X3 TAU-X12 TAU-X23 TAU-X13 STRESS PRINCIPAL STRESSES
9
CENTER 3.2312E-02 -6.9662E-02 4.5570E-01 3.5795E-01 5.9997E+00 2.4598E+01 4.3862E+01 2.5482E+01 1.0094E-01 -2.5165E+01
19 1.4364E+00 1.4670E+00 2.4731E+00 7.1590E-01 5.4867E-01 2.9863E+01 5.1758E+01 3.1822E+01 1.4939E+00 -2.7940E+01
20 1.4364E+00 -2.2583E+00 -1.5436E+00 7.1590E-01 1.1451E+01 2.9863E+01 5.5514E+01 3.1518E+01 -1.3068E+00 -3.2577E+01
24 -1.8198E+00 -2.2583E+00 -2.0291E-01 7.1590E-01 1.1451E+01 1.9334E+01 3.8985E+01 2.1125E+01 -1.5159E+00 -2.3890E+01
23 -1.8198E+00 1.4670E+00 1.0962E+00 7.1590E-01 5.4867E-01 1.9334E+01 3.3669E+01 1.9028E+01 1.5046E+00 -1.9789E+01
27 2.5958E-01 7.3475E-01 2.4731E+00 -2.5466E-08 5.4867E-01 2.9863E+01 5.1772E+01 3.1255E+01 7.3459E-01 -2.8522E+01
28 2.5958E-01 -2.2209E-01 -1.5436E+00 -2.5466E-08 1.1451E+01 2.9863E+01 5.5420E+01 3.1322E+01 -1.6038E-01 -3.2668E+01
32 2.5308E-01 -2.2209E-01 -2.0291E-01 -2.5466E-08 1.1451E+01 1.9334E+01 3.8923E+01 2.2436E+01 -9.8703E-02 -2.2509E+01
31 2.5308E-01 7.3475E-01 1.0962E+00 -2.5466E-08 5.4867E-01 1.9334E+01 3.3509E+01 2.0021E+01 7.3437E-01 -1.8672E+01
12
CENTER -3.2312E-02 6.9662E-02 -4.5570E-01 -3.5795E-01 5.9997E+00 2.4598E+01 4.3862E+01 2.5165E+01 -1.0094E-01 -2.5482E+01
27 -2.5958E-01 -7.3475E-01 -2.4731E+00 -2.5466E-08 5.4867E-01 2.9863E+01 5.1772E+01 2.8522E+01 -7.3459E-01 -3.1255E+01
28 -2.5958E-01 2.2209E-01 1.5436E+00 -2.5466E-08 1.1451E+01 2.9863E+01 5.5420E+01 3.2668E+01 1.6038E-01 -3.1322E+01
32 -2.5308E-01 2.2209E-01 2.0291E-01 -2.5466E-08 1.1451E+01 1.9334E+01 3.8923E+01 2.2509E+01 9.8703E-02 -2.2436E+01
31 -2.5308E-01 -7.3475E-01 -1.0962E+00 -2.5466E-08 5.4867E-01 1.9334E+01 3.3509E+01 1.8672E+01 -7.3437E-01 -2.0021E+01
35 -1.4364E+00 -1.4670E+00 -2.4731E+00 -7.1590E-01 5.4867E-01 2.9863E+01 5.1758E+01 3.1822E+01 1.4939E+00 -2.7940E+01
36 -1.4364E+00 2.2583E+00 1.5436E+00 -7.1590E-01 1.1451E+01 2.9863E+01 5.5514E+01 3.2577E+01 1.3068E+00 -3.1518E+01
40 -1.8198E+00 2.2583E+00 2.0291E-01 -7.1590E-01 1.1451E+01 1.9334E+01 3.8985E+01 2.3890E+01 1.5159E+00 -2.1125E+01
39 1.8198E+00 -1.4670E+00 -1.0962E+00 -7.1590E-01 5.4867E-01 1.9334E+01 3.3669E+01 1.9789E+01 -1.5046E+00 -1.9028E+01
93
CENTER 4.9378E+00 3.8697E-01 4.0281E-01 -2.9372E-02 6.3208E+00 4.8955E+01 8.5618E+01 5.2051E+01 4.5412E-01 -4.6778E+01
20 1.1330E+01 2.2776E+00 1.2126E+00 -5.8743E-02 1.1451E+01 4.4096E+01 7.9495E+01 5.1861E+01 2.8174E+00 -3.9858E+01
265 1.1330E+01 -1.1829E+00 7.1666E-01 -5.8743E-02 1.1907E+00 4.4096E+01 7.7391E+01 4.9797E+01 -1.1769E+00 -3.9255E+01
275 7.9678E+00 -1.1829E+00 -1.3792E+00 -5.8743E-02 1.1907E+00 5.3813E+01 9.3688E+01 5.7323E+01 -1.1810E+00 -5.0736E+01
24 7.9678E+00 2.2776E+00 2.5596E+00 -5.8743E-02 1.1451E+01 5.3813E+01 9.5456E+01 6.0243E+01 2.5002E+00 -4.9938E+01
28 1.5913E-01 7.6055E-01 1.2126E+00 8.2285E-09 1.1451E+01 4.4096E+01 7.8915E+01 4.6286E+01 7.2257E-01 -4.4857E+01
285 1.5913E-01 -3.0739E-01 -7.8166E-01 8.2285E-09 1.1907E+00 4.4096E+01 7.6408E+01 4.3803E+01 -3.0705E-01 -4.4428E+01
295 2.9403E-01 -3.0739E-01 -1.3792E+00 8.2285E-09 1.1907E+00 5.3813E+01 9.3242E+01 5.3290E+01 -3.0710E-01 -5.4376E+01
32 2.9403E-01 7.6055E-01 2.5596E+00 8.2285E-09 1.1451E+01 5.3813E+01 9.5317E+01 5.6467E+01 7.4035E-01 -5.3593E+01

```

94

CENTER 6.6621E+00 -1.4438E-01 -6.7097E-01 -1.7164E-01 6.8800E-01 4.9226E+01 8.5565E+01 5.2365E+01 -1.4785E-01 -4.6370E+01
 265 1.4289E+01 6.2523E-01 2.1609E-02 -3.4329E-01 1.1907E+00 5.3290E+01 9.3378E+01 6.0939E+01 6.1672E-01 -4.6620E+01
 266 1.4289E+01 -4.4792E-01 -8.0471E-01 -3.4329E-01 1.8531E-01 5.3290E+01 9.3501E+01 6.0566E-01 -4.5014E-01 -4.7080E+01
 276 1.3114E+01 -4.4792E-01 -1.6581E+00 -3.4329E-01 1.8531E-01 4.5162E+01 7.9506E+01 5.1493E+01 -4.5056E-01 -4.0034E+01
 275 1.3114E+01 6.2523E-01 -2.4263E-01 -3.4329E-01 1.1907E+00 4.5162E+01 7.9316E+01 5.2110E+01 6.1582E-01 -3.9229E+01
 285 -2.7683E-01 -1.7566E-01 2.1609E-02 3.4200E-08 1.1907E+00 5.3290E+01 9.2324E+01 5.3176E+01 -1.7571E-01 -5.3431E+01
 286 -2.7683E-01 -5.7919E-01 -8.0471E-01 3.4200E-08 1.8531E-01 5.3290E+01 9.2303E+01 5.2750E+01 -5.7918E-01 -5.3832E+01
 296 -4.7801E-01 -5.7919E-01 -1.6581E+00 3.4200E-08 1.8531E-01 4.5162E+01 7.8232E+01 4.4098E+01 -5.7918E-01 -4.6235E+01
 295 -4.7801E-01 -1.7566E-01 -2.4263E-01 3.4200E-08 1.1907E+00 4.5162E+01 7.8251E+01 4.4818E+01 -1.7587E-01 -4.5538E+01

95

CENTER 8.7255E+00 7.2324E-03 -6.6360E-01 -2.7436E-01 2.7693E-02 4.9850E+01 8.6820E+01 5.4103E+01 6.9107E-03 -4.6040E+01
 266 1.7658E+01 1.4541E+00 2.0779E-01 -5.4872E-01 1.8531E-01 5.4680E+01 9.6203E+01 6.4309E+01 1.4504E+00 -4.6440E+01
 267 1.7658E+01 -6.7859E-01 -1.3650E+00 -5.4872E-01 -1.2992E-01 5.4680E+01 9.6540E+01 6.3649E+01 -6.7596E-01 -4.7359E+01
 277 1.7990E+01 -6.7859E-01 -1.1479E+00 -5.4872E-01 -1.2992E-01 4.5021E+01 8.0243E+01 5.4450E+01 -6.7535E-01 -3.7610E+01
 276 1.7990E+01 1.4541E+00 -3.4934E-01 -5.4872E-01 1.8531E-01 4.5021E+01 7.9925E+01 5.4771E+01 1.4496E+00 -3.7126E+01
 286 -3.4267E-01 -1.5986E-01 2.0779E-01 3.1449E-08 1.8531E-01 5.4680E+01 9.4710E+01 5.4613E+01 -1.5986E-01 -5.4748E+01
 287 -3.4267E-01 -5.8669E-01 -1.3650E+00 3.1449E-08 -1.2992E-01 5.4680E+01 9.4713E+01 5.3829E+01 -5.8669E-01 -5.5536E+01
 297 -4.0388E-01 -5.8669E-01 -1.1479E+00 3.1449E-08 -1.2992E-01 4.5021E+01 7.7981E+01 4.4246E+01 -5.8669E-01 -4.5798E+01
 296 -4.0388E-01 -1.5986E-01 -3.4934E-01 3.1449E-08 1.8531E-01 4.5021E+01 7.7979E+01 4.4644E+01 -1.5986E-01 -4.5398E+01

96

CENTER 1.0819E+01 -4.2299E-02 -4.8463E-01 -3.2217E-01 -2.8347E-01 5.0421E+01 8.8036E+01 5.5904E+01 -3.8359E-02 -4.5573E+01
 267 2.0424E+01 1.2167E+00 -4.6396E-01 -8.4434E-01 -1.2992E-01 5.5039E+01 9.7433E+01 6.8004E+01 1.2196E+00 -4.6047E+01
 268 2.0424E+01 -8.4068E-01 -1.5369E+00 -6.4434E-01 -4.3702E-01 5.5039E+01 9.7761E+01 6.5568E+01 -8.2926E-01 -4.6692E+01
 278 2.3998E+01 -8.4068E-01 -2.4427E-01 -6.4434E-01 -4.3702E-01 4.5802E+01 8.2878E+01 5.8881E+01 -8.2596E-01 -3.7610E+01
 277 2.3998E+01 1.2167E+00 3.0664E-01 -6.4434E-01 -1.2992E-01 4.5802E+01 8.2510E+01 5.9091E+01 1.2203E+00 -3.5390E+01
 287 -4.5830E-01 -1.2646E-01 -4.6396E-01 2.8714E-08 -1.2992E-01 5.5039E+01 9.5332E+01 5.4578E+01 -1.2646E-01 -5.5501E+01
 288 -4.5830E-01 -4.1875E-01 -1.5369E+00 2.8714E-08 -4.3702E-01 5.5039E+01 9.5340E+01 5.4046E+01 -4.1876E-01 -5.6041E+01
 298 -8.6911E-02 -4.1875E-01 -2.4427E-01 2.8714E-08 -4.3702E-01 4.5802E+01 7.9336E+01 4.5639E+01 -4.1872E-01 -4.5970E+01
 297 -8.6911E-02 -1.2646E-01 3.0664E-01 2.8714E-08 -1.2992E-01 4.5802E+01 7.9334E+01 4.5913E+01 -1.2646E-01 -4.5693E+01

97

CENTER 1.3066E+01 -1.3408E-02 -8.6496E-02 -3.7722E-01 -6.1966E-01 5.0682E+01 8.8767E+01 5.7596E+01 -2.2396E-03 -4.4628E+01
 268 2.3130E+01 1.1511E+00 -5.9780E-01 -7.5443E-01 -4.3702E-01 5.4614E+01 9.7339E+01 6.7156E+01 1.1641E+00 -4.4636E+01
 269 2.3130E+01 -1.1074E+00 -1.9417E+00 -7.5443E-01 -8.0229E-01 5.4614E+01 9.7776E+01 6.6629E+01 -1.0804E+00 -4.5487E+01
 279 2.9230E+01 -1.1074E+00 8.4962E-01 -7.5443E-01 -8.0229E-01 4.6749E+01 8.6168E+01 6.3896E+01 -1.0712E+00 -3.3852E+01
 278 2.9230E+01 1.1511E+00 1.3439E+00 -7.5443E-01 -4.3702E-01 4.6749E+01 8.5684E+01 6.4073E+01 1.1678E+00 -3.3516E+01
 288 -4.7463E-01 1.1679E-01 -5.9780E-01 3.1032E-08 -4.3702E-01 5.4614E+01 9.4600E+01 5.4080E+01 1.1675E-01 -5.5152E+01
 289 -4.7463E-01 -2.1410E-01 -1.9417E+00 3.1032E-08 -8.0229E-01 5.4614E+01 9.4618E+01 5.3417E+01 -2.1415E-01 -5.5833E+01
 299 3.7732E-01 -2.1410E-01 8.4962E-01 3.1032E-08 -8.0229E-01 4.6749E+01 8.0989E+01 4.7370E+01 -2.1392E-01 -4.6143E+01
 298 3.7732E-01 1.1679E-01 1.3439E+00 3.1032E-08 -4.3702E-01 4.6749E+01 8.0983E+01 4.7614E+01 1.1681E-01 -4.5893E+01

103

CENTER -4.9378E+00 -3.8697E-01 -4.0281E-01 2.9372E-02 6.3208E+00 4.8955E+01 8.5616E+01 4.6778E+01 -4.5412E-01 -5.2051E+01
 28 -1.5913E-01 -7.6055E-01 -1.2126E+00 8.2285E-09 1.1451E+01 4.4096E+01 7.8915E+01 4.4857E+01 -7.2257E-01 -4.6266E+01
 285 -1.5913E-01 3.0739E+01 7.8166E-01 8.2285E-09 1.1907E+00 4.4096E+01 7.6408E+01 4.4426E+01 3.0705E-01 -4.3803E+01
 292 -2.9403E-01 3.0739E-01 1.3792E+00 8.2285E-09 1.1907E+00 5.3813E+01 9.3242E+01 5.4376E+01 3.0710E-01 -5.3290E+01
 32 -2.9403E-01 -7.6055E-01 -2.5596E+00 8.2285E-09 1.1451E+01 5.3813E+01 9.5317E+01 5.3593E+01 -7.4035E-01 -5.6467E+01
 36 -1.1330E+01 -2.2776E+00 -1.2126E+00 5.8743E-02 1.1451E+01 4.4096E+01 7.9495E+01 3.9858E+01 -2.8174E+00 -5.1861E+01
 305 -1.1330E+01 1.1829E+00 7.8166E-01 5.8743E-02 1.1907E+00 4.4096E+01 7.7391E+01 3.9255E+01 1.1789E+00 -4.9797E+01
 315 -7.9678E+00 1.1829E+00 1.3792E+00 5.8743E-02 1.1907E+00 5.3813E+01 9.3688E+01 5.0736E+01 1.1810E+00 -5.7323E+01
 40 -7.9678E+00 -2.2776E+00 -2.5596E+00 5.8743E-02 1.1451E+01 5.3813E+01 9.5456E+01 4.9938E+01 -2.5002E+00 -6.0243E+01

104

CENTER -6.6621E+00 1.4438E-01 6.7097E-01 1.7164E-01 6.8800E-01 4.9226E+01 8.5565E+01 4.6370E+01 1.4785E-01 -5.2365E+01
 285 2.7683E-01 1.7566E-01 -2.1609E-02 3.4200E-08 1.1907E+00 5.3290E+01 9.2324E+01 5.3431E+01 1.7571E-01 -5.3176E+01
 286 2.7683E-01 5.7919E-01 8.0471E-01 3.4200E-08 1.8531E-01 5.3290E+01 9.2303E+01 5.3832E+01 5.7918E-01 -5.2750E+01
 296 4.7801E-01 5.7919E-01 1.6581E+00 3.4200E-08 1.8531E-01 4.5162E+01 7.8232E+01 4.6235E+01 5.7918E-01 -4.4098E+01
 295 4.7801E-01 1.7566E-01 2.4264E-01 3.4200E-08 1.1907E+00 4.5162E+01 7.8251E+01 4.5538E+01 1.7587E-01 -4.4818E+01
 305 -1.4289E+01 -6.2523E-01 -2.1609E-02 3.4329E-01 1.1907E+00 5.3290E+01 9.3378E+01 6.620E+01 -6.1672E-01 -6.0939E+01
 306 -1.4289E+01 4.4792E-01 8.0471E-01 3.4329E-01 1.8531E-01 4.5162E+01 7.9506E+01 4.0034E+01 4.5056E-01 -5.1493E+01
 316 -1.3114E+01 4.4792E-01 1.6581E+00 3.4329E-01 1.8531E-01 4.5162E+01 7.9506E+01 4.0034E+01 4.5056E-01 -5.1493E+01
 315 -1.3114E+01 -6.2523E-01 2.4264E-01 3.4329E-01 1.1907E+00 4.5162E+01 7.9316E+01 3.9229E+01 -6.1582E-01 -5.2110E+01

105

CENTER -8.7255E+00 7.2324E-03 6.6360E-01 2.7436E-01 2.7693E-02 4.9850E+01 8.6820E+01 4.6040E+01 -6.9107E-03 -5.4103E+01
 286 3.4267E-01 1.5986E-01 -2.0779E-01 3.1449E-08 1.8531E-01 5.4680E+01 9.4710E+01 5.4748E+01 1.5986E-01 -5.4613E+01
 287 3.4267E-01 5.8669E-01 1.3650E+00 3.1449E-08 -1.2992E-01 5.4680E+01 9.4713E+01 5.5536E+01 5.8669E-01 -5.3829E+01
 297 4.0388E-01 5.8669E-01 1.1479E+00 3.1449E-08 -1.2992E-01 4.5021E+01 7.7981E+01 4.5798E+01 5.8669E-01 -4.4246E+01
 296 4.0388E-01 1.5986E-01 3.4934E-01 3.1449E-08 1.8531E-01 4.5021E+01 7.7979E+01 4.5398E+01 1.5986E-01 -4.4644E+01
 306 -1.7658E+01 -1.4541E+00 -2.0779E-01 5.4872E-01 1.8531E-01 5.4680E+01 9.6203E+01 6.4309E+01 -1.4504E+00 -6.4309E+01
 307 -1.7658E+01 6.7859E-01 1.3650E+00 5.4872E-01 -1.2992E-01 5.4680E+01 9.6540E+01 4.7359E+01 6.7596E-01 -6.3649E+01
 317 -1.7990E+01 6.7859E-01 1.1479E+00 5.4872E-01 -1.2992E-01 4.5021E+01 8.0243E+01 3.7610E+01 6.7535E-01 -5.4450E+01
 316 -1.7990E+01 -1.4541E+00 3.4934E-01 5.4872E-01 1.8531E-01 4.5021E+01 7.9925E+01 3.7126E+01 -1.4496E+00 -5.4771E+01

106

CENTER -1.0819E+01 4.2299E-02 4.8463E-01 3.2217E-01 -2.8347E-01 5.0421E+01 8.8036E+01 4.5573E+01 3.8359E-02 -5.5904E+01
 287 4.5830E-01 1.2646E-01 4.6396E-01 2.8714E-08 -1.2992E-01 5.5039E+01 9.5332E+01 5.5501E+01 1.2646E-01 -5.4748E+01
 288 4.5830E-01 4.1875E-01 1.5369E+00 2.8714E-08 -4.3702E-01 5.5039E+01 9.5340E+01 5.6041E+01 4.1876E-01 -5.4046E+01
 298 8.6911E-02 4.1875E-01 2.4427E-01 2.8714E-08 -4.3702E-01 4.5802E+01 7.9336E+01 4.5970E+01 4.1872E-01 -4.5639E+01
 297 8.6911E-02 1.2646E-01 3.0664E-01 2.8714E-08 -1.2992E-01 4.5802E+01 7.9334E+01 4.5693E+01 1.2646E-01 -4.5913E+01
 307 -2.0424E+01 -1.2167E+00 4.6396E-01 6.4434E-01 -1.2992E-01 5.5039E+01 9.7433E+01 6.8004E+01 1.2196E+00 -4.6047E+01
 308 -2.0424E+01 8.4068E-01 1.5369E+00 6.4434E-01 -4.3702E-01 5.5039E+01 9.7761E+01 6.692E+01 8.2926E-01 -4.6692E+01
 318 -2.3398E+01 8.4068E-01 2.4427E-01 6.4434E-01 -4.3702E-01 4.5802E+01 8.2878E+01 3.5742E+01 8.2596E-01 -5.8881E+01
 317 -2.3398E+01 -1.2167E+00 3.0664E-01 6.4434E-01 -1.2992E-01 4.5802E+01 8.2510E+01 5.3390E+01 -1.2203E+00 -3.5390E+01

107

CENTER -1.3066E+01 1.3408E-02 8.6496E-02 3.7722E-01 -6.1966E-01 5.0682E+01 8.8767E+01 4.4628E+01 2.2396E-03 -5.7596E+01
 288 4.7463E-01 -1.1679E-01 5.9780E-01 3.1032E-08 -4.3702E-01 5.4614E+01 9.4600E+01 5.5152E+01 -1.1675E-01 -5.4080E+01
 289 4.7463E-01 2.1410E-01 -1.9417E+00 3.1032E-08 -8.0229E-01 5.4614E+01 9.4618E+01 5.5833E+01 2.1415E-01 -5.3417E+01
 299 3.7732E-01 2.1410E-01 -8.4962E-01 3.1032E-08 -8.0229E-01 4.6749E+01 8.0989E+01 4.6143E+01 2.1392E-01 -4.7370E+01
 298 3.7732E-01 -1.1679E-01 -1.3439E+00 3.1032E-08 -4.3702E-01 4.6749E+01 8.0983E+01 4.5893E+01 -1.1681E-01 -4.7614E+01

308 -2.3130E+01 -1.1511E+00 5.9780E-01 7.5443E-01 -4.3702E-01 5.4614E+01 9.7339E+01 4.4636E+01 -1.1641E+00 -6.7156E+01
309 -2.3130E+01 1.1074E+00 1.9417E+00 7.5443E-01 -8.0229E-01 5.4614E+01 9.7776E+01 4.5467E+01 1.0804E+00 -6.6629E+01
319 -2.9230E+01 1.1074E+00 -8.4962E-01 7.5443E-01 -8.0229E-01 4.6749E+01 8.6168E+01 3.3852E+01 1.0712E+00 -6.3896E+01
318 -2.9230E+01 -1.1511E+00 -1.3439E+00 7.5443E-01 -4.3702E-01 4.6749E+01 8.5684E+01 3.3516E+01 -1.1678E+00 -6.4073E+01

STRESS OUTPUT FOR 3/D ELEMENT GROUP 1 CASE NO. 3

ELEMENT		VON MISES					PRINCIPAL STRESSES				
NUMBER	NODE	SIGMA-X1	SIGMA-X2	SIGMA-X3	TAU-X12	TAU-X23	TAU-X13	STRESS	PRINCIPAL STRESSES	PRINCIPAL STRESSES	PRINCIPAL STRESSES
9											
CENTER -1.7513E+01 -3.1990E+00 9.8571E+00 1.5869E+01 -2.5737E-01 7.6650E-01 3.6328E+01 9.9994E+00 6.9170E+00 -2.7772E+01											
19		2.5463E+01	1.5343E+01	2.7494E+01	1.5657E+01	-2.0290E-01	1.0548E+00	2.9427E+01	3.6957E+01	2.7403E+01	3.9401E+00
20		2.5463E+01	-2.2510E+01	2.7767E+01	1.5657E+01	-3.1185E-01	1.0548E+00	5.6180E+01	3.0554E+01	2.7333E+01	-2.7168E+01
24		-6.0658E+01	-2.2510E+01	-1.0016E+01	1.5657E+01	-3.1185E-01	4.7816E-01	5.3145E+01	-9.9838E+00	-1.6937E+01	-6.6263E+01
23		-6.0658E+01	1.5343E+01	-5.8170E+00	1.5657E+01	-2.0290E-01	4.7816E-01	7.3157E+01	1.8446E+01	-5.8173E+00	-6.3760E+01
27		2.4887E+01	1.5179E+01	2.7494E+01	1.6082E+01	-2.0290E-01	1.0548E+00	3.0096E+01	3.6931E+01	2.7404E+01	3.2248E+00
28		2.4887E+01	-2.0807E+01	2.7767E+01	1.6082E+01	-3.1185E-01	1.0548E+00	5.4840E+01	3.0433E+01	2.7313E+01	-2.5900E+01
32		-5.9745E+01	-2.0807E+01	-1.0016E+01	1.6082E+01	-3.1185E-01	4.7816E-01	5.3195E+01	-9.9727E+00	-1.5065E+01	-8.5531E+01
31		-5.9745E+01	1.5179E+01	-5.8170E+00	1.6082E+01	-2.0290E-01	4.7816E-01	7.2513E+01	1.8488E+01	-5.8173E+00	-6.3055E+01
12											
CENTER -1.7513E+01 -3.1990E+00 9.8571E+00 1.5869E+01 2.5738E-01 7.6650E-01 3.6328E+01 9.9994E+00 6.9170E+00 -2.7772E+01											
27		2.4887E+01	1.5179E+01	2.7494E+01	1.6082E+01	2.0290E-01	-1.0548E+00	3.0096E+01	3.6931E+01	2.7404E+01	3.2248E+00
28		2.4887E+01	-2.0807E+01	2.7767E+01	1.6082E+01	3.1185E-01	-1.0548E+00	5.4840E+01	3.0433E+01	2.7313E+01	-2.5900E+01
32		-5.9745E+01	-2.0807E+01	-1.0016E+01	1.6082E+01	3.1185E-01	-1.0548E+00	5.3195E+01	-9.9727E+00	-1.5065E+01	-8.5531E+01
31		-5.9745E+01	1.5179E+01	-5.8170E+00	1.6082E+01	2.0290E-01	-1.0548E+00	7.2513E+01	1.8488E+01	-5.8173E+00	-6.3055E+01
35		2.5463E+01	1.5343E+01	2.7494E+01	1.5657E+01	2.0290E-01	-1.0548E+00	2.9427E+01	3.6957E+01	2.7403E+01	3.9401E+00
36		2.5463E+01	-2.2510E+01	2.7767E+01	1.5657E+01	-3.1185E-01	-1.0548E+00	5.6180E+01	3.0554E+01	2.7333E+01	-2.7168E+01
40		-6.0658E+01	-2.2510E+01	-1.0016E+01	1.5657E+01	-3.1185E-01	-1.0548E+00	5.3145E+01	-9.9838E+00	-1.6937E+01	-6.6263E+01
39		-6.0658E+01	1.5343E+01	-5.8170E+00	1.5657E+01	2.0290E-01	-1.0548E+00	7.3157E+01	1.8446E+01	-5.8173E+00	-6.3760E+01
93											
CENTER -9.3960E+01 -2.3550E+01 -1.7757E+01 -2.3547E+01 -4.5974E-01 8.7621E-01 8.4055E+01 -1.6376E+01 -1.7771E+01 -1.0112E+02											
20		2.3556E+02	-6.5553E+01	8.8086E+01	-2.3668E+01	-3.1185E-01	1.3572E+00	2.6400E+02	2.3742E+02	8.8076E+01	-6.7403E+01
265		2.3556E+02	1.8034E+01	1.2123E+02	-2.3668E+01	-6.0762E-01	1.3572E+00	1.9289E+02	2.3812E+02	1.2122E+02	1.5483E+01
275		-4.2388E+02	1.8034E+01	-1.2401E+02	-2.3668E+01	-6.0762E-01	3.9518E-01	3.9291E+02	1.9300E+01	-1.2401E+02	-4.2515E+02
24		-4.2388E+02	-6.5553E+01	-1.5634E+02	-2.3668E+01	-3.1185E-01	3.9518E-01	3.2526E+02	-6.3996E+01	-1.5634E+02	-4.2544E+02
28		2.3590E+02	-6.3767E+01	8.8086E+01	-2.3426E+01	-3.1185E-01	1.3572E+00	2.6269E+02	2.3773E+02	8.8076E+01	-6.5588E+01
285		2.3590E+02	1.7086E+01	1.2123E+02	-2.3426E+01	-6.0762E-01	1.3572E+00	1.9388E+02	2.3839E+02	1.2122E+02	1.4601E+01
295		-4.2342E+02	1.7086E+01	-1.2401E+02	-2.3426E+01	-6.0762E-01	3.9518E-01	3.9172E+02	1.8331E+01	-1.2401E+02	-4.2466E+02
32		-4.2342E+02	-6.3767E+01	-1.5634E+02	-2.3426E+01	-3.1185E-01	3.9518E-01	3.2600E+02	-6.2247E+01	-1.5634E+02	-4.2494E+02
94											
CENTER -9.4711E+01 6.2863E+00 -4.3534E+00 -2.3165E+01 -5.1763E-01 6.4131E-01 1.0417E+02 1.1355E+01 -4.3563E+00 -9.9776E+01											
265		1.5552E+02	1.7573E+01	9.2799E+01	-2.3633E+01	-6.0762E-01	1.3910E+00	1.2646E+02	1.5948E+02	9.2784E+01	1.3628E+01
266		1.5552E+02	-4.9782E+00	8.9402E+01	-2.3633E+01	-4.2763E-01	1.3910E+00	1.4560E+02	1.5895E+02	8.9381E+01	-8.3899E+00
276		-3.4555E+02	-4.9782E+00	-1.0319E+02	-2.3633E+01	-4.2763E-01	1.0839E-01	3.0637E+02	-3.3442E+00	-1.0319E+02	-3.4718E+02
275		-3.4555E+02	1.7573E+01	-9.6422E+01	-2.3633E+01	-6.0762E-01	1.0839E-01	3.2425E+02	1.9108E+01	-9.6422E+01	-3.4708E+02
285		1.5885E+02	1.6702E+01	9.2799E+01	-2.2696E+01	-6.0762E-01	1.3910E+00	1.2936E+02	1.6241E+02	9.2784E+01	1.3158E+01
286		1.5885E+02	-4.1518E+00	8.9402E+01	-2.2696E+01	-4.2763E-01	1.3910E+00	1.4705E+02	1.6198E+02	8.9381E+01	-7.2566E+00
296		-3.4766E+02	-4.1518E+00	-1.0319E+02	-2.2696E+01	-4.2763E-01	1.0839E-01	3.0876E+02	-2.6567E+00	-1.0319E+02	-3.4916E+02
295		-3.4766E+02	1.6702E+01	-9.6422E+01	-2.2696E+01	-6.0762E-01	1.0839E-01	3.2540E+02	1.8114E+01	-9.6422E+01	-3.4907E+02
95											
CENTER -9.5264E+01 -1.8598E+00 -4.9717E+00 -2.2558E+01 -5.3570E-01 3.4794E-01 9.9856E+01 3.3268E+00 -4.9933E+00 -1.0043E+02											
266		8.1450E+01	-5.3828E+00	6.2157E+01	-2.2605E+01	-4.2763E-01	-2.6999E-02	8.8149E+01	8.6983E+01	6.2158E+01	-1.0917E+01
267		8.1450E+01	7.9780E+01	6.5944E+01	-2.2605E+01	-6.4377E-01	-2.6999E-02	8.3838E+01	8.7355E+01	6.5948E+01	-5.1111E+00
277		-2.7311E+02	7.9780E+01	-7.1418E+01	-2.2605E+01	-6.4377E-01	7.2288E-01	2.4899E+02	2.6551E+00	-7.1420E+01	-2.7497E+02
276		-2.7311E+02	-5.3828E+00	-7.6569E+01	-2.2605E+01	-4.2763E-01	7.2288E-01	2.4336E+02	-3.4859E+00	-7.6568E+01	-2.7501E+02
286		8.2182E+01	4.3691E+00	6.2157E+01	-2.2512E+01	-4.2763E-01	-2.6999E-02	8.7635E+01	8.7688E+01	6.2158E+01	-9.8768E+00
287		8.2182E+01	1.5150E+00	6.5944E+01	-2.2512E+01	-6.4377E-01	-2.6999E-02	8.3562E+01	8.8041E+01	6.5948E+01	-4.3478E+00
297		-2.7158E+02	1.5150E+00	-7.1418E+01	-2.2512E+01	-6.4377E-01	7.2288E-01	2.4800E+02	3.3629E+00	-7.1420E+01	-2.7342E+02
296		-2.7158E+02	-4.3691E+00	-7.6569E+01	-2.2512E+01	-4.2763E-01	7.2288E-01	2.4257E+02	-2.4839E+00	-7.6568E+01	-2.7346E+02
96											
CENTER -9.5176E+01 3.5529E-01 -2.5265E+00 -2.1945E+01 -5.2336E-01 -2.7392E-01 1.0151E+02 5.1975E+00 -2.5683E+00 -9.9976E+01											
267		8.4597E+00	9.8041E-01	3.9591E+01	-2.1758E+01	-6.4377E-01	-3.3150E-01	5.1766E+01	3.9627E+01	2.6762E+01	-1.7358E+01
268		8.4597E+00	-7.6037E-01	3.9914E+01	-2.1758E+01	-4.0296E-01	-3.3150E-01	5.2777E+01	3.9933E+01	2.8072E+01	-1.8392E+01
278		-1.9921E+02	-7.6037E-01	-4.4645E+01	-2.1758E+01	-4.0296E-01	-2.1634E-01	1.8444E+02	1.6011E+00	-4.4649E+01	-2.0156E+02
277		-1.9921E+02	9.8041E-01	-4.4966E+01	-2.1758E+01	-6.4377E-01	-2.1634E-01	1.8550E+02	3.3271E+00	-4.4974E+01	-2.0154E+02
287		8.6671E+00	1.4316E+00	3.9591E+01	-2.2133E+01	-6.4377E-01	-3.3150E-01	5.1996E+01	3.9629E+01	2.7439E+01	-1.7379E+01
288		8.6671E+00	-2.3046E-01	3.9914E+01	-2.2133E+01	-4.0296E-01	-3.3150E-01	5.2952E+01	3.9934E+01	2.6774E+01	-1.8357E+01
298		-1.9862E+02	-2.3046E-01	-4.4645E+01	-2.2133E+01	-4.0296E-01	-2.1634E-01	1.8437E+02	2.2125E+00	-4.4649E+01	-2.0106E+02
297		-1.9862E+02	1.4316E+00	-4.4966E+01	-2.2133E+01	-6.4377E-01	-2.1634E-01	1.8537E+02	3.8600E+00	-4.4974E+01	-2.0104E+02
97											
CENTER -9.4677E+01 -2.2985E-01 -2.1471E+00 -2.1568E+01 -2.4627E-01 -7.0309E-01 1.0070E+02 4.4851E+00 -2.1659E+00 -9.9373E+01											
268		-6.2981E+01	-3.878E-01	1.4267E+01	-2.1352E+01	-4.0296E-01	-6.6575E-01	8.0107E+01	1.4311E+01	6.1141E+00	-8.9579E+01
269		-6.2981E+01	-4.1995E-01	1.4319E+01	-2.1352E+01	-8.9583E-02	-6.6575E-01	8.0140E+01	1.4333E+01	6.1630E+00	-6.9578E+01
279		-1.2654E+02	-4.1995E-01	-1.8737E+01	-2.1352E+01	-8.9583E-02	-7.4044E-01	1.2370E+02	3.0989E+00	-1.8735E+01	-1.3006E+02
278		-1.2654E+02	-3.878E-01	-1.8437E+01	-2.1352E+01	-4.0296E-01	-7.4044E-01	1.2380E+02	3.0910E+00	-1.8446E+01	-1.3006E+02
288		-6.2934E+01	8.9266E-03	1.4267E+01	-2.1783E+01	-4.0296E-01	-6.6575E-01	8.0548E+01	1.4315E+01	6.7669E+00	-6.9741E+01
289		-6.2934E+01	-6.9598E-02	1.4319E+01	-2.1783E+01	-8.9583E-02	-6.6575E-01	8.0551E+01	1.4334E+01	6.7300E+00	-6.9749E+01
299		-1.2625E+02	-6.9598E-02	-1.8737E+01	-2.1783E+01	-8.9583E-02	-7.4044E-01	1.2386E+02	3.5870E+00	-1.8735E+01	-1.2991E+02
298		-1.2625E+02	8.9266E-03	-1.8437E+01	-2.1783E+01	-4.0296E-01	-7.4044E-01	1.2401E+02	3.6736E+00	-1.8445E+01	-1.2991E+02
103											
CENTER -9.3960E+01 -2.3550E+01 -1.7757E+01 -2.3547E+01 -4.5974E-01 8.7622E-01 8.4055E+01 -1.6376E+01 -1.7771E+01 -1.0112E+02											
28		2.3590E+02	-6.3767E+01	8.8086E+01	-2.3426E+01	3.1185E-01	-1.3572E+00	2.6269E+02	2.3773E+02	8.8076E+01	-6.5588E+01
285		2.3590E+02	1.7086E+01	1.2123E+02	-2.3426E+01	6.0762E-01	-1.3572E+00	1.9388E+02	2.3839E+02	1.2122E+02	1.4601E+01

295 -4.2342E+02 1.7086E+01 -1.2401E+02 -2.3426E+01 6.0762E-01 -3.9518E-01 3.9172E+02 1.8331E+01 -1.2401E+02 -4.2466E+02
 32 -4.2342E+02 -6.3767E+01 -1.5634E+02 -2.3426E+01 3.1185E-01 -3.9518E-01 3.2600E+02 -6.2247E+01 -1.5634E+02 -4.2494E+02
 36 2.3556E+02 -8.5553E+01 8.8086E+01 -2.3668E+01 3.1185E-01 -1.3572E+00 2.6400E+02 2.3742E+02 8.8076E+01 -6.7403E+01
 305 2.3556E+02 1.8034E+01 1.2123E+02 -2.3668E+01 6.0762E-01 -1.3572E+00 1.9289E+02 2.3812E+02 1.2122E+02 1.5483E+01
 315 -4.2388E+02 1.8034E+01 -1.2401E+02 -2.3668E+01 6.0762E-01 -3.9518E-01 3.9291E+02 1.9300E+01 -1.2401E+02 -4.2515E+02
 40 -4.2388E+02 -8.5553E+01 -1.5634E+02 -2.3668E+01 3.1185E-01 -3.9518E-01 3.2526E+02 -6.3996E+01 -1.5634E+02 -4.2544E+02
 104
 CENTER -9.4711E+01 6.2863E+00 -4.3534E+00 -2.3165E+01 5.1763E-01 -6.4131E-01 1.0417E+02 1.1355E+01 -4.3563E+00 -9.9776E+01
 285 1.5885E+02 1.6702E+01 9.2799E+01 -2.2696E+01 6.0762E-01 -1.3910E+00 1.2936E+02 1.6241E+02 9.2784E+01 1.3158E+01
 286 1.5885E+02 -4.1516E+00 8.9402E+01 -2.2696E+01 4.2763E-01 -1.3910E+00 1.4705E+02 1.6198E+02 8.9381E+01 -7.2566E+00
 296 -3.4766E+02 -4.1516E+00 -1.0319E+02 -2.2696E+01 4.2763E-01 1.0839E-01 3.0876E+02 -2.6567E+00 -1.0319E+02 -3.4916E+02
 295 -3.4766E+02 1.6702E+01 -9.6422E+01 -2.2696E+01 6.0762E-01 1.0839E-01 3.2540E+02 1.8114E+01 -9.6426E+01 -3.4907E+02
 305 1.5552E+02 1.7573E+01 9.2799E+01 -2.3633E+01 6.0762E-01 -1.3910E+00 1.2646E+02 1.5948E+02 9.2784E+01 1.3628E+01
 306 1.5552E+02 -4.9782E+00 8.9402E+01 -2.3633E+01 4.2763E-01 -1.3910E+00 1.4560E+02 1.5895E+02 8.9381E+01 -8.3899E+00
 316 -3.4555E+02 -4.9782E+00 -1.0319E+02 -2.3633E+01 4.2763E-01 1.0839E-01 3.0637E+02 -3.3442E+00 -1.0319E+02 -3.4718E+02
 315 -3.4555E+02 1.7573E+01 -9.6422E+01 -2.3633E+01 6.0762E-01 1.0839E-01 3.2425E+02 1.9108E+01 -9.6426E+01 -3.4708E+02
 105
 CENTER -9.5264E+01 -1.8598E+00 -4.9717E+00 -2.2558E+01 5.3570E-01 -3.4794E-01 9.9856E+01 3.3268E+00 -4.9933E+00 -1.0043E+02
 286 8.2182E+01 -4.3691E+00 6.2157E+01 -2.2512E+01 4.2763E-01 2.6998E-02 8.7635E+01 8.7688E+01 6.2158E+01 -9.8768E+00
 287 8.2182E+01 1.5150E+00 6.5944E+01 -2.2512E+01 6.4377E-01 2.6998E-02 8.3562E+01 8.8041E+01 6.5948E+01 -4.3478E+00
 297 -2.7158E+02 1.5150E+00 -7.1418E+01 -2.2512E+01 6.4377E-01 -7.2288E-01 2.4800E+02 3.3629E+00 -7.1420E+01 -2.7342E+02
 296 -2.7158E+02 -4.3691E+00 -7.8569E+01 -2.2512E+01 4.2763E-01 -7.2288E-01 2.4257E+02 -2.4839E+00 -7.8568E+01 -2.7346E+02
 306 8.1450E+01 -5.3828E+00 6.2157E+01 -2.2605E+01 4.2763E-01 2.6998E-02 8.8149E+01 8.6983E+01 6.2158E+01 -1.0917E+01
 307 8.1450E+01 7.9760E-01 6.5944E+01 -2.2605E+01 6.4377E-01 2.6998E-02 8.3838E+01 8.7355E+01 6.5948E+01 -5.1111E+00
 317 -2.7311E+02 7.9760E-01 -7.1418E+01 -2.2605E+01 6.4377E-01 -7.2288E-01 2.4899E+02 2.6551E+00 -7.1420E+01 -2.7497E+02
 316 -2.7311E+02 -5.3828E+00 -7.8569E+01 -2.2605E+01 4.2763E-01 -7.2288E-01 2.4336E+02 -3.4859E+00 -7.8568E+01 -2.7501E+02
 106
 CENTER -9.5178E+01 3.5529E-01 -2.5265E+00 -2.1945E+01 5.2336E-01 2.7392E-01 1.0151E+02 5.1975E+00 -2.5683E+00 -9.9976E+01
 287 8.6671E+00 1.4316E+00 3.9914E+01 -2.2133E+01 6.4377E-01 3.3150E-01 5.1996E+01 3.9629E+01 2.7439E+01 -1.7379E+01
 288 8.6671E+00 -2.3046E-01 3.9914E+01 -2.2133E+01 4.0296E-01 3.3150E-01 5.2952E+01 3.9934E+01 2.8774E+01 -1.8357E+01
 298 -1.9862E+02 -2.3046E-01 -4.4645E+01 -2.2133E+01 4.0296E-01 2.1634E-01 1.8437E+02 2.2125E+00 -4.4649E+01 -2.0106E+02
 297 -1.9862E+02 1.4316E+00 -4.4966E+01 -2.2133E+01 6.4377E-01 2.1634E-01 1.8537E+02 3.8600E+00 -4.4974E+01 -2.0104E+02
 307 8.4597E+00 9.8041E-01 3.9591E+01 -2.1758E+01 6.4377E-01 3.3150E-01 5.1766E+01 3.9627E+01 2.6762E+01 -1.7358E+01
 308 8.4597E+00 -7.6037E-01 3.9914E+01 -2.1758E+01 4.0296E-01 3.3150E-01 5.2777E+01 3.9933E+01 2.6072E+01 -1.8392E+01
 318 -1.9921E+02 -7.6037E-01 -4.4645E+01 -2.1758E+01 4.0296E-01 2.1634E-01 1.8444E+02 1.6011E+00 -4.4649E+01 -2.0156E+02
 317 -1.9921E+02 9.8041E-01 -4.4966E+01 -2.1758E+01 6.4377E-01 2.1634E-01 1.8550E+02 3.3271E+00 -4.4974E+01 -2.0154E+02
 107
 CENTER -9.4677E+01 -2.2985E-01 -2.1471E+00 -2.1568E+01 2.4627E-01 7.0309E-01 1.0070E+02 4.4851E+00 -2.1659E+00 -9.9373E+01
 288 -6.2934E+01 8.9267E-03 1.4267E+01 -2.1783E+01 4.0296E-01 6.6575E-01 8.0548E+01 1.4315E+01 6.7669E+00 -6.9741E+01
 289 -6.2934E+01 -6.9598E-02 1.4319E+01 -2.1783E+01 8.9583E-02 6.6575E-01 8.0551E+01 1.4334E+01 6.7300E+00 -6.9749E+01
 299 -1.2625E+02 -6.9598E-02 -1.8737E+01 -2.1783E+01 8.9583E-02 7.4044E-01 1.2386E+02 3.5870E+00 -1.8735E+01 -1.2991E+02
 298 -1.2625E+02 8.9267E-03 -1.8437E+01 -2.1783E+01 4.0296E-01 7.4044E-01 1.2401E+02 3.6736E+00 -1.8445E+01 -1.2991E+02
 308 -6.2981E+01 -4.3878E-01 1.4267E+01 -2.1352E+01 4.0296E-01 6.6575E-01 8.0107E+01 1.4311E+01 6.1141E+00 -6.9579E+01
 309 -6.2981E+01 -4.1995E-01 1.4319E+01 -2.1352E+01 8.9583E-02 6.6575E-01 8.0140E+01 1.4333E+01 6.1630E+00 -6.9578E+01
 319 -1.2854E+02 -4.1995E-01 -1.8737E+01 -2.1352E+01 8.9583E-02 7.4044E-01 1.2370E+02 3.0989E+00 -1.8735E+01 -1.3006E+02
 318 -1.2654E+02 -4.3878E-01 -1.8437E+01 -2.1352E+01 4.0296E-01 7.4044E-01 1.2380E+02 3.0910E+00 -1.8446E+01 -1.3006E+02

APPENDIX E

SENSITIVITY ANALYSIS PROGRAM

In the next pages, the sensitivity analysis program is shown. The program is written in FORTRAN.

The program consists of a main menu and three sub-menus, each offering two analysis options. The main menu prompts for selection of the sensor to be analyzed. When one of the options is selected, the program goes to the appropriate sub-menu and prompts for the type of analysis to be performed, i.e., linear or angular analysis. When one of these options is selected, the program prompts for appropriate values of necessary variables and runs the analysis.

The results of the analysis are written to the corresponding output file, which is ready for a graphical display using a spreadsheet. Finally, the program asks if further analysis is desired or not.

PROGRAM SENSITIVITY

```

*****
* THIS PROGRAM CALCULATES THE SENSITIVITY IN STRESS VARIATION FOR *
* THE DIFFERENT TYPES OF ELASTIC ELEMENTS EMPLOYED IN THREE FORCE *
* SENSORS. *****
C ***** DECLARATION OF VARIABLES *****
CHARACTER ANSWER
INTEGER A,B,J
REAL L,W,H,MI,MA,DELTA,SIG(50),ERR(50),SIGX,SIGY,TXY,EPS(50)
REAL E,POINTS,X(50)
PARAMETER (PI=3.14159265359)
OPEN(UNIT=1,FILE='A:\TRUSSL.DAT',STATUS='UNKNOWN')
OPEN(UNIT=2,FILE='A:\TRUSSA.DAT',STATUS='UNKNOWN')
OPEN(UNIT=3,FILE='A:\STEWARTL.DAT',STATUS='UNKNOWN')
OPEN(UNIT=4,FILE='A:\STEWARTA.DAT',STATUS='UNKNOWN')
OPEN(UNIT=5,FILE='A:\CROSSL.DAT',STATUS='UNKNOWN')
OPEN(UNIT=6,FILE='A:\CROSSA.DAT',STATUS='UNKNOWN')

C ***** MAIN MENU STARTS HERE *****

10 PRINT*, '          MAIN MENU'
PRINT*, ''
PRINT*, '      1) TRUSS SENSOR'
PRINT*, '      2) STEWART PLATFORM'
PRINT*, '      3) CROSS-STRUCTURE SENSOR'
PRINT*, ''
PRINT*, 'TYPE THE NUMBER OF THE OPTION YOU WANT TO ANALYSE'
READ*,A
IF (A.EQ.1) THEN
  GOTO 50
ELSE IF (A.EQ.2) THEN
  GOTO 100
  ELSE IF (A.EQ.3) THEN
    GOTO 150
  ELSE
    PRINT*, 'WRONG NUMBER, TRY AGAIN'
    GOTO 10
END IF

C ***** TRUSS SENSOR ANALYSIS *****

50 PRINT*, '      1) LINEAR SENSITIVITY'
PRINT*, '      2) ANGULAR SENSITIVITY'
PRINT*, ''
PRINT*, 'CHOOSE OPTION AND HIT RETURN'
READ*,B
IF (B.EQ.1) THEN
  GOTO 55
ELSE IF (B.EQ.2) THEN
  GOTO 70
ELSE
  PRINT*, 'NUMBER MUST BE 1 OR 2, TRY AGAIN'
  GOTO 50
END IF

```

```

C ***** LINEAR SENSITIVITY *****
55 PRINT*, ' ENTER LENGHT, WIDTH AND HEIGHT OF THE BEAM '
    READ*,L,W,H
    PRINT*, ' ENTER THE LOAD VALUE '
    READ*,F
56 PRINT*, 'ENTER THE RANGE OF THE BEAM TO BE ANALYZED'
    PRINT*, 'AND THE NUMBER OF POINTS IN THE FOLLOWING'
    PRINT*, 'ORDER: MINIMUM, MAXIMUM, No. OF POINTS '
    PRINT*, 'MINIMUM MUST BE THE REFERENCE POINT'
    PRINT*, ''
    READ*,MI,MA,POINTS
    IF (MA.GT.L) THEN
    PRINT*, 'RANGE CANNOT BE GREATER THAN LENGHT'
    GOTO 56
    END IF
    DELTA=(MA-MI)/POINTS
    X(1)=MI
    DO 57 J=2,POINTS
    X(J)=X(J-1)+DELTA
57 CONTINUE
    DO 58 J=1,POINTS
    SIG(J)=(6*F*X(J))/(W*H**2)
    PRINT*, 'SIG(' ,J, ')=' ,SIG(J)
58 CONTINUE
    DO 59 J=1,POINTS
    ERR(J)=(SIG(J)-SIG(1))/SIG(1)*100.
    PRINT*, 'DIFFERENCE BETWEEN SIG(' ,J, ') AND REF. IS',ERR(J), '%'
59 CONTINUE
    WRITE(1,*) 'POSITION, SIGX, DIFFERENCE (%)'
    DO 60 J=1,POINTS
    WRITE(1,*) X(J),SIG(J),ERR(J)
60 CONTINUE
    GOTO 900

```

```

C ***** ANGULAR SENSITIVITY *****
70 PRINT*, 'PLEASE ENTER THE STRESS FIELD AT THE POINT OF INTEREST'
    PRINT*, 'SIGX, SIGY, AND TAUXY '
    PRINT*, 'THE PROGRAM COMPUTES SIGX AT DIFFERENT ORIENTATIONS'
    PRINT*, 'AND EVALUATES THE DIFFERENCE BETWEEN EACH OF THESE'
    PRINT*, 'VALUES AND THE SIGX ON THE ZERO DEGREES LINE'
    PRINT*, ''
    READ*,SIGX,SIGY,TSY
    PRINT*, 'ENTER THE RANGE AND No.OF POINTS OF ANGLE IN DEGREES'
    PRINT*, 'IN THE FORM: RANGE,No.OF POINTS'
    PRINT*, 'THE REFERENCE POINT IS AT AN ANGLE = 0 DEGREES'
    READ*,MA,POINTS
    MI=0
    MA=MA*PI/180
    DELTA=MA/POINTS
    X(1)=MI
    DO 71 J=2,POINTS
    X(J)=X(J-1)+DELTA

```

```

71 CONTINUE
DO 73 J=1,POINTS
SIG(J)=((SIGX+SIGY)/2)+((SIGX-SIGY)/2)*COS(2*X(J))+TXY*SIN(2*X(J))
PRINT*, 'SIG(',J,')=' ,SIG(J)
73 CONTINUE
DO 75 J=1,POINTS
ERR(J)=(SIG(J)-SIG(1))/SIG(1)*100.
PRINT*, 'DIFF. BETWEEN SIG(',J,') AND REF. IS ',ERR(J),'%'
75 CONTINUE
WRITE(2,*)'POSITION, SIGX, DIFFERENCE (%)'
DO 78 J=1,POINTS
WRITE(2,*) X(J)*180/PI,SIG(J),ERR(J)
78 CONTINUE
GOTO 900

```

C ***** STEWART PLATFORM ANALYSIS *****

```

100 PRINT*, '          1) LINEAR SENSITIVITY '
PRINT*, '          2) ANGULAR SENSITIVITY '
PRINT*, ''
PRINT*, ' CHOOSE OPTION AND HIT RETURN '
READ*,B
IF (B.EQ.1) THEN
GOTO 101
ELSE IF (B.EQ.2) THEN
GOTO 109
ELSE
PRINT*, 'NUMBER MUST BE 1 OR 2, TRY AGAIN'
GOTO 100
END IF

```

C ***** LINEAR SENSITIVITY *****

```

101 PRINT*, 'ENTER LENGHT, AND DIAMETER OF THE BEAM'
READ*,L,D
PRINT*, ' ENTER THE LOAD VALUE '
READ*,F
103 PRINT*, 'ENTER THE RANGE OF THE BEAM TO BE ANALYZED'
PRINT*, 'AND THE NUMBER OF POINTS IN THE FOLLOWING'
PRINT*, 'ORDER: MINIMUM, MAXIMUM, No.OF POINTS '
PRINT*, 'MINIMUM MUST BE THE REFERENCE POINT'
PRINT*, ''
READ*,MI,MA,POINTS
IF (MA.GT.L) THEN
PRINT*, 'RANGE CANNOT BE GREATER THAN LENGHT'
GOTO 103
END IF
DELTA=(MA-MI)/POINTS
X(1)=MI
DO 104 J=2,POINTS
X(J)=X(J-1)+DELTA
104 CONTINUE
DO 105 J=1,POINTS
SIG(J)=(32*F*X(J))/(PI*D**3)

```

```

PRINT*, 'SIG(' , J , ')=' , SIG(J)
105 CONTINUE
DO 107 J=1, POINTS
ERR(J)=(SIG(J)-SIG(1))/SIG(1)*100.
PRINT*, 'DIFFERENCE BETWEEN SIG(' , J , ') AND REF. IS' , ERR(J) , '%'
107 CONTINUE
WRITE(3, *) POSITION, SIGX, DIFFERENCE (%)
DO 108 J=1, POINTS
WRITE(3, *) X(J), SIG(J), ERR(J)
108 CONTINUE
GOTO 900

```

C ***** ANGULAR SENSITIVITY *****

```

109 PRINT*, 'PLEASE ENTER THE STRESS FIELD AT THE POINT OF INTEREST'
PRINT*, 'SIGX, SIGY, AND TAUXY '
PRINT*, 'THE PROGRAM COMPUTES SIGX AT DIFFERENT ORIENTATIONS'
PRINT*, 'AND EVALUATES THE DIFFERENCE BETWEEN EACH OF THESE'
PRINT*, 'VALUES AND THE SIGX ON THE ZERO DEGREES LINE'
PRINT*, ' '
READ*, SIGX, SIGY, TXY
PRINT*, 'ENTER THE RANGE AND NUMBER OF POINTS OF ANGLE IN DEGREES'
PRINT*, 'IN THE FORM: RANGE, No. OF POINTS'
PRINT*, 'THE REFERENCE POINT IS AT AN ANGLE = 0 DEGREES'
READ*, MA, POINTS
MI=0
MA=MA*PI/180
DELTA=MA/POINTS
X(1)=MI
DO 110 J=2, POINTS
X(J)=X(J-1)+DELTA
110 CONTINUE
DO 111 J=1, POINTS
SIG(J)=((SIGX+SIGY)/2)+((SIGX-SIGY)/2)*COS(2*X(J))+TXY*SIN(2*X(J))
PRINT*, 'SIG(' , J , ')=' , SIG(J)
111 CONTINUE
DO 113 J=1, POINTS
ERR(J)=(SIG(J)-SIG(1))/SIG(1)*100.
PRINT*, 'DIFF. BETWEEN SIG(' , J , ') AND REF. IS ' , ERR(J) , '%'
113 CONTINUE
WRITE(4, *) POSITION, SIGX, DIFFERENCE (%)
DO 115 J=1, POINTS
WRITE(4, *) X(J)*180/PI, SIG(J), ERR(J)
115 CONTINUE
GOTO 900

```

C ***** CROSS-STRUCTURE ANALYSIS *****

```

150 PRINT*, '          1) LINEAR SENSITIVITY
PRINT*, '          2) ANGULAR SENSITIVITY
PRINT*, ' '
PRINT*, ' CHOOSE OPTION AND HIT RETURN '
READ*, B
IF (B.EQ.1) THEN

```

```

GOTO 155
ELSE IF (B.EQ.2) THEN
  GOTO 161
ELSE
  PRINT*, 'NUMBER MUST BE 1 OR 2, TRY AGAIN'
  GOTO 150
END IF

C ***** LINEAR SENSITIVITY *****
155 PRINT*, ' ENTER LENGHT, WIDTH AND HEIGHT OF THE BEAM '
  READ*, L, W, H
  PRINT*, ' ENTER THE LOAD VALUE '
  READ*, F
  PRINT*, 'ENTER THE MODULUS OF ELASTICITY IN PSI '
  READ*, E
156 PRINT*, 'ENTER THE RANGE OF THE BEAM TO BE ANALYZED'
  PRINT*, 'AND THE NUMBER OF POINTS IN THE FOLLOWING'
  PRINT*, 'ORDER: MINIMUM, MAXIMUM, No.OF POINTS '
  PRINT*, 'MINIMUM MUST BE THE REFERENCE POINT'
  PRINT*, ' '
  READ*, MI, MA, POINTS
  IF (MA.GT.L) THEN
    PRINT*, 'RANGE CANNOT BE GREATER THAN LENGHT'
    GOTO 156
  END IF
  DELTA=(MA-MI)/POINTS
  X(1)=MI
  DO 157 J=2, POINTS
    X(J)=X(J-1)+DELTA
157 CONTINUE
  DO 158 J=1, POINTS
    EPS(J)=(3*(2*X(J)-L)*F)/(4*E*W*H**2)
    PRINT*, 'EPS(' , J, ')=' , EPS(J)
158 CONTINUE
  DO 159 J=1, POINTS
    ERR(J)=(EPS(J)-EPS(1))/EPS(1)*100.
    PRINT*, 'DIFFERENCE BETWEEN EPS(' , J, ') AND REF.IS' , ERR(J), '%'
159 CONTINUE
  WRITE(5, *) 'POSITION, EPSILON, DIFFERENCE (%)'
  DO 160 J=1, POINTS
    WRITE(5, *) X(J), EPS(J), ERR(J)
160 CONTINUE
  GOTO 900

C ***** ANGULAR SENSITIVITY *****
161 PRINT*, 'PLEASE ENTER THE STRESS FIELD AT THE POINT OF INTEREST'
  PRINT*, 'SIGX, SIGY, AND TAUXY '
  PRINT*, 'THE PROGRAM COMPUTES SIGX AT DIFFERENT ORIENTATIONS'
  PRINT*, 'AND EVALUATES THE DIFFERENCE BETWEEN EACH OF THESE'
  PRINT*, 'VALUES AND THE SIGX ON THE ZERO DEGREE LINE'
  PRINT*, ' '
  READ*, SIGX, SIGY, TXY
  PRINT*, 'ENTER THE RANGE AND No.OF POINTS OF ANGLE IN DEGREES'

```

```
PRINT*, 'IN THE FORM: RANGE, No.OF POINTS '  
PRINT*, 'THE REFERENCE POINT IS AT AN ANGLE = 0 DEGREES'  
READ*, MA, POINTS  
MI=0  
MA=MA*PI/180  
DELTA=MA/POINTS  
X(1)=MI  
DO 162 J=2, POINTS  
X(J)=X(J-1)+DELTA  
162 CONTINUE  
DO 163 J=1, POINTS  
SIG(J)=((SIGX+SIGY)/2)+((SIGX-SIGY)/2)*COS(2*X(J))+TXY*SIN(2*X(J))  
PRINT*, 'SIG(' , J, ')=' , SIG(J)  
163 CONTINUE  
DO 165 J=1, POINTS  
ERR(J)=(SIG(J)-SIG(1))/SIG(1)*100.  
PRINT*, 'DIFF. BETWEEN SIG(' , J, ') AND REF. IS ' , ERR(J), '%'  
165 CONTINUE  
WRITE(6, *) 'POSITION, SIGX, DIFFERENCE (%)'  
DO 170 J=1, POINTS  
WRITE(6, *) X(J)*180/PI, SIG(J), ERR(J)  
170 CONTINUE  
900 PRINT*, 'DO YOU WISH ANOTHER CALCULATION (Y/N)?'  
READ*, ANSWER  
IF (ANSWER.EQ.'Y') THEN  
GOTO 10  
ELSE IF (ANSWER.EQ.'N') THEN  
GOTO 990  
ELSE  
PRINT*, 'ANSWER MUST BE "Y" OR "N", TRY AGAIN'  
GOTO 900  
END IF  
990 STOP  
END
```

APPENDIX F

SINGULAR VALUE DECOMPOSITION PROGRAM

In the next pages, the subroutine that performs the singular value decomposition of an arbitrary matrix A is shown. This program is written in the C language and was taken from ref.[17]. To run the program, the matrix A must be typed in a separate file, using a text editor such as the MS-DOS editor.

The singular value decomposition method is based on the following theorem [17]: any $M \times N$ matrix A whose number of rows M is greater than or equal to its number of columns N , can be written as the product of an $M \times N$ column-orthogonal matrix U , an $N \times N$ diagonal matrix W with positive or zero elements which are called **singular values**, and the transpose of an $N \times N$ orthogonal matrix V .

$$[A] = [U][W][V^T]$$

The program performs the decomposition and returns each of the matrices separately. The first two pages show the main program and printing of results. The next section is the subroutine that actually performs the singular value decomposition.


```

/* Driver for routine SVDCMP */

#include <stdio.h>
#include <conio.h>
#include "nr.h"
#include "nrutil.h"

#define NP 20
#define MP 20
#define MAXSTR 80

main()
{
    int j,k,l,m,n;
    float *w,**a,**u,**v;
    char dummy[MAXSTR];
    FILE *fp;

    w=vector(1,NP);
    a=matrix(1,MP,1,NP);
    u=matrix(1,MP,1,NP);
    v=matrix(1,NP,1,NP);
    /* read input matrices */
    if ((fp = fopen("matrx3.dat","r")) == NULL)
        nrerror("Data file MATRX3.DAT not found\n");
    while (!feof(fp)) {
        fgets(dummy,MAXSTR,fp);
        fgets(dummy,MAXSTR,fp);
        fscanf(fp,"%d %d",&m,&n);
        fgets(dummy,MAXSTR,fp);
        /* copy original matrix into u */
        for (k=1;k<=m;k++)
            for (l=1;l<=n;l++) {
                fscanf(fp,"%f",&a[k][l]);
                u[k][l]=a[k][l];
            }
        if (n > m) {
            for (k=m+1;k<=n;k++) {
                for (l=1;l<=n;l++) {
                    a[k][l]=0.0;
                    u[k][l]=0.0;
                }
            }
            m=n;
        }
        /* perform decomposition */
        svdcmp(u,m,n,w,v);
        /* write results */
        printf("Decomposition matrices:\n");
        printf("Matrix u\n");
        for (k=1;k<=m;k++) {
            for (l=1;l<=n;l++)
                printf("%12.6f",u[k][l]);
        }
    }
}

```

```

        printf("\n");
    }
    printf("Diagonal of matrix w\n");
    for (k=1;k<=n;k++)
        printf("%12.6f",w[k]);
printf("\nPress any key to continue\n"); getch();
    printf("\nMatrix v-transpose\n");
    for (k=1;k<=n;k++) {
        for (l=1;l<=n;l++)
            printf("%12.6f",v[l][k]);
        printf("\n");
    }
    printf("\nCheck product against original matrix:\n"
    printf("Original matrix:\n");
    for (k=1;k<=m;k++) {
        for (l=1;l<=n;l++)
            printf("%12.6f",a[k][l]);
        printf("\n");
    }
    printf("Product u*w*(v-transpose):\n");
    for (k=1;k<=m;k++) {
        for (l=1;l<=n;l++) {
            a[k][l]=0.0;
            for (j=1;j<=n;j++)
                a[k][l] += u[k][j]*w[j]*v[l][j];
        }
        for (l=1;l<=n;l++) printf("%12.6f",a[k][l]);
        printf("\n");
    }
    printf("*****\n");
    printf("press RETURN for next problem\n");
    getch();
}
fclose(fp);
free_matrix(v,1,NP,1,NP);
free_matrix(u,1,MP,1,NP);
free_matrix(a,1,MP,1,NP);
free_vector(w,1,NP);
}

```

```

#include <math.h>

static float at, bt, ct;
#define PYTHAG(a,b) ((at=fabs(a)) > (bt=fabs(b)) ? \
(ct=bt/at, at*sqrt(1.0+ct*ct)) : (bt ? (ct=at/bt, bt*sqrt(1.0+ct*ct)) : 0.0))

static float maxarg1, maxarg2;
#define MAX(a,b) (maxarg1=(a), maxarg2=(b), (maxarg1) > (maxarg2) ? \
(maxarg1) : (maxarg2))
#define SIGN(a,b) ((b) >= 0.0 ? fabs(a) : -fabs(a))

void svdcmp(a,m,n,w,v)
float **a, *w, **v;
int m,n;
{
    int flag, i, its, j, jj, k, l, nm;
    float c, f, h, s, x, y, z;
    float anorm=0.0, g=0.0, scale=0.0;
    float *rv1, *vector();
    void nerror(), free_vector();

    if (m < n) nerror("SVDcmp: You must augment A with extra zero rows")
    rv1=vector(1,n);
    for (i=1; i<=n; i++) {
        l=i+1;
        rv1[i]=scale*g;
        g=s=scale=0.0;
        if (i <= m) {
            for (k=i; k<=m; k++) scale += fabs(a[k][i]);
            if (scale) {
                for (k=i; k<=m; k++) {
                    a[k][i] /= scale;
                    s += a[k][i]*a[k][i];
                }
                f=a[i][i];
                g = -SIGN(sqrt(s), f);
                h=f*g-s;
                a[i][i]=f-g;
                if (i != n) {
                    for (j=l; j<=n; j++) {
                        for (s=0.0, k=i; k<=m; k++) s += a[k][i]*a[k][j];
                        f=s/h;
                        for (k=i; k<=m; k++) a[k][j] += f*a[k][i];
                    }
                }
                for (k=i; k<=m; k++) a[k][i] *= scale;
            }
        }
    }
    w[i]=scale*g;
    g=s=scale=0.0;
    if (i <= m && i != n) {
        for (k=l; k<=n; k++) scale += fabs(a[i][k]);
        if (scale) {

```

```

    for (k=l;k<=n;k++) {
        a[i][k] /= scale;
        s += a[i][k]*a[i][k];
    }
    f=a[i][l];
    g = -SIGN(sqrt(s),f);
    h=f*g-s;
    a[i][l]=f-g;
    for (k=l;k<=n;k++) rv1[k]=a[i][k]/h;
    if (i != m) {
        for (j=l;j<=m;j++) {
            for (s=0.0,k=l;k<=n;k++) s += a[j][k]*a[i][k];
            for (k=l;k<=n;k++) a[j][k] += s*rv1[k];
        }
    }
    for (k=l;k<=n;k++) a[i][k] *= scale;
}
}
anorm=MAX(anorm,(fabs(w[i])+fabs(rv1[i])));
}
for (i=n;i>=1;i--) {
    if (i < n) {
        if (g) {
            for (j=l;j<=n;j++)
                v[j][i]=(a[i][j]/a[i][l])/g;
            for (j=l;j<=n;j++) {
                for (s=0.0,k=l;k<=n;k++) s += a[i][k]*v[k][j];
                for (k=l;k<=n;k++) v[k][j] += s*v[k][i];
            }
        }
        for (j=l;j<=n;j++) v[i][j]=v[j][i]=0.0;
    }
    v[i][i]=1.0;
    g=rv1[i];
    l=i;
}
for (i=n;i>=1;i--) {
    l=i+1;
    g=w[i];
    if (i < n)
        for (j=l;j<=n;j++) a[i][j]=0.0;
    if (g) {
        g=1.0/g;
        if (i != n) {
            for (j=l;j<=n;j++) {
                for (s=0.0,k=l;k<=m;k++) s += a[k][i]*a[k][j];
                f=(s/a[i][i])*g;
                for (k=i;k<=m;k++) a[k][j] += f*a[k][i];
            }
        }
        for (j=i;j<=m;j++) a[j][i] *= g;
    } else {
        for (j=i;j<=m;j++) a[j][i]=0.0;
    }
}

```

```

    }
    ++a[i][i];
}
for (k=n;k>=1;k--) {
    for (its=1;its<=30;its++) {
        flag=1;
        for (l=k;l>=1;l--) {
            nm=l-1;
            if (fabs(rv1[l])+anorm == anorm) {
                flag=0;
                break;
            }
            if (fabs(w[nm])+anorm == anorm) break;
        }
        if (flag) {
            c=0.0;
            s=1.0;
            for (i=1;i<=k;i++) {
                f=s*rv1[i];
                if (fabs(f)+anorm != anorm) {
                    g=w[i];
                    h=PYTHAG(f,g);
                    w[i]=h;
                    h=1.0/h;
                    c=g*h;
                    s=(-f*h);
                    for (j=1;j<=m;j++) {
                        y=a[j][nm];
                        z=a[j][i];
                        a[j][nm]=y*c+z*s;
                        a[j][i]=z*c-y*s;
                    }
                }
            }
        }
        z=w[k];
        if (l == k) {
            if (z < 0.0) {
                w[k] = -z;
                for (j=1;j<=n;j++) v[j][k]=(-v[j][k]);
            }
            break;
        }
    }
    if (its == 30) nerror("No convergence in 30 SVDCMP iterations");
    x=w[l];
    nm=k-1;
    y=w[nm];
    g=rv1[nm];
    h=rv1[k];
    f=((y-z)*(y+z)+(g-h)*(g+h))/(2.0*h*y);
    g=PYTHAG(f,1.0);
    f=((x-z)*(x+z)+h*((y/(f+SIGN(g,f))-h))/x;
    c=s=1.0;

```

```

for (j=1;j<=nm;j++) {
    i=j+1;
    g=rv1[i];
    y=w[i];
    h=s*g;
    g=c*g;
    z=PYTHAG(f,h);
    rv1[j]=z;
    c=f/z;
    s=h/z;
    f=x*c+g*s;
    g=g*c-x*s;
    h=y*s;
    y=y*c;
    for (jj=1;jj<=n;jj++) {
        x=v[jj][j];
        z=v[jj][i];
        v[jj][j]=x*c+z*s;
        v[jj][i]=z*c-x*s;
    }
    z=PYTHAG(f,h);
    w[j]=z;
    if (z) {
        z=1.0/z;
        c=f*z;
        s=h*z;
    }
    f=(c*g)+(s*y);
    x=(c*y)-(s*g);
    for (jj=1;jj<=m;jj++) {
        y=a[jj][j];
        z=a[jj][i];
        a[jj][j]=y*c+z*s;
        a[jj][i]=z*c-y*s;
    }
}
rv1[l]=0.0;
rv1[k]=f;
w[k]=x;
}
}
free_vector(rv1,1,n);
}

```

```

#undef SIGN
#undef MAX
#undef PYTHAG

```

APPENDIX G
TIME AND COST ESTIMATIONS

In this section, a more detailed explanation of the time and cost estimation for each sensor is presented. These estimates were provided by Mr. Charles Maitle from the Electrical Engineering Machine Shop and, according to him, the estimates must be considered only as a rough estimation. The next table shows the time estimate for the Truss sensor. The rate per hour was set as \$26.00/hr.

	ONE SENSOR	SIX SENSORS
OPERATION DESCRP.	TIME (HRS)	TIME (HR)
Square a solid block	2	10
make electrode for holes in frame	4	8
make holes in frame	4	18
make electrode for beams	6	18
make beams	12	60
total time	28	114

Table 5. Time estimation for the Truss sensor.

The next table shows the estimate for the Stewart-Platform. Again, the hourly rate was set at \$26.00/hr.

	ONE SENSOR	SIX SENSORS
OPERATION DESCRIP.	TIME (HRS)	TIME (HRS)
Cut legs and blanks for the plates	3.5	8
set up, drill top and bottom plates	8	20
cut plates from blanks	2	10
assemble and trim with loetite	7	36
dry	8	8
total time	28.5	82

Table 6. Time estimation for the Stewart-Platform.

The final estimate is for the Cross Structure. Again, the rate was set at \$26.00/hr. This estimate is shown in the next table

	ONE SENSOR	SIX SENSORS
	TIME (HRS)	TIME (HRS)
square a solid block	2	10
vice tooling	2	2
brooching ends	6	30
brooching parts	10	39
make electrodes	6	10
EDM tooling	3	3
EDM process	8	36
total time	37	130

Table 7. Time estimation for the Cross sensor.